UNIVERSITY OF KWAZULU-NATAL
INYUVESI YAKWAZULU-NATALI

Metal Complexes with Phosphor-1,1-dithiolato Ligands: Synthesis, Structures, Polymorphism, Antibacterial Studies and Dye-Sensitized Solar Cell Application

By

Gwaza Eric Ayom

2017

Thesis submitted in fulfilment of the academic requirements for the degree of Doctor of Philosophy

School of Chemistry & Physics, College of Agriculture, Engineering and Science, University of KwaZulu-Natal, Durban

As the candidate's supervisor I have approved this Thesis for submission.

Prof. W. E. van Zyl

21 August 2017
Date

DECLARATIONS

DECLARATION 1: PLAGIARISM

I, Gwaza Eric Ayom, declare that:

1. The research reported in this thesis, except where otherwise indicated, is my original research.
2. This thesis has not been submitted for any degree or examination at any other University.
3. This thesis does not contain other persons' data, pictures, graphs or other information, unless specifically acknowledged as being sourced from other persons.
4. This thesis does not contain other persons' writing, unless specifically acknowledged as being sourced from other researchers. Where other written sources have been quoted, then:
    a. Their words have been re-written but the general information attributed to them has been referenced
    b. Where their exact words have been used, then their writing has been placed in italics and inside quotation marks, and referenced.
5. This thesis does not contain text, graphics or tables copied and pasted from the Internet, unless specifically acknowledged, and the source being detailed in the thesis and in the References sections.

Signed

Gwaza Eric Ayom

DECLARATION 2: PUBLICATIONS

DETAILS OF CONTRIBUTION TO PUBLICATIONS that form part and/or include research presented in this thesis.

Publication 1 (manuscript in preparation)

Gwaza E. Ayom and Werner E. van Zyl. **Synthesis and characterization of Zn dithiophosphonate heterocycles.**

Contributions: I carried out the synthesis and characterisation of the compounds. I wrote the initial draft.

Publication 2 (manuscript in preparation)

Gwaza E. Ayom, Richard J. Staples and Werner E. van Zyl. **Coordination and zwitterionic compounds of ethambutol: synthesis, characterization and antibacterial studies**.

Contributions: I carried out the synthesis and characterisation of the compounds. I wrote the initial draft. Dr. Staples provided X- ray crystallographic analysis.

Publication 3 (manuscript in preparation)

Gwaza E. Ayom and Werner E. van Zyl. **Ferrocenyl S-S coupled dithiophosphonates as potential co-sensitizers in dye-sensitized solar cells**.

Contributions: I carried out the synthesis and characterisation of the compounds. I prepared the initial draft.

Signed: Gwaza Eric Ayom

DECLARATION 3: CONFERENCE PROCEEDINGS

1. Gwaza E. Ayom and Werner E. van Zyl. Synthesis and chraracterization of Zn(II) dithiophosphonate heterocycles. (Poster presented at 27th International Conference on Organometallic Chemistry (ICOMC-2016), Melbourne, Australia.

DEDICATION

TO MY PARENTS MR & MRS THOMAS SHAAKAA AYOM

ACKNOWLEDGEMENT

- My Parents Mr & Mrs Ayom and siblings, Doosuur, Nguseer, Tookwase, Doom, Ayom Jr and Bee Ayom for their patience and support. I am immensely grateful to my Parents for bringing me up spiritually, morally and educationally that laid a solid foundation for me in life.

- Prof Werner E. van Zyl, for initiating this study, his useful inputs and constructive criticisms that ultimately produced this thesis.

- Dr. R. J. Staples, Mr Mike Pillay and Sizwe Zamisa for data collection and refinement of the crystal structures presented in this study.

- My appreciation to Dr Lukas Le Roux of CSSIR for helping with the DSSCs measurements at CSSIR and Dr Hafizah Chenia and her student Noyise MB of the microbiology department, UKZN, Westville department for helping out with the anti-microbial screenings.

- The technical and academic staff at UKZN, School of Chemistry and Physics, Westville Campus.

- University of KwaZulu-Natal and the Eskom TESP initiative for financial support for this study.

- My lab mates and friends, Mike Pillay, Vashen Moodley, Vincent Sithole, Zwelihle Ndlovu, Nhlanhla Ntuli, Ibrahim Halliru, Samaila Abubakar, Nasir Lawal, Yerima Iliya, Ogundare Segun, Siyabonga Mcube, Mkubuzi Emmanuel, Olowe Kayode, Ibijola Stephen, Akpan Daniel, Fezile Potwana, Dhimba George and Ajayi Tomilola.

- My love, Avaan Emmanuella

- Grateful to God Almighty, **ALL GLORY TO GOD**.

LIST OF FIGURES

LIST OF SCHEMES

LIST OF CHARTS

LIST OF TABLES

_Toc492279626

ABSTRACT

This thesis describes the isolation, characterization and applications of new dithiophosphonate ligands and their ability to facilitate metal complex formation. New dithiophosphonate ligands, including zwitterionic compounds was obtained from the reaction of 2,4-bis(4-ethoxyphenyl)- and 2,4-diferrocenyl-1,3-dithiadiphosphetane disulfide precursors, $(RP(S)S)_2$ (R = 4-C_6H_4OMe or $FeC_{10}H_9$) with pentaerythritol, diphenylmethanol and ethambutol.

The reaction of PhLR or FcLR, $[ArP(S)(\mu\text{-}S)]_2$ (Ar = p-$CH_3OC_6H_4$ or Fc=Fe(η5-C_5H_4)(η5-C_5H_5)) with pentaerythritol or diphenylmethanol generated 4 dithiophosphonate ligands of the type $[ArP(OR)S_2]^-$, which facilitated the preparation of 14 new Zn(II), Cd(II) and Ni(II) complexes. All the new compounds were characterized by ^1H, ^{31}P, ^{13}C NMR and FTIR. Bulk purity was confirmed by ESI-MS and molecular structures were obtained in select cases using single crystal X-ray crystallography. The representative molecular structures indicated that the geometry around the coordinated Zn(II) and Cd(II) were tetrahedral while that of Ni(II) was square planar. Some of the Zn(II) and Cd(II) compounds exhibited strong solid-state luminescence at room temperature between 315-510 nm following excitation between 220-330 nm based on their UV-Vis electronic absorptions. Solubility tests of the new compounds indicated that while the ligands were generally soluble in polar solvents, the complexes were more soluble in chlorinated solvents; all new compounds were soluble in DMSO and DMF.

The reaction between 2,4-diferrocenyl-1,3-dithiadiphosphetane disulfide, $(RP(S)S)_2$ (R = $FeC_{10}H_9$) and pentaerythritol yielded the corresponding ferrocenyl salt from which Zn(II) and Cd(II) intramolecular S-S coupled dithiophosphonate complexes were made. These complexes were characterised by ^1H, ^{31}P and ^{13}C NMR and FTIR while bulk purity was confirmed by ESI-MS. Representative molecular structures obtained showed that the coordinated Zn(II) and Cd(II) ions adopted an octahedral geometry. Four new polymorphs of a reported intramolecular S-S coupled dithiophosphonate compound are also reported in

this thesis. The molecular structures of these polymorphs obtained were compared to the one already reported in literature and with each other my molecular overlays and crystal packing.

This thesis also report the zwitterionic and coordination compounds obtained by the reaction of ethambutol with PhLR or FcLR, $[ArP(S)(\mu\text{-}S)]_2$ (Ar = p-$CH_3OC_6H_4$ or Fc=Fe(η5-C_5H_4)(η5-C_5H_5)), $NiCl_2.6H_2O$ and $CuCl_2 \cdot 2H_2O$. The zwitterionic and coordination compounds were characterized by ^{1}H, ^{31}P and ^{13}C NMR, except for the paramagnetic coordination compounds. All new compounds were characterized by FTIR while bulk purity was confirmed by ESI-MS. The Ni(II) ethambutol coordination compound formed a hexa-nuclear cluster with an octahedral geometry around each Ni(II) while that of Cu(II) had a square pyramidal orientation.

Some of the new ferrocenyl complexes' application as dye sensitized solar cells, DSSCs, was also investigated. After co-sensitization with the state-of-the-art ruthenium dye, N719, all four tested complexes showed a capacity to improve the performance of the dye as the photovoltaic parameters J_{SC}, V_{OC} and η were all increased. The fabricated device performance decreases in the order **25**/N719 (η = 7.49 %) > **28**/N719 (η = 7.30 %) > **26**/N719 (η = 6.70 %) > **27**/N719 (η = 6.34 %) compared to that of the dye N719 (η = 5.65 %) under similar experimental conditions. These results indicate that these complexes are attractive candidates as co-sensitizers in DSSCs.

Finally, the antibacterial susceptibility screenings showed that selected Gram-negative (*Escherichia coli* ATCC 25922, *E. coli* ATCC 35218, and *Pseudomonas aeruginosa* ATCC 27853) and Gram-positive bacteria (*Staphylococcus aureus* ATCC 29213, *S. aureus* ATCC 43300 and *Enterococcus faecalis* ATCC 51299) were susceptible to some of the synthesized dithiophosphonate compounds at 500 and 1000 µg/L.

LIST OF LIGANDS AND COMPLEXES

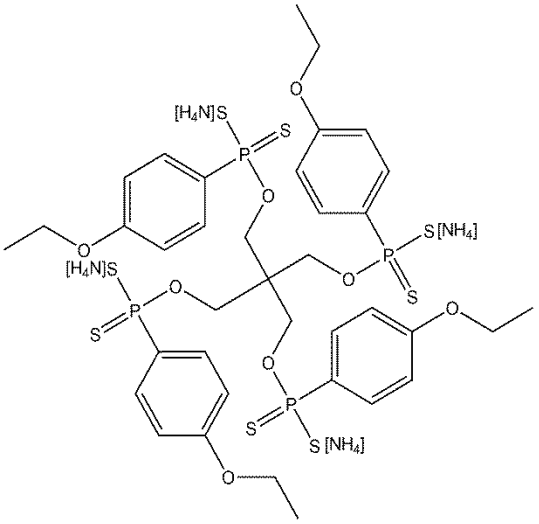

1

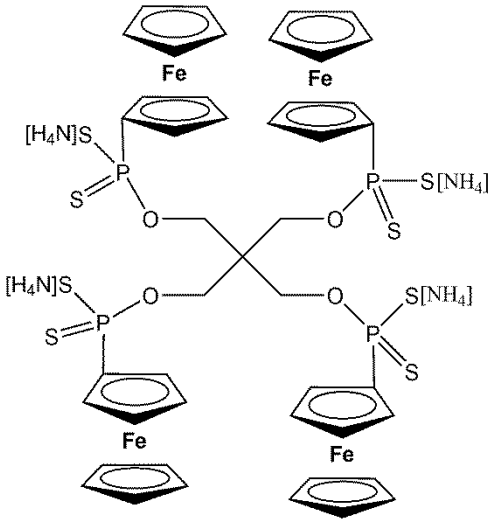

2

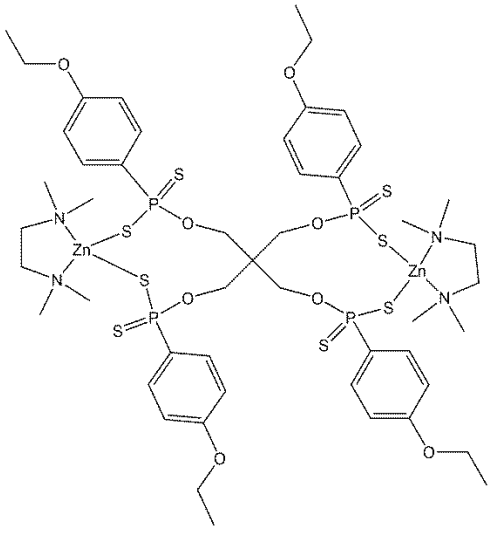

3

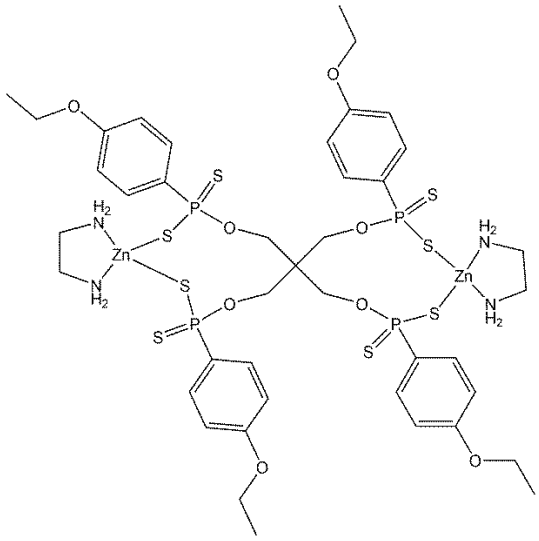

4

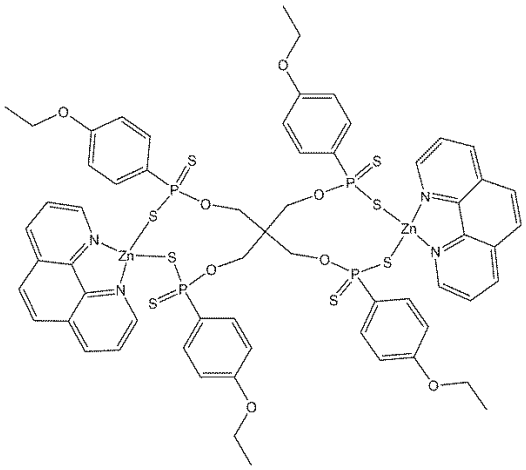

5

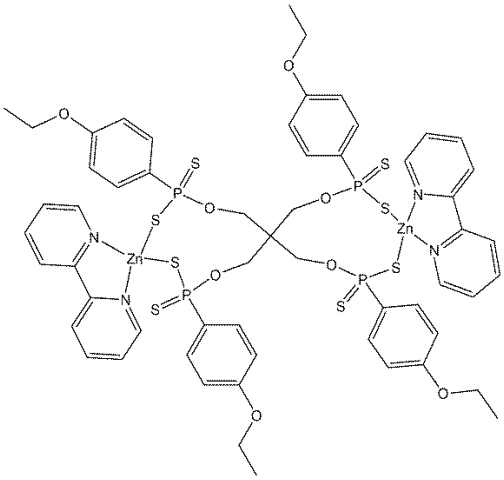

6

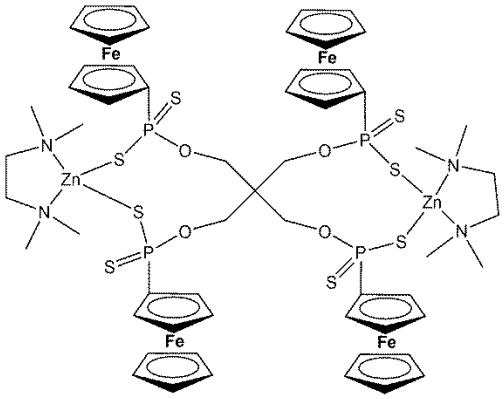

7

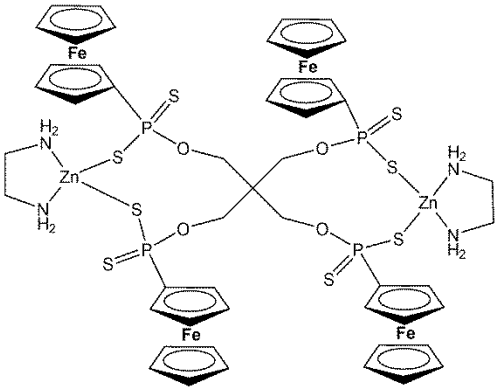

8

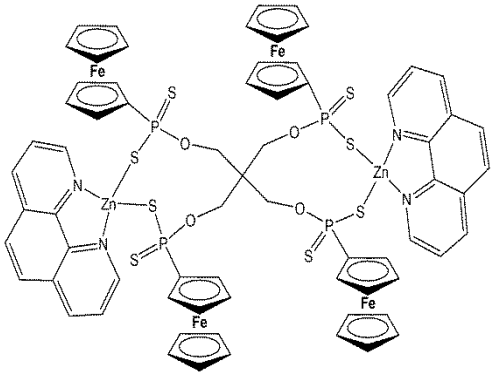

9

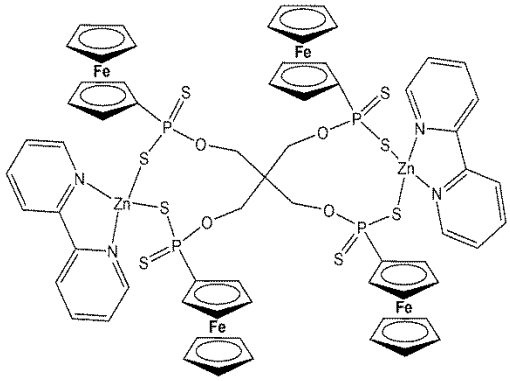

10

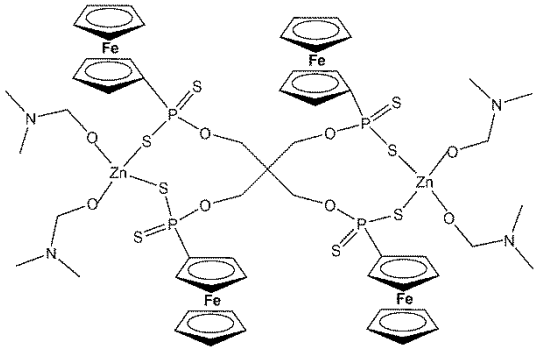

11

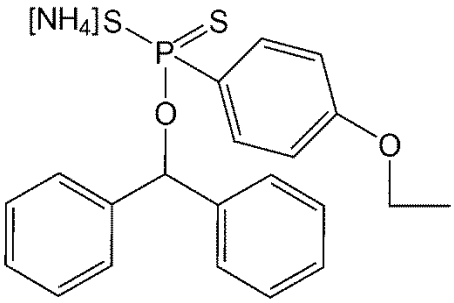

12

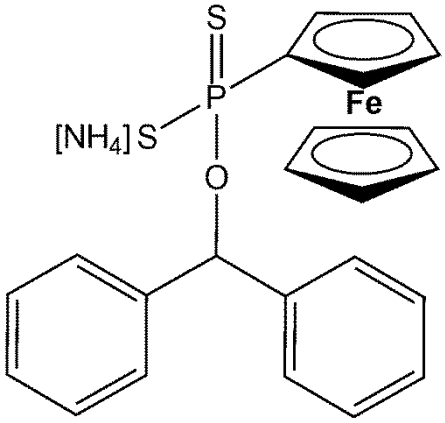

13

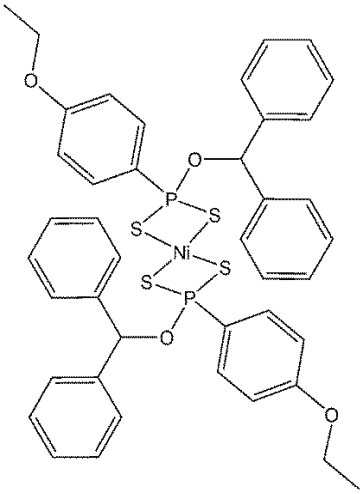

14

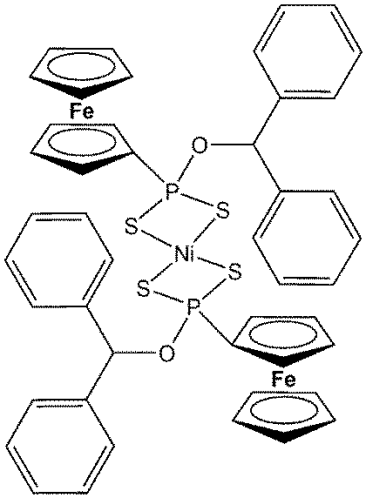

15

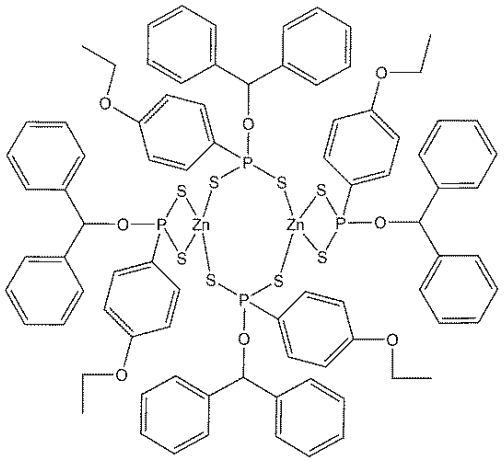

16

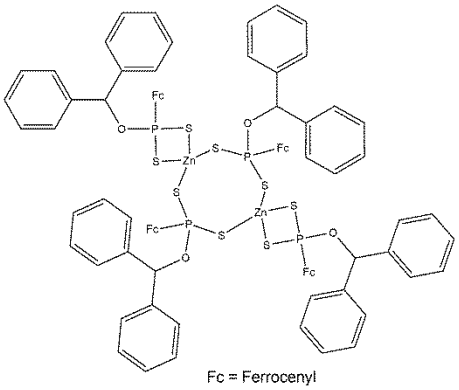

17

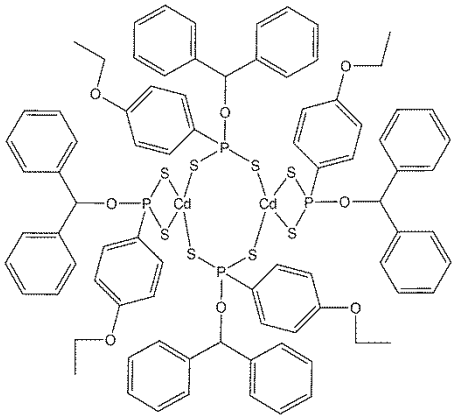

18

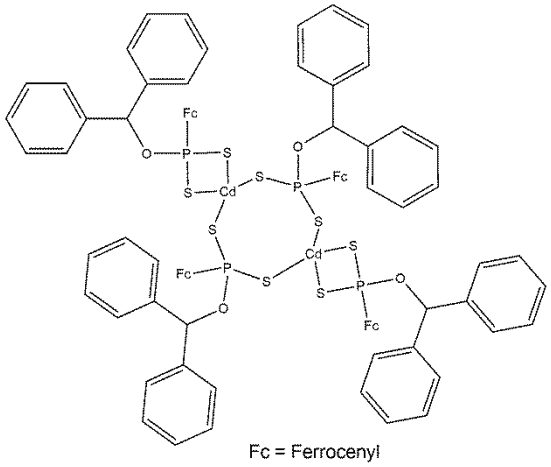
Fc
O
P
S
Cd
Fc = Ferrocenyl

19

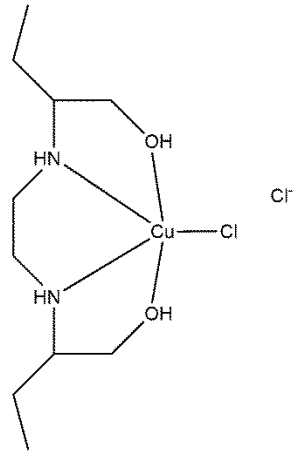
HN
OH
Cu
Cl
Cl-

20

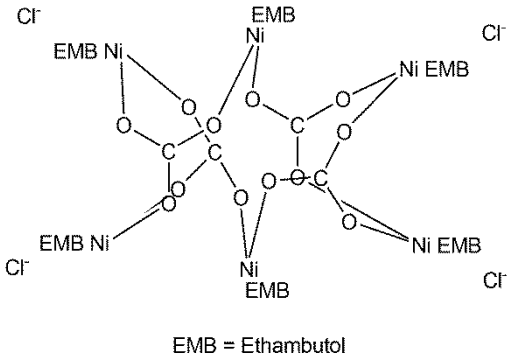
Cl-
EMB Ni
EMB
Ni
Ni EMB
O
C
EMB = Ethambutol

21

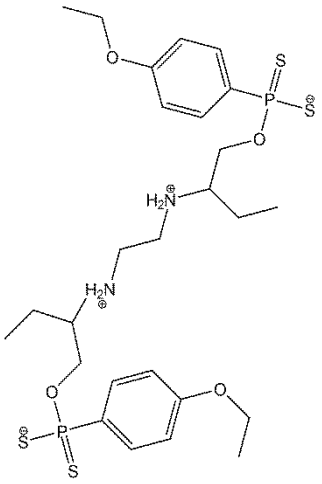
O
S
P
H2N
O

22

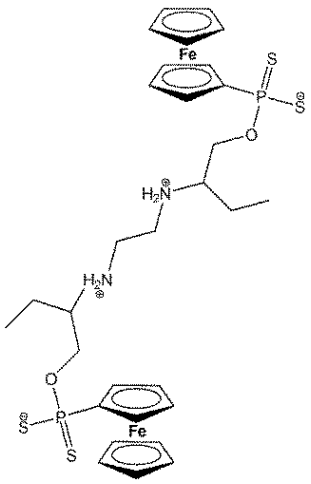

23

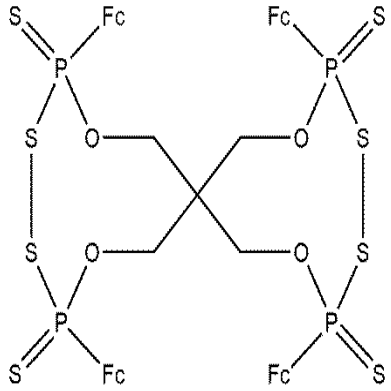

Fc = Ferrocenyl

24

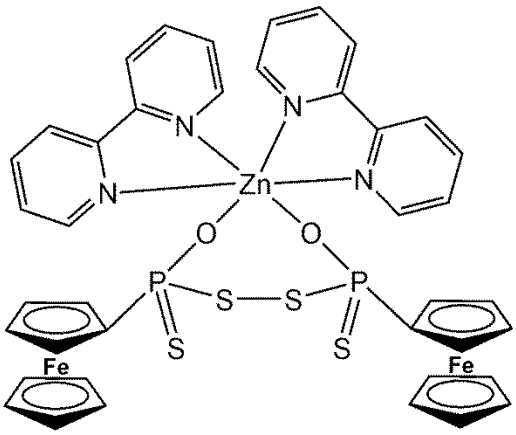

25

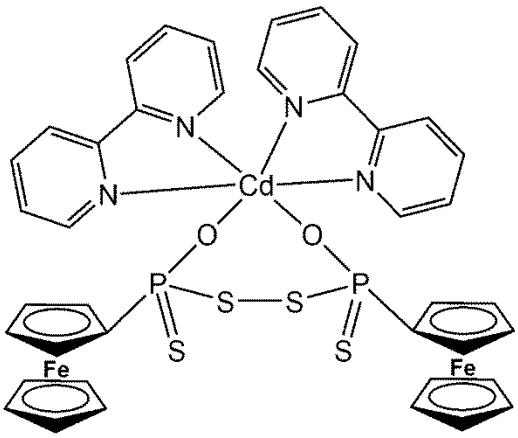

26

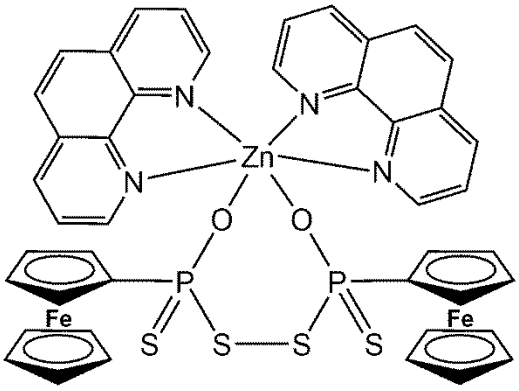

27

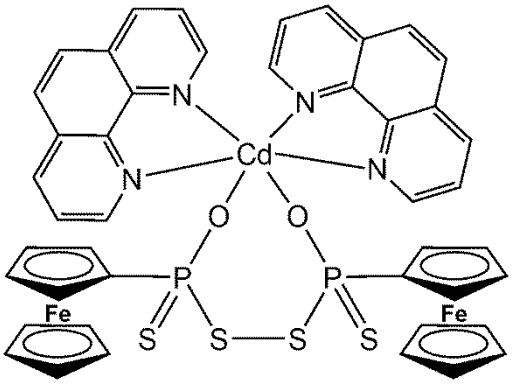

28

ABBREVIATIONS AND SYMBOLS

^{o}C	Degrees Celsius
Å	Ångstrom
MHz	Mega Hertz
cm^{-1}	Wavenumbers
λ	Wavelength
ppm	Parts Per Million
DCM	Dichloromethane (CH_2Cl_2)
THF	Tetrahydrofuran
CH_3CN	Acetonitrile
$CDCl_3$	Deuterated Chloroform
NMR	Nuclear Magnetic Resonance
▪ ^{1}H	Proton Nuclei
▪ ^{13}C	Carbon-13 Nuclei
▪ ^{31}P	Phosphorus-31 Nuclei
▪ s	Singlet
▪ d	Doublet
▪ t	Triplet
▪ quart	Quartet
▪ dd	Doublet Of Doublets
▪ d quart	Doublet Of Quartets

▪ m	Multiplet
FTIR	Fourier Transform Infrared
IR	Infrared
▪ s	Strong
▪ m	Medium
▪ w	Weak
IUPAC	International Union of Pure and Applied Chemistry
PIN	Preferred IUPAC Name
HSAB	Hard and Soft Acid-Base
ORTEP	Oak Ridge Thermal Ellipsoid Plot
DSSC	Dye-sensitized Solar Cells
LR	Lawesson's Reagent
PhLR	Phenetole Lawesson's Reagent
FcLR	Ferrocenyl Lawesson's Reagent
EJ	Exajoules
Fc	Ferrocenyl
EMB	Ethambutol
EMB.2HCl	Ethambutol dihydrochloride

TABLE OF CONTENTS

CHAPTER 1

INTRODUCTION

1.1 OVERVIEW

Thiophosphorus ligands and mixed thio-oxo analogues, as well as dithioarsinates, have been at the center of academic interest for many years.[1] These compounds are versatile ligands, displaying a broad variety of coordination patterns leading to a great diversity of molecular and supramolecular structures.[1] In recent years, the chemistry of compounds containing metal-sulfur bonds has attracted increasing attention.[2] Interest in these compounds has blossomed because they have found use in industry, agriculture, medicine, material chemistry and in other areas.

Scheme 1.1 gives a partial list of sulfur donor ligands that have been used in making several metal complexes which have been the subject of extensive research endeavours. Metal complexes obtained from these bidentate ligands usually have similar electronic properties although their physical properties could vary widely.[1] The focus of this study will be on the dithiophosphonate class of ligand and their metal complexes.

1.2 PHOSPHOR-1,1-DITHIOLATES

The class of compounds phosphor-1,1,-dithiolate is the heavier and "softer" congener of the more common phosphonate derivatives.[3] The S_2P functionality is common to this class of compounds and they can be categorized into several groups like dithiophosphinates, dithiophosphates, dithiophosphonates and amido-dithiophosphonates.

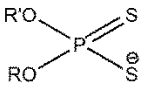

Dithiophosphate
R=alkyl or aryl

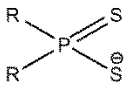

Dithiophosphinate
R= alkyl, aryl or halide

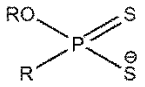

Dithiophosphonate
R=alkyl or aryl

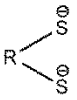

Dithiolate
R= various substituents

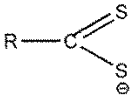

Dithiocarboxylate
R= alkyl, aryl

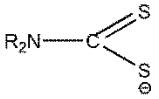

Dithiocarbamate
R= alkyl, aryl

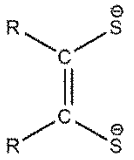

Dithiolene
R= alkyl, aryl, -CN

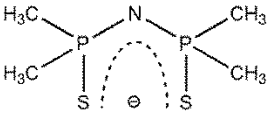

Imidotetramethyldithio-diphosphinate

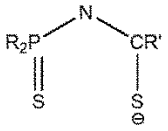

Phosphinoothioyl-thioureas
R= phenyl, R'=alkyl

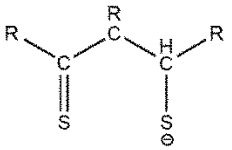

Dithio-β-diketonate
R= alkyl, aryl, H

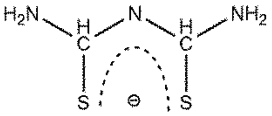

Dithiobiuretate

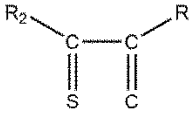

Dithiooxamide
R= alkyl

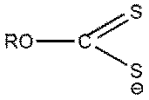

Xanthate
R=alkyl

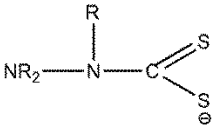

Dithiocarbazate
R= alkyl, aryl

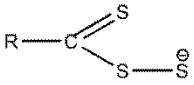

Perthiocarboxylate
R= alkyl, aryl

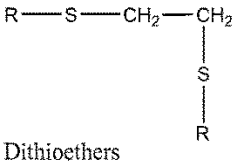

Dithioethers
R= alkyl, aryl and various functional groups

Scheme 1.1: Common sulfur donor ligands.

1.3 DITHIOPHOSPHONATES

The scope and utility of phosphines as a single class of ligand far exceeds others both in organic and inorganic chemistry[4-10] and within this class of ligand the 4-coordinate phosphorus(V) species hold the dubious distinction of being present in systems not only essential to the sustainability of life (DNA, RNA, bone, teeth, etc.) but also as a constituent of the most toxic man-made materials known (nerve gases).[11] The increased air- and moisture stability of metal phosphonates[12] well preceded the isolation and characterization of the heavier metal dithiophosphonates. Unlike the dithiophosphates and dithiophosphinates which have been well studied,[1, 2, 13-17] dithiophosphonates have been scarcely studied until recently. These compounds are hybrid ligands, $S_2PR(R'O)$ (Figure 1.1) of intermediate composition between dithiophosphates $S_2P(R'O)_2$ and dithiophosphinates S_2PR_2. The dithiophosphonate ligand, however, is far less developed but interesting mainly for the following reasons: (i) they can still be considered comparatively rare in the chemical literature and indeed for the majority of main- and transition-metals scarce to non-existent; (ii) the reaction between common dimeric precursors (usually Lawesson's Reagent and its analogues), and any compound that contains a primary or secondary alcohol functionality, a tremendous number of new and varied derivatives can be obtained in a facile manner; (iii) the synthetic methodology allows for control in the design of the ligand (with respect to solubility and materials properties, and steric effects) to perform reactions and yield new products in both organic and also aqueous phases; (iv) the asymmetric nature of the ligand allows for complex isomers to be formed which often impose a unique challenge, a feature not possible for the aforementioned symmetrical ligands; and (v) solution and solid state ^{31}P NMR spectroscopy is a valuable tool to obtain mechanistic and structural information.[3]

1.3.1 NOMENCLATURE

Phosphor-1,1-dithiolate class of compounds are varied and among others include, dithiophosphates, dithiophosphinates, dithiophosphonates and amidodithiophosphonates.

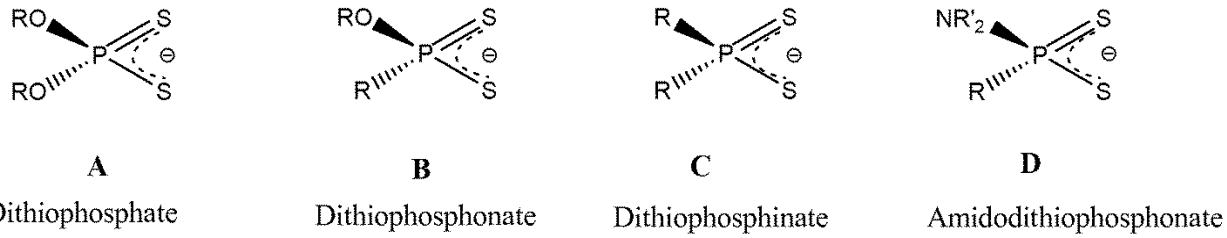

Figure 1.1: Different types of phosphor-1,1-dithiolates.

The dithiophosphonate ligand may be described as a hybrid of the dithiophosphate and dithiophosphinate ligands (Figure 1.1). The nomenclature of metal dithiophosphonates has been applied inconsistently in the open literature. In this respect, phosphonic acid, $HPO(OH)_2$, is the parent acid of the phosphonate anion, $[HPO_3]^{2-}$ from which all dithiophosphonates are derived. The International Union of Pure and Applied Chemistry (IUPAC) standard name for $HPO(OH)_2$ is hydridodihydroxydooxidophosphorus while its common name is phosphonic acid. Preferred IUPAC names (PIN) are commonly used compared to the scientific names giving rise to various nomenclatures for this class of compounds. For example this class of compounds have been called interchangeably as O,O-dialkyldithiophosphonates, O,O'-dialkyldithiophosphonates, O,O-dialkylphosphonodithioate, O,O'-dialkyldithiophosphonates, dithiophosphonates, etc. This then means that as long as there is no ambiguity, the reader being addressed must be considered in the type of nomenclature that is used since no single correct form currently exists.[3] It is also important to note that the 1990, 2001 and 2005 IUPAC recommendation for nomenclature of inorganic chemistry commonly referred to as 'the Red Book' does not give a clear guideline on the naming of a phosphonate derivative containing a phosphorus-carbon bond.[18, 19] The nomenclature of organic chemistry commonly referred to as 'the Blue Book' published in 1979, updated in 1993 and recent draft recommendations of 2004 provides a more useful information with respect to the nomenclature of dithiophosphonates.[20] Going by these recommendations, the acid R(OR')P(S)(SH) is named a phosphonodithoic acid, and anions derived from such acids are named by changing the 'ic'

ending to 'ate', i.e. phosphonodithioate, while neutral salts and esters are both named using the name of the anion derived from the name of the acid.

1.3.2 COORDINATION MODES

The phosphor-1,1,-dithiolate class of ligands can coordinate to virtually all transition metals, giving rise to a variety of coordination patterns.[3] Scheme 1.2 gives a summary of known and potential coordination modes of dithiophosphonate ligands. Coordination patterns and connectivity of metal centers could be mononuclear, dinuclear, trinuclear or tetranuclear. Connectivity here refers to the number of connections between the donating atom of the ligand and the coordinated metal center.[13] These connections are not discriminatory between covalent, dative-coordinate or weak van der Waals interactions.[3]

1.3.3 RESONANCE

Chart 1.1 gives the resonance structure of the dithiophosphonate ligand. The resonance structure of a metal dithiophosphonate complex is predominantly a function of the metal type and its oxidation state.[11] Resonance structures **A** and **B** have been observed in most complexes where the donor atoms of the ligand bind with the metal in a μ_1 – fashion, anisobidentate, with a sulfur atom dangling. Many and Zn(II) Pb(II) and Hg(II), complexes show this resonance structure. Resonance structure **C** is common in many dinuclear Au(I) complexes, as well as in Ni(II) chelating mononuclear complexes. Structure **D** is unknown for metal dithiophosphonate complexes but included here for completeness as the result of a study by Terence and co-workers[21] where a comparison in donor strength between dithiophosphates and dithiocarbamates were made. This resonance structure can however be envisioned alongside **A, B** and **C.** The contrasts between these two dithio-groups was put forward[22] by proposing that the dithiocarbamates, $[S_2C\ NR_2]^-$, having two negative charges on the sulfur atoms, and a positive charge on the nitrogen (related to **C**), gives enhanced electron density on the sulfur atoms while in resonance **C** "the electron density is diminished by back-donation from the sulfur to the 3rd orbitals of the phosphorus." There is thus

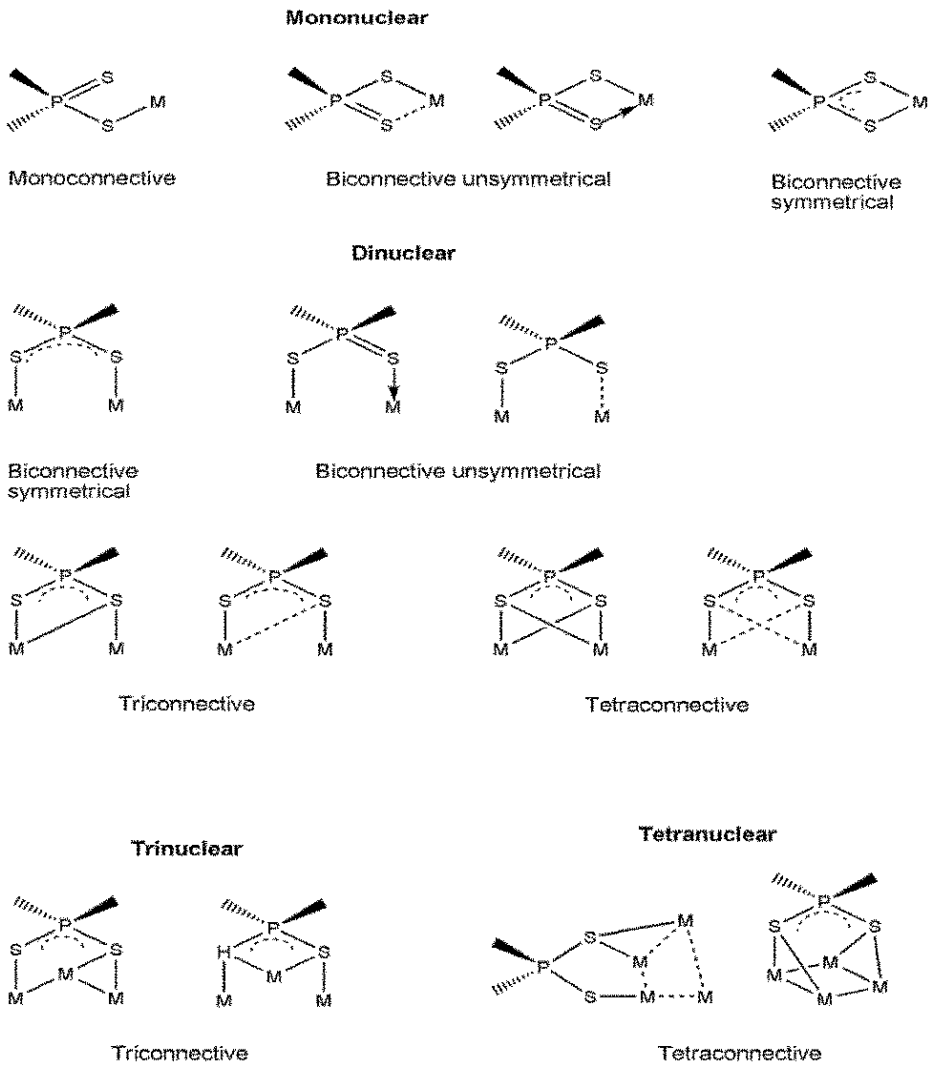

Scheme 1.2: A summary of major known and potential coordination bonding modes of dithiophosphonate ligands.

less covalency in the M-S bond in the dithiophosphates than in the dithiocarbamates, a conclusion in accordance with X-ray photoelectron and UV measurements, as well as quantum mechanical calculations.[3, 21] These resonance structures also play a major part in the description of bonding modes. The slow development of dithiophosphonates as a complexing agent is likely due to its commercial unavailability and sensitivity toward hydrolysis.[3]

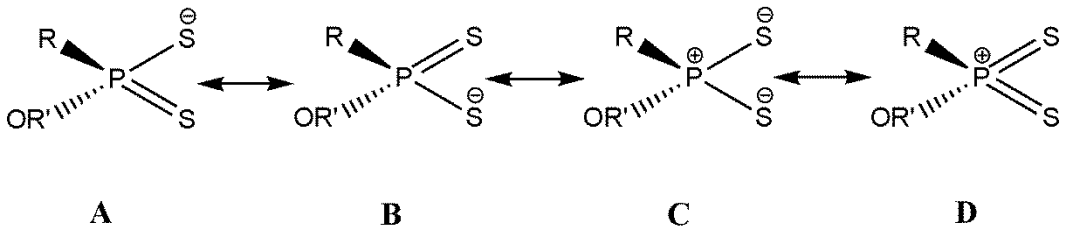

Chart 1.1: Resonance structures of dithiophosphonate ligand.

1.3.4 Disulfides

Oxidation of dithiophosphonate salts, $[S_2PR(OR')]^-$, can be readily achieved with a mild oxidizing agent such as I_2 (with or without activated KI) in aqueous or methanolic solution leading to disulfane products of the type PR(OR')(S)S-SPR(OR')(S) (R = alkyl, aryl).[23] All such S-S compounds are derived from reaction with simple alcohols (MeOH, EtOH, i-PrOH, etc.) and all form intermolecular oxidative couplings because intramolecular bonding was chemically not possible. As early as 1970, the use of diols and polyols were introduced through cumbersome synthesis routes to form disulfides.[24, 25] These compounds can have two dithiophosphonate groups joined by a disulfide bridge (–P–S–S–P–) or have one dithiophosphonate group attached via a disulfide bridge to an organic substituent e.g. an aliphatic or aromatic moiety (–P–S–S–R).[26] Van Zyl and co-workers demonstrated the first structurally characterized intramolecular S-S coupled dithiophosphonates which gave rise to heterocyclic compounds.[23] Figure 1.2 gives the possible geometries of disulfide derivatives of dithiophosphonates. The structural dynamics of these compounds' (S=PSSP=S) geometries has been studied and classified.[27] Three geometries are possible, anti-anti where both S atoms point away from the disulfide bridge; syn-syn where both S atoms point toward the disulfide bridge; and anti-syn which is a hybrid of the other two geometries (Figure 2). Variation in the geometry of the P_2S_4 backbone is a function of several factors like overlapping effect of a filled non-bonding orbital, steric hindrance of bulky substituent groups etc.[27] Some of these compounds have been shown to have very useful application in biological chemistry. Oligo(nucleoside phosphorothioate)s are amongst the most promising of the nucleotide analogues which have been tested

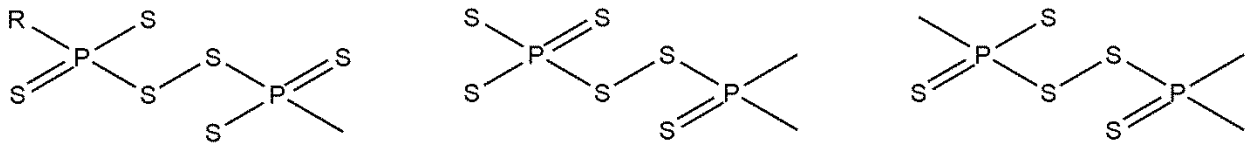

Anti-anti **Syn-syn** **Anti-syn**

Figure 1.2: Possible geometries of dithiophosphonate disulfides.

as antisense modulators of gene expression, bis(O,-O-diisopropoxy phosphinothioyl) disulfide has been shown to be a highly efficient sulfurizing reagent for cost-effective synthesis of oligo(nucleoside phosphorothioate)s.[28]

1.3.5 ZWITTERIONS AND HYDROLYSIS PRODUCTS

Metal complexes of dithiophosphonates are prone to hydrolysis. For example, the reaction between the dithiophosphonato dianion salt, $(NH_4)_2[S_2P(Fc)OCH_2CH_2O(Fc)PS_2]$ and $[Au(PPh_3)Cl]$ yields the complex $[(PPh_3)AuS_2(Fc)P(OC_2H_4O)P(Fc)S_2Au(PPh_3)]$. Van Zyl and coworkers[29] in this study presumed that the moisture content in the DCM solvent used in crystal growth caused the substitution of the terminal P-S bond with P-O bond. There is yet no detailed mechanism for these reactions. Dithiophosphonate zwitterions have been formed from the reaction between amino alcohols or their derivatives and Lawesson's reagent or its ferrocenyl dimer.[30-36] These compounds have been scarcely studied and their molecular structures are rare in literature. Figures 1.3 and 1.4 give the dithiophosphonate zwitterions that have been characterized structurally.

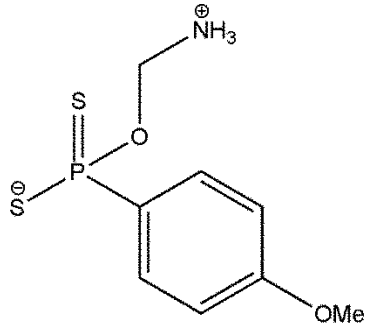

Figure 1.3: A dithiophosphonate zwitterion characterized structurally.

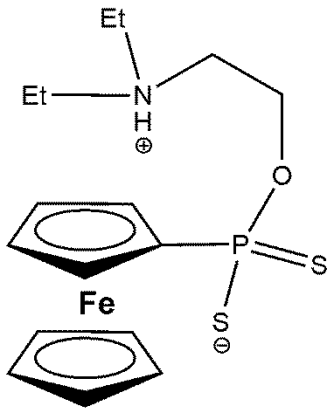

Figure 1.4: A ferrocenyl dithiophosphonate zwitterion characterized structurally.

1.3.6 SYNTHETIC METHODS

It is not clear why the chemistry of the dithiophosphonate ligands were slow to develop compared to that of the dithiophosphates and dithiophosphinates. Commercial unavailability of key starting materials, inherent reactivity (especially susceptibility toward hydrolysis), and the potential toxicity of these compounds and its derivatives, is not much different when compared to the well-established dithiophosphates and dithiophosphonates.[3] The reaction of phosphorus and sulfur dates back centuries. Marggraff reported a fused mixture of phosphorus and sulfur which was distilled as early as in 1740.[37] Berzelius followed up on the study and used white phosphorus and sulfur to synthesize tetraphosphorus decasulfide, P_4S_{10}, by 1843.[38] P_4S_{10}, a malodorous, pale yellow and crystalline solid played a crucial role in the development of the dithiophosphonate chemistry.[3] Vos and Wiebenga[39] obtained the correct structure of P_4S_{10} in 1954 after Mai[40] and Treadwell along co-workers[41] had proposed structures for the

compound. The ^{31}P NMR spectrum of solid P_4S_{10} shows a singlet at 45 ppm (relative to 85% H_3PO_4 (aq)), indicating that all phosphorus nuclei are chemically equivalent.[42] P_4S_{10} have been at the center of many thionation reactions. For example, aromatic hydrocarbons including anisole, phenetole, xylene, naphthalene and thiophene[43] react with P_4S_{10} to form 1,3-dithiadiphosphetanes.[3] Crystalline products of the general formula $[RP(S)S]_2$ have been synthesized from the reaction between P_4S_{10} and aliphatic[44] or aromatic[45] hydrocarbons. Kekule and Liebigs[46] reported the most efficient way to prepare diethyldithiophosphoric acid which was obtained from the reaction between P_4S_{10} and ethanol. This reaction could explain why the dithiophosphate chemistry developed much better compared to that of dithiophosphonates considering also the background that the dithiophosphonates suffered synthetic difficulties in its early stage of development. Pizzotti and Malatesta in 1945 reported a dimeric Ni(II) dithiophosphonate complex, probably the first metal dithiophosphonate complex[47, 48] in a synthetic route difficult to reproduce.[49]

The conversion of ketones to thiones to form dimers of the type $[RP(\mu\text{-}S)S]_2$ (R = aryl) was reviewed in 1965[50] and later in 1980[51] and was pivotal to the development of dithiophosphonate chemistry. Though the procedure was not facile, the phenyldimer of the type $[RP(\mu\text{-}S)S]_2$ were first prepared and characterized in 1962.[52, 53] This procedure is also based upon the reaction between $P(S)PhCl_2$ (liquid) and anhydrous H_2S (gas) introduced subsurface at elevated temperatures (>210 °C) with the release of large quantities of corrosive HCI as a by-product[54] as shown in Figure 1.5.

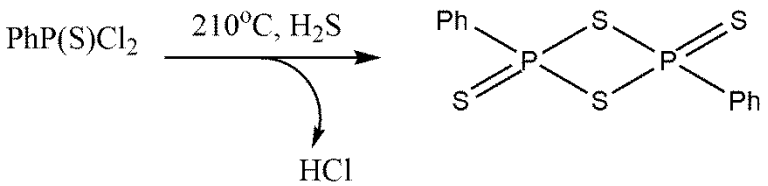

Figure 1.5: Synthesis of the phenyl-dimer $[PhP(\mu\text{-}S)S]_2$.

The analog selenium dimer $[PhP(\mu\text{-}Se)Se]_2$ known as Woollins' Reagent (WR) available commercially is not prepared in a similar manner as the sulfur analog. The chemistry of WR has been described by Woollins[55] who first made it and the dimer's selenation properties are well known.[26, 56-58] The synthesis of the first stable metal dithiophosphonate complex had been described from reaction between RPR_1R_2 [R = 2,4,6-$(Me_3C)_3C_6H_2$; $R_1 = R_2 = H$; $R_1R_2 = CHNMe_2$] with S to give RP(S)(S), which gave RP(OMe)(S)(SH) on treatment with MeOH.[59]

A significant improvement in the synthesis method of dithiophosphonates came in 1978 when Lawesson and co-workers reported[60] reported the reaction between the electron-rich anisole (phenetole is a useful alternative) and P_4S_{10} which leads to the formation of the dimer 2,4-bis(4-methoxyphenyl)-1,3-dithiadiphosphetane-2,4- disulfide, $[(4\text{-}MeOC_6H_4)P(\mu\text{-}S)S]_2$. In the synthesis of this dimer commonly known as Lawesson's Reagent (LR) and commercially available, anisole served as the "solvent" and the reactant which is convenient compared to earlier synthetic methods. The chemistry of LR as a thionation agent is well reported[61-64] and has been reviewed.[65-68] Woollins and co-workers demonstrated that ferrocene, as an electron-rich organometallic with aromatic properties, can replace anisole or phenetole and form the related $[FcP(\mu\text{-}S)S]_2$ or FcLR (Fc = ferrocenyl) type dimer. The FcLR dimer has been used to furnish dithiophosphonate metal complexes with the electron rich ferrocenyl substituent which in turn produces complexes with interesting electrochemistry. FcLR dimer has also been used to form novel 1,2 thiaphosphetanes,[69] P-S-N-type heterocycles[70, 71] and cycloaddition reactions with dienes, alkenes, and thioaldehydes.[72] Figure 1.6 gives a synthesis methodology used in forming these dimers and subsequent ligands.

1.3.7 SPECTROSCOPIC CHARACTERIZATION

NMR spectroscopy has been extensively used for the characterization of dithiophosphonates and for the elucidation of some structural details e.g. molecular conformations. Solution and CP MAS ^{31}P-NMR

spectroscopic studies data have also been correlated with X-ray diffraction structure determination. Van Zyl and co-workers used CP MAS ^{31}P-NMR to propose that the configuration of their gold(I) compounds which were isomers, both in solution and solid state.[23] The ^{31}P NMR spectra of the ammonium salts of dithiophosphonates all resonate with a singlet peak in the approximate range of 90 to 112 ppm (relative to 85% H_3PO_4).[54] Karakus reported lower ^{31}P-NMR pair of values of 72.2 /71.9 ppm and 68.1/67.4 ppm for the neutral and zwitterionic forms of amidodithiophosphonates.[73] Hey-Hawkins and co-workers also reported similar ^{31}P NMR values of 78.7/65.3, 93.1/55.8 and 86.5/65.2 ppm for ferrocenyl amidodithiophosphonates.[74] Vibrational (infrared and Raman) spectroscopy was more popular in the earlier years as a characterization tool.[75]

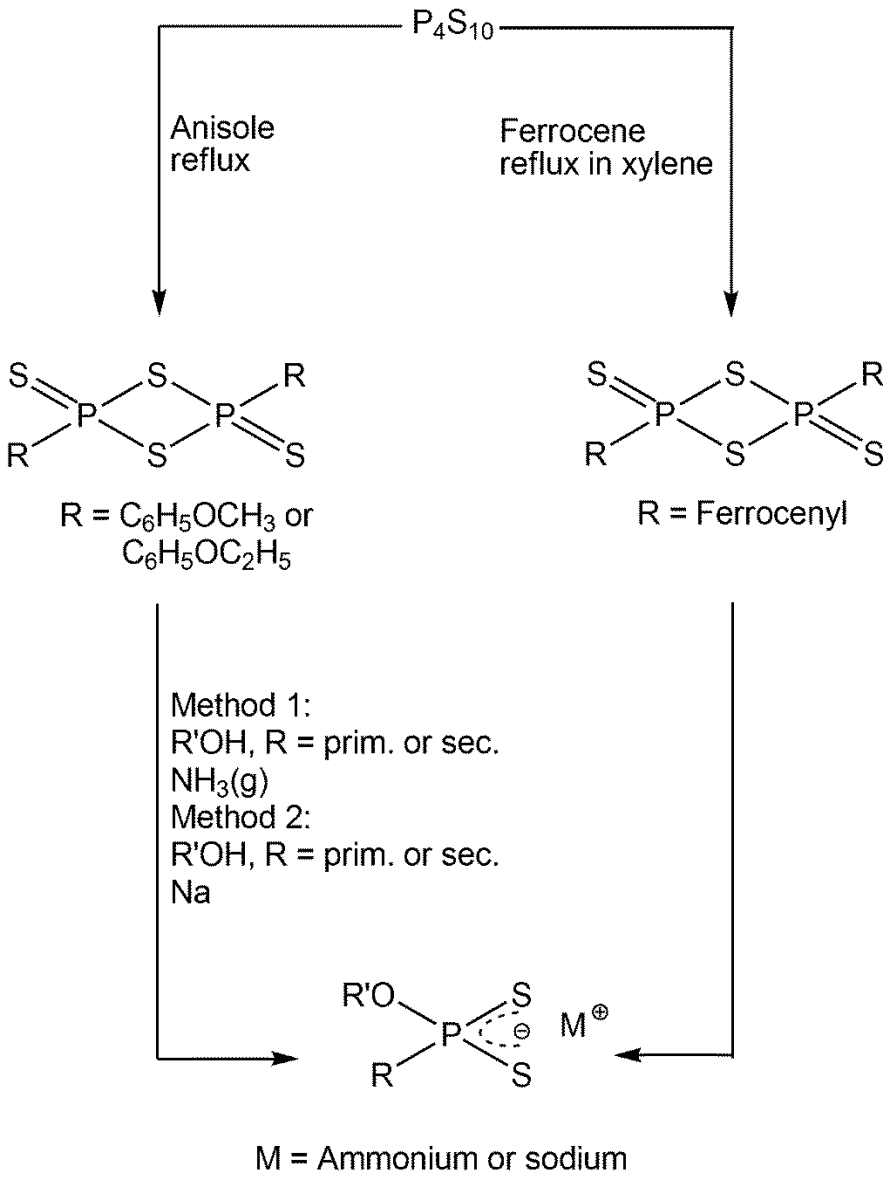

Figure 1.6: Summary of synthesis methodology in forming either sodium or ammonium dithiophosphonate salts.

1.3.8 APPLICATIONS

Thiophosphorus ligands and their metal complexes have found widespread use, not only in basic academic research, but also in industry, agriculture and medicine. Industrially they have been used as anti-oxidant additives in the oil and petroleum industry.[76-78] Zinc diakyldithiophosphates have found

application for many years as anti-oxidant and anti-wear additive in the petroleum industry and have been severally reviewed.[78-81] These complexes have also found use in the industry as metal ore extraction reagents and flotation agents in the mining sector.[82] Studies have also demonstrated that these compounds are useful for agricultural purposes especially as pesticides and insecticides.[83, 84] Metal complexes of these ligands have also shown biological activity.[85]

1.3.9 METALS USED IN THIS STUDY

1.3.9.1 Nickel

A search of literature indicates that the Ni(II) dithiophosphonate complex, [Ni{S_2PPh$(OEt)_2$], reported by Hartung[86] in 1967 is probably the first Ni(II) complex characterized structurally. Many other complexes of Ni(II), neutral and mononuclear have been reported.[26, 87-90] Dinuclear dithiophosphonate Ni(II) complexes have also been reported[91] using diol starting materials. Most of these Ni(II) complexes obtained using LR can be furnished with the ferrocenyl moiety by replacing LR with FcLR.[92, 93] N-donor ligands like bipyridine or pyridinyl-1,4 diamine can be used as linkers in Ni(II) dithiophosphonate complexes to form 6-coordinate polymers.[94] Figure 1.7 gives an interesting aspect of these polymeric complexes where the N-donor linkers are tri sulfides.

One of the key features of the dithiophosphonato ligand is that they are not symmetrical, and as a result can give rise to isomers.[3] The majority of Ni(II) dithiophosphonate complexes exhibit the square planar geometry with either the *trans* configuration in which the ferrocenyl or aromatic groups are above and below the square plane or the *cis* configuration where these groups are on the same side of the plane. The *trans* isomer is formed in most cases compared to the *cis* configuration.

In a rare case, the P–N bond hydrolysis of 4-methoxyphenyl-ammonium ethylamido-phosphonodithionato ligand during its

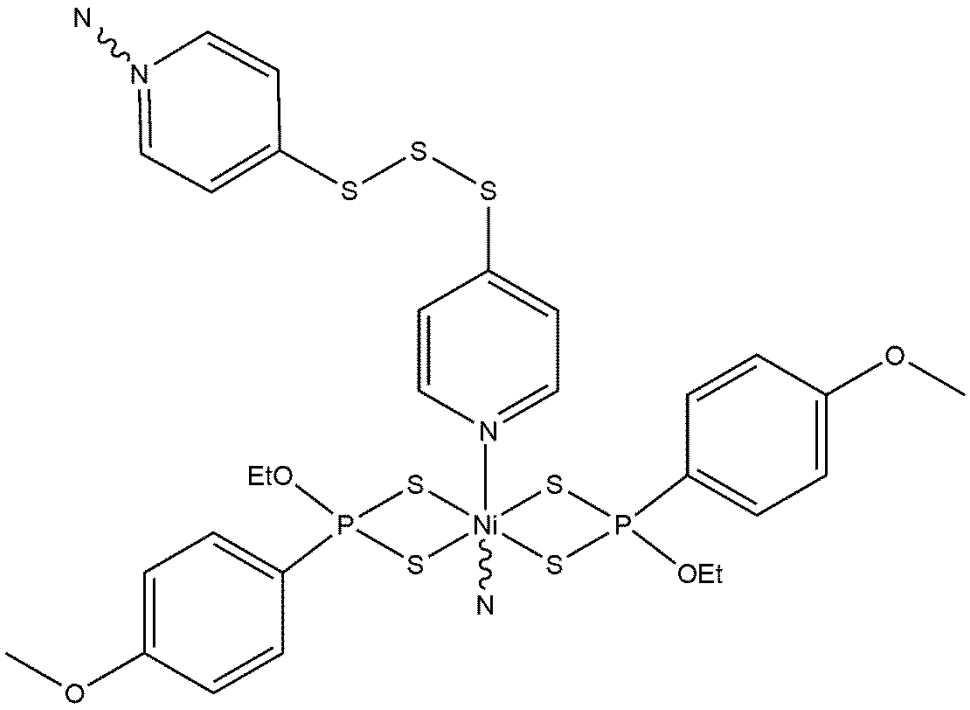

Figure 1.7: A 6-coordinate Ni(II) polymeric complex containing a pyridyl-trisulfide linker.

complexation to Ni(II) led to the first example of phosphonodithioato nickel(II) complex having a *cis* configuration.[95] This complex was reported to be stabilized in the solid state by an extensive and intricate network of hydrogen bonding involving the released ethylenediamine and a water molecule. Isomerization of *cis* and *trans* forms of Ni(II) dithiophosphonates have been demonstrated[96] as shown in Figure 1.8.

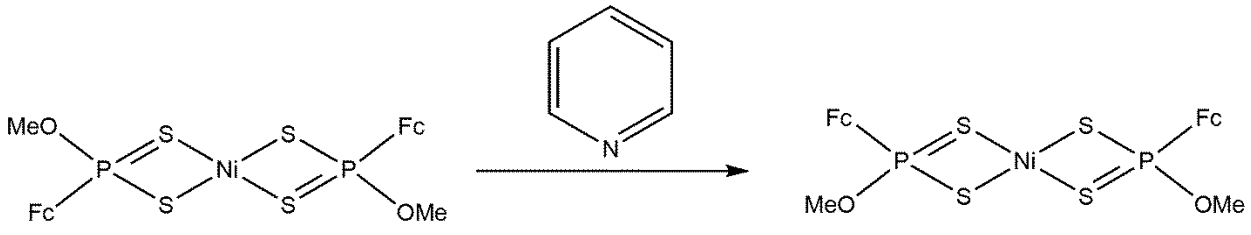

Figure 1.8: Cis/trans isomer interconversion in a square planar Ni(II) complex.

Ni(II) complexes that are 6-coordinate of the type [Ni{$S_2PAr(OMe)\}_2(py)_2$] have also been formed with the addition of the N-donor linker, pyridine to a *trans*-[Ni(II)] complex.[97, 98] Smith and co-workers[99] reported a heterometallic (Ni/Re) luminescent complex in 2010 as shown in Figure 1.9.

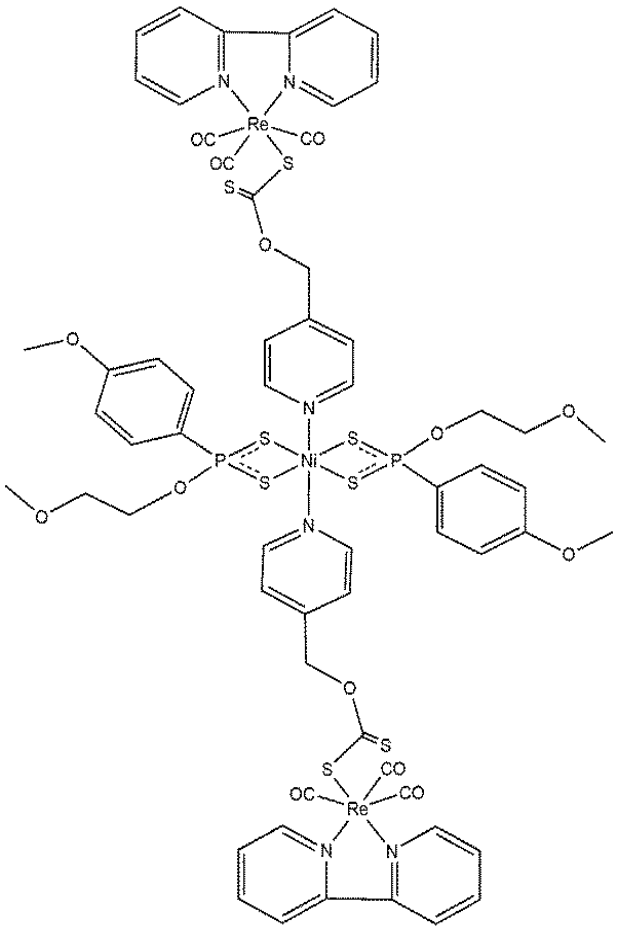

Figure 1.9: A luminescent hetero-metallic Ni/Re complex.

Although the majority of Ni(II) dithiophosphonate complexes reported are mononuclear, there has been one interesting case of a tetranuclear Ni(II) complex[100] (Figure 1.10).

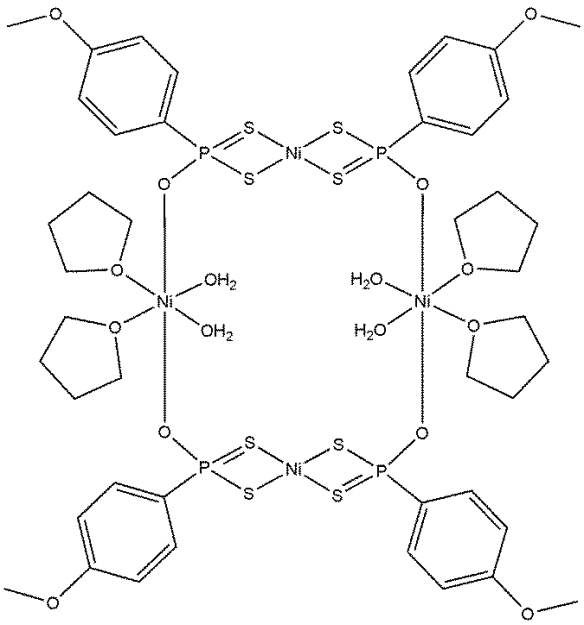

Figure 1.10: A tetra-nuclear Ni(II) complex containing 4- and 6- coordination metal centers.

1.3.9.2 Zn and Cd

The complexes of Zn(II) dithiophosphonates reported to date are structurally remarkably similar and all are 4-coordinate and dinuclear in nature with one ligand S-P-S chelating and the other bridging through the S atoms.[3] Figure 1.11 shows a typical 4-coordinate Zn(II) dithiophosphonate complex. A variety of these complexes have been obtained by use of different simple alcohols and thionation reagents like LR,[91, 92, 101, 102] PhLR[103] and FcLR.[96] The P-S bond lengths in all cases vary by a small but discernible amount i.e. 2.00 and 2.02 Å, the Zn-S bond lengths vary between 2.32 and 2.43 Å for the chelating ligand and between 2.31 and 2.36 Å for the bridging ligand, clearly indicative of an aniso-bidentate bonding mode in all cases.[3] Hursthouse and coworkers reported a rare case of a Zn(II) mononuclear coordination polymer containing two monoconnective S-bound moieties as well as a derivatized bipyridine ligand.[104]

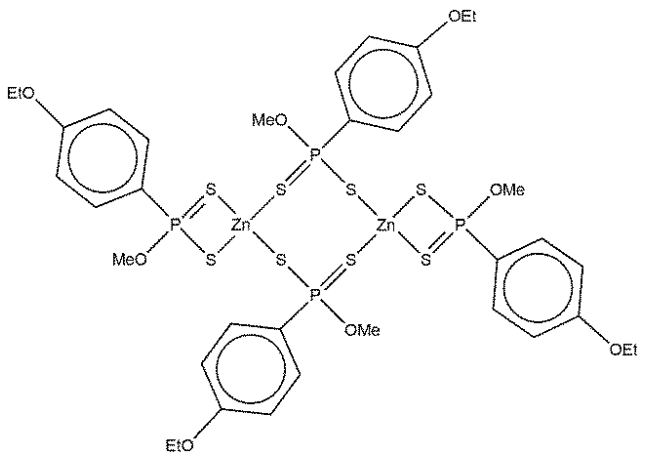

Figure 1.11: A typical example of a 4-coordinate Zn(II) dithiophosphonate complex.

Cadmium dithiophosphonate complexes are closely related to the zinc(II) complexes being dinuclear, but because of the bigger atom size, the metal can accommodate larger coordination numbers.[3] Most of these cadmium complexes are 5-coordinate[102, 105, 106] though 4-coordinate[96] complexes have been reported too. There are also rare examples of mononuclear 6-coordinate polymeric complexes containing dipyridine derivatives.[107, 108]

1.4 ETHAMBUTOL

1.4.1 INTRODUCTION

Ethambutol (EMB) is a symmetrically substituted ethylenediamine [N,N'-bis(1-hydroxy-2 butyl)-ethylenediamine**]** and can be synthesized in three isomeric forms having absolute configurations *R,R,* S,S, and *R,S* at the asymmetric carbons.[109] The *S,S* enantiomer is therapeutically active, unlike the *R,R,* and is used as a drug for tuberculosis. EMB (Figure 1.12) is formulated as the dihydrochloride salt (EMB.2HCl) which is synonymous with the drug.[110-112] This is to minimize the effect of hygroscopicity which leads to the gradual loss of potency of the drug.[110, 111] Cherukuvada and Nangia screened the anti-tuberculosis chiral basic drug with protic acids resulting in the formation of several salts and an ionic liquid which did not show significant improvements in solving the hygroscopicity problem.[113]

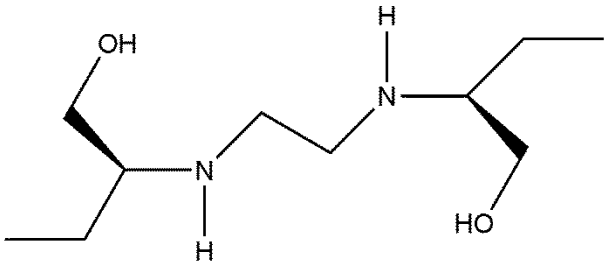

Figure 1.12: Structure of ethambutol.

EMB.2HCl is a white, crystalline powder that is readily soluble in water and dimethyl sulphoxide.[114] The pKa values of the drug have been reported to be 6.3 and 9.5.[110] EMB is the first-line anti-tuberculosis drug administered with Rifampicin, Isoniazid and Pyrazinamide in Fixed Dose Combinations (FDC).[115] In FDC, two or more drugs desired are formulated into a single one. These combination drugs complement each other preventing the emergence of drug resistance in organisms, hence resulting in effective treatment.[115] The free base (EMB) can easily be obtained from the salt (EMB.2HCl).

1.4.2 ETHAMBUTOL AS A THERAPEUTIC DRUG

EMB is a synthetic antimyco-bacterial agent introduced in 1961 as a treatment for patients with tuberculosis (TB).[116] TB has become a worldwide problem stemming from the contagiousness of the disease that is transmitted through the air. It is caused by the bacterium *Mycobacterium tuberculosis*, which can attack different parts of the human body. The first line TB treatment is based on four drugs: isoniazid, rifampicin, pyrazinamide and ethambutol which are available in cheap generic forms and are effective if taken as prescribed.[117]

This drug has a mode of action like many antituberculosis drugs, and is not completely understood.[114] It has been suggested that the drug has the ability to fit a specific enzyme receptor which may account for the structural and stereoisomeric selectivity of the antimycobacterial activity for these diamines. It is also believed that EMB can increase the effectiveness of other antibacterial drugs, such as spermidine, mycolic

acids and arabinogalactin, which through biosynthetic inhibition specifically alter the mycobacterial cell wall.[114] EMB affects primarily the biosynthesis of arabinan in the arabinogalactan (AG) and sequentially lipoarabinomannan (LAM) cell wall of M. tuberculosis. Its targets might possibly be arabinosyl transferases involved in the biosynthesis of AG and LAM.[118]

EMB platinum complexes have also been reported to show anti-cancer activity. The degree of rotational freedom of a coordinated platinum amine complex plays a key role in its potency as an anti-cancer drug.[119] For example, Pt(II) complexes with monodentate enantiomeric primary amines do not show significant differences in their biological activity.[120] A Pt(II) complex of phenethylamine is an example of this class of compounds (Figure 1.13).

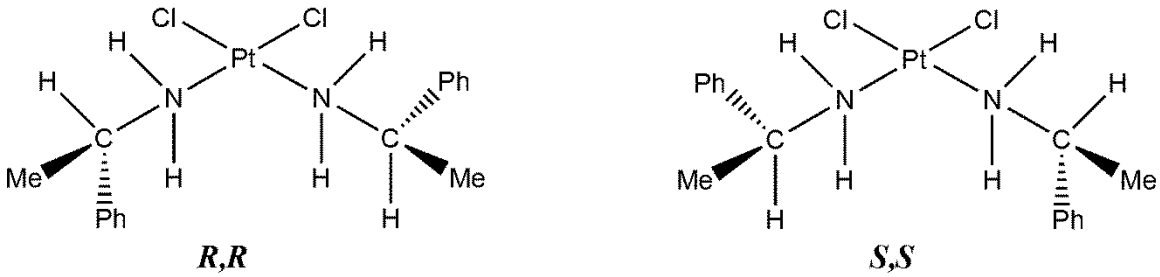

Figure 1.13: Example of the Pt(II) complex with monodentate enantiomeric primary amines.
Ph = phenyl.

Natile and coworkers reported that the biological inactivity of these complexes could possibly be due to the free rotations of the chiral substituents around the carbon–nitrogen (C—N) bond and of the amine around the Pt—N bond. The free rotations average the steric effect due to the ligand asymmetry and offset any stereospecificity in the interaction with biological substrates.[119] The degree of rotational freedom in a complex can be reduced by bridging together the two N of the *cis* amines. EMB is a good example of this kind of an amine[119] (figure 1.14).

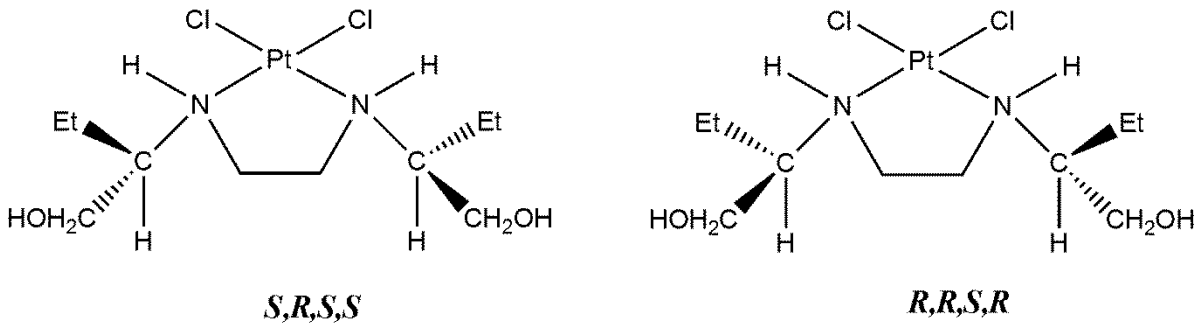

Figure 1.14: Structures of enantiomeric forms of [$PtCl_2$(ethambutol)]. Et, ethyl.

The far less rotational freedom of the asymmetric substituents in these complexes leads to biological activity for the two enantiomers. They exhibit good antitumor activity toward P388 sarcoma and Lewis lung carcinoma.[121]

This study report, in chapter 7, the antimicrobial susceptibility screenings of selected complexes made in this study including coordination complexes of ethambutol reported in chapter 4.

1.4.3 COORDINATION METAL COMPLEXES OF ETHAMBUTOL

In the course of screening randomly selected synthetic compounds, Karlson[122] reported in 1961 that EMB was effective in the treatment of TB in infected guinea pigs. Unfortunately, it soon became apparent that EMB treatment was associated with ocular toxicity. For example, Henkind and Carr[123] reported in 1962 that 8 out of the 18 patients that received 60-100 mg/kg body weight per day of EMB suffered from 'toxic amblyopia.' It was noted, however, that this ocular toxicity improved on cessation of the drug. This gave good indication that the drug (EMB) could be chelating essential elements in the body. EMB has four sites (2 NHs and 2 OHs) that it can potentially be used in forming coordination complexes. Spectroscopic studies have also revealed that ethambutol can form chelates with metal ions.[124] Studies on metal complexes of ethambutol are largely limited to copper[125-127] with isolated reports on other metals like Zn, Pt,[119] Co and Ni.[114] To the best of our knowledge only the Cu ethambutol complex molecular structure[117] has so far been reported (Figure 1.15).

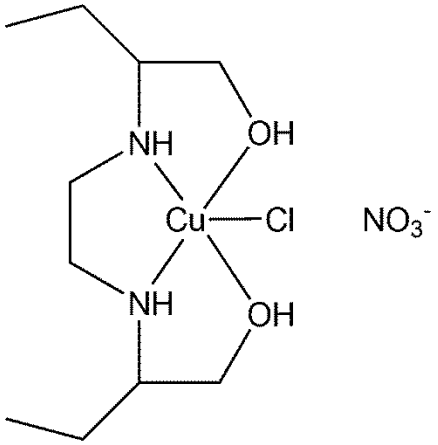

Figure 1.15. Structure of reported Cu-EMB complex.

1.5 DYE SENSITIZED SOLAR CELLS (DSSCs)

It is clear that access to economically viable renewable energy sources is essential for the development of a globally sustainable society.[128] The growing concern about sustainable energy is important considering the increase in energy consumption of our planet which has accelerated the depletion of the earth's oil reserves, leading to environmental contamination and the greenhouse effect.[129] The continued use of fossil fuels cannot be a long-term solution as they come from a limited stock and the deleterious environmental consequences of their combustion have become self-evident.[130] Currently, worldwide concerns of such problems significantly spur the technological endeavor of renewable and green energy.[129] For example the European Union (EU) and the American Recovery and Reinvestment Act in the United States has set goals in clean energy development aiming to reduce greenhouse gas emission by 2020.[131, 132]

Among all the renewable energy forms, solar energy has showed that it holds the key in its potential for power generation. Solar radiation amounts to 3.8 million EJ/year, which is approximately 10,000 times more than current energy needs.[133] The sun is the one source that on its own could supply the world's projected energy demand and in a sustainable fashion too.[134] To put it in perspective, the amount of solar energy reaching the earth in one day could power the planet for an entire year.[135] From the perspective of energy conservation and environmental protection, it is desirable to directly convert solar radiation into electrical power by the application of photovoltaic devices.

The development of dye-sensitized solar cells (DSSCs) based on nanocrystalline TiO_2 thin films by O'Regan and Grätzel and co-workers[136] have attracted considerable attention in the field of photovoltaics.[137-143] This interest stems from the ability of these systems to convert the freely and abundantly available sunlight into the desired electrical energy with low fabrication cost compared with conventional silicon-based solar cells.[136] The major hurdle facing chemists however are how to improve cell efficiency so that these devices can replace conventional Si-based solar cells. The operational principle of the DSSC is given in Figure 1.16. The operational principle can be summarized in the steps given below as outlined by Sumathy and coworkers in 2012.[129]

I. a transparent anode made up of a glass sheet treated with a transparent conductive oxide layer;
II. a mesoporous oxide layer (typically TiO_2) deposited on the anode to activate electronic conduction;
III. a monolayer charge transfer dye covalently bonded to the surface of the mesoporous oxide layer to enhance light absorption;
IV. an electrolyte containing redox mediator in an organic solvent effecting dye-regenerating; and
V. a cathode made of a glass sheet coated with a catalyst (typically platinum) to facilitate electron collection.

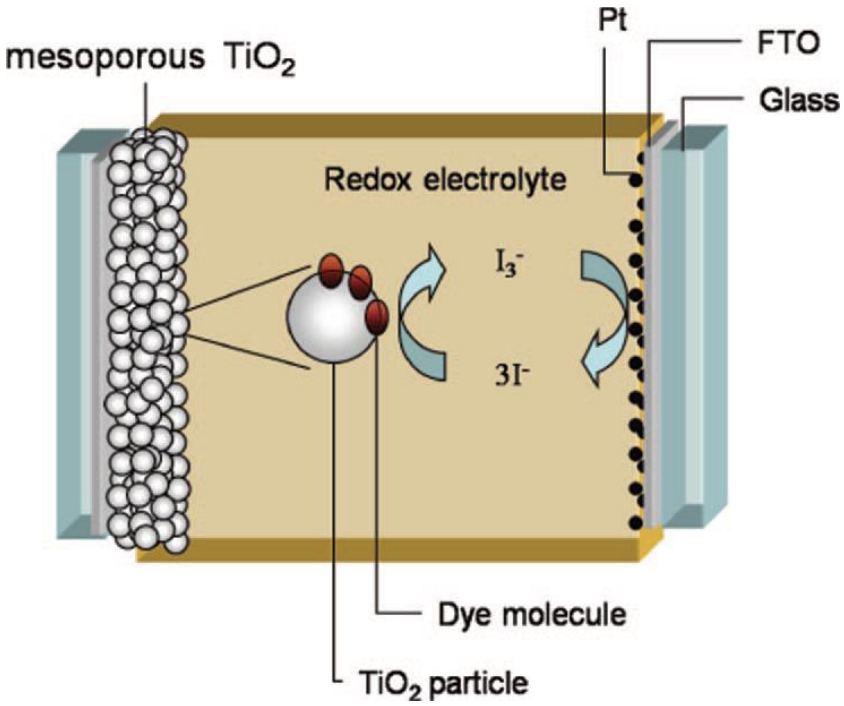

Figure 1.16: Schematic diagram of the dye-sensitized solar cell, DSSC.[128]

A conducting glass which enhances electrical conductivity and light transmittance is used as the substrate. The most commonly used substrate is glass coated with fluorine-doped tin oxide (FTO) or indium-doped tin oxide (ITO). The criteria to select a proper type is sometimes not straightforward because of the variety of cell configurations and materials.[129] The semiconductor electrode is usually a layer of nanocrystalline titanium dioxide (TiO_2), a thin film deposited on the conducting glass film with the thickness ca. 5–30 mm, which plays an important role in both the exciton and the electron transfer process. The porosity and morphology of theTiO_2 layer are dominant factors that determine the amount of dye molecules absorbed on its surface which can provide an enormous area of reaction sites for the monolayer dye molecules to harvest incident light. A large number of artificial dye molecules have been synthesized since the first introduction of dye-sensitized solar cells and some of them have already been successfully commercialized such as N3, N719 and Z907. In this study the state of the art dye N719 (Figure 1.17) was used as a sensitizer. Desirable dye molecules have to meet certain criteria, such as provide a proper match with the solar spectrum, long-term operational stability, and firm graft onto the

semiconductor surface. In addition, their redox potential should be high enough to facilitate the regeneration reaction with a redox mediator.[128]

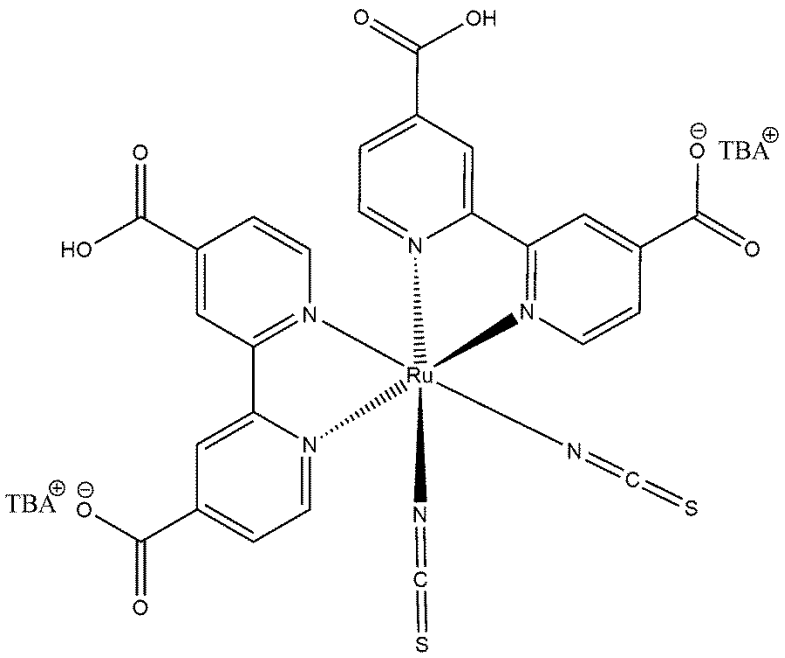

Figure 1.17: The chemical structure of the N719 dye ($TBA^+ = {}^+N(C_4H_9)_4$).

When exposed to sunlight, the dye sensitizer absorbs light to form a molecular excited state which can inject an electron into the conduction band of mesoporous TiO_2. The excited electrons injected into the mesoporous layer can diffuse to the anode and be utilized by an external load. The photo-excited molecules of the dye sensitizer are in an unstable oxidized state and are restored to the stable ground state by electron transfer from the electrolyte, typically an organic solvent containing the iodide/triiodide redox system (Figure 1.16). The regeneration of the sensitizer by iodide intercepts the recapture of the conduction band electron by the oxidized dye. The I_3^- ions formed by oxidation of I^- diffuse a short distance (<50 μm) through the electrolyte to the cathode, which is coated with a thin layer of platinum catalyst, where the regenerative cycle is completed by electron transfer to reduce I_3^- to I^-.[128]

Typical materials and relative concentrations of the different species used in the mesoporous system under normal working conditions are summarized below in a study by O'Regan and Durrant.[144]

- Under working conditions, there are about 10 electrons per TiO_2 particle.
- More than 90% of electrons in TiO_2 are trapped and <10% are in the conduction band.
- There are ~10 000 adsorption sites for H^+ on an 18 nm (diameter) TiO_2 particle.
- A TiO_2 particle (18 nm) has ~600 dye molecules on the surface.
- Each dye molecule absorbs a photon once per second.
- The flux of electron injection into the TiO_2 particle is ~600 s^{-1}.
- Under working conditions, about 1 dye per 150 TiO_2 particles is in its oxidized state.
- The total volume fraction of the solutes in the electrolyte is ~10-20%.
- In the pore volume around the TiO_2 particle, there will be ~1000 I^- and 200 I_3^- ions.
- The concentration of iodine, I_2, is <1 μM, that is, about one free iodine per 10 000 TiO_2 particles.

One of the problems complicating the use of DSSCs is low conversion efficiencies compared to Si based solar cells which are widely in use commercially. For example, conversion efficiencies of about 26% have been achieved in a study by Yamamoto and colleagues[145] in 2017 using Si based solar cells while Hanaya and collaborators[146] reported conversion efficiencies of about 14% in 2015 using silyl-anchor and carboxy-anchor dyes as co-sensitizers. Co-sensitization is one of the strategies employed by chemists to solve the problem of low conversion efficiencies so that the DSSC can replace the Si based solar cells. Co-sensitization involves the use of a combination of two or more dyes on the same semiconducting film, which can extend the light-harvesting spectrum of the cells and can in turn increase the photocurrent of the device.[147] Different materials have been used as co-sensitizers in various studies[138, 146-153] including metal–organic complexes[147, 154-159] containing d^{10} transition metals to improve DSSC performance. Literature survey indicates that dithiophosphonates have so far not been employed as sensitizers or co-sensitizers in DSSC.

Considering this background, this study reports in chapter 7, Zn(II) and Cd(II) dithiophosphonates as co-sensitizers (N719 dye used as a sensitizer) in DSSCs.

1.6 AIMS AND OBJECTIVES OF THIS STUDY

The study aims were as follows:

1. Synthesis and characterization of new dithiophosphonate salts, to be used as ligands.
2. Synthesis and characterization of new Zn(II), Cd(II), Ni(II) dithiophosphonate complexes.
3. Synthesis and characterization of Ni(II) and Cu(II) coordination complexes of ethambutol.
4. Investigation of light harvesting properties of selected complexes in dye sensitized solar cells.
5. Investigation of antimicrobial susceptibility screenings of selected complexes.

The aims of this study were achieved by meeting the following objectives:

- Synthesis of new dithiophosphonate ligands using pentaeryhritol (tetraol), diphenylmethanol (aromatic alcohol) and ethambutol (TB drug).
- Synthesis of new dithiophosphonate Zn(II), Cd(II), and Ni(II) complexes using above ligands.
- Synthesis of Ni(II) and Cu(II) coordination compounds of ethambutol.
- Characterization of all new complexes by NMR (^{1}H, ^{31}P, ^{13}C), FTIR and mass spectroscopy and melting points.
- Characterization by X-ray crystallographic analysis of selected complexes.
- Investigation of optical properties (solid state luminescence and UV) of selected complexes.
- Investigation of light harvesting properties of some dithiophosphonate complexes synthesized.
- Anti-microbial susceptibility screenings of synthesized complexes.

1.7 OVERVIEW

This thesis is divided into 8 chapters as outlined below:

Chapter 1 provides a broad literature survey of this study beginning with an overview that highlights a wide range of sulfur donor ligands that have been studied. The survey also looks at phosphor-1,1-dithiolates generally and narrows it down to the central focus of this study, the dithiophosphonates. This chapter also reviews the nomenclature, coordination modes, resonance, disulfides, zwitterion and hydrolysis products, synthetic methods, spectroscopic characterization and applications of dithiophosphonates. Ethambutol as a therapeutic drug and its coordination compounds as well as metal complexes relevant to this study that have been studied, were also surveyed. This chapter concludes by reviewing dye sensitized solar cells as cheap and simple alternatives to other power sources and its working principle.

Chapter 2 presents dithiophosphonate ligands synthesized using pentaerythritol and the corresponding metal heterocycles synthesized. The chapter also gives experimental data and characterization (^{1}H, ^{31}P, ^{13}C NMR, FTIR and mass spectroscopic results, melting points, yields and X-ray crystallography of representative compounds) of all compounds and their discussion.

Chapter 3 describes new dithiophosphonate ligands and complexes made from diphenyl methanol. The chapter also reports the experimental data and characterization (^{1}H, ^{31}P, ^{13}C NMR, FTIR and mass spectroscopic results, melting points, yields and X-ray crystallography of the representative compound) of these compounds with discussions.

Chapter 4 describes the synthesis and characterization (^{1}H, ^{31}P, ^{13}C NMR, FTIR and mass spectroscopic results, melting points, yields and X-ray crystallography of the representative compound) of compounds of ethambutol.

Chapter 5 presents dithiophosphonate intramolecular S-S compounds synthesized, their experimental data, characterization (^{1}H, ^{31}P, ^{13}C NMR, FTIR and mass spectroscopic results, melting points, yields and X-ray crystallography of the representative compound) and discussions. The chapter also describes a comparison of four polymorphs of a known S-S coupled dithiophosphonate earlier synthesized via molecular overlays and crystallographic packing.

Chapter 6 discusses the light harvesting properties of selected synthesized complexes as potential co-sensitizers in DSSCs. The fabricated device performance of these co-sensitized compounds decreases in the order **25**/N719 (η = 7.49 %) > **28**/N719 (η = 7.30 %) > **26**/N719 (η = 6.70 %) > **27**/N719 (η = 6.34 %) compared to that of the dye N719 (η = 5.65 %) under similar experimental conditions. These results indicate that these complexes are attractive candidates as co-sensitizers in DSSCs.

Chapter 7 presents results of antimicrobial susceptibility screenings of synthesized complexes and their discussions. The antibacterial susceptibility screenings showed that selected Gram-negative (*Escherichia coli* ATCC 25922, *E. coli* ATCC 35218, and *Pseudomonas aeruginosa* ATCC 27853) and Gram-positive bacteria (*Staphylococcus aureus* ATCC 29213, *S. aureus* ATCC 43300 and *Enterococcus faecalis* ATCC 51299) were susceptible to some of the synthesized dithiophosphonate compounds at 500 and 1000 µg/L.

Chapter 8 rounds up this thesis by presenting a summary of the main findings of this study and an outlook of potential further work. In total 28 new compounds were synthesized and characterized spectroscopically. Representative Molecular structures were also obtained in this study.

1.8 REFERENCES

1. I. Haiduc, *J. Organomet. Chem*, **2001**, 623, 29-42.
2. J. R. Wasson, G. M. Woltermann and H. J. Stoklosa, in *Inorg. Chem*, Springer, **1973**, pp. 65-129.
3. W. E. van Zyl and J. D. Woollins, *Coord. Chem. Rev*, **2013**, 257, 718-731.
4. J. H. Nelson, *Synth. and React. in Inorg. and Metal-Organic Chem*, **1992**, 22, 487-488.
5. J. Tsuji, *Trans Metal Reagents Cat: Innovations Organic Synth*, John Wiley & Sons, **2002.**
6. R. H. Crabtree, *The organomet. Chem Trans. Metals*, John Wiley & Sons, **2009**.
7. A. F. Cotton, G. Wilkinson, M. Bochmann and C. A. Murillo, *Advanced Inorg.Chem*, Wiley, **1999**.
8. L. S. Hegedus, *Trans. Metals Synth. Complex Organic Mol*, University Science Books, **1999**.
9. F. A. Cotton and B. Hong, *Progress Inorg. Chem, Volume 40*, **2007**, 179-289.
10. L. D. Quin, *A Guide Organophos. Chem*, John Wiley & Sons, **2000**.
11. W. E. Van Zyl, *Comments. Inorg. Chem*, **2010**, 31, 13-45.
12. J. Wasson, *Inorg. Chem. The Chem. of Phos. E. Fluck. Trans Metal Dithio-and Diselenophosphate Complexes JR Wasson, GM Woltermann HJ Stoklosa*, Springer-Verlag, **1973**.
13. I. Haiduc, D. B. Sowerby and S.-F. Lu, *Polyhedron*, **1995**, 14, 3389-3472.
14. R. Mehrotra, G. Srivastava and B. Chauhan, *Coord. Chem. Rev.*, **1984**, 55, 207-259.
15. K. C. Molloy and J. J. Zuckerman, *Acc. Chem. Res.*, **1983**, 16, 386-392.
16. E. Tiekink, *Main Group Metal Chem*, **1992**, 15, 161-161.
17. E. R. Tiekink, *CrystEngComm*, **2003**, 5, 101-113.
18. J. A. McCleverty and N. G. Connelly, *Nomen. Inorg. Chem: Recommendations 2000. II*, RSC, **2001**.
19. S. R. Batten, N. R. Champness, X.-M. Chen, J. Garcia-Martinez, S. Kitagawa, L. Öhrström, M. O'Keeffe, M. P. Suh and J. Reedijk, *CrystEngComm*, **2012**, 14, 3001-3004.

20. I. U. o. Pure, A. C. C. o. t. N. o. O. Chemistry, R. Panico, W. H. Powell and J.-C. Richer, *A guide to IUPAC Nomen. of Organic Compounds: Recommendations 1993*, Blackwell Scientific Publications Oxford, **1993**.

21. M. G. Drew, W. A. Hopkins, P. C. Mitchell and T. Colclough, *J. Chem Soc, Dalton Trans*, **1986**, 351-354.

22. A. Bond and R. Martin, *Coord. Chem. Rev*, **1984**, 54, 23-98.

23. M. N. Pillay, H. van der Walt, R. J. Staples and W. E. van Zyl, *J. Organomet. Chem.*, **2015**, 794, 33-39.

24. W. Przychodzeń and J. Chojnacki, *Hetero. Chem*, **2008**, 19, 271-282.

25. O. Grishina and N. Andreev, *Chemischer Informationsdienst*, **1976**, **7**.

26. I. P. Gray, P. Bhattacharyya, A. M. Slawin and J. D. Woollins, *Chem–A Euro J*, **2005**, 11, 6221-6227.

27. P. Knopik, L. Łuczak, M. J. Potrzebowski, J. Michalski, J. Błaszczyk and M. W. Wieczorek, *J. Chem. Soc, Dalton Trans*, **1993**, 2749-2757.

28. W. J. Stec, B. Uznanski, A. Wilk, B. L. Hirschbein, K. L. Fearon and B. J. Bergot, *Tetrahedron lett*, **1993**, 34, 5317-5320.

29. H. van der Walt, A. Muller, R. J. Staples and W. E. Van Zyl, *Acta Cryst. Sec. E: Structure Reports Online*, **2010**, 66, m1364-m1365.

30. M. Karakus, P. Lönnecke, D. Yakhvarov and E. Hey-Hawkins, *Zeitschrift für anorganische und allgemeine Chemie*, **2004**, 630, 1444-1450.

31. V. Garcia-Montalvo, R. A. Toscano, A. Badillo-Delgado and R. Cea-Olivares, *Polyhedron*, **2001**, 20, 203-208.

32. A. M. Z. S. M.R.S. Foreman, J.D. Woollins, *J. Chem. Soc. Dalton Trans*, **1996**, 3653.

33. S. F. Martin, A. S. Wagman, G. G. Zipp and M. K. Gratchev, *J. Org. Chem.*, **1994**, 59, 7957-7958.

34. P. Gryaznov, O. Naumova, D. Alimova, D. Krivolapov, I. Litvinov and V. Al'fonsov, *Russ. J. Gen. Chem*, **2005**, 75, 1744-1749.

35. M. Karakus, P. Lönnecke and E. Hey-Hawkins, *Polyhedron*, **2004**, 23, 2281-2284.

36. C. Aydemir, M. Karakus, I. Kara, A. Ö. Kiraz and N. Kolsuz, *J. Mol. Structure*, **2016**, 1111, 61-68.

37. A. S. Marggraff, *Miscellanea Berolinensia*, **1740**, 6, 54.

38. J. L. J. Berzelius, *Ann. Chem*, **1843**, 59 593.

39. E. H. W. A. Vos, *Proc. Kon. Ned. Akad. Wetensch*, **1954**, 57B, 497.

40. J. Mai, *Berichte Der Deutschen Chemischen Gesellschaft*, **1911**, 44, 1229-1233.

41. W. Treadwell and C. Beeli, *Helvetica Chimica Acta*, **1935**, 18, 1161-1171.

42. E. Andrew and V. Wynn, Proceedings of the Royal Society of London A: Mathematical, Physical and Engineering Sciences, **1966**.

43. H. Y. H. Hirai, *Chem. Abs.* , **1969**, 71 50213h.

44. P. Fay and H. P. Lankelma, *J. American Chem. Soc*, **1952**, 74, 4933-4935.

45. H. Lecher, R. Greenwood, K. Whitehouse and T. Chao, *J. American Chem. Soc*, **1956**, 78, 5018-5022.

46. A. Kekulé, *Justus Liebigs Annalen der Chemie*, **1854**, 90, 309-316.

47. L. Malatesta, *Gazz. Chim. Ital*, **1946**, 76, 167.

48. L. Malatesta, *Chin. I d (Milan)*, **1945**, 27, 6.

49. P. Shetty, P. Jose and Q. Fernando, *Chem Comm (London)*, **1968**, 788-790.

50. L. Maier, *Topics Phos. Chem*, **1965**, 2, 43.

51. L. Maier, *Topics. Phos Chem*, **1980**, 10, 129.

52. J. P. Chupp and P. E. Newallis, *The J. Org. Chem*, **1962**, 27, 3832-3835.

53. J. P. C. P.E. Newallis, L.C.D. Groenwege, *J. Org. Chem*, **1962**, 3829.

54. W. E. Van Zyl and J. P. Fackler, *Phosphorus, Sulfur Silicon Relat. Elem*, **2000**, 167, 117-132.

55. J. D. Woollins, *Synlett*, 2012, **2012**, 1154-1169.

56. M. J. Pilkington, A. M. Slawin, D. J. Williams, P. T. Wood and J. D. Woollins, *Hetero. Chem*, **1990**, 1, 351-355.

57. G. Hua, Y. Li, A. M. Slawin and J. D. Woollins, *Tetrahedron*, **2008**, 64, 5442-5448.

58. P. Bhattacharyya, A. M. Slawin and J. D. Woollins, *Angew. Chem. Int. Edition*, **2000**, 39, 1973-1975.

59. J. Navech, J. Majoral and R. Kraemer, *Tetrahedron lett*, **1983**, 24, 5885-5886.

60. S. S. B.S. Pederson, N.H. Nilsson, S.O. Lawesson, *Bull. Soc. Chim. Belg*, **1978**, 223.

61. M. R. J. Navech, S. Mathieu, *Phosphorus Sulfur Silicon Relat. Elem*, **1988**, 107, 306.

62. N. Yousif and M. Salama, *Phosphorus Sulfur Relat. Elem*, **1987**, 32, 51-53.

63. R. Shabana, *Phosphorus Sulfur Relat. Elem*, **1987**, 29, 293-296.

64. A. El-Barbary, *Monatshefte für Chemie/Chemical Monthly*, **1984**, 115, 769-777.

65. R. Cherkasov, G. Kutyrev and A. Pudovik, *Tetrahedron*, **1985**, 41, 2567-2624.

66. E. S. B. I.S. Nizamov, V.A. Al'fonsov, *Russ. J. Gen. Chem*, **1993**, 63, 1840.

67. M. Jesberger, T. P. Davis and L. Barner, *Synthesis*, 2003, **2003**, 1929-1958.

68. T. Ozturk, E. Ertas and O. Mert, *Chem. Rev*, **2007**, 107, 5210-5278.

69. A. M. Slavin, M.S.J. Foreman, J.D. Woollins, *J. Chem. Soc. Chem. Commun*, **1997**, 855.

70. A. M. Slavin, M.S.J. Foreman, J.D. Woollins, *J. Chem. Soc. Chem. Commun*, **1997**, 1269.

71. A. M. Slavin, M.S.J. Foreman, J.D. Woollins, *Phosphorus Sulfur Silicon Relat. Elem*, **1997**, 469.

72. M. S. J. Foreman and J.D. Woollins, *J. Chem. Soc. Dalton Trans*, **2000**, 1533-1543.

73. M. Karakus, *Phosphorus, Sulfur Silicon Relat Elem*, **2011**, 186, 1523-1530.

74. M. Karakus, Y. Aydogdu, O. Celik, V. Kuzucu, S. Ide and E. Hey-Hawkins, *Zeitschrift für anorganische und allgemeine Chemie*, **2007**, 633, 405-410.

75. I. Haiduc and L. Y. Goh, *Coord. Chem. Rev*, **2002**, 224, 151-170.

76. P. T. Wood and J. D. Woollins, *Trans. Met. Chem*, **1987**, 12, 403.

77. I. P. Alimarin and V. M. Ivanov, *Russ. Chem. Rev*, **1989**, 58, 863.

78. M. Fuller, M. Kasraia, J. S. Sheasby, G. M. Bancroft, K. Fyfe and K. H. Tan, *Tribology Lett*, **1995**, 1, 367-378.

79. A. M. Barnes, K. D. Bartle and V. R. Thibon, *Tribology Int*, **2001**, **34**, 389-395.

80. M. A. Nicholls, T. Do, P. R. Norton, M. Kasrai and G. M. Bancroft, *Tribology Int*, **2005**, 38, 15-39.

81. H. Spikes, *Lubricat Sci*, **2008**, 20, 103-136.

82. L. Bromberg, I. Lewin and A. Warshawsky, *Hydrometallurgy*, **1993**, 33, 59-71.

83. P. Patnaik, *A Comprehensive Guide to the Hazardous Properties of Chemical Substances*, John Wiley & Sons, **2007**.

84. T. B. Gaines, *Toxic and Applied Pharm*, **1969**, 14, 515-534.

85. S. E. Livingstone and A. E. Mihkelson, *Inorg. Chem*, **1970**, 9, 2545-2551.

86. H. Hartung, *Zeitschrift für Chemie*, **1967**, 7, 241-241.

87. M. C. Aragoni, M. Arca, F. A. Devillanova, M. B. Hursthouse, S. L. Huth, F. Isaia, V. Lippolis, A. Mancini, S. Soddu and G. Verani, *Dalton Trans*, **2007**, 2127-2134.

88. Y. Özcan, S. Ide, M. Karakus and H. Yilmaz, *Anal Sci*, **2002**, 18, 1285-1286.

89. H.-L. Liu, H.-Y. Mao, C. Xu, H.-Y. Zhang, H.-W. Hou, Q.-a. Wu, Y. Zhu, B.-X. Ye and L.-J. Yuan, *Polyhedron*, **2004**, 23, 1799-1804.

90. M. Arca, A. Cornia, F. A. Devillanova, A. C. Fabretti, F. Isaia, V. Lippolis and G. Verani, *Inorg. Chimica Acta*, **1997**, 262, 81-84.

91. M. Karakus and H. Yilmaz, *Russian J. of Coord. Chem*, **2006**, 32, 437-443.

92. I. P. Gray, A. M. Slawin and J. D. Woollins, *Zeitschrift für anorganische und allgemeine Chemie*, **2004**, 630, 1851-1857.

93. M. Karakus, P. Lönnecke and E. Hey-Hawkins, *Polyhedron*, **2004**, 23, 2281-2284.

94. M. A. M.C. Aragoni, N.R. Champness, A.V. Chemikov, F.A. Devillanova, F. and V. L. Isiaia, N.S. Oxtoby, G. Verani, S.Z. Vatsadze, C. Wilson, *Eur. J. Inorg. Chem*, **2004**, 2008.

95. V. G. Albano, M. C. Aragoni, M. Arca, C. Castellari, F. Demartin, F. A. Devillanova, F. Isaia, V. Lippolis, L. Loddo and G. Verani, *Chem. Comm*, **2002**, 1170-1171.

96. I. P. Gray, H. L. Milton, A. M. Slawin and J. D. Woollins, *Dalton Trans*, **2003**, 3450-3457.

97. M. C. Aragoni, M. Arca, F. Demartin, F. A. Devillanova, C. Graiff, F. Isaia, V. Lippolis, A. Tiripicchio and G. Verani, *J. Chem. Soc, Dalton Trans*, **2001**, 2671-2677.

98. M. Karakus, P. Lönnecke and E. Hey-Hawkins, *Zeitschrift für anorganische und allgemeine Chemie*, **2004**, 630, 1249-1252.

99. R. F. Semeniuc, T. J. Reamer, J. P. Blitz, K. A. Wheeler and M. D. Smith, *Inorg. Chem*, **2010**, 49, 2624-2629.

100. W. Shi, M. Shafaei-Fallah, C. E. Anson and A. Rothenberger, *Dalton Trans*, **2005**, 3909-3912.

101. M. Karakus, H. Yilmaz and E. Bulak, *Russ. J. of Coord. Chem*, **2005**, 31, 316-321.

102. M. Karakus, H. Yilmaz, E. Bulak and P. Lönnecke, *Applied Organomet. Chem*, **2005**, 19, 396-397.

103. S. Blaurock, F. T. Edelmann, I. Haiduc, G. Mezei and P. Poremba, *Inorg. Chimica Acta*, **2008**, 361, 407-410.

104. C. A. F. Devillanova, M. Arca, M.B. Hursthouse, S.L. Huth, *Univ. of Southampton*, **2006**, p. 238.

105. I. P. Gray, A. M. Slawin and J. D. Woollins, *New J. of Chem*, **2004**, 28, 1383-1389.

106. W. Shi, M. Shafaei-Fallah, C. E. Anson and A. Rothenberger, *Dalton Trans*, **2006**, 3257-3262.

107. C. A. F. Devillanova, M. Arca, M.B. Hursthouse, S.L. Huth, *Univ. of Southampton*, **2006**, p. 248.

108. C. A. F. Devillanova, M. Arca, M.B. Hursthouse, S.L. Huth, *Univ. of Southampton*, **2006**, p. 235.

109. M. Coluccia, F. Fanizzi, G. Giannini, D. Giordano, F. Intini, G. Lacidogna, F. Loseto, M. Mariggio, A. Nassi and G. Natile, *Anticancer research*, **1990**, 11, 281-287.

110. S. Singh and B. Mohan, *The Inter J. Tuberculosis and Lung. Disease*, **2003**, 7, 298-303.

111. H. Bhutani, S. Singh, K. Jindal and A. K. Chakraborti, *J. Pharm. and Biomed. Analysis*, **2005**, 39, 892-899.

112. B. Blomberg, S. Spinaci, B. Fourie and R. Laing, *Bullet.WHO*, **2001**, 79, 61-68.

113. S. Cherukuvada and A. Nangia, *Cryst. Growth & Des*, **2013**, 13, 1752-1760.

114. G. N. Rao and M. M. Annapurna, *J. Pharm. Edu. and Research*, **2010**, 1, 44.

115. M. V. N. de Souza, *Current Opinion Pulmonary Medicine*, **2006**, 12, 167-171.

116. A. M. I. Rageh, F. A. Mohamed, N. N. Atia and S. M. Botros, .*J Liq Chromat & Relat Tech*, **2015**, 38, 1061-1067.

117. A. F. Faria, L. F. Marcellos, J. P. Vasconcelos, M. V. de Souza, S. Júnior, L. Antônio, W. R. d. Carmo, R. Diniz and M. A. de Oliveira, *J. Brazilian Chem. Soc*, **2011**, 22, 867-874.

118. T. C. Ramalho, E. F. da Cunha and R. B. de Alencastro, *J. of Mol. Structure: THEOCHEM*, **2004**, 676, 149-153.

119. M. Benedetti, J. Malina, J. Kasparkova, V. Brabec and G. Natile, *Environ. Health Persp*, **2002**, **110**, 779.

120. M. Collucia, M. Correale, D. Giordano, M. A. Marrigiò, S. Moscelli, F. P. Fanizzi, G. Natile and L. Maresca, *Inorg. Chimica Acta*, **1986**, 123, 225-229.

121. M. Coluccia, F. P. Fanizzi, G. Giannini and D. Giordano, *Anticancer Rresearch*, **1991**, 11, 281-288.

122. A. G. Karlson, *American Rev.Resp. Disease*, **1961**, 84, 902-904.

123. R. E. Carr and P. Henkind, *Archives Ophthalmology*, **1962**, 67, 566-571.

124. C. Hawkins, *Acta Chem. Scand*, **1964**, 18, 1564-1566.

125. A. Cole, P. M. May and D. R. Williams, *Agents and Actions*, **1981**, 11, 296-305.

126. V. K. Gupta, R. Prasad and A. Kumar, *Talanta*, **2003**, 60, 149-160.

127. G. Bemski, M. Rieber and H. Reyes, *FEBS lett*, **1972**, 23, 59-60.

128. A. Hagfeldt, G. Boschloo, L. Sun, L. Kloo and H. Pettersson, *Chem. Rev*, **2010**, 110, 6595-6663.

129. J. Gong, J. Liang and K. Sumathy, *Ren. Sust Energy Rev*, **2012**, 16, 5848-5860.

130. S. Ardo and G. J. Meyer, *Chem. Soc. Rev*, **2009**, 38, 115-164.

131. https://ec.europa.eu/energy/en/topics/renewable-energy./Retrieved from the internet on **23/05/2017**

132. https://www.whitehouse.gov/america-first-energy./ Retrieved from the internet on **15/05/2017**

133. M. A. Hasan and K. Sumathy, *Renew Sust. Energy Rev*, **2010**, 14, 1845-1859.

134. N. S. Lewis and D. G. Nocera, *Proceedings Nat. Academy of Sci*, **2006**, 103, 15729-15735.

135. N. S. a. C. Lewis, George, *US Department of Energy, Office of Basic Energy Science , Washington, DC.*, **2005**.

136. B. O'Regan and M. Gratzel, *Nature*, **1991**, 353, 737-740.

137. F. Bella, S. Galliano, M. Falco, G. Viscardi, C. Barolo, M. Grätzel and C. Gerbaldi, *Green Chem*, **2017**.

138. M. E. Ragoussi, J. J. Cid, J. H. Yum, G. de la Torre, D. Di Censo, M. Grätzel, M. K. Nazeeruddin and T. Torres, *Angew. Chem. Int. Ed*, **2012**, 51, 4375-4378.

139. M. K. Nazeeruddin, F. De Angelis, S. Fantacci, A. Selloni, G. Viscardi, P. Liska, S. Ito, B. Takeru and M. Grätzel, *J. American Chem. Soc*, **2005**, 127, 16835-16847.

140. Z. Zhang, S. M. Zakeeruddin, B. C. O'Regan, R. Humphry-Baker and M. Grätzel, *J. Phys. Chem. B*, **2005**, 109, 21818-21824.

141. J. J. Cid, J. H. Yum, S. R. Jang, M. K. Nazeeruddin, E. Martínez-Ferrero, E. Palomares, J. Ko, M. Grätzel and T. Torres, *Angew. Chem*, **2007**, 119, 8510-8514.

142. M. Grätzel, *Nature*, **2001**, 414, 338-344.

143. U. Bach, D. Lupo, P. Comte, J. E. Moser, F. Weissortel, J. Salbeck, H. Spreitzer and M. Gratzel, *Nature*, **1998**, 395, 583-585.

144. B. C. O'Regan and J. R. Durrant, *Acc. Chem. Res*, **2009**, 42, 1799-1808.

145. K. Yoshikawa, H. Kawasaki, W. Yoshida, T. Irie, K. Konishi, K. Nakano, T. Uto, D. Adachi, M. Kanematsu, H. Uzu and K. Yamamoto, *Nature Energy*, **2017**, 2, 17032.

146. K. Kakiage, Y. Aoyama, T. Yano, K. Oya, J.-i. Fujisawa and M. Hanaya, *Chem. Comm*, **2015**, 51, 15894-15897.

147. R. Yadav, M. Trivedi, G. Kociok-Köhn, R. Chauhan, A. Kumar and S. W. Gosavi, *Euro. J. Inorg. Chem*, **2016**.

148. H. Choi, S. Kim, S. O. Kang, J. Ko, M. S. Kang, J. N. Clifford, A. Forneli, E. Palomares, M. K. Nazeeruddin and M. Grätzel, *Angew. Chemie Int. Ed*, **2008**, 47, 8259-8263.

149. C.-M. Lan, H.-P. Wu, T.-Y. Pan, C.-W. Chang, W.-S. Chao, C.-T. Chen, C.-L. Wang, C.-Y. Lin and E. W.-G. Diau, *Energy Environ. Sci*, **2012**, 5, 6460-6464.

150. M. Mojiri-Foroushani, H. Dehghani and N. Salehi-Vanani, *Electrochim. Acta*, **2013**, 92, 315-322.

151. L. Han, A. Islam, H. Chen, C. Malapaka, B. Chiranjeevi, S. Zhang, X. Yang and M. Yanagida, *Energy & Environ. Sci*, **2012**, 5, 6057-6060.

152. H. Ozawa, R. Shimizu and H. Arakawa, *RSC Advances*, **2012**, 2, 3198-3200.

153. R. Y.-Y. Lin, Y.-S. Yen, Y.-T. Cheng, C.-P. Lee, Y.-C. Hsu, H.-H. Chou, C.-Y. Hsu, Y.-C. Chen, J. T. Lin and K.-C. Ho, *Organic lett*, **2012**, 14, 3612-3615.

154. X. Wang, Y.-L. Yang, P. Wang, L. Li, R.-Q. Fan, W.-W. Cao, B. Yang, H. Wang and J.-Y. Liu, *Dalton Trans*, **2012**, 41, 10619-10625.

155. X. Wang, Y. Yang, R. Fan and Z. Jiang, *New J. Chem*, **2010**, 34, 2599-2604.

156. L. Zhang, Y. Yang, R. Fan, P. Wang and L. Li, *Dyes and Pigments*, **2012**, 92, 1314-1319.

157. S. Gao, R. Q. Fan, X. M. Wang, L. S. Qiang, L. G. Wei, P. Wang, H. J. Zhang, Y. L. Yang and Y. L. Wang, *J. Mat. Chem A*, **2015**, 3, 6053-6063.

158. X.-M. Wang, P. Wang, R.-Q. Fan, M.-Y. Xu, L.-S. Qiang, L.-G. Wei, Y.-L. Yang and Y.-L. Wang, *Dalton Trans*, **2015**, 44, 5179-5190.

159. Y.-W. Dong, R.-Q. Fan, P. Wang, L.-G. Wei, X.-M. Wang, S. Gao, H.-J. Zhang, Y.-L. Yang and Y.-L. Wang, *Inorg. Chem*, **2015**, 54, 7742-7752.

CHAPTER 2

SYNTHESIS AND CHARACTERIZATION OF ZINC DITHIOPHOSPHONATE HETEROCYCLES

2.1 INTRODUCTION

Thiophosphorus species, as an important class of S-donor ligands, have been studied for many years. This class of compounds includes the dithiophosphates, dithiophosphinates and the least studied dithiophosphonates. These compounds are versatile ligands, displaying a broad variety of coordination patterns leading to a great diversity of molecular and supramolecular structures.[1] Lawesson's reagent (LR), Phenetole Lawesson's Reagent (PhLR) (Figure 2.1) and the ferrocenyl dimer (FcLR) (Figure 2.2) are well known thionation agents and undergo cyclization reactions with alcohols to form sulfur containing heterocycles, which incorporate the alkoxyl or ferrocenyl moiety. A literature survey indicate studies where LR[2] and FcLR[3-5] have been used in synthesizing sulfur containing heterocycles.

In this chapter, the ring opening reactions of PhLR and FcLR are exploited using pentaerythritol (a tetraol) (Figure 2.3) to form sulfur rich heterocycles. The chapter also presents the experimental data, characterization and discussion of these data.

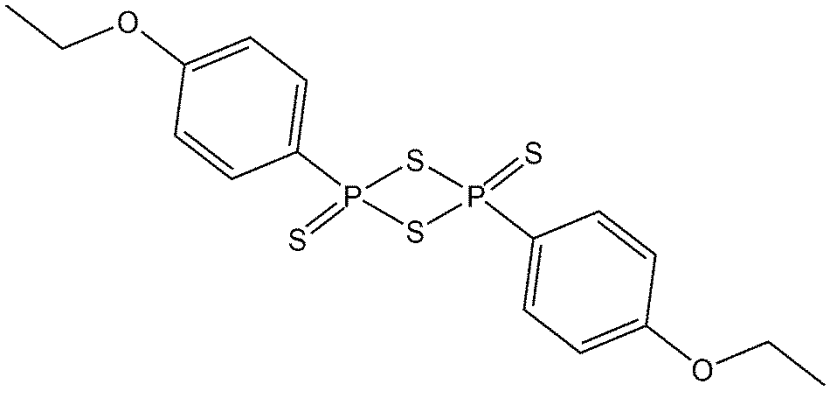

Figure 2.1: Phenetole Lawesson's Reagent (PhLR).

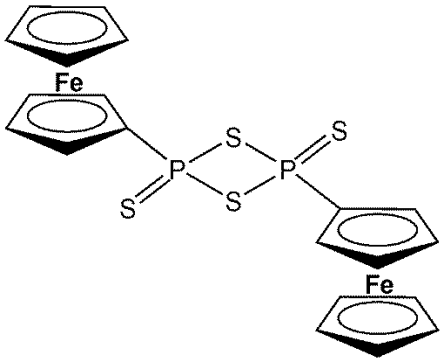

Figure 2.2: Ferrocenyl Lawesson's Reagent (FcLR).

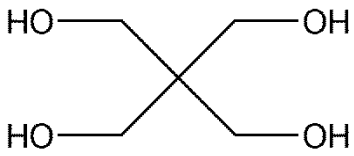

Figure 2.3: Structure of pentaerythritol.

2.2 RESULTS AND DISCUSSION

2.2.1 SYNTHESIS

The synthesis of compound **2** has been reported[5] and the synthesis of the salts **1** and **2** followed this procedure. Dithiophosohonate salts **1** and **2** were prepared by heating the alcohol (pentaerythritol) with PhLR or FcLR in small amounts of toluene at 70°C and subsequent deprotonation. The reaction was essentially complete once dissolution of all solids took place. The dithiophosphonic acids formed were deprotonated *in-situ* with the weak base ammonia at 0°C (ice bath) forming dithiophosphonate salt derivatives **1** and **2** as shown in Scheme 2.1. Each mole of pentaerythritol is used in cleaving two moles of the dimeric PhLR for **1** and FcLR for **2**. **1** and **2** were found to be relatively stable and could be stored indefinitely under a N_2 atmosphere. Prolonged exposure of **1** and **2** to air eventually lead to the release of malodourous H_2S due to hydrolysis and oxidation. Compounds **1** and **2** are also hygroscopic.

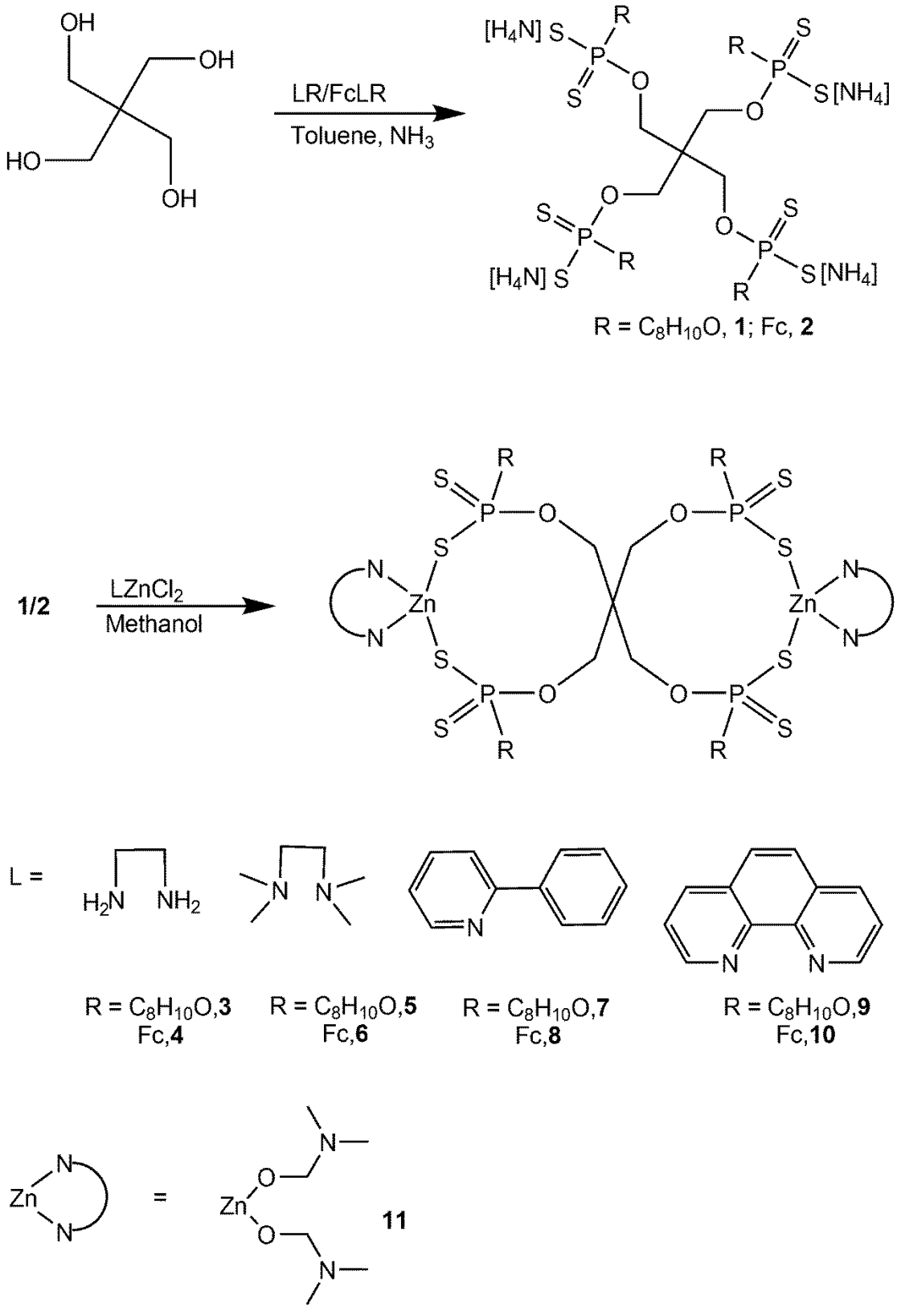

Scheme 2.1: Synthesis of compounds **3-11**.

Metal complexes **3-10** were obtained by drop-wise addition of the zinc precursors ($LZnCl_2$) dissolved in a methanol solution of **1** and **2** as shown in Scheme 2.1. Complexes **3-6** were obtained as colorless solids while **7-10** were obtained as yellow solids typical of ferrocenyl compounds. Compounds **3-10** are relatively stable for a long period when exposed to the atmosphere.

2.2.2 SPECTROSCOPY

The ^{1}H NMR of compounds **1-10** was well resolved and integrated to the number of the corresponding hydrogen atoms in all cases. The aromatic protons appeared between 6 and 9 ppm for complexes **3-6** as can be seen for complex **1** and **3** in Figure 2.4 and 2.5. The chemical shifts of the ligand (**1)** compared to that of the complexes (**3-6**) indicate complexation as seen in Figures 2.4 and 2.5. The protons of the metal precursors were also an indication for complexation, for example, the CH_3 and CH_2 protons of tetramethylethylenediamine (TMEDA) for complex **3** appear at about 2.6 ppm as shown in Figure 2.5. The ^{1}H NMR spectra of the compounds (**1, 3-6**) also confirm the presence of the anisyl and alkoxy moieties as expected. The unsubstituted cyclopentadienyl ring in all cases gave a singlet peak, with the substituted ring giving two sets of signals for the pair of equivalent protons for compounds **7-10.** The ^{31}P NMR spectra of compounds **1-10** gave singlet peaks between 94-107 ppm which lies within the expected region[6] as shown in Table 2.1. This suggests that these compounds are present in a single isomer configuration in solution. ^{31}P NMR chemical shifts could also be a good indicator of complexation for instance the ^{31}P NMR of **1** (103.40 ppm) shifts upfield to 100.03 ppm for **3** after complexation as shown in Figures 2.4 and 2.5. The different ^{31}P NMR chemical shifts of compounds **1-10** arises from the different chemical environment of the P atoms. The IR spectra show distinct bands at 1185–1179 cm^{-1}, 1028–1025 cm^{-1}, 678–674 cm^{-1} and 559–557 cm^{-1}, corresponding to ν[(P)–O–C], ν[P–O–(C)], $\nu(PS)_{asym}$ and $\nu(PS)_{sym}$ absorptions respectively.[7] The prominent band around 2974 cm^{-1} corresponding to the N-H of the ammonium ion cation in the ligand (compound **1** and **2**) disappears in the complexes (compounds **3-10**) indicating complexation which is consistent with literature.[7]

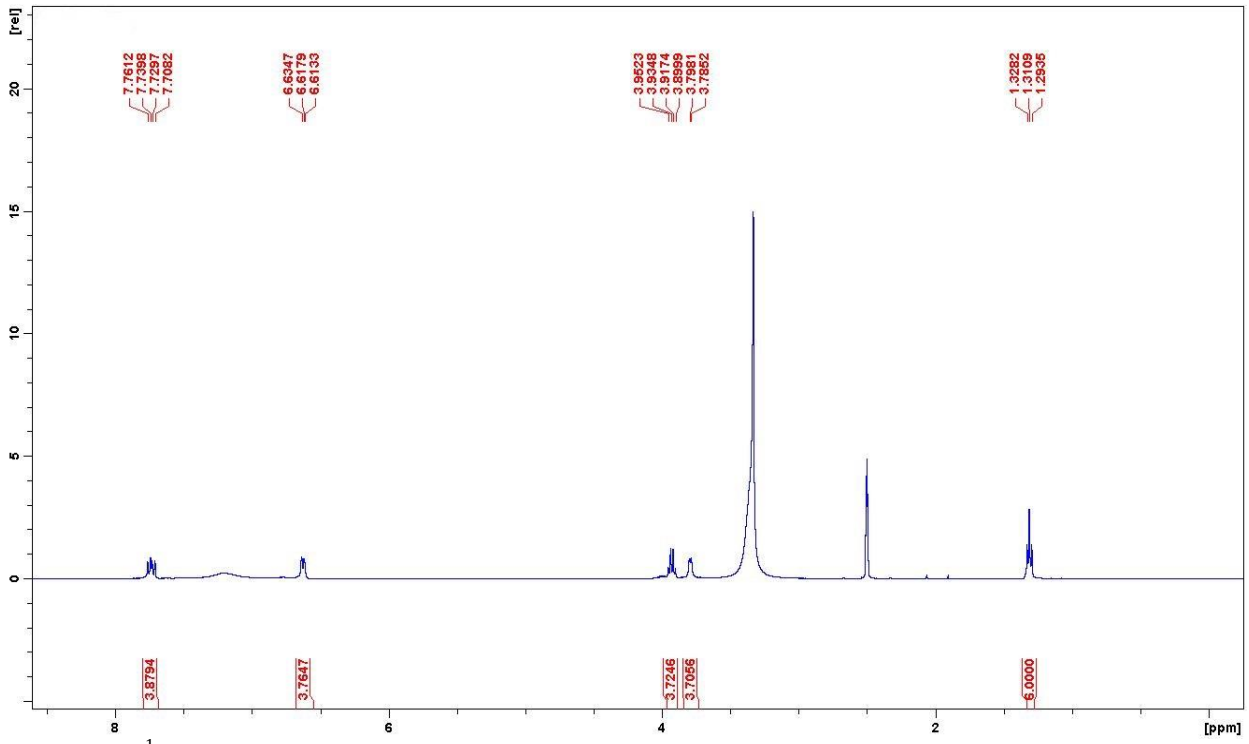

Figure 2.4: ^{1}H NMR spectrum of compound **1**.

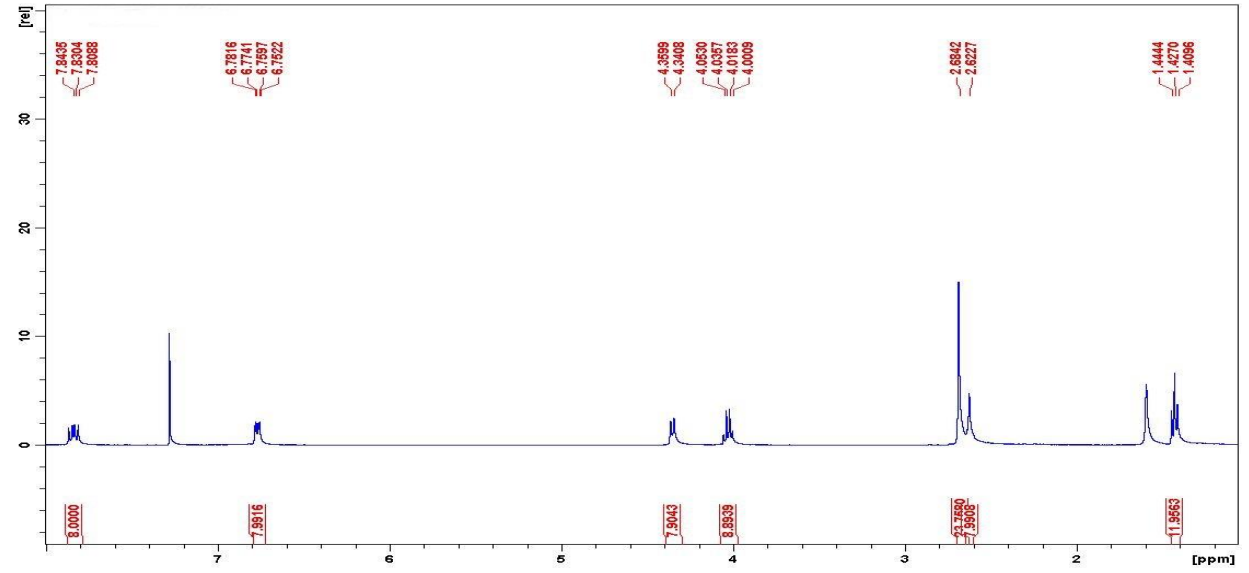

Figure 2.5: ^{1}H NMR spectrum of compound **3**.

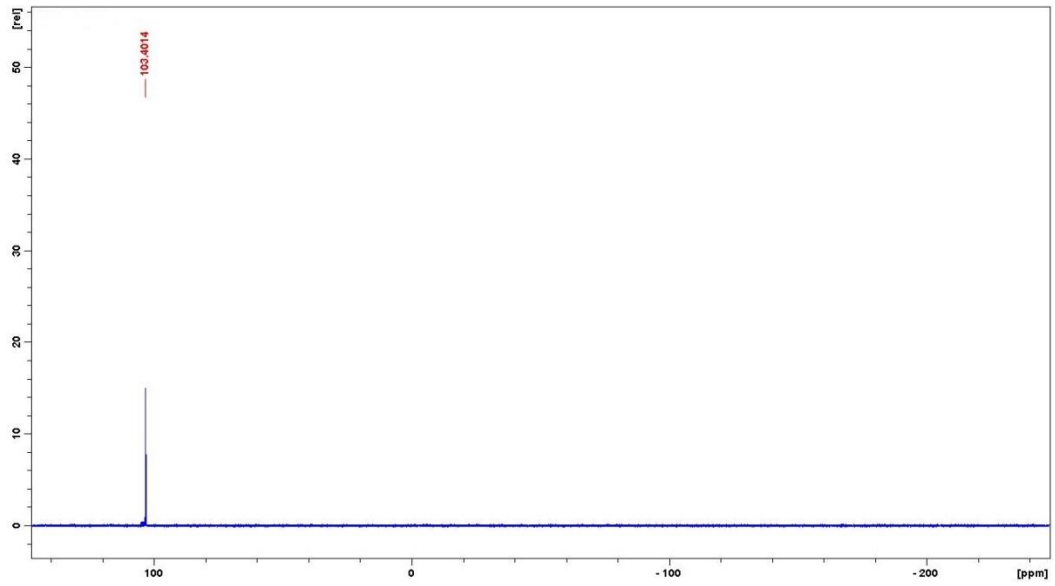

Figure 2.6: ^{31}P NMR spectrum of compound **1**.

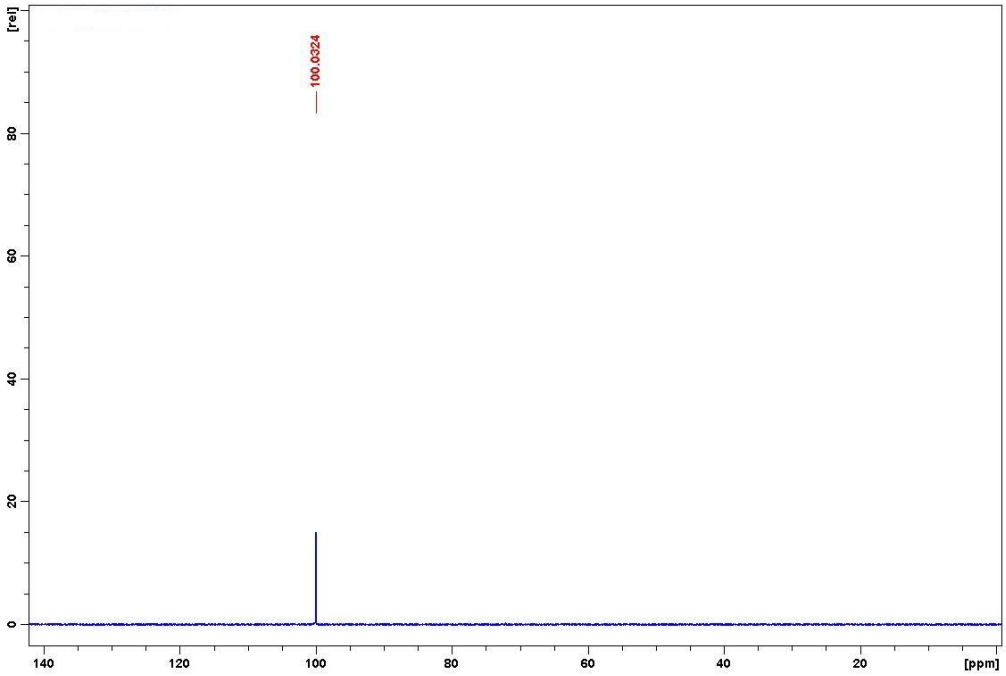

Figure 2.7: ^{31}P NMR spectrum of compound **3**.

Table 2.1: Yield, melting points, and ^{31}P NMR data of compounds **1-10**.

Compound	Yield(%)	M.p.(°c)	^{31}P NMR(ppm)	Colour
1	61	168	103.40	Colourless
2[a]	83	193	96.20	Yellow
3	71	[b]198	100.03	Colorless
4	60	[b]270	101.76	Colorless
5	50	208	102.34	Colorless
6	70	[b]240	97.55	Colorless
7	84	[b]332	95.29	Yellow
8	75	[b]240	101.42	Yellow
9	38	[b]322	106.52	Yellow
10	55	[b]260	105.38	Yellow

[a] = Literature values

[b] = Decompose

The presence of the ammonium capping moieties of the complexes is indicated in the IR at bands between 2920 and 2985 cm^{-1}. Mass spectrometry of compounds **1-10** gave fragmented ions. Compounds **1** and **2** melts at 168 and 193 °C respectively while compounds **3-10** decompose to black solid between 95-107 °C. Compounds **1** and **2** which are ligands melted at the given temperatures while the bulkier metal complexes of the ligands decomposed. Compounds **2, 7-10** which contain the ferrocenyl moiety were typically yellow compared to compounds **1, 3-6** that contain the phenetolic group.

2.3 QUALITATIVE SOLUBILITY STUDIES OF COMPOUND 1-10

Knowledge about the solubility of compounds, either to make the appropriate choice of solvent for spectroscopic measurements or as an aid in preparative chemistry, is useful.[6] Considering this

background, a series of solubility tests were performed on compounds **1-10**. Different solvents of varying polarity were used to obtain the data given in Table 2.2. This data is based on the criteria of dissolving a specified amount (0.03 g) of the compound of interest in the relevant solvent (0.2 mL), shaking for 10 seconds and then filtration at 25°c.

Table 2.2: Solubility data for **1-10**.

Compound	CH_3OH	C_2H_5OH	DCM	Hexane	THF	H_2O	DMF	DMSO
1	S	S	I	I	I	VS	VS	VS
2	S	S	PS	I	PS	VS	VS	VS
3	I	I	I	I	I	I	VS	VS
4	I	I	I	I	I	I	VS	VS
5	I	I	I	I	I	I	VS	VS
6	I	I	I	I	I	I	VS	VS
7	I	I	PS	I	PS	I	VS	VS
8	I	I	PS	I	PS	I	VS	VS
9	I	I	PS	I	PS	I	VS	VS
10	I	I	PS	I	PS	I	VS	VS

I = insoluble. PS = partly soluble. S = soluble. VS = very soluble. The symbol I means the compound is quantitatively recovered after filtration, PS means small amount of the compound (about 10%) is dissolved, S means a large amount of the compound is dissolved (about 80%) and VS means a clear solution of the compound emerged immediately.

Compounds **1** and **2** are soluble in polar solvents and not soluble in non-polar solvents except for compound **2** that is partly soluble in DCM (Table 2.2). Compounds **3-10** are all soluble in DMF and DMSO. Compounds **7-10** are partly soluble in THF and DCM while compounds **3-6** are not soluble. The solubility of compounds **1** and **2** and Zn metal precursors (L) in polar solvents like water, methanol and ethanol when compared to the insolubility of compounds **3-10** in these solvents play a key role in the precipitation of the desired complexes **3-10**. The solubility of the by-product (NH_4Cl) upon metal complexation in polar solvents mentioned above is useful as the NH_4Cl is removed in one step.

2.4 SOLID STATE STRUCTURES

Figures 2.8 and 2.9 give the molecular structures of **3** and **11** while important X-ray crystallographic data and parameters are shown in Table 2.3. Table 2.4 gives selected bond lengths and angles of **3** and **11**.

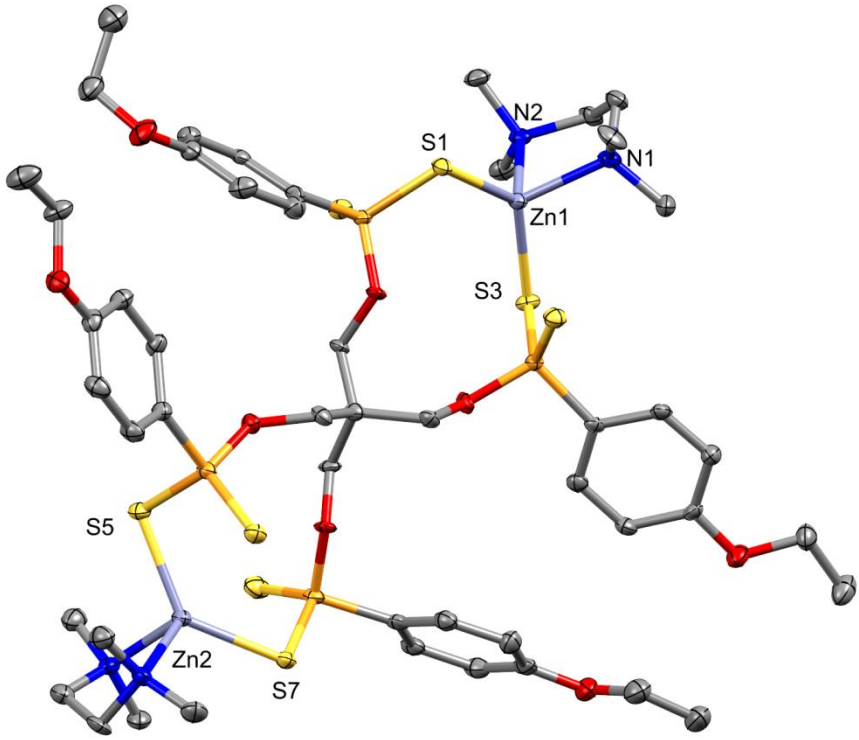

Figure 2.8: Molecular structure of **3**, thermal ellipsoids drawn at the 50% probability.
Hydrogen atoms are omitted for clarity.

Single crystals of compound **3** were obtained by slow diffusion of hexane into a concentrated solution of **3** in DCM. Compound **3** crystallizes in the triclinic space group P-1 with 2 molecules in the asymmetric unit cell. A perspective view of compound **3** is shown in Figure 2.8. The structure consists of two Zn atoms, each coordinated to two sulfur atoms from the two adjoining dithio groups while the other two S atoms from the dithio groups dangle in space, capping the derivitized pentaerythritol at both ends with a

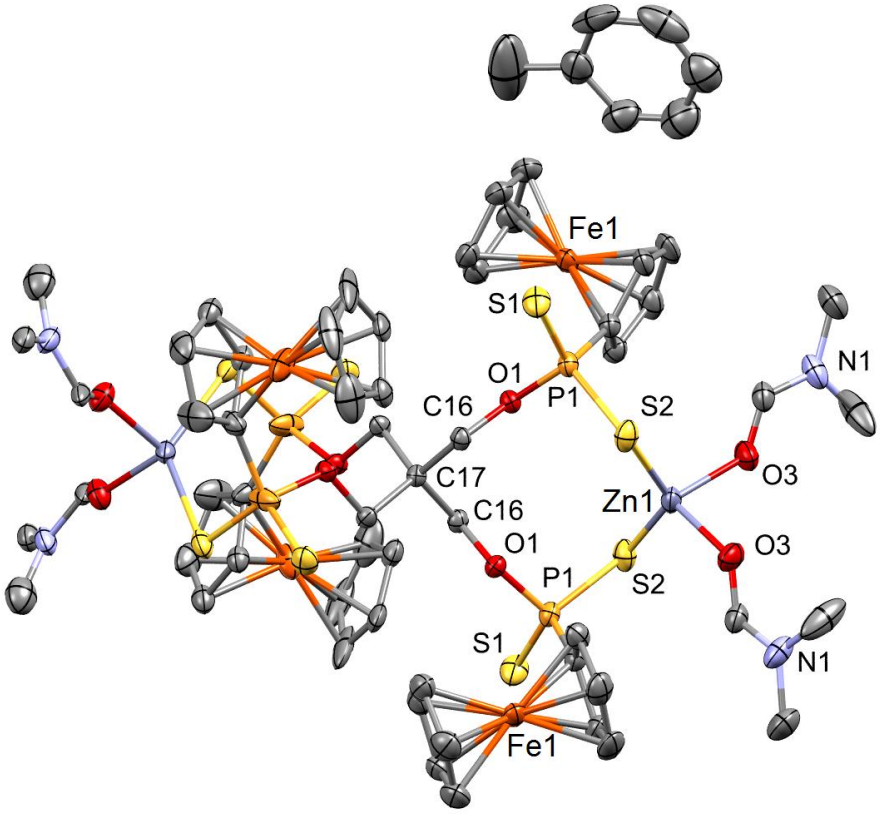

Figure 2.9: Molecular structure of **11**, thermal ellipsoids drawn at the 50% probability. Hydrogen atoms are omitted for clarity.

TMEDA group to give a dinuclear complex as shown in Figure 2.8. Thus, two ten membered rings in saddle-shape geometry similar to that obtained by Liu and co-workers[8] in 2003 were formed for the solid structure of **3**. Each metallo-ring in the molecular structure of **3** contains a Zn atom, two S atoms, 2 P atoms, 2 O atoms and 3 C atoms and both hetero-cycles share a geometric center (C17) as shown in Figure 2.8. The coordinated Zn atoms have a slightly distorted tetrahedral geometry which could be due to the steric hindrance of the TMEDA group. Crystals of compound **11** were obtained while trying to grow crystals of compound **8** in excess DMF in the refrigerator for 8 months.

Table 2.3: X-ray crystallographic data for compounds **3** and **11**.

Compound	**3**	**11**
Empirical formula	$C_{50}H_{78}Cl_2N_4O_8P_4S_8Zn_2$	$C_{71}H_{88}Fe_4N_4O_8P_4S_8Zn_2$
Formula weight	1445.21	1859.95
Temperature	100(2) K	100(2) K
Wavelength	0.71073 Å	0.71073 Å
Crystal system	Triclinic	Monoclinic
Space group	P -1	C 2/c
Unit cell dimensions	a = 14.3666(5) Å	a = 23.9986(7) Å
	b = 14.5315(5) Å	b = 21.3749(6) Å
	c = 19.3305(6) Å	c = 15.9950(5) Å
Volume	3467.4(2) $Å^3$	8196.9(4) $Å^3$
α	95.208(2)°	90°
β	99.567(2)°	92.5300(10)°
γ	117.417(2)°	90°
Z	2	4
Density (calculated)	1.384 Mg/m^3	1.507 Mg/m^3
Absorption coefficient	1.150 mm^{-1}	1.600 mm^{-1}
F(000)	1588	3832
Crystal size	0.245 x 0.241 x 0.126 mm^3	0.098 x 0.092 x 0.085 mm^3
Completeness to theta = 25.242°	99.5 %	99.9 %
Goodness-of-fit on F^2	1.511	1.059
Final R indices [I>2sigma(I)]	R1 = 0.0556, wR2 = 0.1831	R1 = 0.0674, wR2 = 0.1390
R indices (all data)	R1 = 0.0722, wR2 = 0.1957	R1 = 0.1213, wR2 = 0.1620

Compound **11** crystallizes in the monoclinic space group C2/c with 4 molecules per asymmetric unit cell, and with a toluene molecule in the crystal lattice (Figure 2.9). The molecular structure of **11** has two Zn atoms each coordinating to two sulfur atoms to form a ten membered ring similar to the molecular structure of **3**. The rings have a saddle-like shape similar to that obtained by Liu and co-workers[8] in 2003 and have a common centroid (C17). The coordinated Zn atoms are capped at each end by two molecules of DMF which binds to the Zn through the O atoms giving rise to a dinuclear complex. The geometry around the coordinated Zn atoms is slightly distorted tetrahedral. All four ferrocenyl groups are attached to the P atom in a *cis*- conformation. Figure 2.10 and 2.11 shows the hydrogen bonding in compound **3**. There is intra molecular hydrogen bonding between the oxygen atoms (O_1) of the phenetolic groups and the protons (H_{26}) of the opposite aromatic groups depicted as green dotted lines as shown in Figure 2.10. Green dotted lines also indicate inter-hydrogen bonding between aromatic protons (H_{24}) and oxygen atoms (O_3) of adjacent molecules of compound **3** (Figure 2.11).

Table 2.4: Selected bond lengths (Å) and angles (°) for compounds **3** and **11**.

Compound 3			
Zn(1)-S(3)	2.3006(13)	Zn(1)-N(1)	2.114(4)
Zn(1)-S(1)	2.3248(13)	Zn(1)-N(2)	2.129(4)
Zn(2)-S(7)	2.2977(13)	Zn(2)-N(5)	2.122(4)
Zn(2)-S(5)	2.3129(13)	Zn(2)-N(3)	2.154(4)
S(3)-P(2)	2.0320(17)	P(2)-O(6)	1.613(3)
S(4)-P(2)	1.9506(17)	P(3)-O(7)	1.601(4)
S(6)-P(3)	1.9513(17)	P(4)-O(8)	1.612(3)
S(5)-P(3)	2.0319(17)	P(1)-O(5)	1.611(3)
S(7)-P(4)	2.0267(18)	N(1)-Zn(1)-N(2)	85.93(16)
S(8)-P(4)	1.9498(17)	N(1)-Zn(1)-S(3)	113.11(12)

Compound 3			
S(2)-P(1)	1.9536(17)	N(2)-Zn(1)-S(3)	100.27(11)
S(1)-P(1)	2.0256(17)	N(1)-Zn(1)-S(1)	106.30(12)
N(5)-Zn(2)-S(5)	112.12(12)	N(2)-Zn(1)-S(1)	112.65(11)
N(3)-Zn(2)-S(5)	99.74(11)	S(3)-Zn(1)-S(1)	129.76(5)
S(7)-Zn(2)-S(5)	132.68(5)	N(5)-Zn(2)-N(3)	86.04(17)
P(2)-S(3)-Zn(1)	99.75(6)	N(5)-Zn(2)-S(7)	105.37(12)
P(3)-S(5)-Zn(2)	97.76(6)	N(3)-Zn(2)-S(7)	110.86(11)
P(4)-S(7)-Zn(2)	98.40(6)	P(1)-S(1)-Zn(1)	97.85(6)
Compound 11			
O(1)-P(1)	1.609(3)	O(3)#1-ZN2-O(3)	94.9(2)
O(2)-P(2)	1.603(3)	O(3)#1-ZN2-S(2)#1	113.86(12)
O(3)-ZN2	2.015(4)	O(3)-ZN2-S(2)#1	98.22(12)
P(1)-S(1)	1.9434(18)	O(3)#1-ZN2-S(2)	98.22(12)
P(1)-S(2)	2.0417(18)	O(1)-P(1)-S(1)	114.74(13)
P(2)-S(3B)	1.778(4)	C(9)-P(1)-S(1)	113.70(18)
P(2)-S(4A)	1.876(4)	O(1)-P(1)-S(2)	107.49(13)
P(2)-S(3A)	2.114(4)	C(9)-P(1)-S(2)	110.96(17)
P(2)-S(4B)	2.278(5)	S(1)-P(1)-S(2)	110.55(8)
S(2)-ZN2	2.2807(14)	O(2)-P(2)-C(13)	99.3(2)
ZN2-O(3)#1	2.015(4)	O(2)-P(2)-S(3B)	120.9(2)
ZN2-S(2)#1	2.2807(14)	C(13)-P(2)-S(3B)	118.9(2)

This intra- and inter molecular hydrogen bonding produces a one dimensional polymer that grows along the crystallographic *c* axis as shown in Figure 2.12. The TMEDA groups are arranged at the peripheral of the crystal packing of compound **3** along the crystallographic *c* axis.

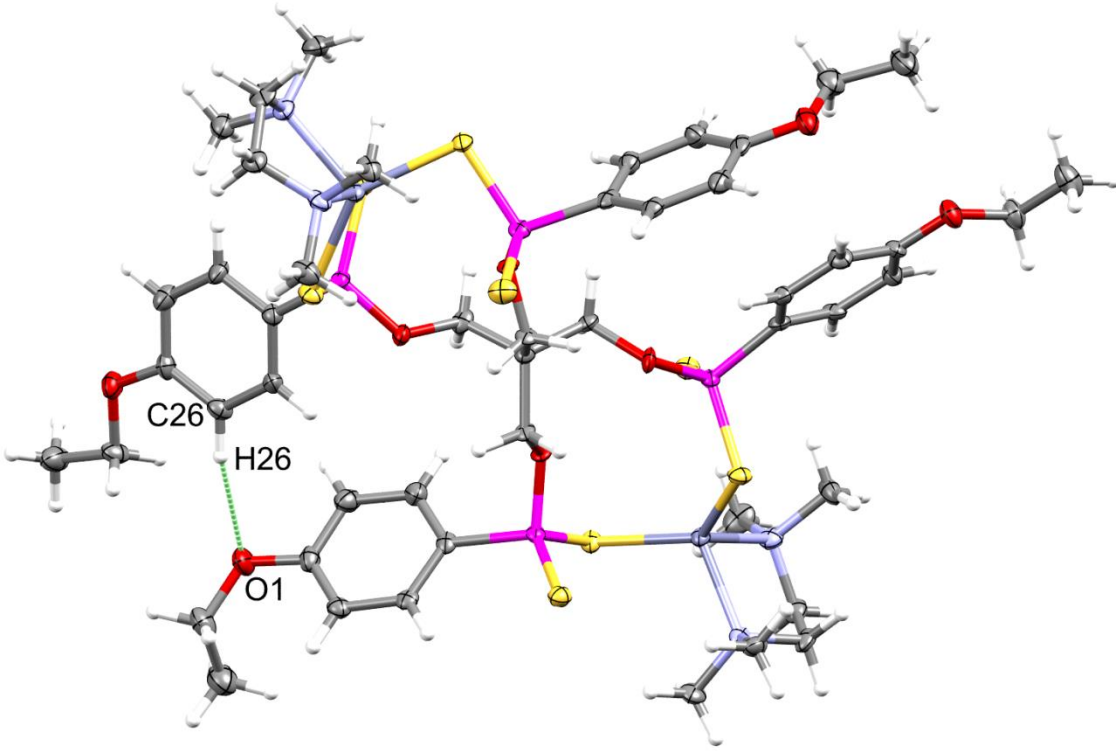

Figure 2.10: Molecular structure of compound **3** showing intra hydrogen bonding. Hydrogen atoms are omitted for clarity.

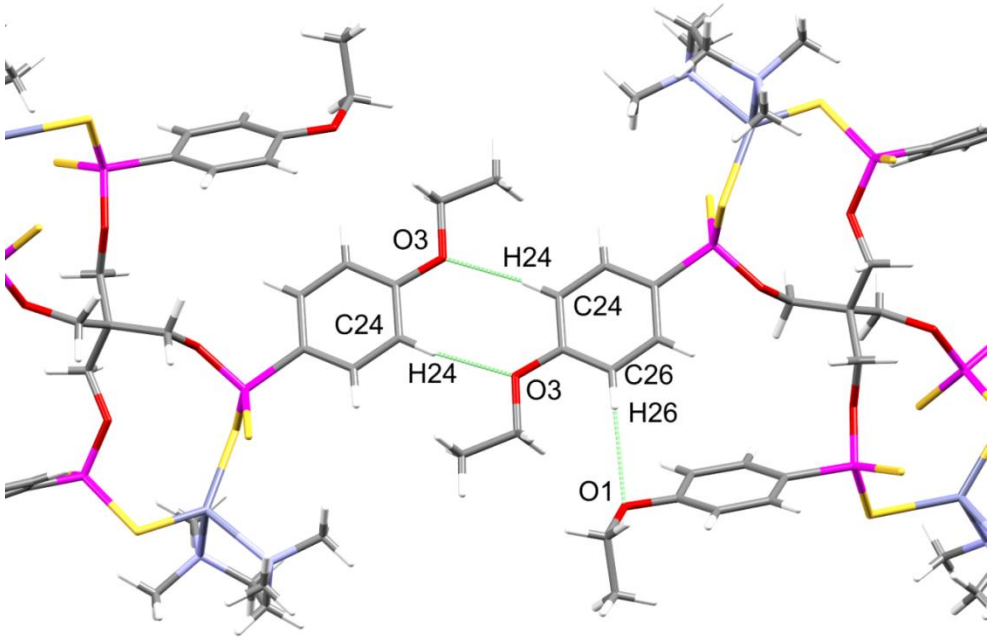

Figure 2.11: Molecular structure of compound **3** showing inter hydrogen bonding. Hydrogen atoms are omitted for clarity.

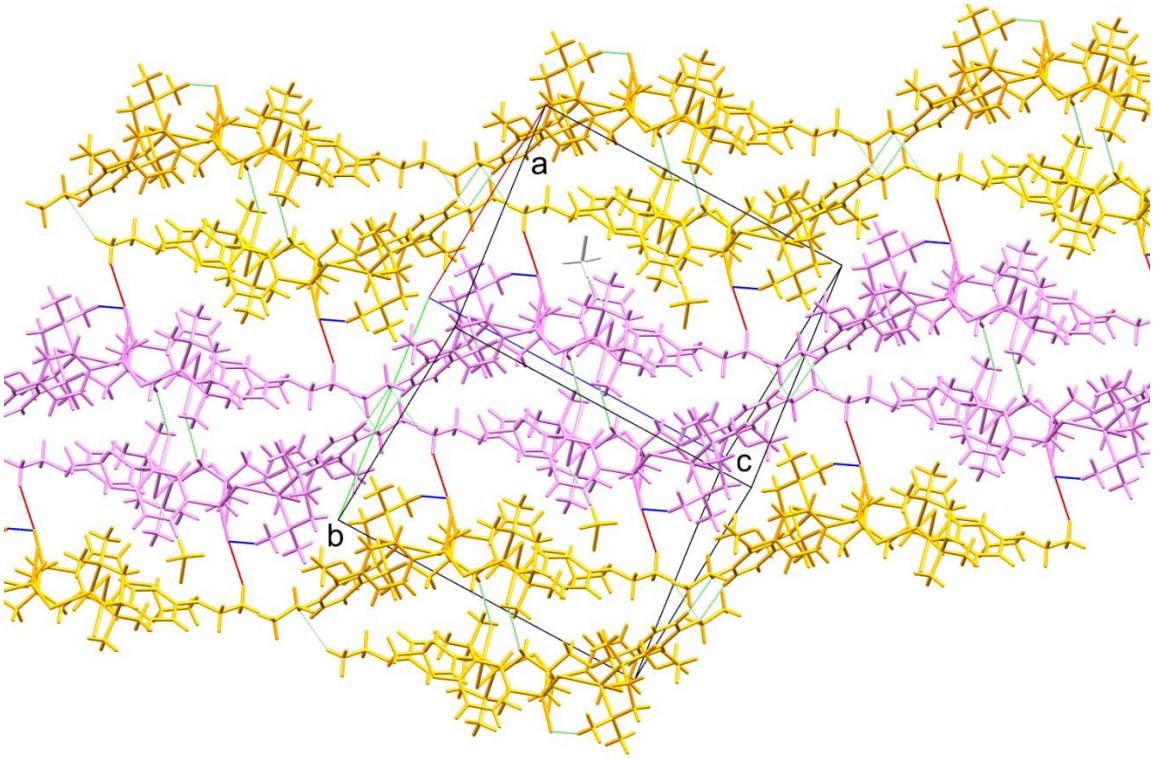

Figure 2.12: Crystal packing of compound **3**.

2.5 OPTICAL PROPERTIES

Previous studies[9-12] have shown that Zn(II) coordination complexes exhibit photoluminescence and taking into account the excellent luminescent properties of d^{10} metal complexes and bipyridine and phenanthroline ligands, the luminescence of compounds **7-10** were investigated as shown in Figure 2.13.

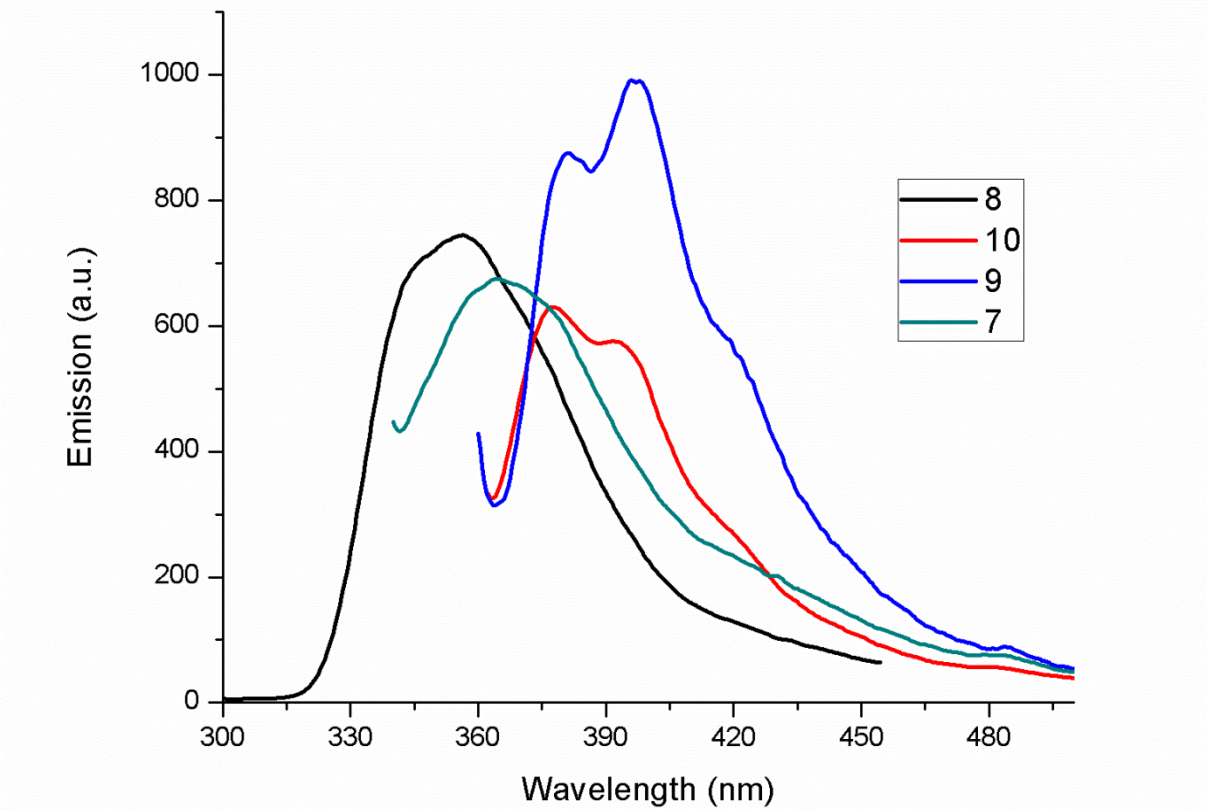

Figure 2.13: Solid state photoemission spectra of complexes **7–10** at room temperature.

The solid state luminescence of compounds **7-10** were done at room temperature based on their UV-Vis spectra (Figure 2.14).

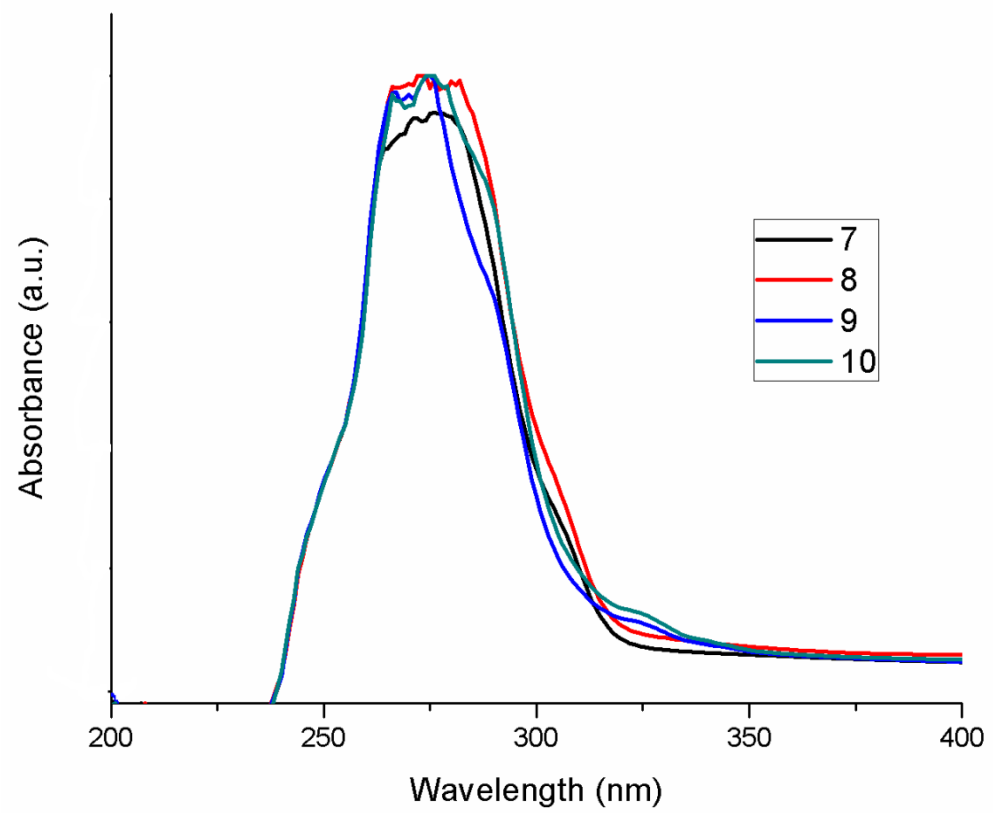

Figure 2.14: UV-Vis spectra of complexes **7-10** recorded in 10^{-6} M DMF solution.

The emissions of compounds **7-10** were observed between 315 to 480 nm (Figure 2.13) when excited between 320 to 330 nm. The emission intensity or maxima is higher for the compounds with the phenetole moiety compared to those with the ferrocenyl moiety. For example considering the compounds containing the phenanthroline zinc capping group, compound **9** (contains a phenetole group) has a higher emission intensity compared to that of compound **10** (contains a ferrocenyl group) as shown in Figure 2.13. On the other hand, for compounds with the bipyridinyl capping group, compound **7** (contains a phenetole group) has a higher emission maximum of 365 nm compared to that of compound **8** (contains a ferrocenyl group) with a maximum of 340 nm. This could be due to the luminescence quenching effect of the ferrocenyl moiety.[13-15] Compounds **1-6,** however, were not emissive. This suggests that the conjugated groups, phenanthroline and bipyridine, are responsible for the luminescence of complexes **7-10**. The fluorescent intensity of complexes with the phenanthroline moiety (compounds **9** and **10**) is higher

compared to those with the bipyridinyl group (Compounds **7** and **8**) which may be attributed to higher conjugation in the phenanthroline moiety compared to that of bipyridine.[16]

2.6 CONCLUSION

This chapter reported the synthesis and characterization of zinc dithiophosphonate heterocycles. The ring opening reaction of Phenetole Lawesson's reagent and its ferrocenyl dimer were exploited using pentaerythritol to synthesize these new complexes. The geometry of all the zinc complexes was distorted tetrahedral as indicated by the two complexes that were characterised by single crystal X-ray. The optical properties of some of these complexes were also studied and indicated that they could be useful candidates as co-sensitizers in DSSCs.

2.7 EXPERIMENTAL

2.7.1 METHOD

Unless otherwise noted, all reactions and manipulations were carried out under an inert atmosphere with a positive nitrogen gas flow using standard Schlenk lines and tubes. Standard Schlenk techniques are critical for these reactions and manipulations to minimize contact with atmospheric oxygen that can oxidize and/or reduce desired compounds.

2.7.2 MATERIALS

Phenetole Lawesson's reagent and ferrocenyl Lawesson's reagent were prepared according to established literature.[6] Tetramethylethylenediamine (TMEDA), ethylenediamine (EDA), bipyridine (Bipy) and phenanthroline (Phenan) zinc metal precursors were also prepared according to established literature.[9, 17] Phosphorus-pentasulfide, ferrocene, phenetole, tetramethylethylenediamine, ethylenediamine, bipyridine, phenanthroline and pentaerythritol were purchased from Sigma Aldrich and used without further purification. Ammonia gas was obtained from Afrox (South Africa). Diethyl ether, THF and hexane were distilled under dinitrogen over a Na wire with the formation of a benzophenone ketyl indicator. Dichloromethane was distilled over P_4O_{10}. Methanol and ethanol were distilled from I_2/Mg turnings.

2.7.3 CHARACTERIZATION METHODS

^{1}H and ^{31}P NMR spectra were recorded on a Bruker Avance 400 MHz spectrometer. NMR data are expressed in parts per million (ppm) and referenced internally to the residual proton impurity in the deuterated solvent whilst ^{31}P spectra chemical shifts are reported relative to an 85% H_3PO_4 in D_2O external standard solution, all at 298 K. Data are reported as chemical shift position (δ_H), multiplicity, relative integral intensity and assignment. Melting points were determined using a Stuart SMP3 melting point apparatus. Infrared spectra were recorded on a Perkin-Elmer Spectrum 100 FT-IR spectrometer. Mass spectral analyses were performed on a Waters API Quattro Micro spectrometer. UV-Vis spectra were recorded on UV-3600 Plus-UV-VIS-NIR spectrometer while the emission/excitation spectra were recorded on a Perkin–Elmer LS55 fluorescence spectrometer.

2.7.4 X-RAY STRUCTURE DETERMINATION

Crystals were mounted on glass fibers with epoxy resin, and all geometric and intensity data were collected on a Bruker APEXII CCD diffractometer equipped with graphite monochromated Mo-Ka radiation ($\lambda = 0.71073$ Å). The data reduction was carried out with SAINT-Plus software.[18] The SADABS program was used to apply empirical absorption corrections.[19] All structures were solved by direct methods and refined by full-matrix least-squares on F2 with SHELXTL software package[20] found in SHELXTL/PC version 5.10.[21] Thermal ellipsoid plots are generated with OLEX2.[22]

2.5 EXPERIMENTAL

Synthesis of $(NH_4)_4[C\{CH_2OPS_2(4\text{-}C_2H_5OC_6H_4)\}_4]$ (1)

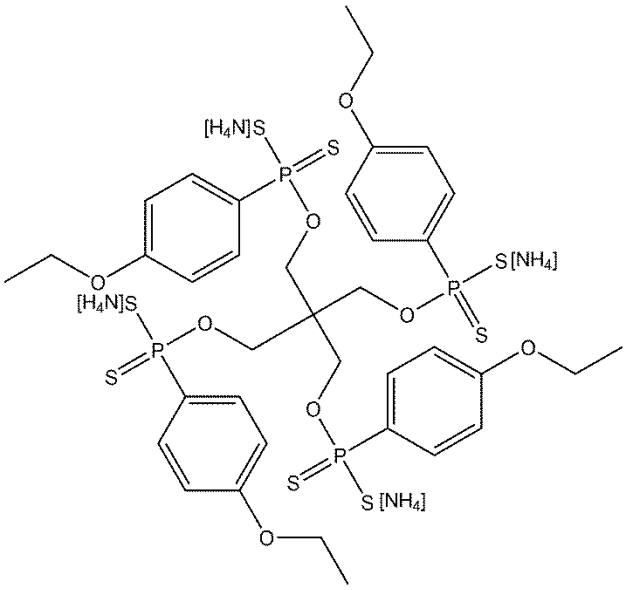

A 25 mL Schlenk tube equipped with a magnetic stirrer bar was charged with $\{PS(S)C_6H_4OC_2H_5\}_2$ (4.00 g, 9.25 mmol) and placed under vacuum for 30 minutes. The solid was then heated to 75°C and then pentaerythritol (0.63 g, 4.62 mmol) and toluene (3 mL) added. The temperature was maintained at 75°C until dissolution of all solids was observed. The ensuing solution was further heated at this temperature for another 20 minutes and then placed in ice bath for 15 minutes. Anhydrous ammonia was then bubbled into the solution slowly via a Pasteur pipette which formed an immediate precipitate. The sticky white solid was consolidated with hexane and a free flowing powder was obtained after removing the solvent under reduced pressure. Colourless solid was isolated. Yield: 6.0 g, 61%. M.p.: 168 °C. ^{1}H-NMR (400 MHz, DMSO-d_6, ppm): δ 1.31 (12H, t, *J*=6.94 Hz, Ar-CH_3), 3.79 (8H, d, *J*=5.16 Hz, Ar-OCH_2), 3.93 (8H, q, *J*=6.99 Hz, CH_2), 6.63 (8H, d, *J*=6.72 Hz, *m*-ArH), 7.73 (8H, dd, *J*=8.58, 12.63 Hz, *o*-ArH). ^{31}P NMR (400 MHz, DMSO-d_6, ppm): δ 103.40 (s). ^{13}C NMR (400 MHz, DMSO-d_6, ppm): δ 161.52, 161.49, 136.72, 135.58, 133.15, 133.02, 114.54, 114.40, 65.25, 64.56, 15.25. Selected FTIR (ν cm^{-1}): 2976 (m), 1568 (s), 1593 (s), 1496 (s), 1393 (m), 1245 (s), 994 (m). ESI-MS: $(M\text{-}4H)^+$ 1064.

Synthesis of $(NH_4)_4[C\{CH_2OPS_2(Fc)\}_4]$ (2)

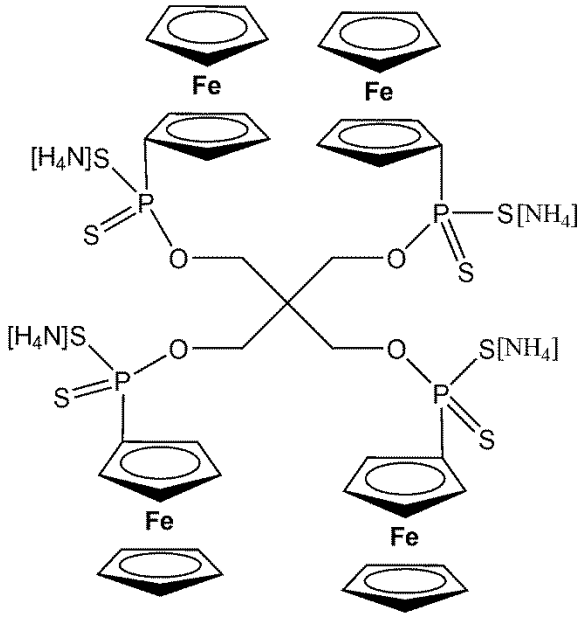

Synthesis of compound **2** was according to established literature.[5] A 25 mL Schlenk tube equipped with a magnetic stirrer bar was charged with FcLR (4.00 g, 9.25 mmol) and placed under vacuum for 30 minutes. The solid was then heated to 75°C and pentaerythritol (0.63 g, 4.62 mmol) in toluene (3 mL) added. The temperature was maintained at 75°C until dissolution of all solids was observed. The ensuing brown solution was further heated at this temperature for another 20 minutes and then placed in ice bath for 15 minutes. Anhydrous ammonia was bubbled into the solution slowly via a Pasteur pipette which formed an immediate precipitate. The ammonium salt was then dissolved in THF (10 mL), filtered through anhydrous $MgSO_4$/Celite yielding orange colored filtrate. The filtrate was then concentrated under reduced pressure. Ether was then added to precipitate the product once the yellow solution became concentrated. The product was filtered and washed with ether.

Synthesis of [{Zn(TMEDA)}$_2$C$_5$H$_8$O$_4$(C$_2$H$_5$OC$_6$H$_4$PS$_2$)$_4$] (3)

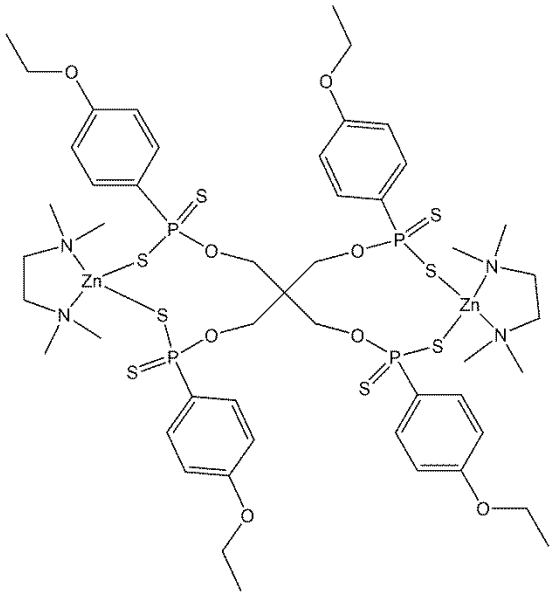

To a stirred solution of **1** (0.20 g, 0.019 mmol) dissolved in 20 mL of methanol was added drop-wise a solution of (TMEDA)$ZnCl_2$ (0.010 g, 0.037 mmol) in 20 mL of methanol. The resulting precipitate was allowed to stir for 30 minutes at room temperature, vacuum filtered, washed with de-ionized water and then diethyl ether. The colorless free flowing powder was isolated. Colourless solid was isolated. Yield: 0.18 g, 71% yield. M.p.: 198 °C (dec). ^{1}H NMR (400 MHz, $CDCl_3$, ppm): δ 1.43 (12H, t, *J*=6.96 Hz, Ar-CH_3), 2.62 (8H, s, N-CH_2), 2.68 (24H, s, N-CH_3), 4.03 (8H, q, *J*=6.95 Hz, Ar-CH_2), 4.35 (8H, d, *J*=7.64 Hz, CH_2), 6.77 (8H, q, *J*=3.92 Hz, *m*-ArH), 7.84 (8H, q, *J*=7.52 Hz, *o*-ArH). ^{31}P NMR (400 MHz, $CDCl_3$, ppm): δ 100.03 (s). ^{13}C NMR (400 MHz, DMSO-d_6, ppm): δ 133.90, 131.26, 131.13, 113.95, 113.79, 63.41, 57.38, 47.36, 14.75. Selected FTIR (ν cm^{-1}): 3281 (m), 2940 (m), 1595 (m), 1465 (m), 1252 (s), 1174 (s), 1108 (s), 1001 (s). ESI-MS: (M-2$C_6H_{18}N_2Zn$)$^+$ 1024.

Synthesis of $[\{Zn(EDA)\}_2C_5H_8O_4(C_2H_5OC_6H_4PS_2)_4]$ (4)

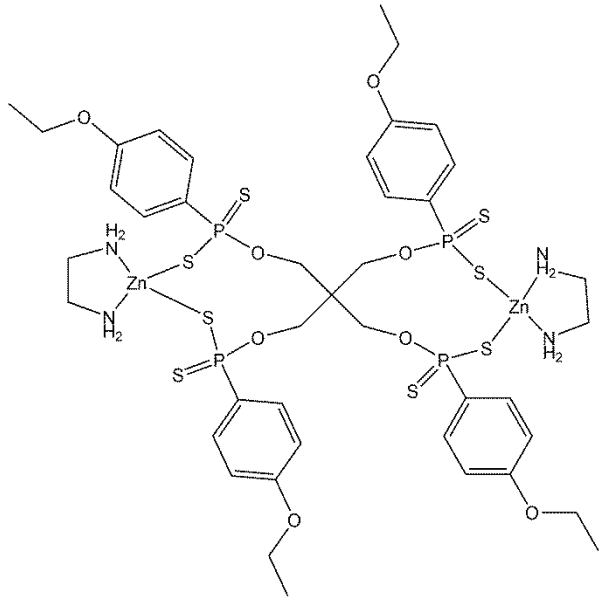

To a stirred solution of **1** (0.30 g, 0.28 mmol) dissolved in 30 mL of methanol was added drop-wise a solution of $(EDA)ZnCl_2$ (0.28 g, 0.94 mmol) in 30 mL of methanol. The resulting precipitate was allowed to stir for 30 minutes at room temperature, vacuum filtered, washed with de-ionized water and diethyl ether. The colorless free flowing powder was then isolated. Yield: 0.21 g, 60%. M.p.: 270 °C (dec). ^{1}H-NMR (400 MHz, DMSO-d_6, ppm): δ 1.34 (12H, t, *J*=7.04 Hz, Ar-CH_3), 2.63 (8H, s, N-CH_2), 3.79 (8H, q, *J*=9.55 Hz, CH_2), 4.05 (8H, q, *J*=6.68 Hz, N-CH_2), 6.86 (8H, m, *J*=3.72 Hz, *m*-ArH), 7.78 (8H, m, *J*=4.79 Hz, *o*-ArH). ^{31} P NMR (400 MHz, DMSO-d_6, ppm): δ 101.76 (s). ^{13}C NMR (400 MHz, DMSO-d_6): δ 161.52, 161.49, 136.72, 135.58, 133.15, 133.02, 114.54, 114.40, 65.25, 64.56, 15.25. Selected FTIR (ν cm^{-1}): 3282 (m), 2951 (m), 1595 (s), 1568 (s), 1495 (s), 1455 (m), 1252 (s), 1001 (s). ESI-MS: $(M\text{-}2C_6H_{18}N_2O_2Zn)^+$ 827.

Synthesis of [{Zn(Phenan)}$_2$C$_5$H$_8$O$_4$(C$_2$H$_5$OC$_6$H$_4$PS$_2$)$_4$] (5)

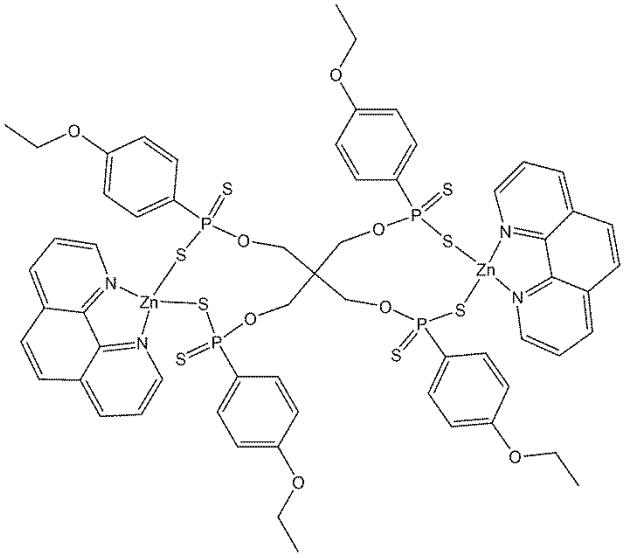

To a stirred solution of **1** (0.30 g, 0.28 mmol) dissolved in 40 mL of methanol was added drop-wise a solution of (Phenan)$ZnCl_2$ (0.18 g, 0.56 mmol) in 40 mL of methanol. The resulting precipitate was allowed to stir for 30 minutes at room temperature, vacuum filtered, washed with de-ionized water and diethyl ether. The colorless free flowing powder was then isolated. Yield: 0.21g, 50%. M.p.: 208 °C (dec). ^{1}H-NMR (400 MHz, DMSO-d_6, ppm): δ 1.28 (12H, t, J=6.94 Hz, Ar-CH_3), 3.78 (8H, d, J=7.08 Hz, CH_2), 3.94 (8H, q, J=5.62 Hz, Ar-OCH_3), 6.68 (8H, m, J=5.80 Hz, *m*-ArH), 7.70 (8H, m, J=6.56 Hz, *o*-ArH), 8.03 (4H, s, Ar-CH), 8.26 (4H, s, Ar-CH), 8.86 (4H, d, J=7.60 Hz, Ar-CH). ^{31} P NMR (400 MHz, DMSO-d_6, ppm): δ 102.34 (s). ^{13}C NMR (400 MHz, DMSO-d_6): δ 148.85, 139.70, 139.61, 131.22, 128.75, 127.13, 125.59, 112.77, 62.86, 14.55. Selected FTIR (ν cm^{-1}): 3280 (m), 2940 (m), 1595 (s), 1518 (s), 1495 (s), 1426 (s), 1105 (s), 1004 (s).ESI-MS: $(M-S)^+$ 1451.

Synthesis of [{Zn(Bipy) }$_2$$C_5H_8O_4(C_2H_5OC_6H_4PS_2)_4$] (6)

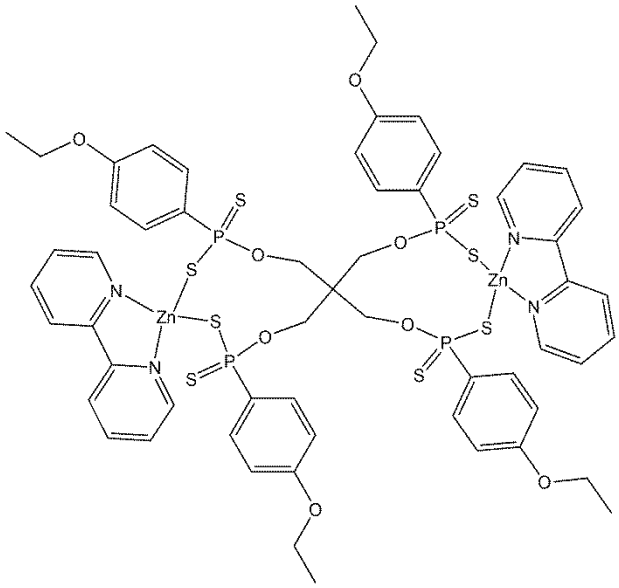

To a stirred solution of **1** (0.30 g, 0.28 mmol) dissolved in 40 mL of methanol was added drop-wise a solution of (Bipy)$ZnCl_2$ (0.16 g, 0.56 mmol) in 40 mL of methanol. The resulting precipitate was allowed to stir for 30 minutes at room temperature, vacuum filtered, washed with de-ionized water and diethyl ether. The colorless free flowing powder was then isolated. Yield: 0.33 g, 70%. M.p.:240 °C (dec). ^{1}H-NMR (400 MHz, DMSO-d_6, ppm): δ 1.36 (12H, t, J=6.96 Hz, Ar-CH_3), 3.89 (8, d, J=7.04 Hz, CH_2), 4.06 (8H, q, J=3.79 Hz, Ar-OCH_3), 6.87 (8H, q, J=3.78 Hz, *m*-ArH), 7.65 (4H, s, Ar-CH), 7.80 (8H, m, J=6.24 Hz, *o*-ArH), 8.17 (4H, s, Ar-CH), 8.57 (4H, s, Ar-CH), 8.73 (4H, s, Ar-CH). ^{31}P NMR (400 MHz, DMSO-d_6) δ: 97.55 (s). ^{13}C NMR (400 MHz, DMSO-d_6): δ 148.30, 139.15, 139.06, 130.68, 128.20, 126.59, 125.04, 112.23, 62.32, 14.01. Selected FTIR (ν cm^{-1}): 3281 (m), 2940 (m), 1596 (s), 1568 (m), 1494 (s), 1473 (s), 1443 (s), 1108 (s), 1004 (s). ESI-MS: $(M-2C10H8N2Zn)^+$ 1165.

Synthesis of $[\{Zn(TMEDA)\}_2C_5H_8O_4(FcPS_2)_4]$ (7)

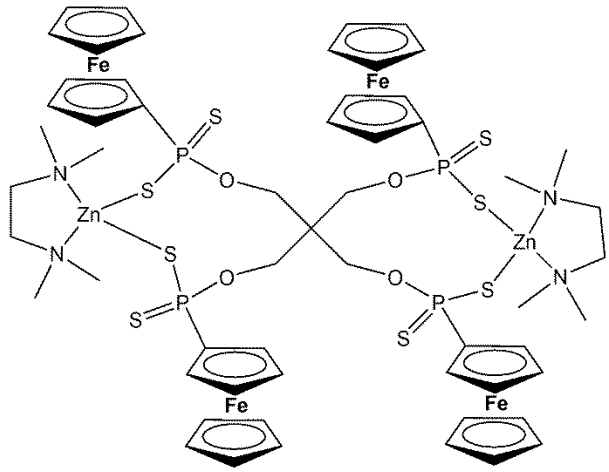

To a stirred solution of **2** (0.50 g, 0.47 mmol) dissolved in 40 mL of methanol was added drop-wise a solution of $(TMEDA)ZnCl_2$ (0.28 g, 0.94 mmol) in 40 mL of methanol. The resulting precipitate was allowed to stir for 30 minutes at room temperature, vacuum filtered, washed with de-ionized water and diethyl ether. The yellow free flowing powder was then isolated. Yield: 0.14 g, 84%. M.p.:332 °C (dec). ^{1}H NMR (400 MHz, $CDCl_3$): δ 2.64 (24H, s, N-CH_3), 2.74 (8H, s, N-CH_2), 3.86 (8H, d, J=7.04 Hz, CH_2), 4.23 (3H, d, J=9.85 Hz, Fc), 4.34 (20H, s, Fc), 4.55 (7H, d, J=17.21 Hz, Fc), 4.66 (3H, s, Fc), 4.76 (3H, s, Fc). ^{31}P NMR (400 MHz, $CDCl_3$): δ 95.29 (s). ^{13}C NMR (400 MHz, DMSO-d_6): δ 69.83, 69.56, 57.65, 57.58, 48.70, 48.64, 27.23. Selected FTIR (ν cm^{-1}): 3281 (m), 2948 (m), 1573 (m), 1456 (s), 1412 (m), 1176 (m), 1003 (s), 819 (s). ESI-MS: $(M\text{-}Fc)^+$ 1484.

Synthesis of $[\{Zn(EDA)\}_2C_5H_8O_4(FcPS_2)_4]$ (8)

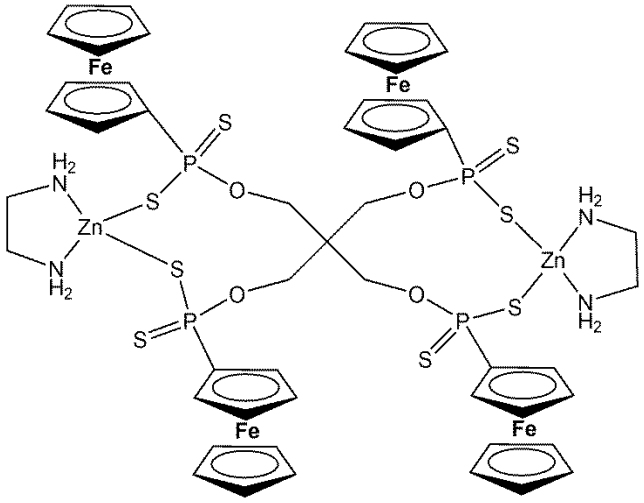

To a stirred solution of **2** (0.20 g, 0.15 mmol) dissolved in 40 mL of ethanol was added drop-wise a solution of $(EDA)ZnCl_2$ (0.015 g, 0.076 mmol) in 40 mL of ethanol. The resulting precipitate was allowed to stir for 30 minutes at room temperature, vacuum filtered, washed with de-ionized water and diethyl ether. The yellow free flowing powder was then isolated. Yield: 0.17 g, 75%. M.p.: 240 °C (dec). ^{1}H-NMR (400 MHz, $CDCl_3$): δ 2.65 (8H, s, N-CH_2), 3.86 (8H, d, J=7.06 Hz, CH_2), 4.45 (3H, d, J=9.75 Hz, Fc), 4.56 (20H, s, Fc), 4.77 (7H, d, J=17.21 Hz, Fc), 4.88 (3H, s, Fc), 4.99 (3H, s, Fc). ^{31}P NMR (400 MHz, $CDCl_3$): δ 101.42 (s). ^{13}C NMR (400 MHz, DMSO-d_6): δ 69.67, 69.47, 69.21, 47.97, 47.13, 39.33. Selected FTIR (ν cm^{-1}): 3281 (m), 3230 (m), 2952 (m), 1573 (m), 1454 (s), 1412 (w), 1338 (m), 1128 (s), 1004 (s), 820 (s). ESI-MS: $(M\text{-}2C6H28N2)^+$ 1355.

Synthesis of $[\{Zn(Phenan)\}_2C_5H_8O_4(FcPS_2)_4]$ (9)

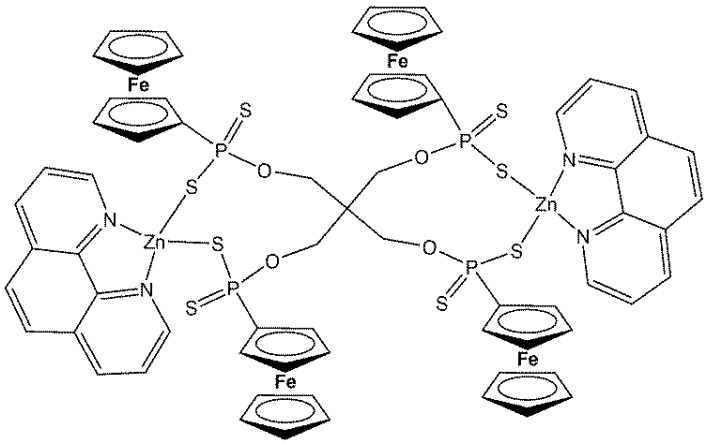

To a stirred solution of **2** (0.30 g, 0.23 mmol) dissolved in 30 mL of ethanol was added drop-wise a solution of (Phenan)$ZnCl_2$ (0.14 g, 0.45 mmol) in 30 mL of ethanol. The resulting precipitate was allowed to stir for 30 minutes at room temperature, vacuum filtered, washed with de-ionized water and diethyl ether. The yellow free flowing powder was then isolated. Yield: 0.15 g, 38%. M.p.: 322 °C (dec). ^{1}H-NMR (400 MHz, DMSO-d_6, ppm): δ 1H-NMR ($CDCl_3$) 3.81 (8H, d, J=7.04 Hz, CH_2), 4.21 (3H, d, J=9.75 Hz, Fc), 4.32 (20H, s, Fc), 4.53 (7H, d, J=17.21 Hz, Fc), 4.64 (3H, s, Fc), 4.75 (3H, s, Fc), 7.79 (4H, t, J=5.63 Hz, Ar-CH), 8.05 (4H, s, Ar-CH), 8.59 (4H, s, Ar-CH), 8.83 (4H, s, Ar-CH). ^{31} P NMR (400 MHz, $CDCl_3$): δ 106.52 (s). ^{13}C NMR (400 MHz, DMSO-d_6): 148.86, 139.75, 139.58, 128.75, 127.13, 125.56, 69.68, 68.46. Selected FTIR (ν cm^{-1}): 3277 (m), 2940 (m), 1573 (s), 1455 (m), 1138 (m), 1004 (s), 819 (s). ESI-MS: $(M\text{-}C_{12}H_8N_2)^+$ 1021.

Synthesis of [{Zn(Bipy) }$_2$$C_5H_8O_4(FcPS_2)_4$] (10)

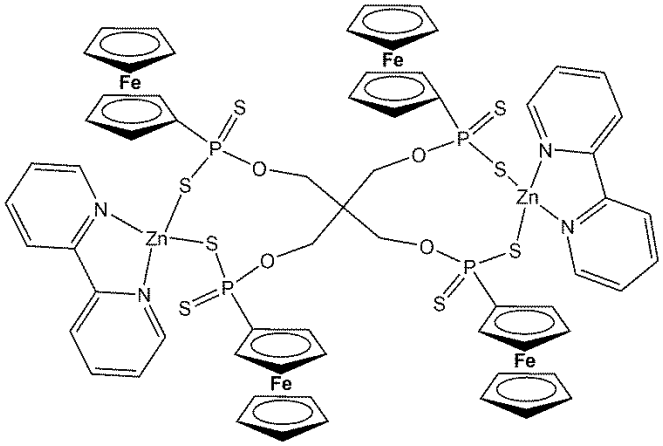

To a stirred solution of **1** (0.50 g, 0.47 mmol) dissolved in 40 mL of methanol was added drop-wise a solution of (Bipy)$ZnCl_2$ (0.28 g, 0.94 mmol) in 40 mL of methanol. The resulting precipitate was allowed to stir for 30 minutes at room temperature, vacuum filtered, washed with de-ionized water and diethyl ether. The colorless free flowing powder was then isolated. Yield: 0.21 g, 55%. M.p.: 260 °C (dec). ^{1}H-NMR (400 MHz, $CDCl_3$): δ 1H-NMR ($CDCl_3$) 3.89 (8H, d, J=7.04 Hz, CH_2), 4.21 (3H, d, J=9.88 Hz, Fc), 4.32 (20H, s, Fc), 4.53 (7H, d, J=17.27 Hz, Fc), 4.63 (3H, s, Fc), 4.74 (3H, s, Fc), 7.84 (4H, s, Ar-CH), 8.34 (4H, s, Ar-CH), 8.76 (4H, d, J=7.37 Hz, Ar-CH), 8.98 (4H, d, J=3.62 Hz, Ar-CH). ^{31}P NMR (400 MHz, $CDCl_3$): δ 105.38 (s). ^{13}C NMR (400 MHz, DMSO-d_6): δ 151.34, 143.18, 129.11, 124.80, 69.68, 69.47, 69.31, 69.21, 65.83. Selected FTIR (ν cm^{-1}): 3281 (m), 2952 (m), 1598 (s), 1573 (s), 1444 (s), 1177 (m), 1005 (s), 819 (s). ESI-MS: $(1/2M\text{-}Fc)^+$ 829.

2.6 REFERENCES

1. I. Haiduc, *J. of Organomet Chem*, **2001**, 623, 29-42.
2. T. Nishio, *Tetrahedron lett*, **1995**, 36, 6113-6116.
3. I. P. Gray, H. L. Milton, A. M. Slawin and J. D. Woollins, *Dalton Trans*, **2003**, 3450-3457.
4. M. S. J. Foreman, A. M. Slavin and J. D. Woollins, *Hetero Chem*, **1999**, 10, 651-657.
5. M. N. Pillay, H. van der Walt, R. J. Staples and W. E. van Zyl, *J. of Organomet Chem*, **2015**, 794, 33-39.
6. W. E. Van Zyl and J. P. Fackler, *Phos, Sulfur, and Silicon and the Relat Elem*, **2000**, 167, 117-132.
7. L. Thomas and R. A. Chittenden, *Spectrochimica Acta*, **1964**, 20, 489-502.
8. B. K. Santra, B.-J. Liaw, C.-M. Hung, C. Liu and J.-C. Wang, *Inorg Chem*, **2003**, 42, 8866-8871.
9. G. H. Eom, H. M. Park, M. Y. Hyun, S. P. Jang, C. Kim, J. H. Lee, S. J. Lee, S.-J. Kim and Y. Kim, *Polyhedron*, **2011**, 30, 1555-1564.
10. X.-L. Chen, B. Zhang, H.-M. Hu, F. Fu, X.-L. Wu, T. Qin, M.-L. Yang, G.-L. Xue and J.-W. Wang, *Crystal Growth and Design*, **2008**, 8, 3706-3712.
11. Y.-W. Dong, R.-Q. Fan, P. Wang, L.-G. Wei, X.-M. Wang, S. Gao, H.-J. Zhang, Y.-L. Yang and Y.-L. Wang, *Inorg Chem*, **2015**, 54, 7742-7752.
12. M. Allendorf, C. Bauer, R. Bhakta and R. Houk, *Chem Soc Rev*, **2009**, 38, 1330-1352.
13. D. Albagli, G. Bazan, R. Schrock and M. Wrighton, *The J. of Phy Chem*, **1993**, 97, 10211-10216.
14. D. Dorokhin, N. Tomczak, A. H. Velders, D. N. Reinhoudt and G. J. Vancso, *J. Phys. Chem C*, **2009**, 113, 18676-18680.
15. X.-B. Xia, Z.-F. Ding and J.-Z. Liu, *J. of Photochem and Photobio A: Chem*, **1995**, 88, 81-84.
16. K.-L. Zhang, H.-Y. Gao, Z.-C. Pan, W. Liang and G.-W. Diao, *Polyhedron*, **2007**, 26, 5177-5184.
17. D. J. Awad, F. Conrad, A. Koch, U. Schilde, A. Pöppl and P. Strauch, *Inorganica Chimica Acta*, **2010**, 363, 1488-1494.
18. V. SAINT, *Siemens Analytical Instruments Division, Madison, WI*, **1995**.

19. G. Sheldrick, *University of Göttingen, Germany*, **2010**.

20. G. Sheldrick, *University of Göttingen, Germany*, **1997**.

21. V. SHELXTL, *Inc., Madison, WI*, **2001**.

22. C. Júnior and P. de Sousa, Universidade de São Paulo, **2017**.

CHAPTER 3

SYNTHESIS AND CHARACTERIZATION OF NEW DITHIOPHOSPHONATE COMPOUNDS

3.1 INTRODUCTION

Organodithio- derivatives of phosphorus have been widely studied since the beginning of the twentieth century.[1-3] These compounds have found use in academic research, industry and agriculture. This chapter describes new dithiophosphonate complexes obtained from the reaction between PhLR or FcLR with diphenylmethanol. The chapter also reports on the characterization of these compounds and discussion of experimental data obtained. The photoluminescence of some of the complexes were also investigated. The anti-bacterial susceptibility screenings of these compounds are reported in Chapter 7.

3.2 RESULTS AND DISCUSSION

3.2.1 Synthesis

Symmetrical cleavage of PhLR or FcLR, $[ArP(S)(\mu\text{-}S)]_2$ (Ar = p-$C_2H_5OC_6H_4$ or Fc=$Fe(C_5H_4)(\eta^5\text{-}C_5H_5)$) with diphenylmethanol generates $[ArP(OR)S_2]^-$, which can act as a bidentate ligand.[4] The phosphonodithioate salts **12** and **13** were prepared by the reaction of FcLR/PhLR with 2 molar equivalents of diphenylmethanol. Diphenylmethanol was heated with PhLR or FcLR in small amounts of toluene at 70°C. The reaction was essentially complete once dissolution of all solids took place. The formed dithiophosphonic acids were deprotonated *in-situ* with the weak base ammonia at 0°C (ice bath) forming dithiophosphonate salt derivatives **12** and **13** as shown in Scheme 3.1.

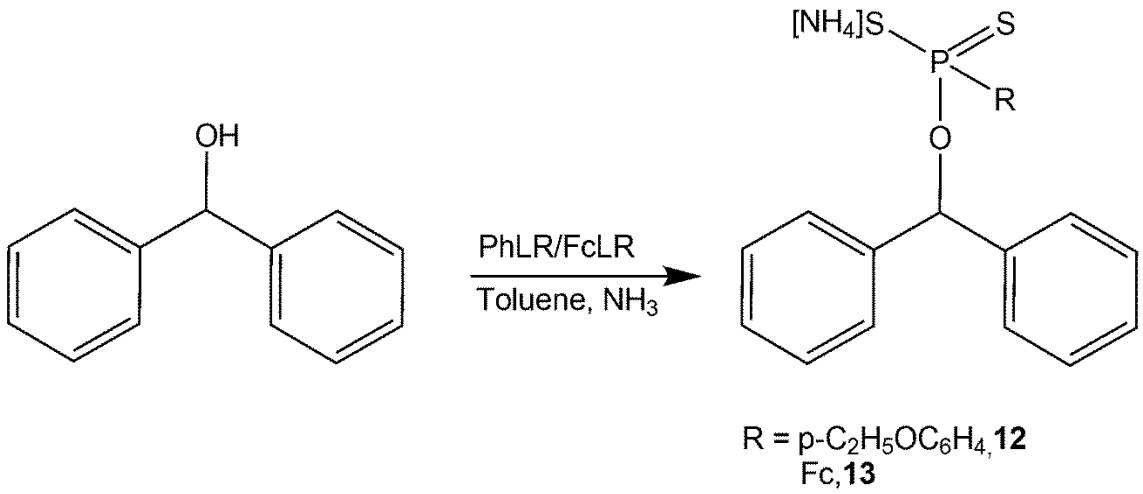

Scheme 3.1: Synthesis of compounds **12** and **13**.

Ligands **12** and **13** were found to be stable and could be stored indefinitely under a N_2 atmosphere. Prolonged exposure of **12** and **13** to air eventually lead to the release of H_2S due to oxidation and hydrolysis. Ligands **12** and **13** are hygroscopic. The reaction between **12** and **13** with Ni(II), Zn(II), or Cd(II) metal precursors afforded a series of new metal dithiophosphonate complexes as shown in Scheme 3.2. In all cases, to a dissolved solution of **12** or **13** in methanol was added dropwise a solution of the metal precursor also dissolved in methanol yielding an immediate precipitate. Compounds **12**, **14, 16** and **18** were obtained as colourless solids while **13**, **15, 17** and **19** as yellow solids.

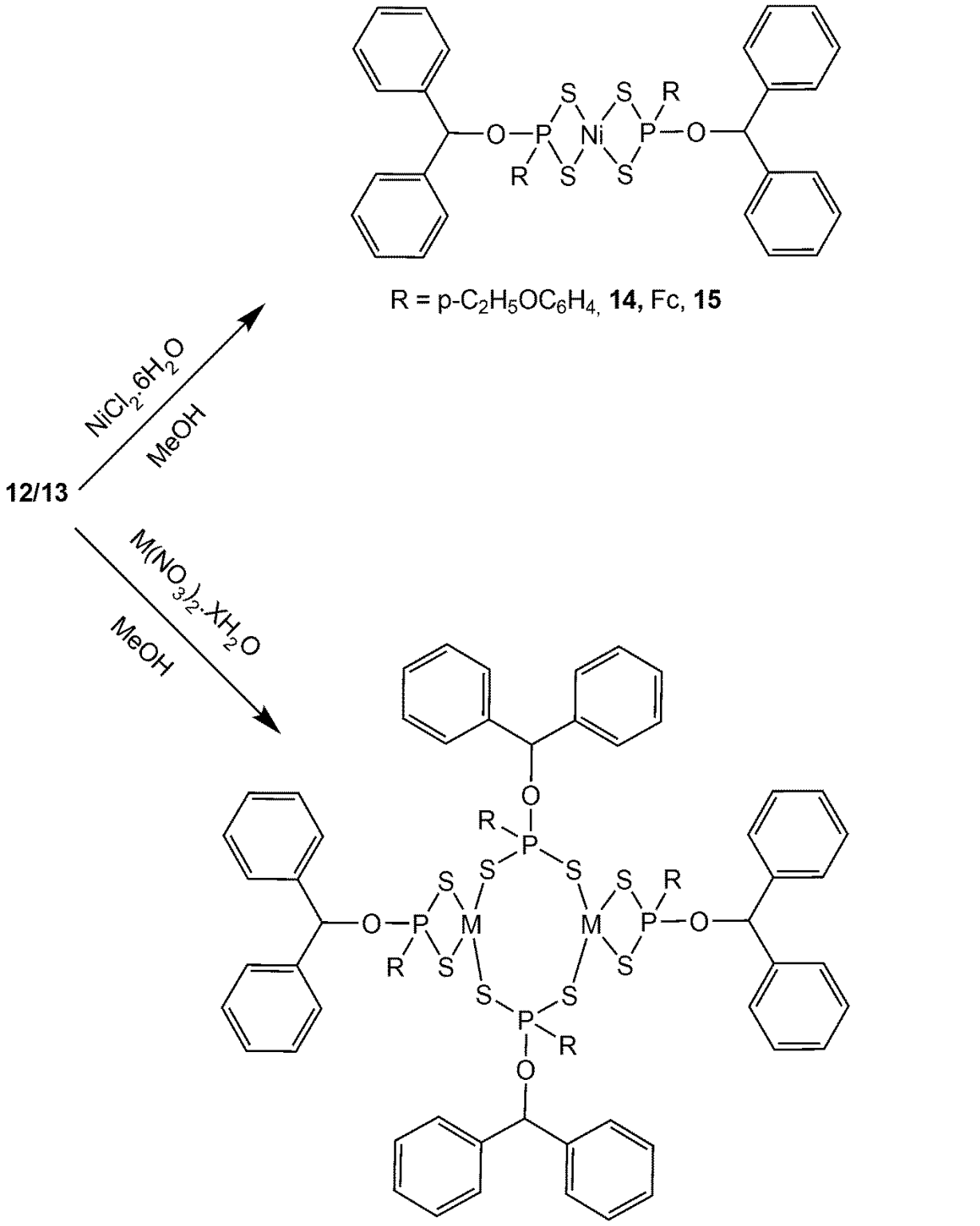

Scheme 3.2: Synthesis of compounds **14** to **19**.

3.2.2 Spectroscopy

The ^{1}H NMR of compounds **12-19** was well resolved and integrated to the number of the corresponding hydrogen atoms in all cases. The ^{1}H NMR spectra of the phenetolic groups and the phenyl rings of the diphenylmethanol appear in the aromatic region of between 6 and 8 ppm. Comparisons of the ^{1}H NMR of the ligands (**12** and **13**) to that of the complexes (**15 - 18**) showed a slight shift in proton peaks suggestive of complexation. The unsubstituted cyclopentadienyl ring in all cases gave a singlet peak, with the substituted ring giving two sets of signals for the pair of equivalent protons for the compounds. Fackler and Van Zyl reported in 2000 that ^{31}P NMR of dithiophosphonates is obtained in the region of about 90 to 112 ppm. The ^{31}P NMR of all compounds was obtained as singlets and fall within the expected region. ^{31}P NMR can also be a good indicator of complexation. For example the shift in ^{31}P NMR of about 7 ppm from 107 ppm for the ligand (**12)** to 100 ppm for compound (**14)** as shown in Figures 3.1 and 3.2 suggest complex formation. The appearance of the ^{31}P NMR as singlets suggests that compounds **12** to **19** exist in single isomer conformation in solution. Table 3.1 gives the ^{31}P NMR, yield and melting of compounds **12 - 19**. The IR spectra show distinct bands at 1185–1179 cm^{-1}, 1028–1025 cm^{-1}, 678–674 cm^{-1} and 559–557 cm^{-1}, corresponding to ν[(P)–O–C], ν[P–O–(C)], $\nu(PS)_{asym}$ and $\nu(PS)_{sym}$ absorptions, respectively.[5] The prominent band around 2974 cm^{-1} corresponding to the NH_4^+ (ligands **12** and **13**) disappears in the complexes (complexes **14-19**) suggesting complexation. Electrospray ionization (negative) mass spectrometry (ES-MS) was obtained for compounds **12 – 19**. ESI-MS of ligand **12** showed a peak at m/z 399 corresponding to $(M\text{-}NH_4)^+$ while that of ligand **13** gave m/z 466 corresponding to $(M\text{-}NH_4)^+$. The ESI-MS of complexes **14 – 19** gave fragmented ions. Compounds **12-13, 16**, **18-19** melt at different temperatures ranging from 106 to159 °C while compounds **14, 15** and **17** decompose to black solids at different temperatures (Table 3.1).

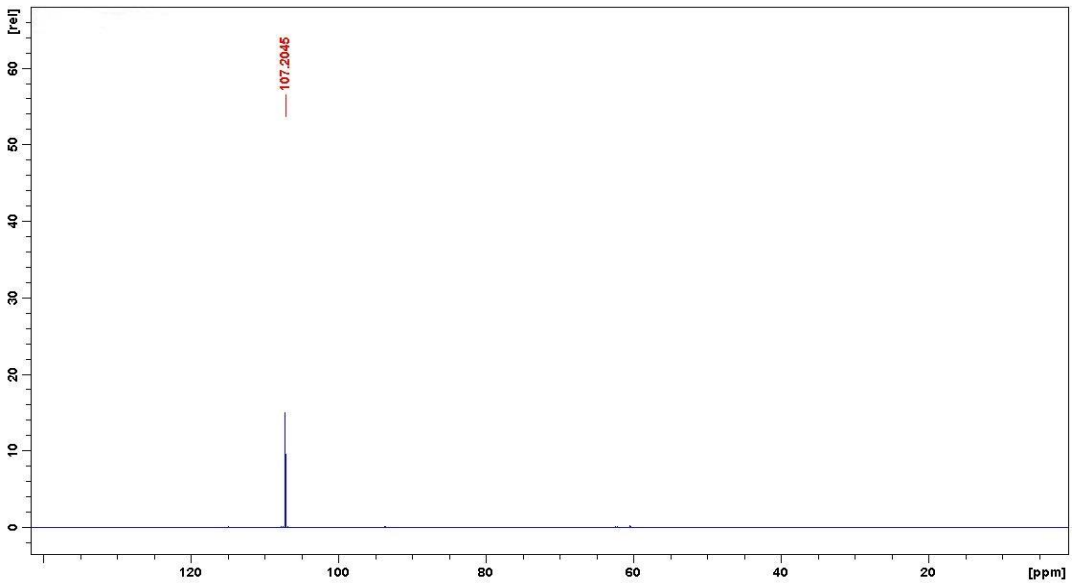

Figure 3.1: ^{1}H NMR spectrum of compound **12**.

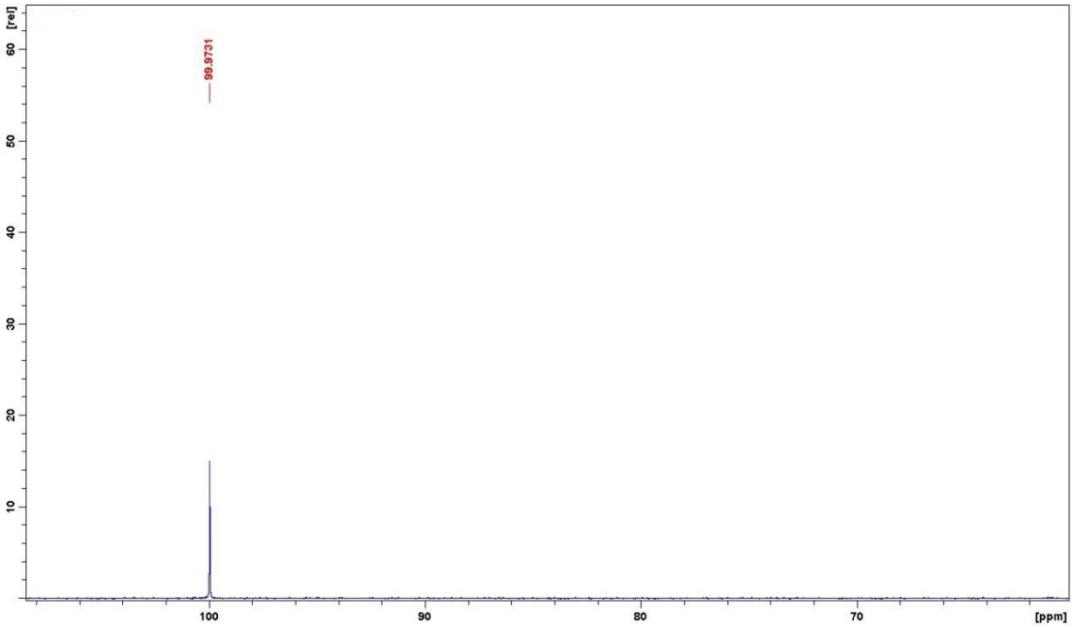

Figure 3.2: ^{1}H NMR spectrum of compound **14**.

Table 3.1: Yield, melting point, ^{31}P NMR data and colour of compounds **12-19**.

Compound	Yield(%)	Melting point (°C)	^{31}PNMR/ppm	Colour
12	71	106	107.24	Colourless
13	64	116	108.38	Yellow
14	87	123[d]	99.97	Colourless
15	63	140[d]	108.38	Colourless
16	49	132	106.29	Colourless
17	36	142[d]	108.38	Yellow
18	42	159	78.90	Yellow
19	44	123	109.89	Yellow

d = decompose

3.2.3 Solubility studies

Solubility of compounds is important because such information is not only useful for spectroscopic studies but also for preparative aid.[6] For example the solubility of compounds **12-19** in common solvents like DCM, Hexane, $CHCl_3$, DMF, DMSO, THF, CH_3OH etc will be useful in characterizing these complexes by solution ^{31}P NMR, ^{1}H NMR, UV, X-ray crystallography and even in complexation.

Considering this background, compounds **12-19** were qualitatively tested for solubility with different solvents of varying polarity and dielectric constants. Tesed solubility data of compounds **12-19** are given in Table 3.2 and this data is based on the criteria of dissolving a specified amount (0.03 g) of the compound of interest in the relevant solvent (0.2 mL), shaking for 10 seconds and then filtration at 25°C.

Table 3.2: Solubility test for compounds **12-19**.

Compound	H_2O	DCM	Hexane	Toluene	MeOH	EtOH	DMF	DMSO	CH_3CN
12	VS	I	I	I	VS	VS	VS	VS	I
13	VS	I	I	I	VS	VS	VS	VS	I
14	I	S	I	I	I	I	VS	VS	I
15	I	S	I	I	I	I	VS	VS	I
16	I	S	I	I	I	I	VS	VS	I
17	I	S	I	I	I	I	VS	VS	I
18	I	S	I	I	I	I	VS	VS	I
19	I	S	I	I	I	I	VS	VS	I

I = insoluble. PS = partly soluble. S = soluble. VS = very soluble. The symbol I means the compound is quantitatively recovered after filtration, PS means small amount of the compound (about 10%) is dissolved, S means a large amount of the compound is dissolved (about 80%) and VS means a clear solution of the compound emerged immediately.

Ligands **12** and **13** are soluble in polar solvents and insoluble in non-polar solvents, while complexess **14-19** are soluble in DCM, DMF and DMSO and insoluble in polar solvents. The solubility of the starting materials (metal precursors) and compounds **12-19** played an important role in the preparation of these complexes. For example, the starting materials and compounds **12** and **13** are soluble in polar solvents such as methanol and this was exploited in the complexation of complexes **14-19** which are not soluble in polar solvents. By-products of this complexations (NH_4Cl) was easily removed in one step due to solubility in polar solvents.

3.2.4 Solid state structures

Figure 3.3 gives a perspective view of the molecular structure of compound **14** while Tables 3.2 and 3.3 give important X-ray crystallographic data, parameters and selected bond lengths, angles respectively.

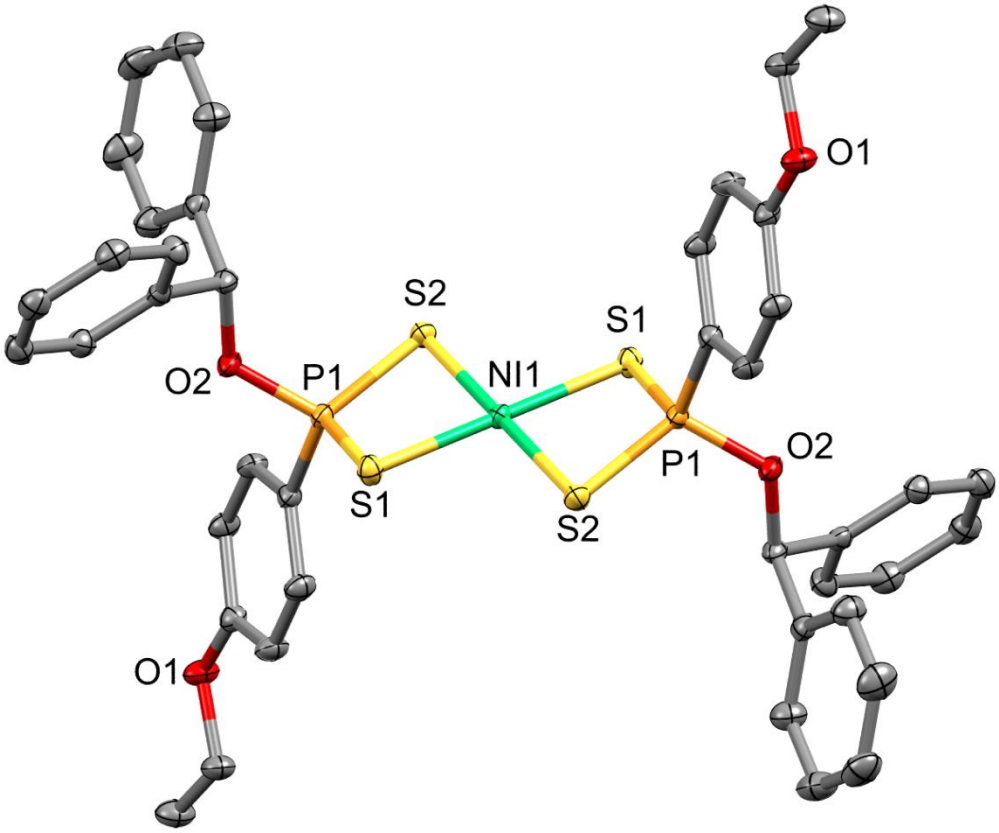

Figure 3.3: Molecular structure of **14**, thermal ellipsoids drawn at the 50% probability. Hydrogen atoms are omitted for clarity.

Single crystals suitable for X-ray analysis of **14** were obtained by layering of hexane on a concentrated solution of compound **14** dissolved in DCM. Compound **14** crystallizes in the triclinic space group *P-1* with 1 molecule per asymmetric unit cell.

Table 3.3: X-ray crystallographic data for compounds **14**.

Compound	**14**
Empirical formula	C_{42} H_{40} Ni O_4 P_2 S_4
Formula weight	857.63
Temperature	100(2) K
Wavelength	0.71073 Å
Crystal system	Triclinic
Space group	*P -1*
Unit cell dimensions	a = 8.9611(2) Å
	b = 9.5520(2) Å
	c = 12.0497(3) Å
	α= 102.9240(10)°
	β = 94.856(2)°
	γ = 94.381(3)°
Volume	996.84(4) $Å^3$
Z	1
Density (calculated)	1.429 Mg/m^3
Crystal size	0.306 x 0.121 x 0.108 mm^3

Table 3.4: Selected bond lengths (Å) and angles (°) for compound **14**.

Compound 14			
O(2)-P(1)	1.5970(9)	O(1)-C(4)-C(3)	124.39(12)
P(1)-S(1)	1.9992(4)	O(1)-C(4)-C(7)	115.49(11)
P(1)-S(2)	2.0051(5)	O(1)-C(5)-C(6)	107.48(11)
P(1)-NI1	2.8076(3)	O(1)-C(5)-H(5A)	110.2
S(1)-NI1	2.2270(3)	O(1)-C(5)-H(5B)	110.2
S(2)-NI1	2.2317(3)	O(2)-C(9)-C(16)	108.94(10)
NI1-S(1)#1	2.2270(3)	O(2)-C(9)-C(10)	108.59(10)
NI1-S(2)#1	2.2317(3)	O(2)-C(9)-H(9)	109.2
NI1-P(1)#1	2.8077(3)	C(4)-O(1)-C(5)	117.22(10)
S(2)-P(1)-NI1	52.060(12)	C(9)-O(2)-P(1)	120.50(8)
P(1)-S(1)-NI1	83.076(15)	O(2)-P(1)-C(1)	99.33(5)
P(1)-S(2)-NI1	82.821(14)	O(2)-P(1)-S(1)	114.31(4)
S(1)-NI1-S(1)#1	180.0	C(1)-P(1)-S(1)	114.37(5)
S(1)-NI1-S(2)	88.492(12)	O(2)-P(1)-S(2)	112.83(4)
S(1)#1-NI1-S(2)	91.508(12)	C(1)-P(1)-S(2)	114.69(5)
S(1)-NI1-S(2)#1	91.509(12)	S(1)-P(1)-S(2)	101.957(19)
S(1)#1-NI1-S(2)#1	88.491(12)	O(2)-P(1)-NI1	141.51(4)
S(2)-NI1-S(2)#1	180.0	C(1)-P(1)-NI1	119.15(4)
S(1)-NI1-P(1)	44.981(11)	S(1)-P(1)-NI1	51.943(12)
S(1)#1-NI1-P(1)	135.019(10)	P(1)-NI1-P(1)#1	180.0
S(2)-NI1-P(1)	45.119(11)	S(2)#1-NI1-P(1)#1	45.119(11)
S(2)#1-NI1-P(1)	134.881(11)	S(2)-NI1-P(1)#1	134.881(11)
S(1)-NI1-P(1)#1	135.019(11)	S(1)#1-NI1-P(1)#1	44.981(11)

The X-ray structure of compound **14** revealed a square planar geometry with symmetric MS_2P rings which is consistent with related studies[7-9] and contrasts to others[10] where the P-S bond lengths are unsymmetrical. The phenetolic groups (p-$C_2H_5OC_6H_4$) of the two ligands are arranged above and below the metal coordination plane resulting in a *'trans'* arrangement. This geometry is usually favourable for Ni(II) dithiophosphonate complexes because it gives room for less steric hindrance and hence higher stability compared to the *'cis'* conformation

3.3 SOLID STATE LUMINESCENSE

Previous studies[11-14] have shown that d^{10} systems exhibit photoluminescence and the solid state luminescence of complexes **16 -19** was therefore investigated. The solid state emissions of complexes **16** and **18** were observed between 390 to 510 nm (Figures 3.4 and 3.5) when excited at 227 and 210 nm respectively.

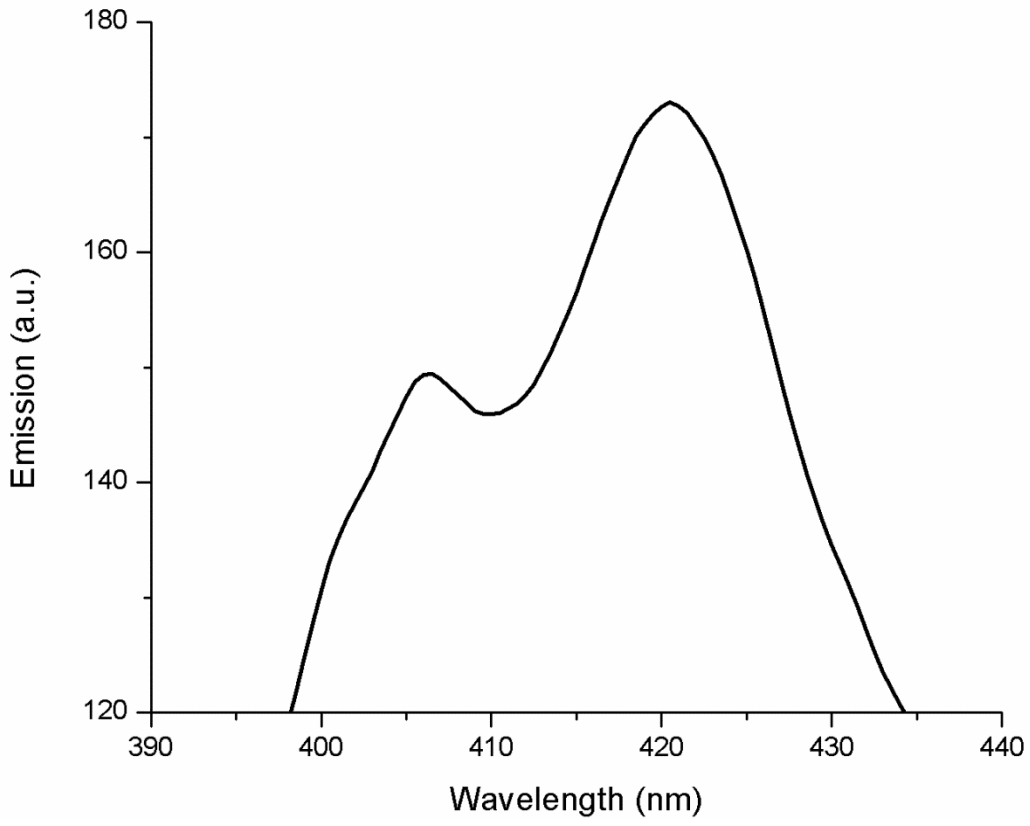

Figure 3.4: Solid state luminescence of compound **16**.

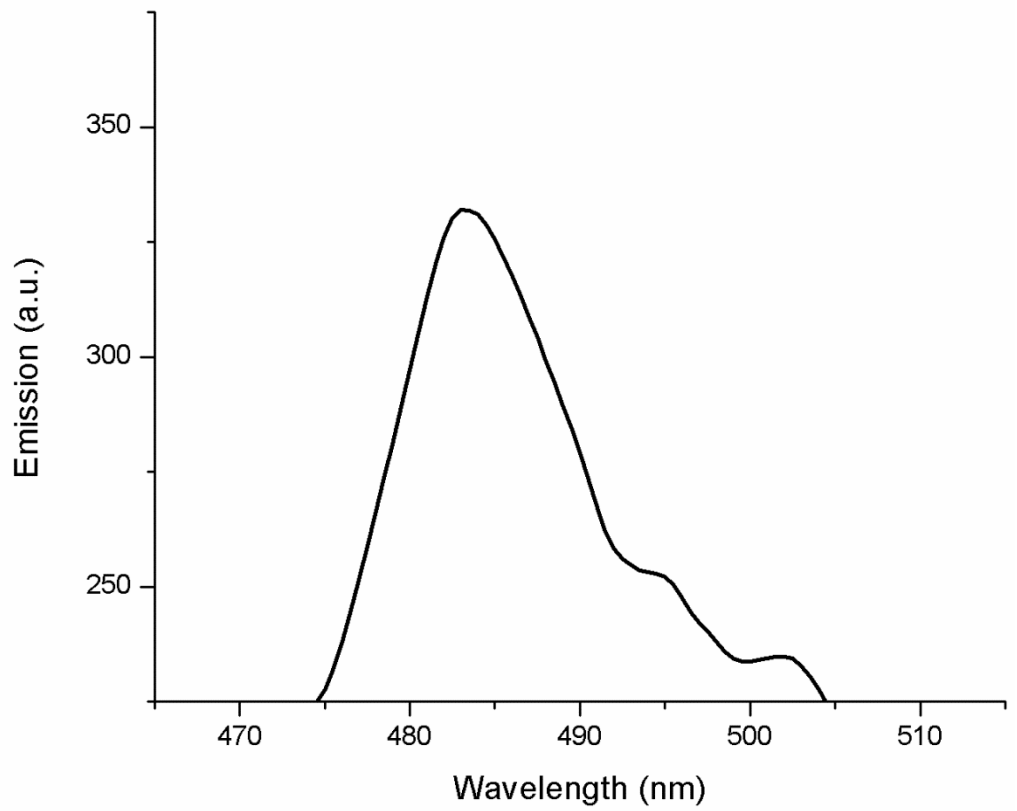

Figure 3.5: Solid state luminescence of compound **18**.

Compound **16** has an emission maximum of 420 nm as shown in Figure 3.4 while compound **18** has a maximum of 485 nm (Figure 3.5). Compounds **17** and **19** were not emissive which may be attributed to the luminescence quenching effect of the ferrocenyl moiety.[15-17] Allendorf and co-workers[14] in their review noted that ligand-to-metal charge transfer (LMCT) is exhibited by a range of Zn(II) and Cd(II) metal organic frameworks primarily in structures containing benzene derivatives. The solid state emission of complexes 16 and 19 can be assigned to LMCT. The emission shoulder at 405 nm for complex 16 could indicate competition between energy transfer states to Zn(II) and the diphenyl rings.[14]

3.4 CONCLUSION

This chapter reports new dithiophosphonate compounds obtained by the ring opening reaction of phenetole Lawesson's reagent and the ferrocenyl dimer using diphenylmethanol. Two of these

compounds exhibited solid state luminescence. These compounds were screened for antibacterial activity reported in Chapter 7.

3.5 EXPERIMENTAL

3.5.1 Method

Unless otherwise noted, all reactions and manipulations were carried out under an inert atmosphere with a positive nitrogen gas flow using standard Schlenk lines and tubes. Standard Schlenk techniques are critical for these reactions and manipulations to minimize contact with atmospheric oxygen that can oxidize and/or reduce desired compounds.

3.5.2 Materials

Phenetole Lawesson's reagent and ferrocenyl Lawesson's reagent were prepared according to established literature procedures.[6] Diphenylmethanol (DPM) was purchased from Sigma Aldrich and used without further purification. Ammonia gas was obtained from Afrox (South Africa). Diethyl ether, THF, toluene and hexane were distilled under dinitrogen over a Na wire with the formation of a benzophenone ketyl indicator. Dichloromethane was distilled over P_4O_{10}. Methanol was distilled from I_2/Mg turnings.

3.5.3 Characterization methods

^{1}H and ^{31}P NMR spectra were recorded on a Bruker Avance 400 MHz spectrometer. NMR data are expressed in parts per million (ppm) and referenced internally to the residual proton impurity in the deuterated solvent whilst ^{31}P spectra chemical shifts are reported relative to an 85% H_3PO_4 in D_2O external standard solution, all at 298 K. Data are reported as chemical shift position (δ_H), multiplicity, relative integral intensity and assignment. Melting points were determined using a Stuart SMP3 melting point apparatus. Infrared spectra were recorded on a Perkin-Elmer Spectrum 100 FT-IR spectrometer. Mass spectral analyses were performed on a Waters API Quattro Micro spectrometer. Solid state emission spectra were recorded on a Perkin–Elmer LS55 fluorescence spectrometer.

3.5.4 X-ray structure determination

Crystals were mounted on glass fibers with epoxy resin, and all geometric and intensity data were collected on a Bruker APEXII CCD diffractometer equipped with graphite monochromated Mo-Ka radiation (λ = 0.71073 Å). The data reduction was carried out with SAINT-Plus software.[18] The SADABS program was used to apply empirical absorption corrections.[19] All structures were solved by direct methods and refined by full-matrix least-squares on F2 with SHELXTL software package[20] found in SHELXTL/PC version 5.10.[21] Thermal ellipsoid plots are generated with OLEX2.[22]

3.6 EXPERIMENTAL

Synthesis of $NH_4[(DPM)OPS_2(p\text{-}C_2H_5OC_6H_{14})]$ (12)

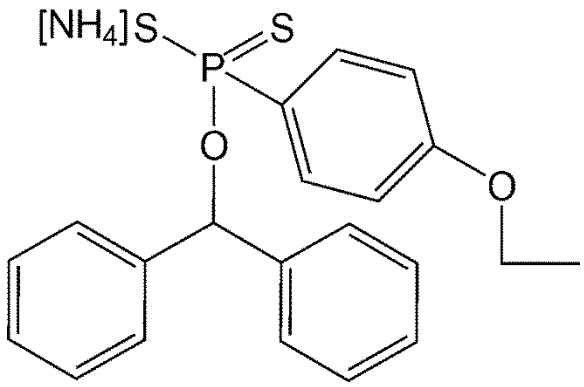

A 25 mL Schlenk tube equipped with a magnetic stirrer bar was charged with PhLR (0.59 g, 1.36 mmol) and placed under vacuum for 30 minutes. The solid was then heated to 75°C and then diphenylmethanol (0.50 g, 2.71 mmol) and toluene (1 mL) added. The temperature was maintained at 75°C until dissolution of all solids was observed. The ensuing solution was further heated at this temperature for another 20 minutes and then placed in ice bath for 15 minutes. Anhydrous ammonia was then bubbled into the solution slowly via a Pasteur pipette which formed an immediate precipitate. The sticky white solid was consolidated with hexane and a free flowing powder was obtained after removing the solvent under reduced pressure. Colourless solid was isolated. Yield: 4.0 g, 71%. M.p.: 106 °C. ^{1}H-NMR (400 MHz, DMSO-d_6, ppm): δ 1.28 (3.0H, t, J=6.90 Hz, Ar-CH_3), 3.97 (2.1H, q, J=6.91 Hz, Ar-OCH_2), 5.73 (1.0H, s, CH), 6.67 (1.7H, d, J=7.92 Hz, Ar-CH_2), 7.17 (9.3H, m, J=8.79 Hz, Ar-CH_2), 7.78 (1.8H, t, J=9.89 Hz, Ar-CH_2). ^{31}P NMR (400 MHz, DMSO-d_6, ppm): δ 107.24 (s). ^{13}C NMR (400 MHz, DMSO-d_6, ppm): δ 161.47, 144.36, 144.31, 137.56, 136.44, 133.21, 133.08, 129.28, 128.80, 128.65, 128.23, 127.86, 127.72, 113.84, 113.69, 79.82, 79.75, 64.43, 15.12. Selected FTIR (ν cm^{-1}): 2974 (m), 1594 (s), 1568 (m), 1494 (s), 1305 (w), 1104(s), 868 (w). ESI-MS: $(M\text{-}NH_4)^+$ 399.

Synthesis of $NH_4[(DPM)OPS_2(Fc)]$ (13)

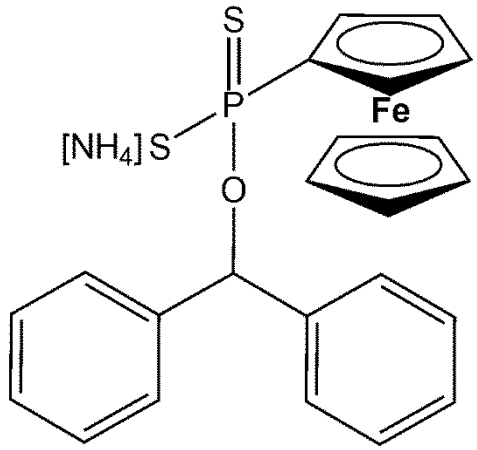

A 25 mL Schlenk tube equipped with a magnetic stirrer bar was charged with FcLR (1.52 g, 2.71 mmol) and placed under vacuum for 30 minutes. The solid was then heated to 75°C and then diphenylmethanol (1.00 g, 5.43 mmol) and toluene (2 mL) added. The temperature was maintained at 75°C until dissolution of all solids was observed. The ensuing solution was further heated at this temperature for another 20 minutes and then placed in ice bath for 15 minutes. Anhydrous ammonia was then bubbled into the solution slowly via a Pasteur pipette which formed an immediate precipitate. The ammonium salt was extracted in THF, filtered through Celite and the filtrare concentrated to about 1 mL. The yellow concentrate was precipitated with hexane and consolidated into a free flowing powder in hexane. Yellow solid was isolated. Yield: 0.8 g, 64%. M.p.: 116 °C. ^{1}H-NMR (400 MHz, $CDCl_3$, ppm): δ 4.36 (5H, s, Fc), 4.57 (2H, d, J=17.17 Hz, Fc), 4.67 (1H, s, Fc), 4.78 (1H, s, Fc), 7.35 (5H, m, J=3.71 Hz, Ar-H), 7.47 (5H, t, J=4.21 Hz, Ar-H). ^{31} P NMR (400 MHz, $CDCl_3$, ppm): δ 108.38 (s). ^{13}C NMR (400 MHz, DMSO-d_6, ppm): δ 114.63, 114.31, 128.79, 128.65, 127.86, 79.82, 79.75, 71.88, 71.10, 70.45, 70.36, 70.22, 70.12. Selected FTIR (ν cm^{-1}): 2979 (s), 2935 (s), 1594 (s), 1569 (s), 1252 (s), 1111 (s), 977(m), 823 (s). ESI-MS: (m/z 100%) 463, (m/z 6.3%) 461.

Synthesis of $Ni[(DPM)OPS_2(p\text{-}C_2H_5OC_6H_{14})]_2$ (14)

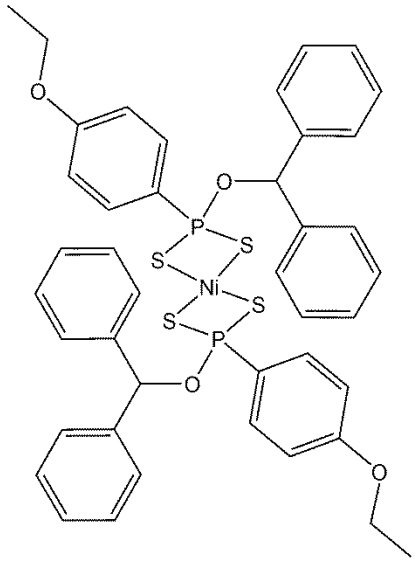

To a stirred solution of **12** (0.10 g, 0.24 mmol) dissolved in 10 mL of methanol was added drop-wise a solution of $NiCl_2.6H_2O$ (0.028 g, 0.12 mmol) in 10 mL of methanol. The resulting precipitate was allowed to stir for 30 minutes at room temperature, vacuum filtered, washed with de-ionized water and diethyl ether. The colorless free flowing powder was then isolated. Yield: 0.90 g, 87%. M.p.: 123 °C (dec). ^{1}H-NMR (400 MHz, $CDCl_3$, ppm): δ 1.47 (6.0H, t, J=6.98 Hz, Ar-CH_3), 4.13 (4.0H, q, J=6.98 Hz, Ar-OCH_3), 7.01 (6.0H, m, J=3.66 Hz, Ar-CH_2), 7.35 (10.0H, m, J=4.58 Hz, Ar-CH_2), 7.45 (7.6H, t, J=4.22 Hz, Ar-CH_2), 8.05 (4.0H, q, J=7.62 Hz, Ar-CH_2). ^{31} P NMR (400 MHz, $CDCl_3$, ppm): δ 99.97 (s). ^{13}C NMR (400 MHz, CDCl): δ 162.35, 143.40, 140.57, 131.94, 131.87, 131.79, 128.90, 128.56, 128.40, 128.03, 127.80, 127.74, 127.55, 127.19, 114.56, 114.48, 114.40, 63.80, 47.81, 14.67. Selected FTIR (ν cm^{-1}): 2979 (m), 2934 (m), 1594 (s), 1497 (s), 1252 (s), 1111 (s), 981 (s). ESI-MS: $(M\text{-}S)^+$ 822, (1/2MSH) 401.

Synthesis of $Ni[C_{13}H_{12}OPS_2(Fc)]_2$ (15)

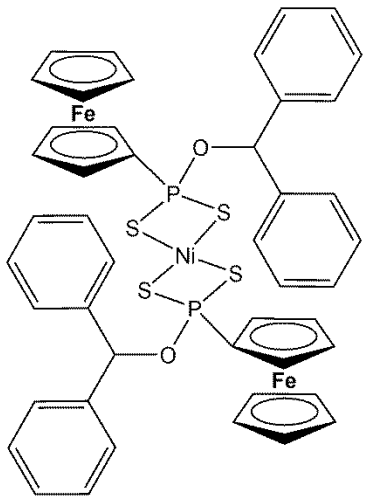

To a stirred solution of **13** (0.15 g, 0.31 mmol) dissolved in 20 mL of methanol was added drop-wise a solution of $NiCl_2.6H_2O$ (0.37 g, 0.16 mmol) in 20 mL of methanol. The resulting precipitate was allowed to stir for 30 minutes at room temperature, vacuum filtered, washed with de-ionized water and diethyl ether. The yellow free flowing powder was then isolated. Yield: 0.10 g, 63%. M.p.: 140 °C (dec). ^{1}H-NMR (400 MHz, $CDCl_3$, ppm): δ 4.46 (10H, s, Fc), 4.67 (4H, d, J=17.19 Hz, Fc), 4.78 (2H, s, Fc), 4.88 (2H, s, Fc), 7.25 (20H, m, J=3.66 Hz, Ar-H), 7.36 (20H, t, J=4.25 Hz, Ar-H). ^{31} P NMR (400 MHz, $CDCl_3$, ppm): δ 108.38 (s). ^{13}C NMR (400 MHz, DMSO-d_6, ppm): δ 114.36, 114.31, 128.79, 128.65, 127.86, 79.82, 79.75, 71.88, 71.10, 70.45, 71.22,

71.12. Selected FTIR (ν cm^{-1}): 2938 (m), 1595 (s), 1494 (s), 1449 (s), 1108 (s), 1024 (m). ESI-MS: $(M-2Fc)^+$ 583.

Synthesis of $Zn_2[(DPM)OPS_2(p\text{-}C_2H_5OC_6H_{14})]_4$ (16)

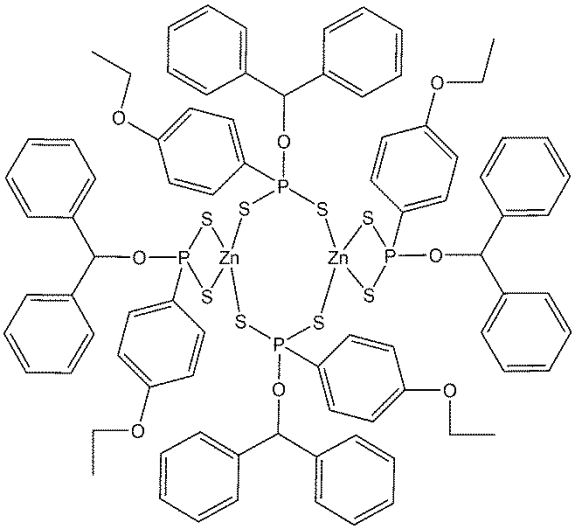

To a stirred solution of **12** (0.29 g, 0.72 mmol) dissolved in 20 mL of methanol was added drop-wise a solution of $Zn(NO_3)_2.6H_2O$ (0.10 g, 0.36 mmol) in 20 mL of methanol. The resulting precipitate was allowed to stir for 30 minutes at room temperature, vacuum filtered, washed with de-ionized water and diethyl ether. The colourless free flowing powder was then isolated. Yield: 0.30 g, 49%. M.p.: 132 °C. ^{1}H-NMR (400 MHz, DMSO-d_6, ppm): δ 1.29 (12.0H, t, J=6.92 Hz, Ar-CH_3), 3.99 (8H, q, J=6.95 Hz, Ar-OCH_2), 6.65 (8H, m, J=13.79 Hz, Ar-CH_2), 7.20 (40H, m, J=3.87 Hz, Ar-CH_2), 7.80 (8H, q, J=7.32 Hz, Ar-CH_2). ^{31} P NMR (400 MHz, DMSO-d_6, ppm): δ 106.29 (s). ^{13}C NMR (400 MHz, CDCl): δ 158.99, 143.39, 143.34, 132.13, 131.45, 131.32, 128.06, 127.94, 127.86, 127.65, 127.08, 126.52, 113.33, 112.47, 112.33, 76.38, 76.32, 63.03, 62.62, 14.54. Selected FTIR (ν cm^{-1}): 2978 (m), 1593 (s), 1497 (s), 1252 (s), 1112 (s), 551 (w). ESI-MS: $(1/4M)^+$ 401.

Synthesis of $Zn_2[(DPM)OPS_2(Fc)]_4$ (17)

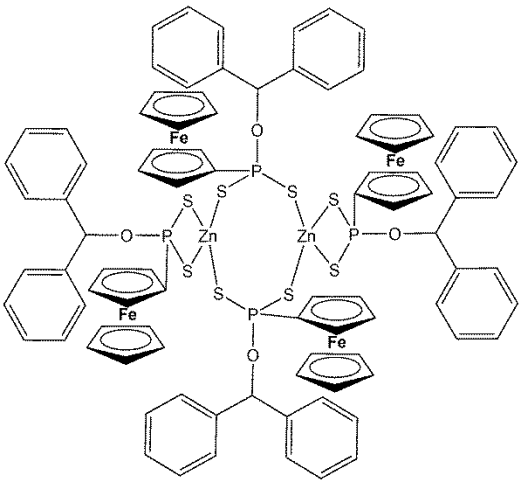

To a stirred solution of **13** (0.10 g, 0.21 mmol) dissolved in 20 mL of methanol was added drop-wise a solution of $Zn(NO_3)_2.6H_2O$ (0.12 g, 0.41 mmol) in 10 mL of methanol. The resulting precipitate was allowed to stir for 30 minutes at room temperature, vacuum filtered, washed with de-ionized water and diethyl ether. The colourless

free flowing powder was then isolated. Yield: 0.15 g, 36%. M.p.: 142 °C (dec). ^{1}H-NMR (400 MHz, $CDCl_3$, ppm): δ 4.47 (10H, s, Fc), 4.68 (4H, d, J=17.21 Hz, Fc), 4.78 (2H, s, Fc), 4.89 (2H, s, Fc), 7.26 (20H, m, J=3.75 Hz, Ar-H), 7.37 (20H, t, J=4.26 Hz, Ar-H). ^{31} P NMR (400 MHz, DMSO-d_6, ppm): δ 108.38 (s). ^{13}C NMR (400 MHz, CDCl): δ 145.25, 145.21, 129.69, 129.54, 128.76, 80.71, 80.64, 71.83, 71.05, 70.40, 70.31, 70.17, 70.07. Selected FTIR (ν cm^{-1}): 2938 (m), 1593 (s), 1494 (m), 1449 (m), 1108 (s), 1024 (w), 583 (w). ESI-MS: $(1/4M)^+$ 593.

Synthesis of $Cd_2[(DPM)OPS_2(p\text{-}C_2H_5OC_6H_{14})]_4$ (18)

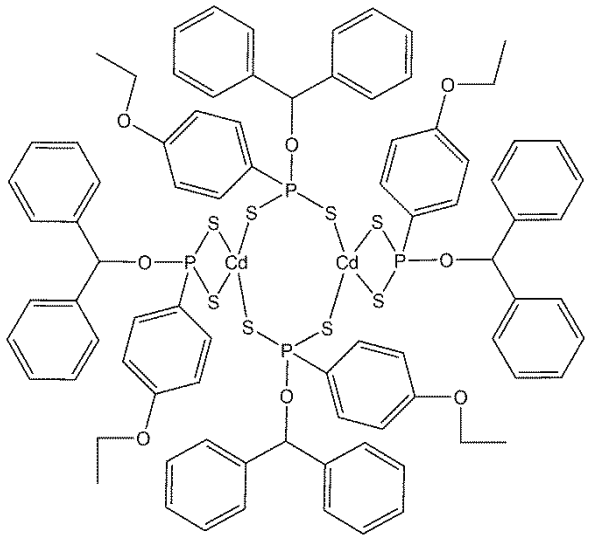

To a stirred solution of **12** (0.10 g, 0.24 mmol) dissolved in 20 mL of methanol was added drop-wise a solution of $Cd(NO_3)_2.4H_2O$ (0.037 g, 0.12 mmol) in 20 mL of methanol. The resulting precipitate was allowed to stir for 30 minutes at room temperature, vacuum filtered, washed with de-ionized water and diethyl ether. The colourless free flowing powder was then isolated. Yield: 0.091 g, 42%. M.p.: 159 °C. ^{1}H-NMR (400 MHz, DMSO-d_6, ppm): δ 1.32 (12H, d, J=2.96 Hz, Ar-CH_3), 4.06 (8H, d, J=6.76 Hz, Ar-OCH_2), 6.64 (1.0H, d, J=6.32 Hz), 6.94 (6.0H, dd, J=2.68, 8.60 Hz, Ar-CH_2), 7.20 (6.0H, d, J=18.69 Hz, Ar-CH_2), 7.22 (8.0H, dd, J=9.53, 16.53 Hz, Ar-CH_2), 7.29 (10.0H, d, J=16.61 Hz, Ar-CH_2), 7.31 (9.0H, d, J=16.97 Hz, Ar-CH_2), 7.51 (1.0H, dd, J=8.58, 12.67 Hz, Ar-CH_2), 7.70 (2.0H, d, J=4.36 Hz, Ar-CH_2), 7.72 (1.0H, d, J=3.48 Hz, Ar-CH_2), 7.85 (4.5H, dd, J=8.58, 14.03 Hz, Ar-CH_2), 7.95 (1.0H, dd, J=8.64, 14.21 Hz, Ar-CH_2). P NMR (400 MHz, DMSO-d_6, ppm): δ 78.90 (s).^{13}C NMR (400 MHz, DMSO-d_6, ppm): δ 132.00, 131.88, 131.64, 131.49, 128.63, 128.33, 128.12, 128.04, 127.81, 127..38, 127.18, 126.98, 126.16, 113.69, 113.54, 112.85, 63.27, 63.11, 62.94, 55.02, 14.54. Selected FTIR (ν cm^{-1}): 2938 (m), 1595 (s), 1494 (s), 1181 (s), 1108 (s), 602 (w). ESI-MS: $(1/4M)^+$ 401.

Synthesis of $Cd_2[(DPM)OPS_2(Fc)]_4$ (19)

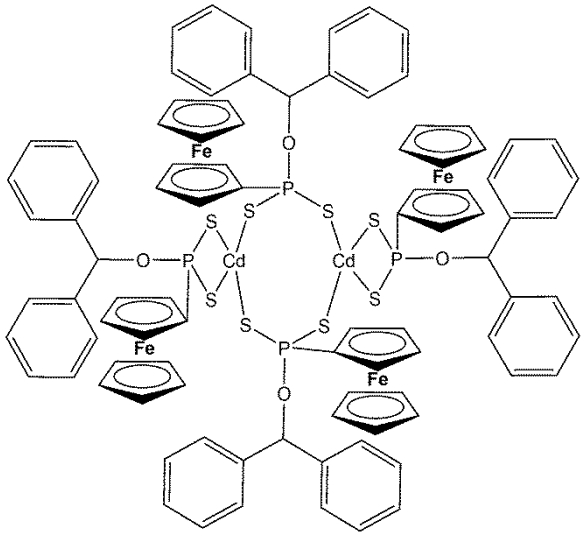

To a stirred solution of **13** (0.10 g, 0.21 mmol) dissolved in 20 mL of methanol was added drop-wise a solution of $Cd(NO_3)_2.4H_2O$ (0.032 g, 0.10 mmol) in 10 mL of methanol. The resulting precipitate was allowed to stir for 30 minutes at room temperature, vacuum filtered, washed with de-ionized water and diethyl ether. The colourless free flowing powder was then isolated. Yield: 0.09 g, 44%. M.p.: 123 °C (dec).

^{1}H-NMR (400 MHz, $CDCl_3$, ppm): δ 4.47 (810H, s, Fc), 4.68 (4H, d, J=17.26 Hz, Fc), 4.78 (2H, s, Fc), 4.89 (2H, s, Fc), 7.18 (20H, m, J=3.76 Hz, Ar-H), 7.30 (20H, t, J=4.21 Hz, Ar-H). ^{31} P NMR (400 MHz, $CDCl_3$, ppm): δ 109.89 (s). ^{13}C NMR (400 MHz, CDCl): δ 145.36, 145.31, 129.79, 129.65, 128.86, 80.82, 80.75, 72.83, 72.05, 71.40, 71.17, 71.07. Selected FTIR (ν cm^{-1}): 2979 (m), 1594 (s), 1495 (m), 1409 (w), 1108 (s), 823 (s). ESI-MS: $(1/4M)^+$ 464.

3.7 REFERENCES

1. P. Pishchimuka, *J. Russ. Phys. Chem. Soc*, **1912**, 44, 1406.
2. L. Malatesta and R. Pizotti, *Chimica e Industria (Milan)*, **1945**, 27, 6-10.
3. N. Meinhardt, S. Z. CARDON and P. Vogel, *The J of Organic Chem*, **1960**, 25, 1991-1992.
4. W. E. van Zyl and J. D. Woollins, *Coord. Chem. Rev.*, **2013**, 257, 718-731.
5. L. Thomas and R. A. Chittenden, *Spectrochimica Acta*, **1964**, 20, 489-502.
6. W. E. Van Zyl and J. P. Fackler, *Phos, Sulfur, and Silicon and the Relat Elem*, **2000**, 167, 117-132.
7. I. P. Gray, H. L. Milton, A. M. Slawin and J. D. Woollins, *Dalton Trans*, **2003**, 3450-3457.
8. M. N. Pillay, H. van der Walt, R. J. Staples and W. E. van Zyl, *J. Organomet. Chem*, **2015**, 794, 33-39.
9. X.-Y. Wang, Y. Li, Q. Ma and Q.-F. Zhang, *Organometallics*, **2010**, 29, 2752-2760.
10. J. S. Casas, A. Castiñeiras, M. a. C. Rodríguez-Argüelles, A. n. Sánchez, J. Sordo, A. V. López, S. Pinelli, P. Lunghi, P. Ciancianaini and A. Bonati, *J. Inorg. Biochem*, **1999**, 76, 277-284.
11. G. H. Eom, H. M. Park, M. Y. Hyun, S. P. Jang, C. Kim, J. H. Lee, S. J. Lee, S.-J. Kim and Y. Kim, *Polyhedron*, **2011**, 30, 1555-1564.
12. X.-L. Chen, B. Zhang, H.-M. Hu, F. Fu, X.-L. Wu, T. Qin, M.-L. Yang, G.-L. Xue and J.-W. Wang, *Cryst Growth and Des*, **2008**, 8, 3706-3712.
13. Y.-W. Dong, R.-Q. Fan, P. Wang, L.-G. Wei, X.-M. Wang, S. Gao, H.-J. Zhang, Y.-L. Yang and Y.-L. Wang, *Inorg. Chem*, **2015**, 54, 7742-7752.
14. M. Allendorf, C. Bauer, R. Bhakta and R. Houk, *Chem. So.c Rev*, **2009**, 38, 1330-1352.
15. D. Albagli, G. Bazan, R. Schrock and M. Wrighton, *J. Phys. Chem.*, **1993**, 97, 10211-10216.
16. D. Dorokhin, N. Tomczak, A. H. Velders, D. N. Reinhoudt and G. J. Vancso, *The J. Phys. Chem. C*, **2009**, 113, 18676-18680.
17. X.-B. Xia, Z.-F. Ding and J.-Z. Liu, *J. Photochem. and Photobio. A: Chem*, **1995**, 88, 81-84.
18. V. SAINT, *Siemens Analytical Instruments Division, Madison, WI*, **1995**.

19. G. Sheldrick, *University of Göttingen, Germany*, **2010**.

20. G. Sheldrick, *University of Göttingen, Germany*, **1997**.

21. V. SHELXTL, *Inc., Madison, WI*, **2001**.

22. C. Júnior and P. de Sousa, Universidade de São Paulo, **2017**.

CHAPTER 4

DITHIOPHOSPHONATE ZWITTERIONIC COMPOUNDS OF ETHAMBUTOL

4.1 INTRODUCTION

Ethambutol (EMB), chemically known as (+) 2, 2′ -(ethane-1,2 diyldiimino)dibutan-1-ol, is a potent synthetic antimyco-bacterial agent introduced in 1961 as a treatment for patients with tuberculosis (TB).[1] It is a synthetic diamine derivative, which possess four coordinating sites (Figure 4.1) and forms chelate complexes with bivalent metal ions such as Cu^{2+}, Ni^{2+}, Co^{2+} and $Zn.^{2+}$ [2] It is also used in combination with other drugs like isoniazid, rifampicin, and pyrazinamide for the effective treatment of tuberculosis.[3] Studies on metal complexes of ethambutol have been restricted to copper,[4-7] zinc and platinum.[8, 9] To the best of my knowledge, apart from copper ethambutol complex that has been structurally characterized,[7] all other studies on metal complexes of ethambutol have been speculative on the actual geometry and structure of such complexes.

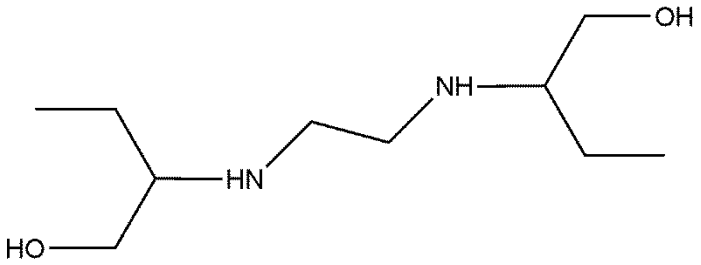

Figure 4.1: Structure of ethambutol.

On the other hand, thiophosphorus ligands as S-donor compounds have been widely studied in the last decade. This class of compounds includes the dithiophosphates, dithiophosphinates and dithiophosphonates. Dithiophosphorus ligands and complexes have found applications in industry, agriculture and medicine. Unlike the dithiophosphonates which have been reasonably well studied, their

zwitterionic analogues are still scarce in the literature. To the best of my knowledge, the only dithiophosphonate zwitterions structurally characterized were the ones reported by Karakus and co-workers.[10, 21]

This chapter reports on Cu and Ni coordination compounds of ethambutol as well as dithiophosphonate zwitterionic derivatives of ethambutol.

4.2 RESULTS AND DISCUSSION

4.2.1 Synthesis of coordination compounds of ethambutol

Compounds **20** and **21** were prepared as shown in Scheme 4.1. They were obtained in aqueous solution by drop-wise addition of Cu(II) and Ni(II) chlorides. K_2CO_3 was also used for the synthesis of compound **20** (Scheme 4.1). EMB was first stirred with KOH to neutralize the HCl that is typically added to EMB to reduce hygroscopicity. After 1 hr, coloured solutions obtained were centrifuged and excess KCl removed via precipitation by drop-wise addition of ether and decantation. Re-centrifugation and concentration were then performed to yield coloured crystalline powders. Obtained crystalline powders are hygroscopic and turn to solutions within minutes when exposed to the atmosphere.

4.2.2 Synthesis of dithiophosphonate zwitterions

Compounds **22** and **23** were prepared by reaction of one mole equivalent of PhLR or FcLR with one mole of EMB. The mixtures were stirred together in THF until it turned clear and then turned to a colourless solid for compound **22** or yellow solid for compound **23**, as shown in Figure 4.3. Our efforts to prepare metal coordination complexes of these zwitterions were unsuccessful and this is consistent with similar and earlier studies reported in leiterature.[10, 21]

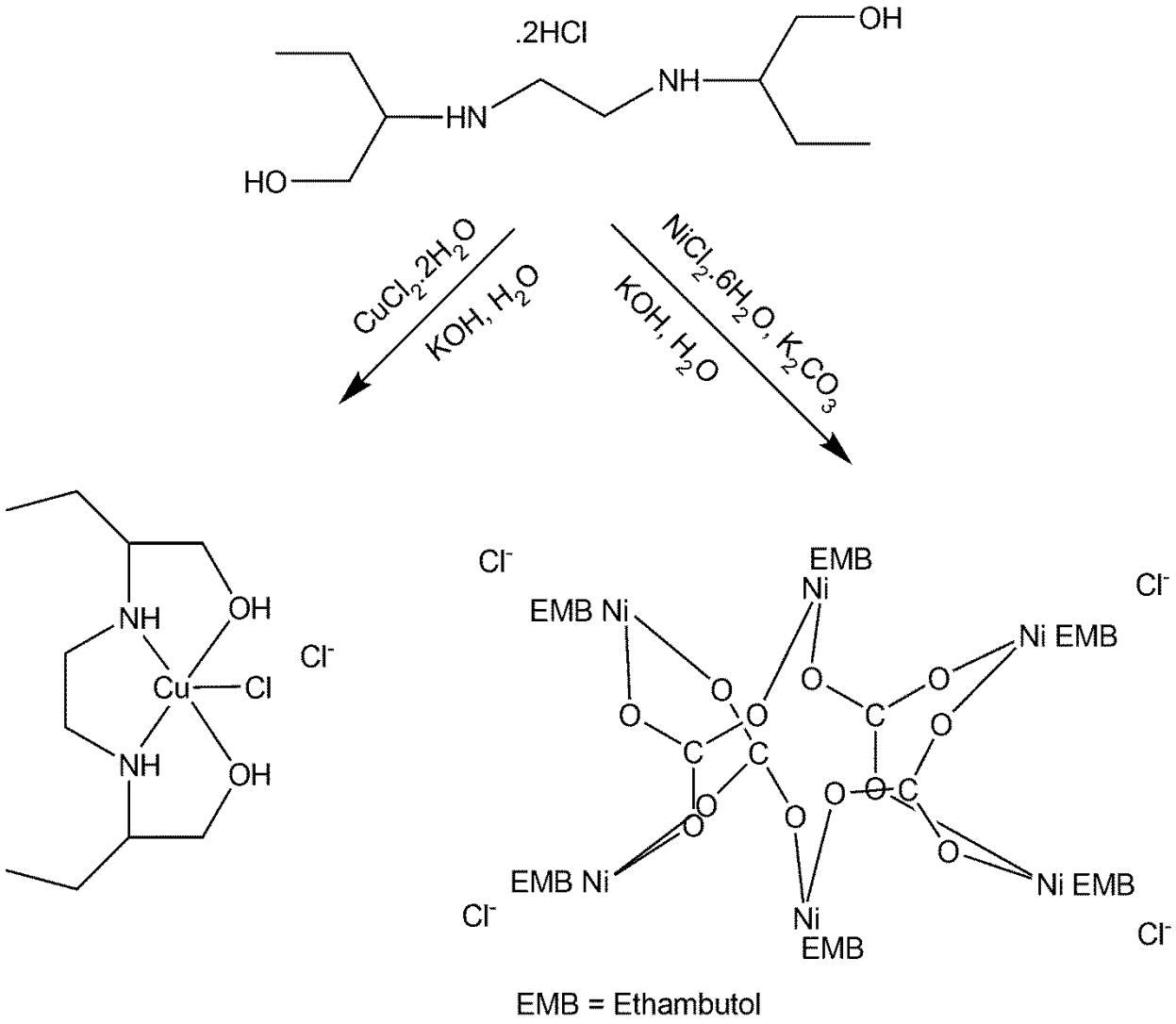

Figure 4.2: Synthesis of Cu (**20)** and Ni(**21)** EMB compounds.

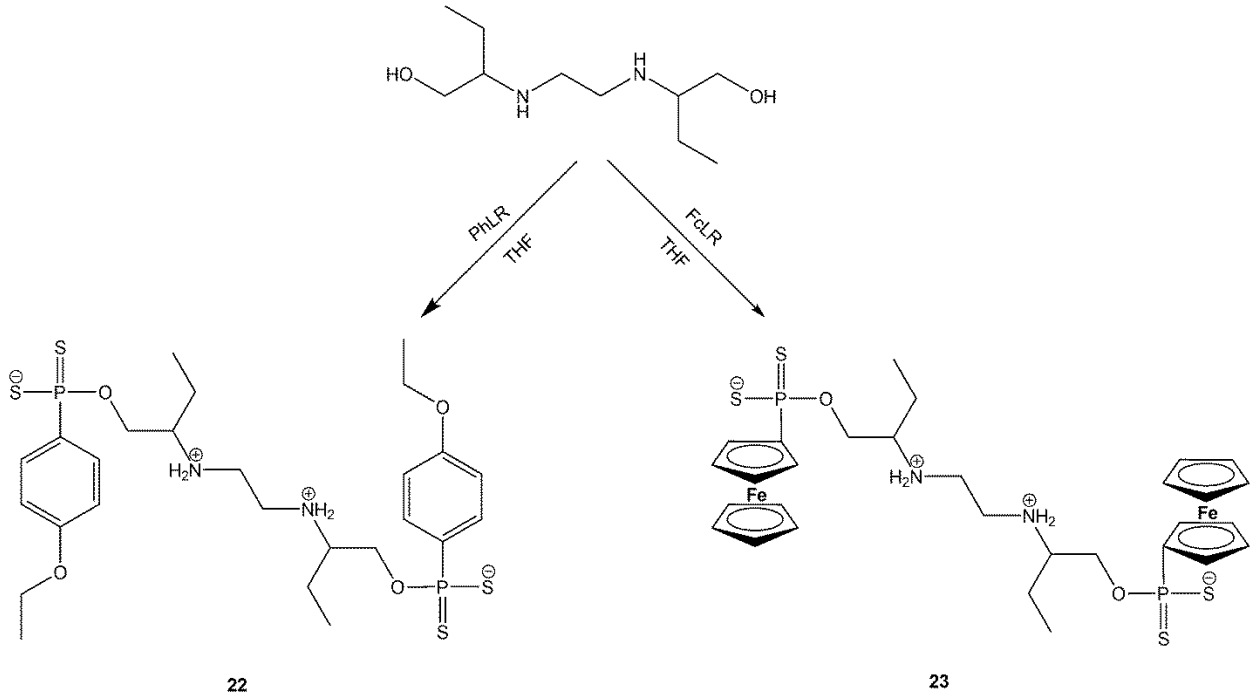

Figure 4.3: Synthesis of EMB dithiophosphonate zwitterions.

4.2.3 Spectroscopy

4.2.3.1 Spectroscopy for compounds 21 and 22

The ^{1}H and ^{13}C NMR spectra of compounds **20-21** provided no useful information about these compounds because the octahedral Ni^{2+} and square pyramidal Cu^{2+} complexes (Figures 4.7 and 4.10) are paramagnetic. Figure 4.4 shows comparative FTIR spectra of EMB.2HCl and compounds **20-21.** A shift in the vibrational frequency for compound **20-21** compared to the starting material (EMB.2HCl) indicates the formation of multicomponent adducts.[11] For example, the strong band around 3300 cm^{-1} in EMB.2HCl broadens and shifts to about 3200 cm^{-1} due to hydrogen bonding. The band around 1635 cm^{-1} in compound **20** is due the carbonate group. The sharp peak around 1600 cm^{-1} in EMB.2HCl is assigned to the NH in the compound.

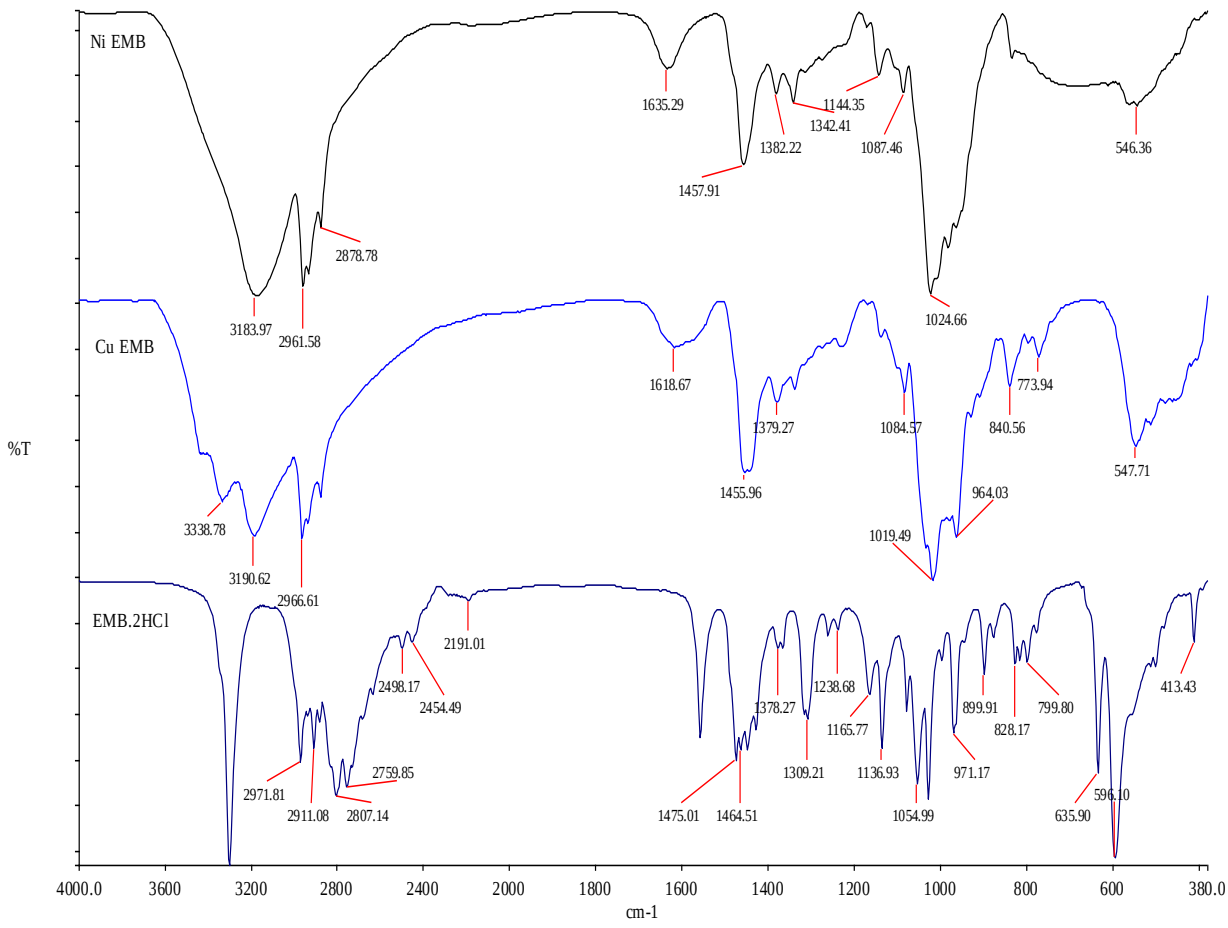

Figure 4.4: Comparative FTIR of EMB.2HCl and compounds **20** & **21** (Cu EMB = Compound **19**; Ni EMB = Compound **20**).

The FTIR results are consistent with those obtained by Nangia and Cherukuvada in 2013.[12]

4.2.3.2 Spectroscopy for ethambutol dithiophosphonate zwitterions

The ^{1}H NMR of compounds **22** and **23** were well resolved and integrated to the number of the corresponding hydrogen atoms in both cases. The ^{1}H NMR spectrum of **22** showed the presence of the aromatic protons which appeared between 6 and 8 ppm. The unsubstituted cyclopentadienyl ring in the ^{1}H NMR of **23** gave a singlet peak, with the substituted ring giving two sets of signals for the pair of equivalent protons. ^{31}P NMR spectra gave a singlet peak at 108.84 and 108.38 ppm for compounds **22** and **23**, respectively, indicating that the compounds exist in a single isomeric form in solution. The purity

of compounds **22** and **23** were also ascertained by mass spectrometry. Electrospray ionization (negative) mass spectrometry of compound **22** showed the expected parent ion as $(M+H)^+$ at *m*/*z* 636.15 and other fragmented ions at *m*/*z* (32%) 637.14 and *m*/*z* (5.7%) 639.52 (Figure 4.5). The ESI-MS of compound **23** showed the parent ion as $(M-H)^+$ at *m*/*z* 763.01 and other fragmented ions as *m*/*z* (41%) 765.02, *m*/*z* (21.9%) 766.03 and *m*/*z* (7.5%) 767.03. The FTIR spectra showed distinct bands at 1185–1179 cm^{-1}, 1028–1025 cm^{-1}, 678–674 cm^{-1} and 559–557 cm^{-1}, corresponding to ν[(P)–O–C], ν[P–O–(C)], $\nu(PS)_{asym}$ and $\nu(PS)_{sym}$ absorptions, respectively.[13] The N present in compounds **21** and **22** is indicated in the FTIR at bands between 2920 and 2985 cm^{-1}.

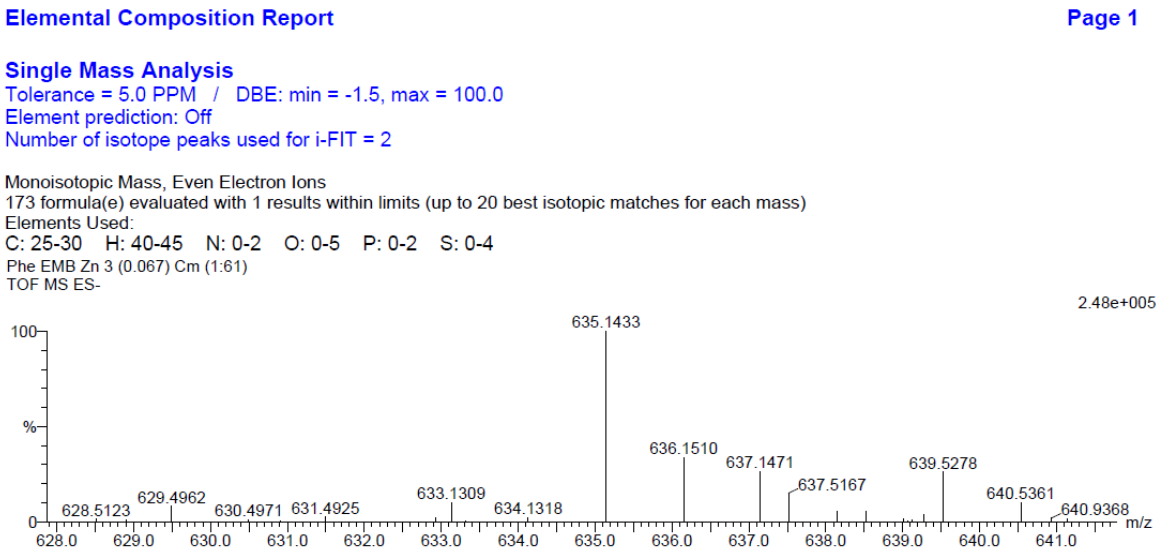

Figure 4.5: ESI-MS spectrum of compound **22**.

Elemental Composition Report **Page 1**

Single Mass Analysis
Tolerance = 5.0 PPM / DBE: min = -1.5, max = 100.0
Element prediction: Off
Number of isotope peaks used for i-FIT = 2

Monoisotopic Mass, Even Electron Ions
434 formula(e) evaluated with 1 results within limits (up to 20 best isotopic matches for each mass)
Elements Used:
C: 25-30 H: 40-45 N: 0-2 O: 0-2 S: 0-5 Fe: 0-2 P: 0-2

Fe EMB Zn 21 (0.674) Cm (1:61)
TOF MS ES-

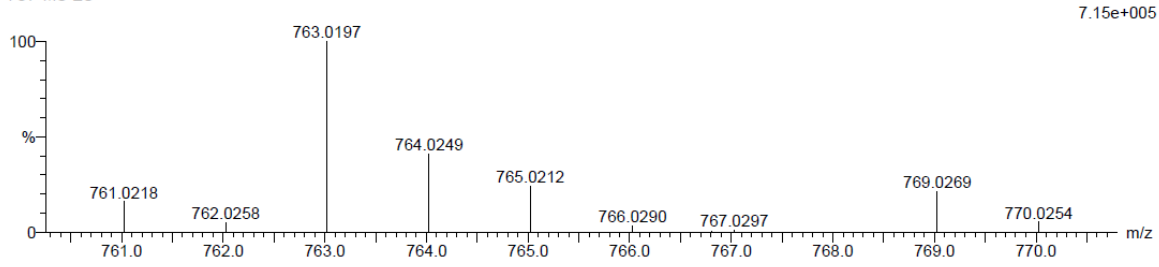

Minimum:				-1.5			
Maximum:		5.0	5.0	100.0			
Mass	Calc. Mass	mDa	PPM	DBE	i-FIT	i-FIT (Norm)	Formula
763.0197	763.0225	-2.8	-3.7	12.5	65.4	0.0	C30 H41 N2 O2 S4 Fe2 P2

Figure 4.6: ESI-MS spectrum of compound **23**.

4.2.4 Solubility

Knowledge about the solubility of compounds, either to make the appropriate choice of solvent for spectroscopic measurements or as an aid in preparative chemistry is useful.[14] Compounds **20-21** also turn watery on exposure to the atmosphere, due to their hygroscopicity. Against this background, a series of solubility tests were performed on **20-23**. Different solvents of varying polarity were used to obtain the data given in Table 4.1. This data is based on the criteria of dissolving a specified amount (0.03 g) of the compound of interest in the relevant solvent (0.2 mL), shaking for 10 seconds and then filtration at 25°C.

Table 4.1: Solubility data for complexes **20**-**23**.

Compound	CH_2OH	C_2H_5OH	DCM	Hexane	THF	H_2O	DMF	DMSO
20	VS	VS	I	I	PS	VS	VS	VS
21	VS	VS	I	I	PS	VS	VS	VS
22	I	I	I	I	I	I	VS	VS
23	PS	PS	PS	I	PS	I	VS	VS

I = insoluble. PS = partly soluble. S = soluble. VS = very soluble. The symbol I means the compound is quantitatively recovered after filtration, PS means small amount of the compound (about 10%) is dissolved, S means a large amount of the compound is dissolved (about 80%) and VS means a clear solution of the compound emerged immediately.

Compounds **20** and **21** are mostly soluble in polar solvents like CH_3OH, C_2H_5OH, H_2O and DMF and DMSO as shown in Table 4.1. These compounds are not soluble in non-polar solvents like hexane and DCM. The solubility of compounds **20** and **21** in polar and non-polar solvents was exploited in the synthesis of these compounds and in the removal of excess KCl from the reaction system. Compound **22** was largely not soluble in the polar and non-polar solvents tested as shown in Table 4.1 but very soluble in DMF and DMSO. Compound **23** on the other hand is partially soluble in CH_3OH, C_2H_5OH and DCM and very soluble in DMF and DMSO. This information was useful in the spectroscopic characterization of the complexes and in crystal growth.

4.2.4 Solid state structures

Figures 4.7, 4.10 and 4.11 give the molecular structures of compound **20** and **21** while important X-ray crystallographic data and parameters are shown in Table 4.2. Table 4.3 gives selected bond lengths and angles of **20** and **21**. Single crystals of compound **20** were obtained by slow evaporation of a concentrated solution of compound **20** dissolved in water. Compound **20** crystallizes in the orthorhombic space group $P2_12_12_1$ with 4 molecules in the asymmetric unit cell. The molecular structure of complex **19** is cationic, similar to that obtained by Oliveira and co-workers in 2011.[7] The neutrality of the mono cationic complex is obtained by the presence of a Cl^- ion in the crystal lattice as shown in Figure 4.7. EMB acts as a tetradentate ligand with two

NH and OH groups each. The copper atom is coordinated to five atoms (2 NH, 2 OH & Cl atoms) giving rise to a square pyramidal geometry (Figure 4.7). The molecular structure of compound **20** has a basal plane occupied by 2 N, 1 O, 1 Cl, and 1 Cu atom while the second O atom of EMB occupies the apical position as shown in Figure 4.7. The apical Cu(2)-O(0aa) distance [2.351(6) Å] is longer than that of the basal Cu(2)-O(1) [1.943(6) Å] (Table 4.3) giving rise to a Jahn-Teller distortion in the structure. The crystal structure of compound **20** is stabilized by intermolecular N-H…Cl hydrogen bonds resulting in a one dimensional supramolecular assembly (Figures 4.8 and 4.9).

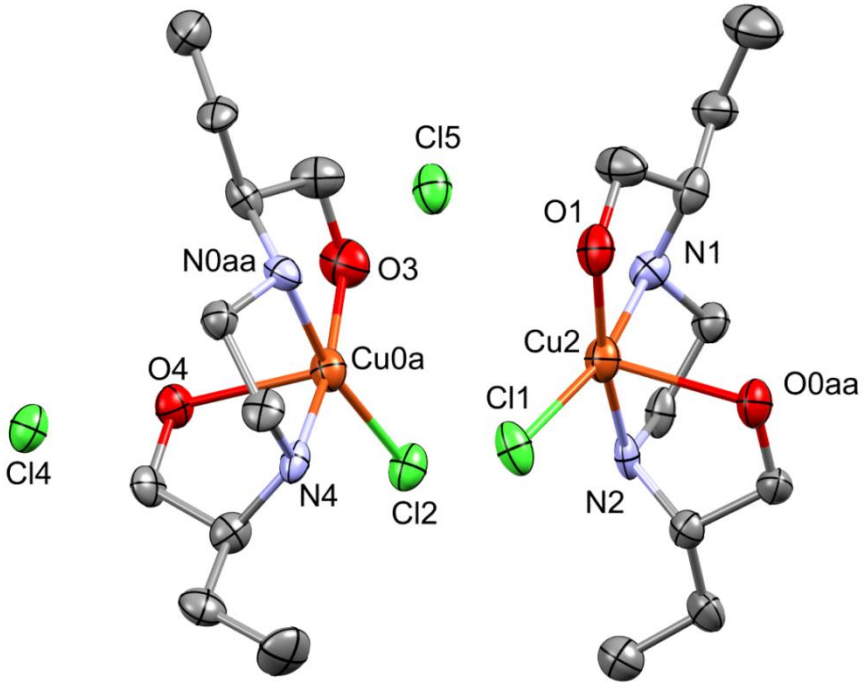

Figure 4.7: Molecular structure of compound **19**, thermal ellipsoids drawn at the 50% probability. Hydrogen atoms are omitted for clarity.

Table 4.2: X-ray crystallographic data for compounds **20** and **21**.

Compound	**20**	**21**
Chemical formula	$2(C_{10}H_{24}ClCuN_2O_2)\cdot 2(Cl)$	$C_{64}H_{129}N_{12}Ni_6O_{24}$
M_r	677.53	1802.93
Crystal system, space group	Orthorhombic, $P2_12_12_1$	Trigonal, $R3{:}H$
Temperature (K)	173	100
a, *b*, *c* (Å)	8.0876 (19), 18.540 (4), 20.311 (5)	16.1440 (3), 16.1440 (3), 39.8098 (10)
V (Å^3)	3045.6 (12)	8985.5 (4)
Z	4	3
Radiation type	Mo *K*a	Mo *K*a
□ (mm^{-1})	1.78	0.98
Crystal size (mm)	0.22 × 0.13 × 0.02	0.50 × 0.37 × 0.17
Data collection		
Diffractometer	Bruker *APEX*-II CCD diffractometer	Bruker *APEX*-II CCD diffractometer
T_{min}, T_{max}	0.611, 0.745	0.631, 0.859
No. of measured, independent and observed [I □ 2u(I)] reflections	24648, 5554, 2942	80970, 10100, 9379
R_{int}	0.151	0.020
Refinement		
$R[F^2 > 2\square(F^2)]$, $wR(F^2)$, S	0.062, 0.146, 0.98	0.026, 0.114, 0.53
No. of reflections	5554	10100
No. of parameters	325	322
No. of restraints	12	1
H-atom treatment	H atoms treated by a mixture of independent and constrained refinement	H-atom parameters constrained
Peak diff. $_{max}$, $_{min}$ (e Å^{-3})	1.09, -0.86	0.56, -0.25
Absolute structure	Flack, H. D.	Refined as an inversion twin
Flack parameter	-0.02 (3)	0.008 (11)

Table 4.3: Selected bond lengths (Å) and angles (°) for compounds **20** and **21**.

Compound **20**

Cu2—Cl1	2.270 (2)	Cu0a—Cl2	2.263 (2)
Cu2—O1	1.943 (6)	Cu0a—O4	2.354 (6)
Cu2—N2	1.975 (7)	Cu0a—N0aa	2.002 (7)
Cu2—O0aa	2.351 (6)	Cu0a—O3	1.962 (6)
Cu2—N1	2.000 (7)	Cu0a—N4	1.995 (7)
O1—Cu2—Cl1	95.30 (17)	N1—Cu2—Cl1	165.7 (2)
N2—Cu2—Cl1	95.8 (2)	N1—Cu2—O1	83.2 (3)
N2—Cu2—O1	168.8 (3)	N1—Cu2—N2	86.3 (3)
O0aa—Cu2—Cl1	104.05 (17)	N1—Cu2—O0aa	90.2 (3)
O0aa—Cu2—O1	98.3 (3)	O4—Cu0a—Cl2	102.46 (16)
O0aa—Cu2—N2	77.5 (3)	N0aa—Cu0a—Cl2	168.4 (2)

Compound **21**

Ni(1)-O(6)	2.052(2)	Ni(2)-O(3)	2.0447(19)
Ni(1)-O(5)	2.059(2)	Ni(2)-O(4)#2	2.055(2)
Ni(1)-O(7)	2.103(2)	Ni(2)-O(1)	2.119(2)
Ni(1)-O(8)	2.126(2)	Ni(2)-O(2)	2.125(2)
O(5)-Ni(1)-N(3)	163.38(10)	N(3)-Ni(1)-O(7)	81.90(10)
N(4)-Ni(1)-N(3)	83.47(10)	O(6)-Ni(1)-O(8)	84.27(9)
O(6)-Ni(1)-O(7)	92.28(9)	O(5)-Ni(1)-O(8)	90.43(8)
O(5)-Ni(1)-O(7)	82.15(8)	N(4)-Ni(1)-O(8)	80.71(10)

N(4)-Ni(1)-O(7)	103.41(10)	N(3)-Ni(1)-O(8)	105.76(10)
O(7)-Ni(1)-O(8)	171.81(9)	O(3)-Ni(2)-N(2)	163.87(10)
O(3)-Ni(2)-O(4)#2	90.37(8)	O(4)#2-Ni(2)-N(2)	93.94(10)

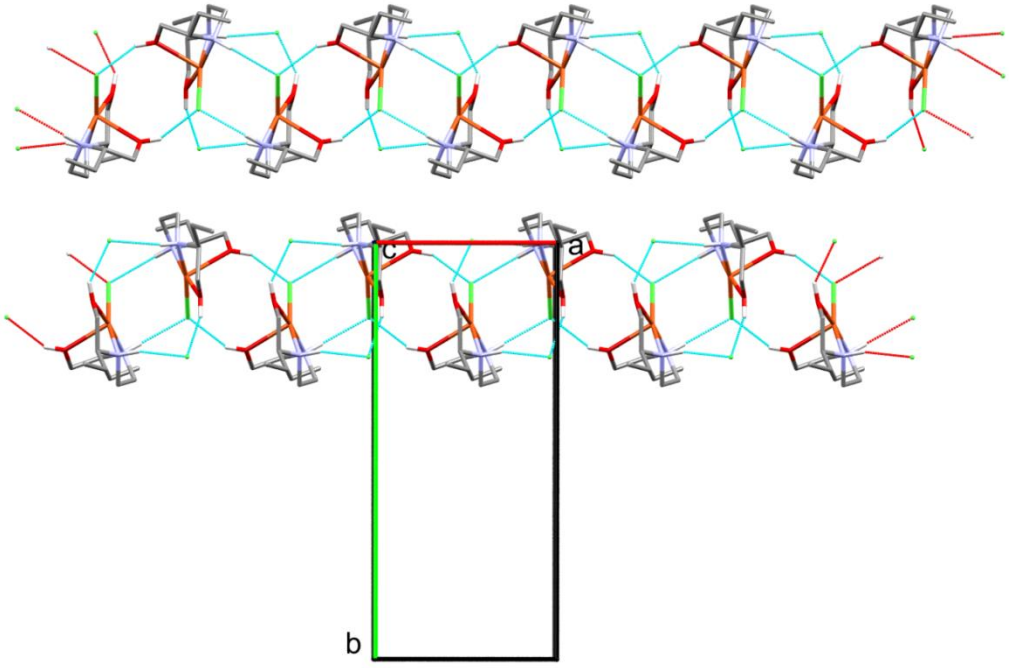

Figure 4.8: Crystal structure of compound **20** showing a supramolecular assembly extending along crystallographic *a* axis (hydrogen bonds shown in green lines).

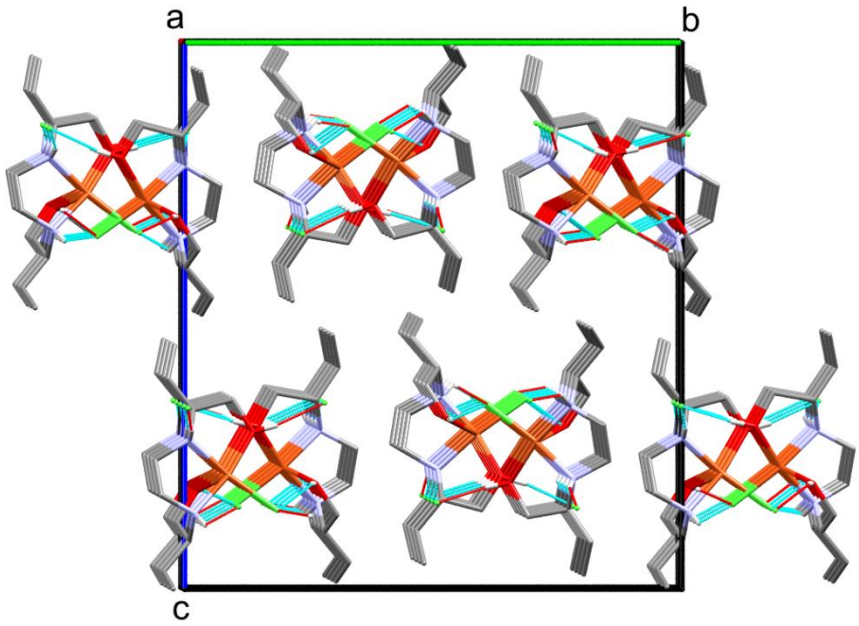

Figure 4.9: Crystal structure of compound **20** viewed along crystallographic *b* axis.

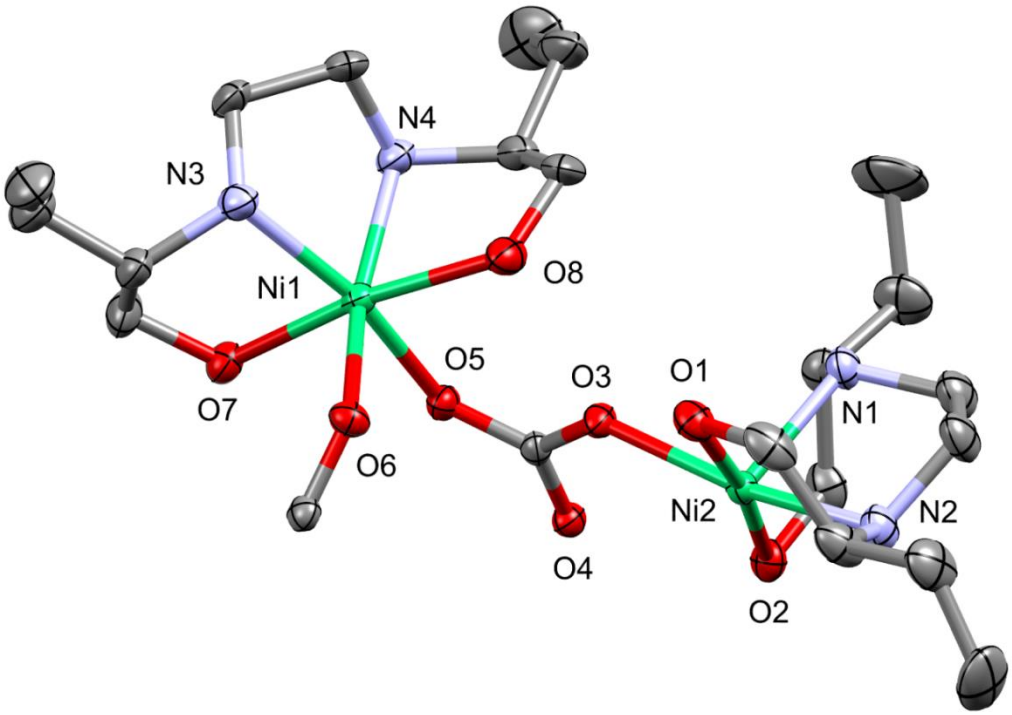

Figure 4.10: Perspective view of asymmetric unit (for clarity) of compound **21**, thermal ellipsoids drawn at the 50% probability. Hydrogen atoms are omitted for clarity.

Single crystals of compound **21** were obtained by slow evaporation of a concentrated solution of compound **21** dissolved in water. Compound **21** crystallizes in the trigonal space group *R*3:*H* with 3 molecules per asymmetric unit cell. The molecular structure of compound **21** shows it is a hexa-nuclear cluster made up of 6 EMB molecules and 6 Ni atoms held together by four carbonate CO_3^{2-} units as shown in Figure 4.10. Each EMB molecule is coordinated to a Ni atom via its 2 N and 2 O atoms. 2 O atoms from a neighboring coordinating CO_3^{2-} unit complete a 6 coordination for each Ni atom giving rise to a distorted octahedral geometry around each of the 6 Ni atoms (Figures 4.10 & 4.11). The coordination of EMB through its four binding sites to Ni forms 3 Ni/O/C/N cycles for each of the 6 EMB units (Figure 4.10). These heterocycles are held together by 4 CO_3^{2-} to form an 18 heterocyclic cluster (Figure 4.11).

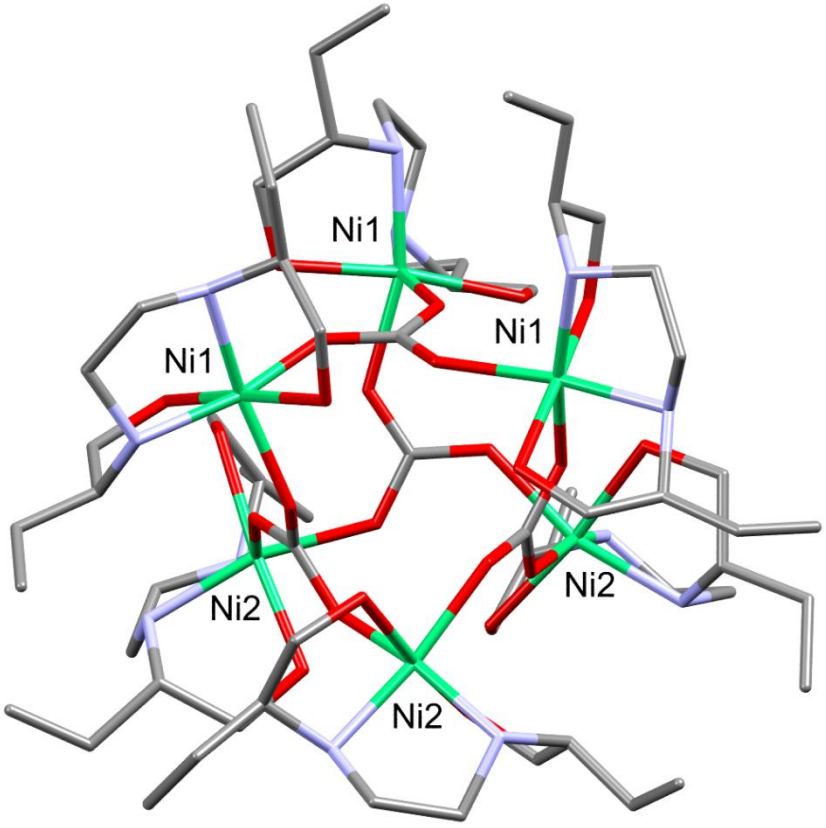

Figure 4.11: Perspective view of the molecular structure of compound **21**, thermal ellipsoids drawn at the 50% probability. Hydrogen atoms are omitted for clarity.

In compound **21**, the solvent molecules in the channels were intractably disordered and the SQUEEZE option in PLATON[15] was employed.

4.3 CONCLUSION

Nickel(II) and copper(II) coordination compounds of EMB are reported. Two new zwitterionic dithiophosphonate complexes were also reported. Considering that EMB has been effectively used as an anti-TB drug, its derivatives made in this chapter were screened for anti-microbial activity and the results are reported in Chapter 7.

4.4 EXPERIMENTAL

4.4.1 Method

Unless otherwise noted, all reactions and manipulations were carried out under an inert atmosphere with a positive nitrogen gas flow using standard Schlenk lines and tubes. Standard Schlenk techniques are critical for these reactions and manipulations to minimize contact with atmospheric oxygen that can oxidize and/or reduce desired compounds.

4.4.2 Materials

Phenetole Lawesson's reagent and ferrocenyl Lawesson's reagent were prepared according to established leiterature.[14] The free base of ethambutol (EMB) was prepared according to established literature.[12] Ethambutol dihydrochloride (EMB.2HCl) was purchased from Sigma Aldrich and used without further purification. Ammonia gas was obtained from Afrox (South Africa). Diethyl ether, THF and hexane were distilled under dinitrogen over a Na wire with the formation of a benzophenone ketyl indicator. Dichloromethane was distilled over P_4O_{10}. Methanol was distilled from I_2/Mg turnings.

4.4.3 Characterization methods

^{1}H and ^{31}P NMR spectra were recorded on a Bruker Avance 400 MHz spectrometer. NMR data are expressed in parts per million (ppm) and referenced internally to the residual proton impurity in the deuterated solvent whilst ^{31}P spectra chemical shifts are reported relative to an 85% H_3PO_4 in D_2O external standard solution, all at 298 K. Data are reported as chemical shift position (δ_H), multiplicity, relative integral intensity and assignment. Melting points were determined using a Stuart SMP3 melting point apparatus. Infrared spectra were recorded on a Perkin-Elmer Spectrum 100 FT-IR spectrometer. Mass spectral analyses were performed on a Waters API Quattro Micro spectrometer.

4.4.4 X-ray structure determination

Crystals were mounted on glass fibers with epoxy resin, and all geometric and intensity data were collected on a Bruker APEXII CCD diffractometer equipped with graphite monochromated Mo-Ka radiation (λ = 0.71073 Å). The data reduction was carried out with SAINT-Plus software.[16] The SADABS program was used to apply empirical absorption corrections.[17] All structures were solved by direct methods and refined by full-matrix least-squares on F2 with SHELXTL software package[18] found in SHELXTL/PC version 5.10.[19] Thermal ellipsoid plots are generated with OLEX2.[20]

4.5 EXPERIMENTAL

Synthesis of (EMB)CuCl·Cl (20)

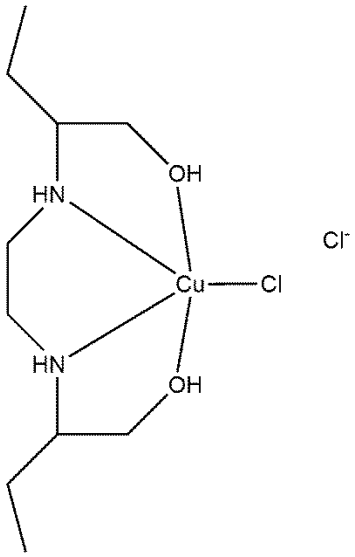

To a 100 mL beaker was added EMB.2HCl (0.200 g, 0.721 mmol) and KOH (0.081 g, 1.443 mmol) in 10 mL of deionized water. After stirring for 5 mins, $CuCl_2.5H_2O$ (0.180 g, 0.721 mmol) was added as a solid yielding an immediate blue solution. This was further stirred for 30 and diethyl ether (6 mL) was added in aliquots (2 mL) to the blue solution, with a white precipitate of residual potassium chloride forming from solution. The solution was re-centrifuged and the supernatant was decanted and stored at room temperature. Blue crystals that formed from the solution after about 14 days were filtered and rinsed with diethyl ether. Yield: 0.15 g, 65%; no NMR spectra owing to para-magnetism. Mp: hygroscopic. Selected FTIR (ν cm^{-1}): 3183 (w), 2961 (s), 2878 (s), 1635 (w), 1457 (s), 1382 (w), 1024 (s). EI-MS $(1/6M)^+$ 261.

Synthesis of 6(EMB)4(CO_3).4Cl (21)

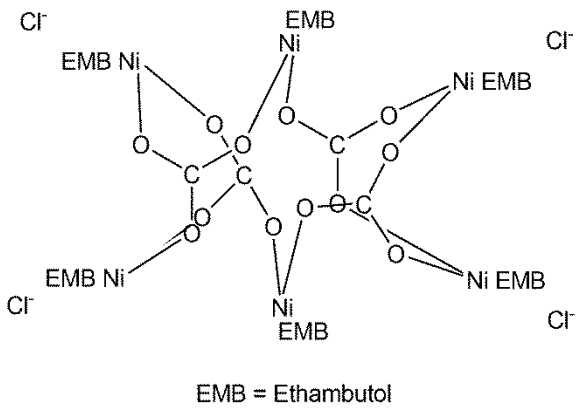

EMB = Ethambutol

To a 100 mL beaker was added EMB.2HCl (0.200 g, 0.721 mmol) and KOH (0.0269 g, 0.481 mmol) in 10 mL of deionized water. After stirring the suspension for 5 mins, K_2CO_3 (0.0665 g, 0.481 mmol) and $NiCl.6H_2O$ (0.171 g, 0.721 mmol) were added yielding an immediate green colored solution. The solution was further stirred for 30 min and diethyl ether (6 mL) was added in aliquots (2 mL) to the blue solution, with a white precipitate of residual potassium chloride forming from solution. The solution was re-centrifuged and the supernatant was decanted and stored at room temperature. Olive green crystals that formed from the solution after about 20 days were filtered and rinsed with diethyl ether. Yield: 0.16 g, 81%; no NMR spectra owing to para-

magnetism. Mp: 110 °c. Selected FTIR (ν cm^{-1}): 3338 (w), 3190 (m), 2966 (w), 1618 (w), 1455 (m), 1379 (w), 1019 (s), 547 (m). EI-MS $(1/6M)^+$ 261.

Synthesis of O,O'-2,2'-(ethane-1,2-diylbis(ammonionediyl))bis(butane-2,1-diyl) bis(4-ethoxyphenylphosphonodithioate) zwitterion (22)

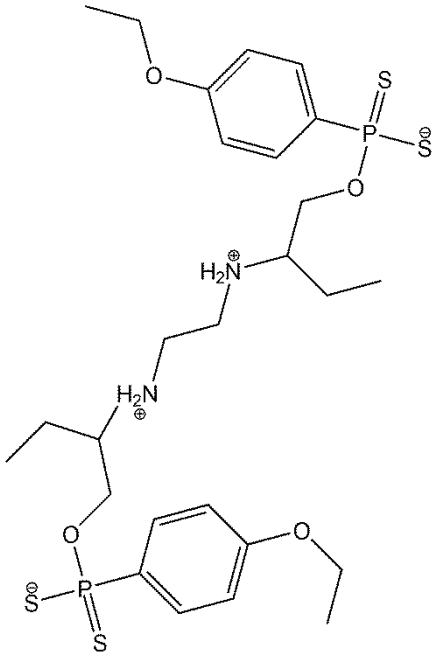

Ethambutol free base (0.100 g, 0.49 mmol) and PhLR (0.21 g, 0.49 mmol) were stirred together in THF (20 mL) in a 100 mL schlenk tube at room temp until the milky suspension went clear. The clear solution was further stirred for 30 min and all THF was removed under reduced pressure yielding a colorless precipitate. This colorless precipitate was consolidated in hexane into a free flowing powder. Colourless solid 0.19 g, 61% yield. M.p.: 193 °C. ^{1}H-NMR (400 MHz, DMSO-d_6, ppm): δ 0.87 (3.0H, t, J=7.34 Hz, CH_3), 1.32 (4.0H, q, J=6.94 Hz, Ar-CH_3), 1.60 (2.0H, d, J=7.28 Hz, CH_2), 3.86 (1.0H, d, J=4.32 Hz, CH), 4.04 (3.4H, q, J=6.94 Hz, CH_2), 6.88 (2.0H, dd, J=2.30, 8.74 Hz, Ar-H), 7.93 (2.0H, dd, J=8.62, 13.27 Hz, Ar-H). ^{31}P NMR (400 MHz, DMSO-d_6, ppm): δ 108.84 (S, 2P). ^{13}C NMR (400 MHz, CDCl3, ppm): δ 161.24, 131.89, 131.75, 113.12, 112.97, 59.84, 55.34, 46.11, 43.12, 22.89, 10.39, 8.68. Selected FTIR (ν cm^{-1}): 2973 (w), 2931 (w), 2722 (w), 1592 s), 1102 (s), 1034 (s), 665 (s). ESI-MS: $(M+H)^+$ 636.15.

Synthesis of O,O'-2,2'-(ethane-1,2-diylbis(ammonionediyl))bis(butane-2,1-diyl bis(ferrocenylphosphonodithioate) zwitterion (23)

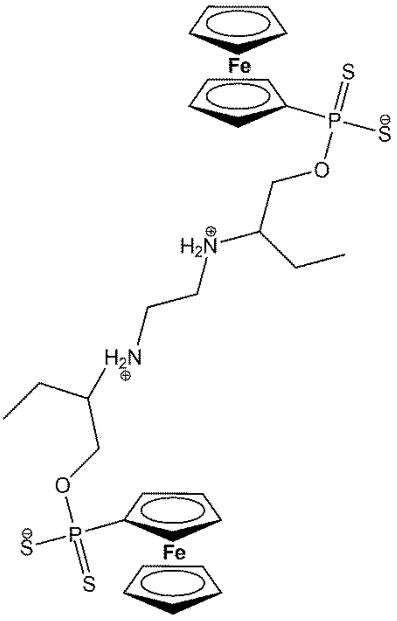

Ethambutol free base (0.100 g, 0.49 mmol) and PhLR (0.27 g, 0.49 mmol) were stirred together in THF (20 mL) in a 100 mL schlenk tube at room temp until the brown suspension went clear. The clear brown solution was further stirred for 30 min and all THF was removed under reduced pressure yielding a yellow precipitate. The yellow precipitate was consolidated in hexane into a free flowing powder. The yellow powder was purified by column chromatography. Yield: 0.12 g, 32%. M.p.: 196 °C. ^{1}H-NMR (400 MHz, DMSO-d_6, ppm): δ 0.83 (6H, t, J=7.44 Hz, CH_3), 1.33 (4H, q, J=7.19 Hz, CH_2), 2.35 (2H, t, J=5.66 Hz, CH), 2.57 (4H, s, CH_2), 3.24 (2H, q, J=5.55 Hz, CH_2), 3.33 (2H, q, J=5.24 Hz,CH_2), 4.05 (2H, d, J=9.85 Hz, Fc), 4.16 (10H, s, Fc), 4.37 (4H, d, J=17.37 Hz, Fc), 4.48 (1H, s, Fc), 4.58 (1H, s, Fc). ^{31}P NMR (400 MHz, DMSO-d_6, ppm): δ 108.38 (S, 2P). ^{13}C NMR (400 MHz, CDCl3, ppm): δ 77.50, 77.19, 76.87, 71.83, 71.05, 70.71, 70.40, 70.31, 70.17, 70.07, 67.89, 62.41, 61.60, 58.93, 31.61, 31.51, 25.84, 21.13, 19.19, 19.14, 13.88, 10.42. Selected FTIR (ν cm^{-1}): 2933 (w), 1591 (w), 1456 (m), 1173 (s), 1020 (s), 649 (s). ESI-MS: $(M-H)^+$ 763.01.

4.6 REFERENCES

1. A. M. I. Rageh, F. A. Mohamed, N. N. Atia and S. M. Botros, *J of Liquid Chromat & Relat Tech*, **2015**, 38, 1061-1067.
2. R. Bhattacharyya, U. Paul, A. Chatterjee and S. Bag, *INDIAN J OF CHEM SECTION A-INORG BIO-INOR PHY THEO & ANALY CHEM*, **1990**, 29, 986-995.
3. M. V. N. de Souza, *Current opinion in pulmonary medicine*, **2006**, 12, 167-171.
4. A. Cole, P. M. May and D. R. Williams, *Agents and actions*, **1981**, 11, 296-305.
5. V. K. Gupta, R. Prasad and A. Kumar, *Talanta*, **2003**, 60, 149-160.
6. G. Bemski, M. Rieber and H. Reyes, *FEBS letters*, **1972**, 23, 59-60.
7. A. F. Faria, L. F. Marcellos, J. P. Vasconcelos, M. V. de Souza, S. Júnior, L. Antônio, W. R. d. Carmo, R. Diniz and M. A. de Oliveira, *J. Brazilian Chem. Soc*, **2011**, 22, 867-874.
8. M. Benedetti, J. Malina, J. Kasparkova, V. Brabec and G. Natile, *Environ Health Perspectives*, **2002**, 110, 779.
9. J. E. Heng, C. K. Vorwerk, E. Lessell, D. Zurakowski, L. A. Levin and E. B. Dreyer, *Investigative ophthalmology & visual science*, **1999**, 40, 190-196.
10. M. Karakus, P. Lönnecke and E. Hey-Hawkins, *Polyhedron*, **2004**, 23, 2281-2284.
11. Z. J. Li, Y. Abramov, J. Bordner, J. Leonard, A. Medek and A. V. Trask, *J. Am. Chem. Soc.*, **2006**, 128, 8199-8210.
12. S. Cherukuvada and A. Nangia, *Cryst. Growth & Des*, **2013**, 13, 1752-1760.
13. L. Thomas and R. A. Chittenden, *Spectrochimica Acta*, **1964**, 20, 489-502.
14. W. E. Van Zyl and J. P. Fackler, *Phosphorus, Sulfur Silicon Relat. Elem*, **2000**, 167, 117-132.
15. A. Spek, *Inc., Madison, WI*, **2003**.
16. V. SAINT, *Siemens Analytical Instruments Division, Madison, WI*, **1995**.
17. G. Sheldrick, *University of Göttingen, Germany*, **2010**.
18. G. Sheldrick, *University of Göttingen, Germany*, **1997**.
19. V. SHELXTL, *Inc., Madison, WI*, **2001**.

20. C. Júnior and P. de Sousa, Universidade de São Paulo, **2017**.

21. M. Karakus, Y. Aydogdu, O. Celik, V. Kuzucu, S. Ide, E. Hey-Hawkins. Z. Anorg. Allg. Chem, **2007**, 633, 405-410

CHAPTER 5

DITHIOPHOSPHONATE S-S COUPLED COMPOUNDS: SYNTHESIS, CHARACTERIZATION AND POLYMORPHS

5.1 INTRODUCTION

Thiophosphorus compounds, their acids and metal complexes have been utilized for a variety of applications in academia, industry and commerce. For example, they have been used in the industry as anti-oxidant additives in the oil and petroleum industry.[1-3] Zinc diakyldithiophosphates have found application for many years as anti-oxidant and anti-wear additive in the petroleum industry and have been reviewed.[3-6] These complexes have also found use as metal ore extraction reagents and flotation agents in the mining sector.[7] Studies have also demonstrated that these compounds are useful for agricultural purposes especially as pesticides and insecticides.[8, 9] Metal complexes of these ligands have also shown biological activity.[10]

Recent studies on thiophosphorus compounds have aimed largely at the use of these compounds as ligands for metal complexation.[11-15] Thiophosphorus compounds can also be used as precursors in the synthesis of S-S coupled disulfides. These disulfides can be formed by two thiophosphorus groups joined by a disulfide bridge (–P–S–S–P–) or one thiophosphorus group attached *via* a disulfide bridge to an organic substituent e.g. an aliphatic or aromatic moiety (–P–S–S–R).[16] Compounds of the former type have been subject of recent studies.[16, 17] Previously such studies[18-20] offered little information on spectroscopic characterization of disulfide compounds, but later studies[16, 17] reported ^{1}H NMR, ^{31}P NMR, ^{13}C NMR, mass spectrometric and elemental analyses characterization of disulfides and in some cases molecular structures. Most of the thiophosphorus disulfides formed from simple alcohols such as MeOH, EtOH, i-PrOH, etc are intermolecular S-S coupled compounds (intramolecular S-S coupled disulfides are chemically not possible for simple alcohols). Van Zyl and co-workers[17] reported dithiophosphonate S-S coupled heterocycles obtained by oxidative intramolecular coupling. The geometry of the starting

alcohols gave room for these intramolecular S-S couplings and they also reported the molecular structures of these heterocycles.

The properties of a solid material depend not only on the identity of its constituents but also on their arrangement (packing) in the solid. Crystalline solids are those in which the component atoms, molecules, or ions are arranged in a regularly ordered, repeating pattern in three dimensions. It is therefore not unusual for a single constituent to be able to exist in more than one crystalline arrangement[21] and this can give rise to variation in physical properties. It is important to note that polymorphism exist only in the solid state and not in the liquid or gaseous state. This is because crystal structures are discreet, repeating units held together by weak forces like van der Waals, hydrogen bonding, ionic interactions etc. Chemical energies sufficient enough to break up the forces holding the crystalline solids together will also disrupt these weak forces hence giving no room for polymorphism. The existence of the same crystalline solid in two or more different arrangements can be influenced by factors like solvent[22, 23] and temperature.[24]

This chapter reports synthesis and characterization of dithiophosphonate S-S coupled compounds obtained by oxidative intramolecular coupling. Four different polymorphs of pentaerthritol derived ferrocenyl dithiophosphonate compounds are described, compound **2** has been synthesized and molecular structure reported by our group in literature.[17] The polymorph reported in literature has also been compared with four others obtained in this study.

5.2 RESULTS AND DISCUSSION

5.2.1 Synthesis of polymorphs

The ferrocenyl dithiophosphonate salt **2** was prepared by heating a mixture of 2 molar equivalents of FcLR with 1 molar equivalent of pentaerythritol while stirring at 70°C until dissolution of all solids (Scheme 5.1). The dithiophosphonic acid was then deprotonated at ice bath temperature (0°C) using anhydrous ammonia. S-S coupled disulfide **24** derived from intramolecular oxidation were obtained by precipitation from methanol in the presence of I_2 following an established literature procedure.[17] Different polymorphs were obtained by growing the crystals of compound **24** in different solvents. Crystals of polymorphs **A, B** and **C** were grown from layering hexane, ether or toluene onto concentrated solutions of compound **24** dissolved in $CHCl_3$, respectively. Crystals of polymorph **D** were grown by layering toluene onto a concentrated solution of compound **24** dissolved in DCM.

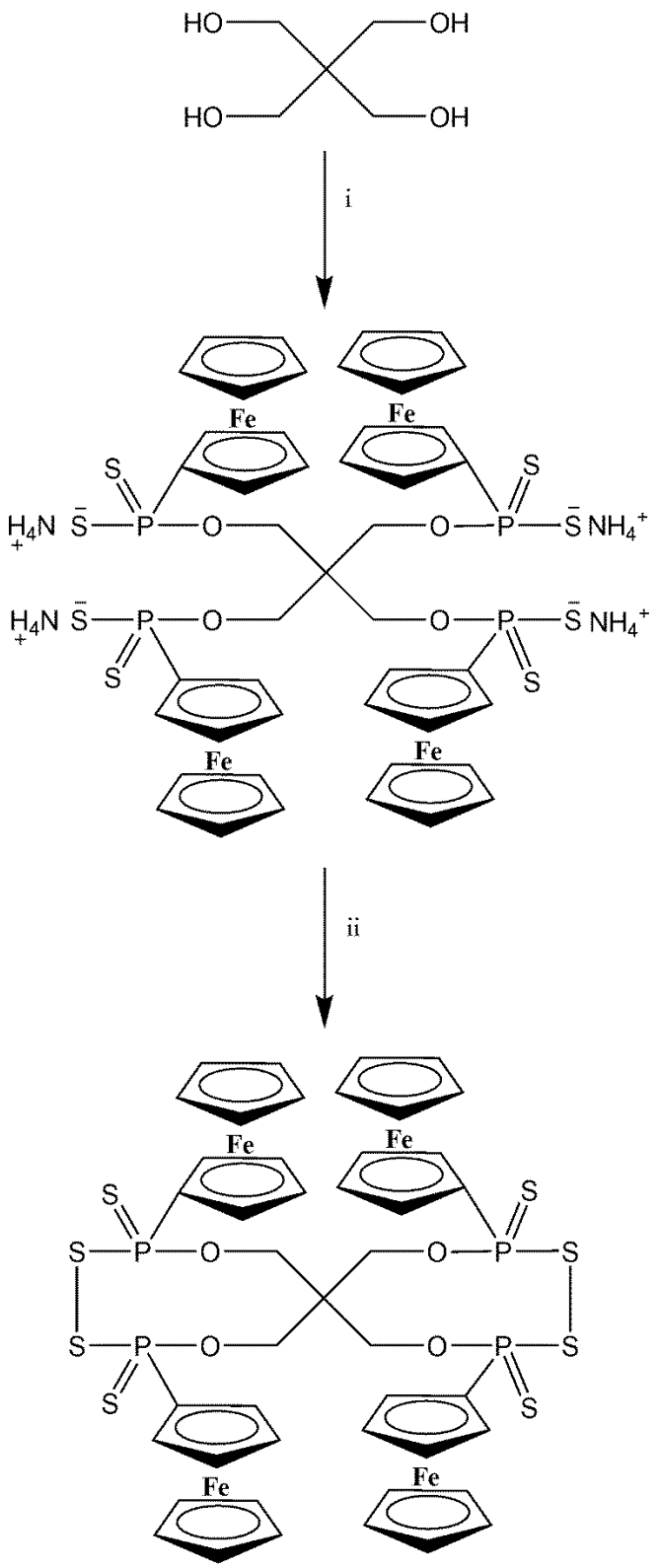

Scheme 5.1: Synthesis of compound **24**. Conditions: i) Toluene, 70 °C, ammonia gas, ii) Iodine in MeOH at room temperature.[17]

5.2.2 Synthesis of dithiophosphonate disulfides.

Scheme 5.2 gives the route to the synthesis of complexes **25-28**. Many derivatives of the dithiophosphonate ligand are obtainable from the reaction between a common thionation precursor (usually Lawesson's Reagent or a derivative thereof), and a primary or a secondary alcohol.[25] In the right stoichiometric amount, the alcohol cleaves the dimeric LR/FcLR unit to form a dithiophosphonic acid and subsequently the ammonium salt can be formed. The ligand salt can then react with a metal precursor to form a metal complex, or can also be used to generate the disulfide in the presence of iodine. The synthesis of compounds **25-28** (Scheme 5.2) did not follow this common synthetic route. The reaction started with a pentaerythritol derivitized dithiophosphonate ammonium salt (ligand **2**) and yielded a bimetallic dithiophosphonate disulfide (Scheme 5.2). Ligand **2** was stirred in methanol with the Zn(II) or Cd(II) bipyridine or phenanthroline precursors to yield the dithiophosphonate disulfides. The mechanism for the formation of these disulfides is not fully understood and is similar to that reported by Rauchfuss and Zank[26] in 1986, as well as Hey-Hawkins and coworkers[27] in 2012. There is a C-O bond cleavage followed by M-O and S-S bond formation.

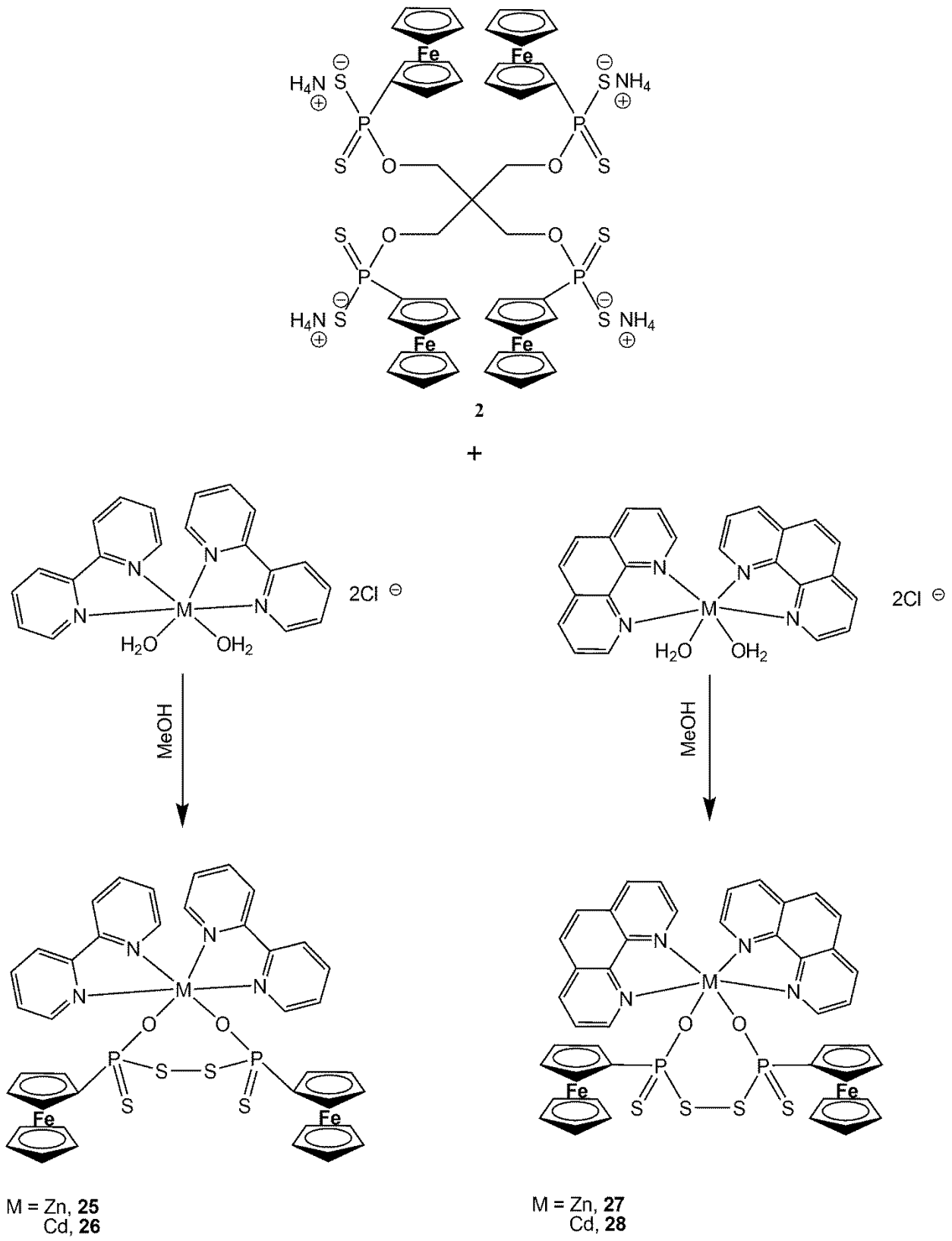

Scheme 5.2: Synthesis of dithiophosphonate disulfide heterocycles.

5.2.3 Spectroscopy

The ^{1}H NMR of compounds **25-28** showed peaks in the expected region. The aromatic protons gave signals between 7 to 9 ppm which integrated to the equivalent number of protons. The substituted ferrocenyl protons gave two set of peaks equivalent to the protons while the unsubstituted ferrocenyl protons gave a singlet signal. The ^{31}P NMR gave singlets for compounds **25-28** indicating that these compounds are single isomers in solution. Compounds **25-28** decomposed between 220-320°C and the ESI-MS gave fragmented ions in all cases.

5.2.4 Comparison of polymorphs

5.2.4.1 Molecular structures

The molecular structures of all the polymorphs are essentially the same as shown in Figure 5.1. Polymorphs **A-D** have the following crystallographic parameters: Monoclinic space group $P2_1/c$ with 4 molecules per unit cell (polymorph **A**); *Pn* with 2 molecules per unit cell (polymorph **B**); *C*2/*c* with 4 molecules per unit cell (polymorph **C**); and *C*2/*c* with 4 molecules per unit cell (polymorph **D**), respectively, as shown in Table 5.1. Polymorphs **A** and **B** crystallize without any solvated molecules while polymorphs **C** and **D** crystallize with 1 and 2 molecules of toluene, respectively. In both polymorphs **C** and **D** the toluene molecules in the channels were intractably disordered and the SQUEEZE option in PLATON[28] was employed. All the 4 polymorphs are made up of two heterocycles each similar to that obtained by van Zyl and co-workers[17] (**Z**) with a common centroid. The two heterocycles in each polymorph are a 9-membered ring made up of 2 C, 2 O, 2 P, and 2 C atoms with a common C atom (centroid) as shown in Figure 5.2. Table 5.1 gives the differences in crystal data of all the polymorphs and **Z**. Molecular overlays were used in comparing the different polymorphs and this is presented in Figure 5.3.

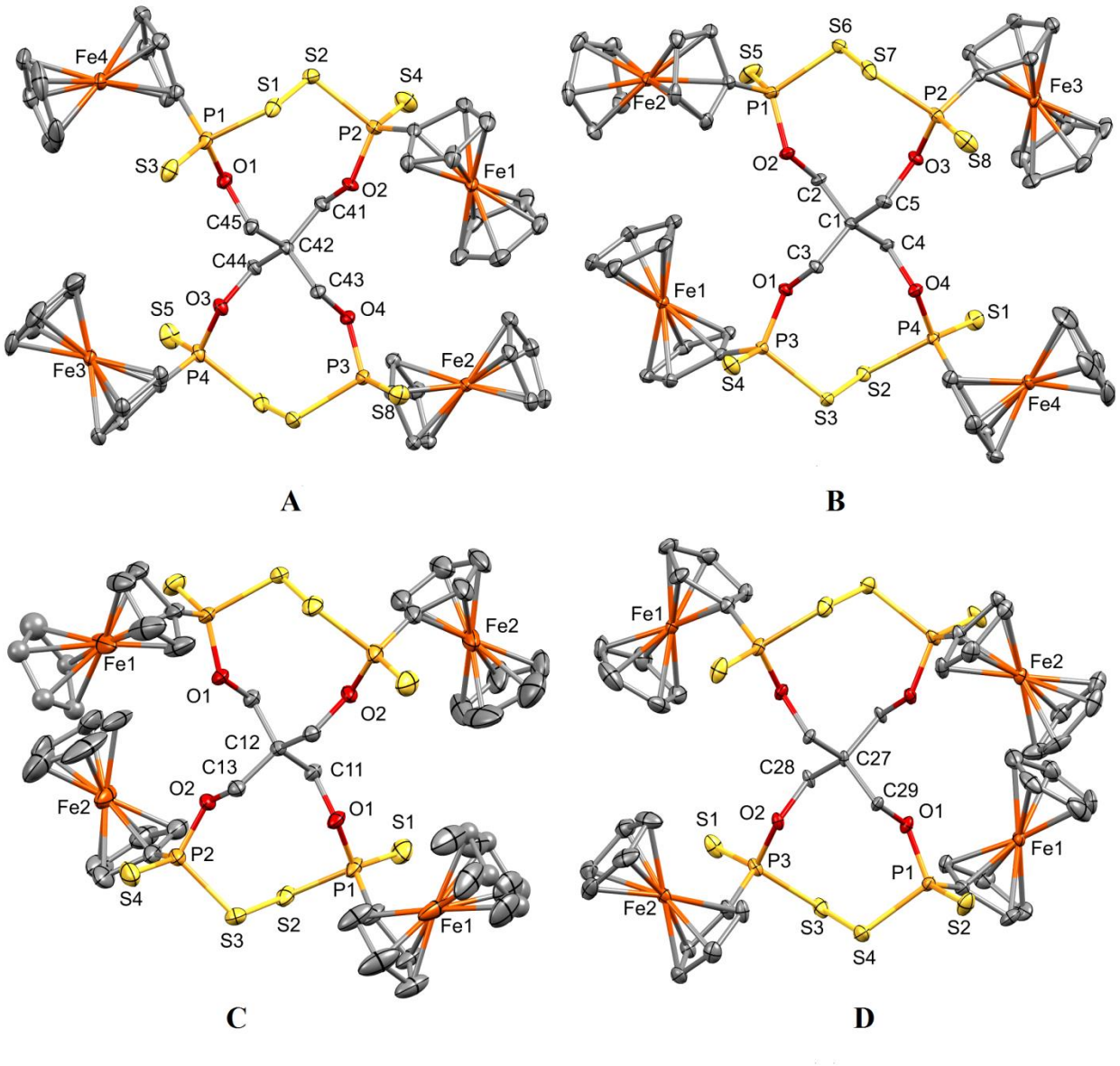

Figure 5.1: Perspective view of polymorphs **A-D**.

Table 5.1 gives important crystal data of all the polymorphs obtained (**A-D**) and the one reported by van Zyl and co-workers[17] (**Z**).

Table 5.1 : X-ray crystallographic data for polymorphs **(A-D)** of compound **24** and **Z**.[17]

Polymorphs	(**A**)	(**B**)	(**C**)	(**D**)	(**Z**)[17]
Crystal data					
Chemical formula	$C_{45}H_{44}Fe_4O_4P_4S_8$	$C_{45}H_{44}Fe_4O_4P_4S_8$	$C_{45}H_{44}Fe_4O_4P_4S_8$	$C_{45}H_{44}Fe_4O_4P_4S_8$	$C_{45}H_{44}Fe_4O_4P_4S_8 \cdot 2(CH_2Cl_2)$
M_r	1252.56	1252.56	1252.56	1252.56	1418.38
Crystal system, space group	Monoclinic, $P2_1/c$	Monoclinic, *Pn*	Monoclinic, $C2/c$	Monoclinic, $C2/c$	Orthorhombic, *Pbca*
Temperature (K)	173	173	173	173	173
a, *b*, *c* (Å)	23.8600 (4), 15.4101 (3), 13.5420 (2)	14.5094 (3), 12.4013 (2), 15.0364 (3)	28.1141 (7), 9.0649 (3), 23.5989 (6)	28.127 (2), 8.9825 (7), 28.406 (2)	27.4485 (13), 14.5982 (7), 28.2672 (14)
□ (°)	96.091 (1)	112.288 (1)	96.732 (1)	112.957 (8)	90
V (Å^3)	4951.08 (15)	2503.44 (8)	5972.7 (3)	6608.5 (10)	11326.6 (9)
Z	4	2	4	4	8
Radiation type	Mo *K*α	Mo *K*α	Mo *K*α	Mo *K*α	Mo *K*α
Absorption coefficient (mm^{-1})	1.66	1.64	1.38	1.24	1.64
Crystal size (mm)	0.30 × 0.19 × 0.14	0.46 × 0.34 × 0.21	0.21 × 0.17 × 0.13	0.26 × 0.08 × 0.04	0.20 × 0.18 × 0.18

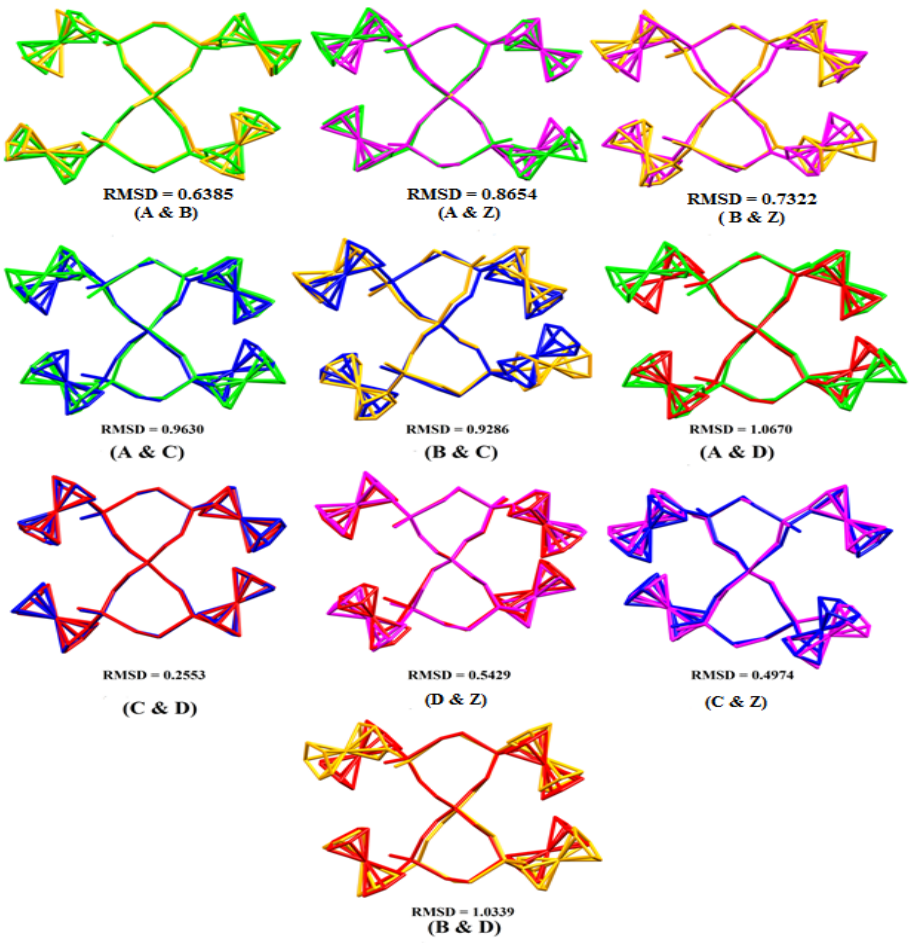

Figure 5.2: Molecular overlay between polymorphs **A-D** and **Z** (Polymorphs **A** in green, **B** in yellow, **C** in blue, **D** in red and **Z** in pink).

The degree of deviation between these polymorphs is statistically expressed as root mean square deviation (RMSD) for each pair (Figure 5.2). The highest deviation is about 10 % between polymorphs **B** & **D** and **A** & **D**. Polymorphs **B** & **C** and **A** & **C** have a deviation of about 9 %. The least deviation occurs between polymorphs **C** & **D** with about 2 %. The degree of deviation between the polymorphs could be linked to the presence of a solvent in the crystal lattice. For example, polymorphs **C** and **D** crystallized with 1 and 2 toluene molecules, respectively, and have the least molecular deviation (2 %). Polymorphs **1** and **2** however crystallized without any solvent in the crystal lattice and have higher deviations when compared to **C** and **D** than among themselves. The RMSD (%) between polymorphs **A** & **C** and **B** & **C** are 9 % each and **A** & **D** and **B** & **D** are 10 % each, respectively. The RMSD (%) between **A** & **B** is about 6 % as

shown in Figure 5.2. This trend is observable with the polymorph reported in literature[17] (**Z**) compared to polymorphs **A**-**D**. Polymorph **Z** crystallized with 2 molecules of DCM (Table 5.1). Polymorph **Z** differs least when compared to **C** & **D** (4 & 5 %) that crystallized with a solvent compared to **A** & **B** (8 & 7 %) that crystallized without a solvent. The use of different solvents can be said to have influenced the crystallization of different polymorphs and may have also have played a role in the deviations observed in the molecular displays (Figure 5.2).

5.2.4.2 Crystal packing

A perspective view of portions of the crystal packing for polymorphs **A**-**D** and **Z** are given in Figure 5.3. When viewed along the same crystallographic axis (*b*), it can be seen that the packing of all polymorphs are not the same as shown (Figure 5.3). All the polymorphs contain a variety of intermolecular non-classical hydrogen bonding interactions which form hydrogen bonded supramolecular architectures. The hydrogen bonding parameters are given in Tables 5.2 to 5.6.

The hydrogen atoms of the substituted ferrocenyl molecule and the adjacent sulfur atoms (P=S) in polymorph **A** interact through intermolecular hydrogen bonding that forms chains which extends along the crystallographic *c* axis (Figure 5.4).

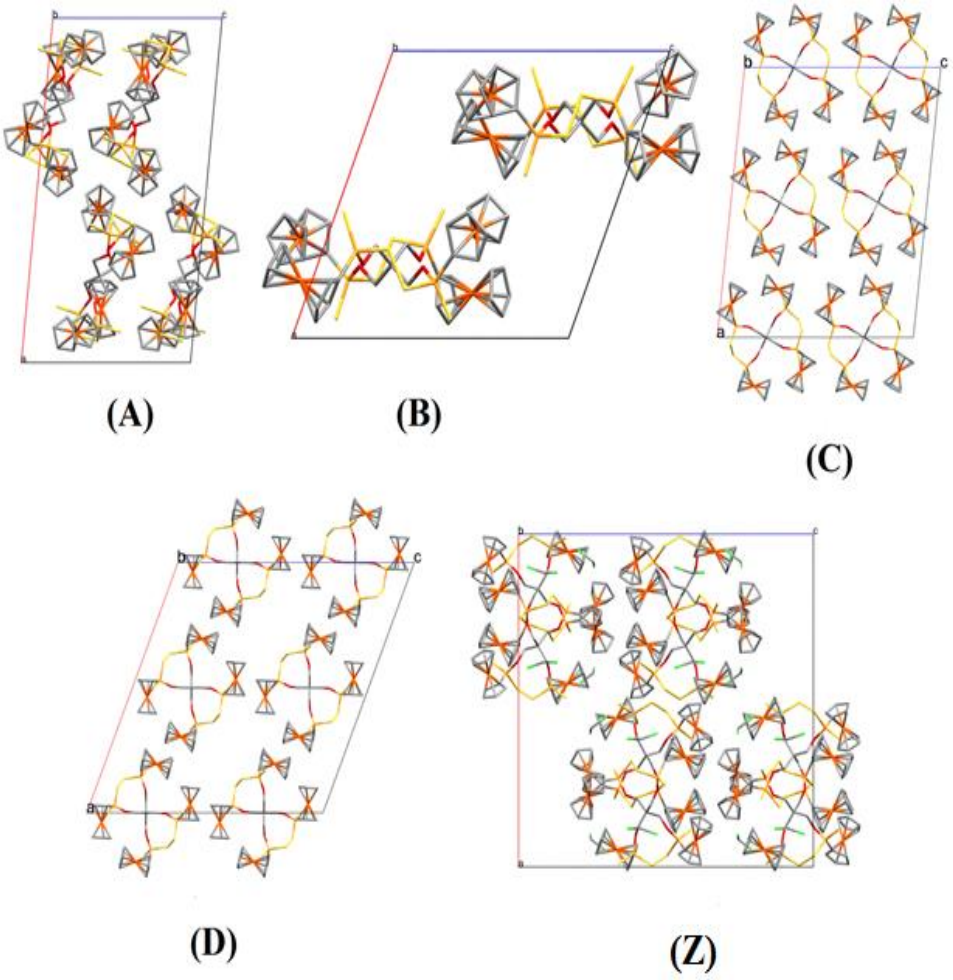

Figure 5.3: Representations of the crystal structure packing of polymorphs **A-D** and **Z**[17].

The hydrogen atoms of the substituted ferrocenyl moiety of polymorph **A** are also linked to the neighboring sulfur atoms (P=S) by C—H…S hydrogen bonds resulting into a 10 membered ring described by a $R_2^2(10)$ graph-set notation which forms a 2 dimensional polymer. The methylene hydrogen atoms from the dithiophosphonate are linked to neighbouring sulfur atoms (P=S) by C—H···S hydrogen bonds that align along the crystallographic *c* axis. All these intermolecular hydrogen bonding in polymorph **A** give rise to a two dimensional supramolecular assembly that extends along the crystallographic *a* and *b* axes as shown in Figure 5.4.

Table 5.2: Hydrogen-bond geometry (Å, º) for polymorph **A**.

D—H···*A*	*D*—H	H···*A*	*D*···*A*	*D*—H···*A*
C5—H5···S4^{i}	1.00	2.81	3.786 (3)	166
C12—H12···S3^{ii}	1.00	2.94	3.855 (3)	152
C32—H32···S8^{iii}	1.00	2.84	3.800 (3)	162
C41—H41*A*···S8^{iii}	0.99	2.89	3.652 (3)	135
C45—H45*B*···S4^{i}	0.99	2.64	3.443 (3)	138

Symmetry codes: (i) *x*, −*y*+1/2, *z*−1/2; (ii) −*x*, −*y*+1, −*z*+1; (iii) *x*, −*y*+1/2, *z*+1/2.

Table 5.3: Hydrogen-bond geometry (Å, º) for polymorph **B**.

D—H···*A*	*D*—H	H···*A*	*D*···*A*	*D*—H···*A*
C2—H2*B*···S8^{i}	0.99	2.90	3.644 (3)	132
C4—H4*A*···S2	0.99	2.98	3.481 (3)	113
C7—H7···S5^{ii}	1.00	2.73	3.561 (3)	141
C37—H37···S6	1.00	2.89	3.412 (3)	114

Symmetry codes: (i) *x*−1/2, −*y*+1, *z*−1/2; (ii) *x*+1/2, −*y*+1, *z*+1/2.

Table 5.4: Hydrogen-bond geometry (Å, º) for polymorph **C**.

D—H···*A*	*D*—H	H···*A*	*D*···*A*	*D*—H···*A*
C5—H5···S2^{i}	1.00	2.94	3.559 (4)	121
C11—H11*A*···S2	0.99	2.96	3.465 (4)	113
C13—H13*A*···S3	0.99	2.97	3.475 (3)	113
C5—H5···S2^{i}	1.00	2.94	3.559 (4)	121
C11—H11*A*···S2	0.99	2.96	3.465 (4)	113
C13—H13*A*···S3	0.99	2.97	3.475 (3)	112

Symmetry code: (i) −*x*+1, −*y*+1, −*z*.

Table 5.5: Hydrogen-bond geometry (Å, º) for polymorph **D**.

D—H···*A*	*D*—H	H···*A*	*D*···*A*	*D*—H···*A*
C4—H4···S2^{i}	1.00	2.82	3.5924 (3)	135
C14—H14···S1^{ii}	1.00	2.77	3.7408 (3)	165

Symmetry codes: (i)1/2 –*x*, -1/2+y, ½-z (ii) x, 1+y, z

Table 5.6: Hydrogen-bond geometry (Å, º) for **Z**.

D—H···*A*	*D*—H	H···*A*	*D*···*A*	*D*—H···*A*
C9A—H9A···S3^{i}	1.00	2.75	3.624(6)	146
C19—H19···S2^{ii}	1.00	2.86	3.821 (6)	162

Symmetry codes: (i)1/2 –*x*, -1/2+y, ½+yz (ii) 1-x, -y,-z

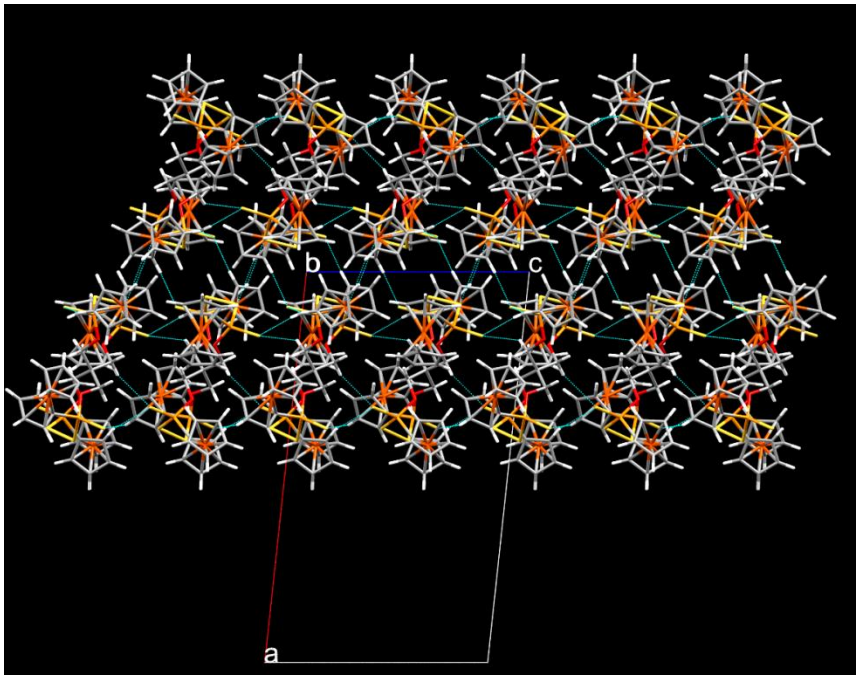

Figure 5.4: Representation of the crystal structure of polymorph **A** showing a 2 D supramolecular assembly (green lines show hydrogen bonding).

In polymorph **B**, hydrogen atoms of the substituted ferrocenyl moiety are linked to neighboring sulfur atoms (P=S) by C—H···S hydrogen bonds forming chains that extend along crystallographic *c* axis. On the other hand, hydrogen atoms of the dithiophosphonate's methylene group also interact by hydrogen bonding to neighbouring sulfur atoms (P=S) forming chains that extends along crystallographic *a* and *c* axes. A combination of these interactions results into a polymer that extends diagonally with respect to *a* and *c* crystallographic axes (Figure 5.5).

Hydrogen atoms of substituted ferrocenyl moiety interact by intermolecular hydrogen bonding with neighboring sulfur atoms (S-S) to form a 10 membered heterocycle ring described by a $R_2^2(10)$ graph-set notation resulting in a one dimensional polymer that extends long the crystallographic *c* axis for polymorph **C** (figure 5.6). The sulfur hydrogen bond acceptor in this case is the S-S coupled atoms and not the P=S atoms unlike polymorphs **A** and **B**.

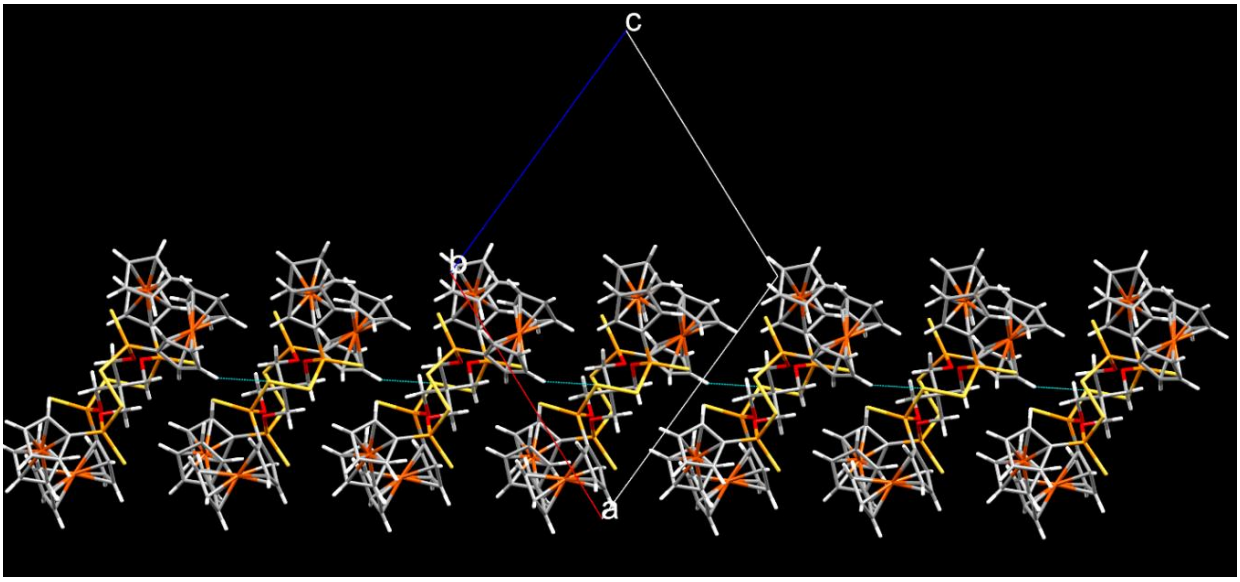

Figure 5.5: Representation of the crystal structure of polymorph **B** with diagonal chains that extends with respect to crystallographic **a** and *c* axes (hydrogen bonds shown as green lines).

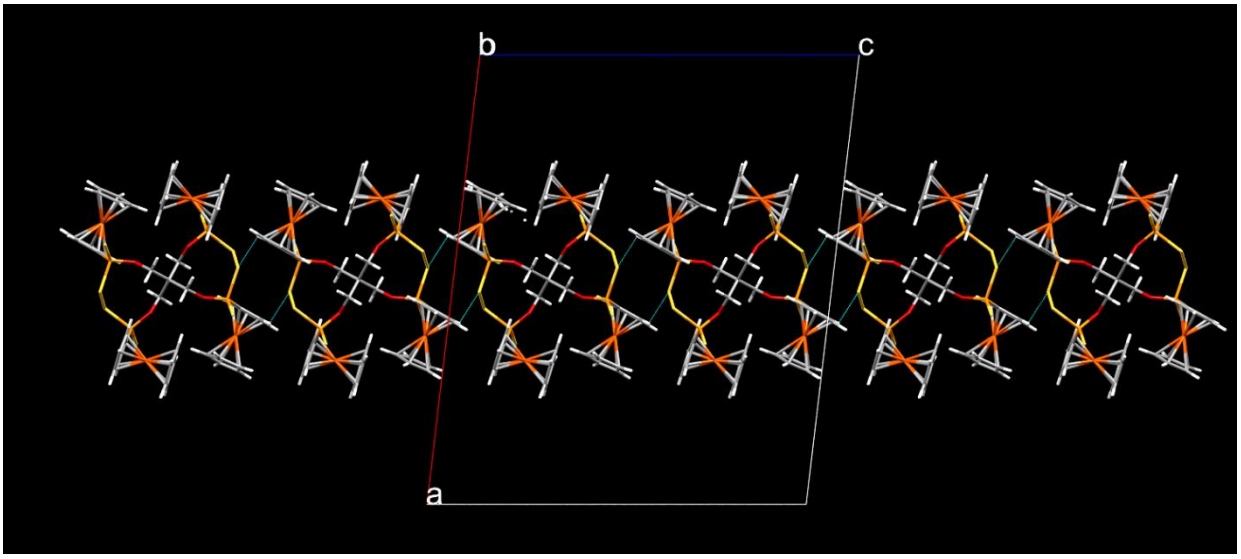

Figure 5.6: Representation of crystal structure of polymorph **C** forming one dimensional polymer (hydrogen bonds shown in green lines).

These hydrogen bonds, shown as green lines, form squares running parallel between the dithiophosphonate molecules in the polymeric assembly as shown in Figure 5.6.

In polymorph **D,** hydrogen atoms of both the substituted and unsubstituted ferrocenyl moiety interact with neighboring sulfur atoms (P=S). In the first case, hydrogen atoms of the substituted ferrocenyl molecule form intermolecular hydrogen bonds with neighboring sulfur atoms resulting into chains that extend along *b* axis (Figures 5.7 & 5.8) while in the second one, hydrogen atoms of the unsubstituted ferrocenyl molecule are linked to the neighboring sulfur atoms by C—H···S hydrogen bonds which links up the chains formed in the first case along the crystallographic *a* axis (figure 5.8). The overall effect of these intermolecular hydrogen bonds is a two dimensional supramolecular assembly with the representations shown in figure 5.7 and 5.8.

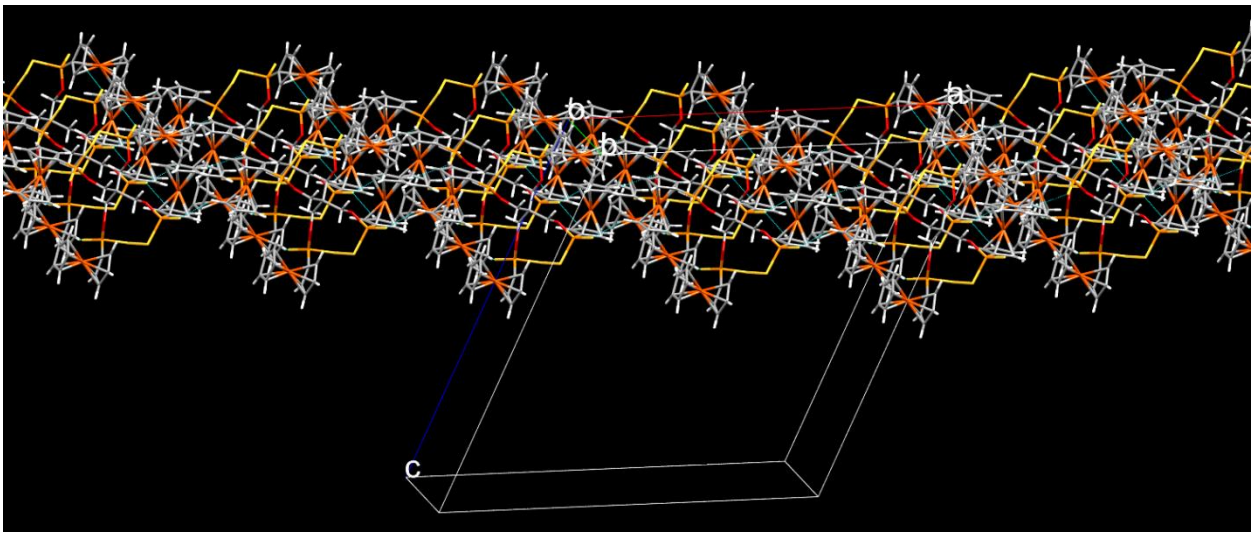

Figure 5.7: A representation of the crystal structure of polymorph **D** (green lines show hydrogen bonding).

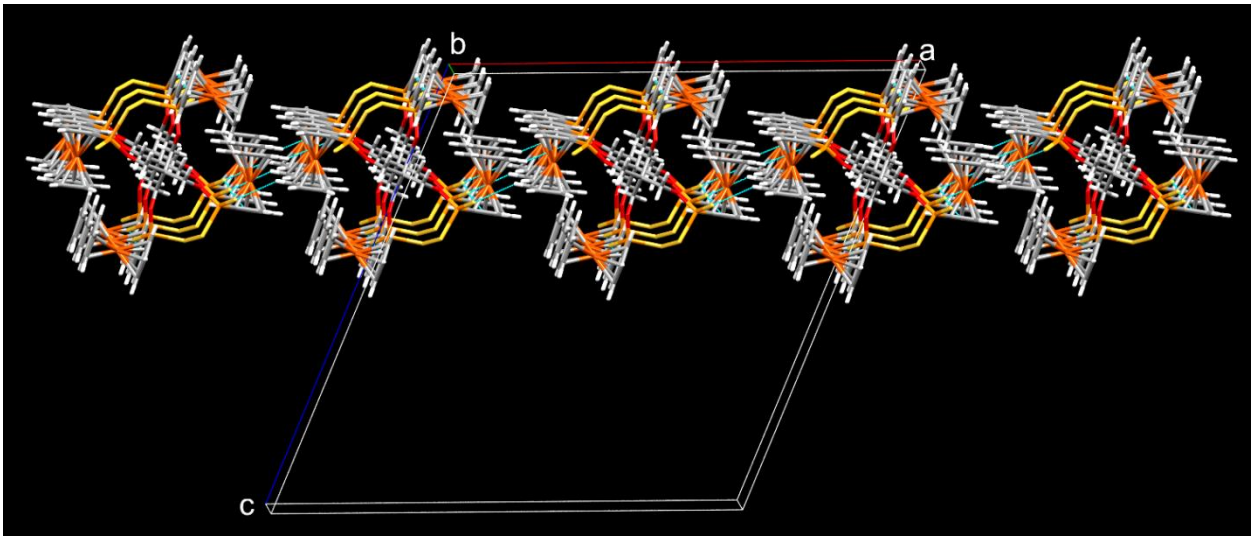

Figure 5.8: Another representation of the crystal structure of polymorph **D** showing side by side linkage of chains (green lines show hydrogen bonds) in the supramolecular assembly.

The crystal packing of polymorph **Z**[17] also shows a different pattern. Linking the hydrogen atoms of the substituted ferrocenyl moiety to the neighbouring sulfur atoms (P=S) are C—H···S hydrogen bonds that form chains which extends along *b* axis. The hydrogen atoms of the substituted ferrocenyl moiety also interact with the neighbouring S atoms (S-S) to form a 14 membered heterocycle ring described by a

$R_2^2(14)$ graph-set notation linking up the chains formed from the first case and resulting into a corrugated two dimensional supramolecular architecture (Figure 5.9).

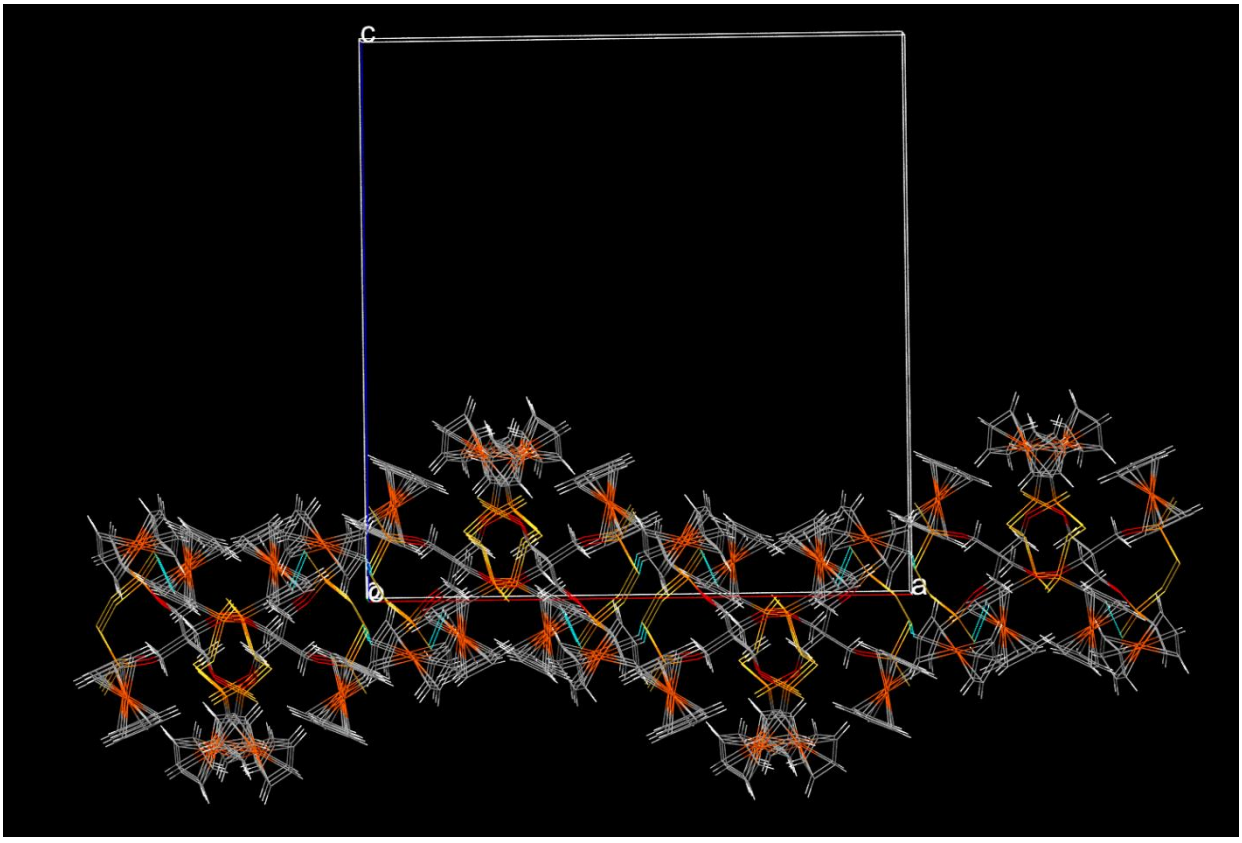

Figure 5.9: A representation of the crystal structure of polymorph **Z** showing corrugated supramolecular assembly (green lines show hydrogen bonding).

5.3 MOLECULAR STRUCTURES OF DISULFIDES

X-ray structures of compounds **25** and **27** were obtained in this study. Single crystals of **25** and **27** suitable for X-ray analysis were obtained by slow diffusion of hexane into concentrated solutions of **25** and **27** dissolved in DCM. This thesis reports new solid-state structures of intramolecular S-S coupled dithiophosphonates, van Zyl and co-workers[17] previously reported some. The S-S coupled dithiophosphonate molecular structures reported here are the first examples of bimetallic intramolecular S-S coupled dithiophosphonates. Compound **25** crystallizes in the monoclinic space group C2/c. A

perspective view of the molecular structure of compound **25** is depicted in Figure **5.10** while important X-ray crystallographic data and selected bond lengths and angles are shown in Tables **5.7** and **5.8**, respectively.

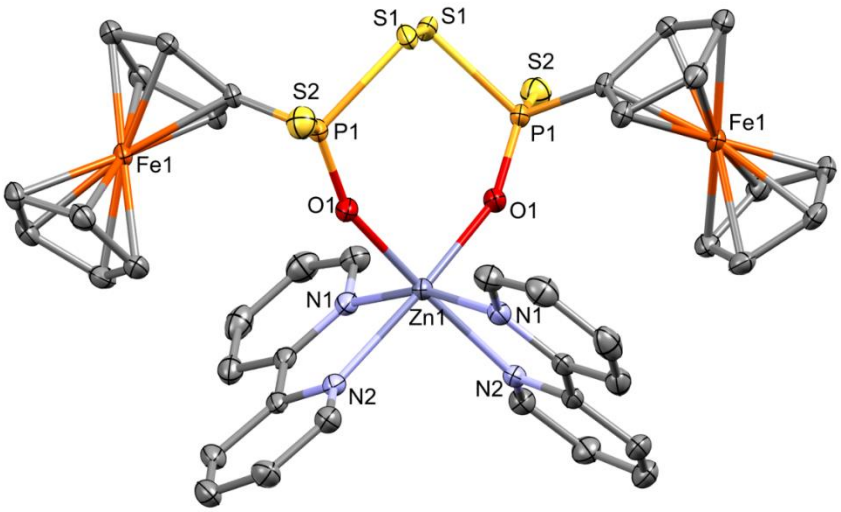

Figure 5.10: Perspective view of the molecular structure of compound **25**. Hydrogen atoms are omitted for clarity.

Variation between bond lengths of P=S and P-S are seen in the bond lengths of 1.95 and 2.10 Å, respectively, which are in close agreement to that of literature.[17] The S-S coupling of compound **25** results in the formation of a 7-membered heterocycle as shown in Figure 5.10. The coordination geometry around the Zn(II) centre is distorted octahedral comprising of four atoms of N and two atoms of O. The S1-S1 bond length of 2.07 Å of the molecular structure of compound **25** is in good agreement with literature.[17] The structural dynamics of the S=PSSP=S geometry have been studied and classified into *anti-anti* where both S atoms point away from the disulfide bridge; *syn-syn* where both point toward the disulfide bridge; and *anti-syn* which is a hybrid of the aforementioned[29] as shown earlier in Chapter 1 (Figure 1.2). The molecular structure of compound **25** displays the *anti-anti* geometry as shown in Figure 5.10. A perspective view of the molecular structure of compound **27** is shown in Figure 5.11.

Table 5.7: X-ray crystallographic data for compounds **25** and **27**.

Compound	**25**	**27**
Empirical formula	$C_{40}H_{34}FeN_4O_2P_2S_4Zn$	$C_{44}H_{34}Fe_2N_4O_2P_2S_4Zn$
Formula weight	969.96	1018.00
Temperature	100(2) K	100(2) K
Wavelength	0.71073 Å	0.71073 Å
Crystal system	Monoclinic	Monoclinic
Space group	C 2/c	C 2/c
Unit cell dimensions	a = 12.8817(17) Å	a = 13.163(5) Å
	c = 18.419(3) Å	c = 17.214(5) Å
	b = 17.633(2) Å	b = 19.405(5) Å
	α= 90°.	α= 90°.
	β= 108.928(3)°.	β= 108.817(5)°.
	γ = 90°.	γ = 90°.
Volume	3957.6(9) $Å^3$	4162(2) $Å^3$
Z	4	4
Density (calculated)	1.628 Mg/m^3	1.625 Mg/m^3
Absorption coefficient	1.659 mm^{-1}	1.582 mm^{-1}
F(000)	1976	2072
Crystal size	0.180 x 0.120 x 0.090 mm^3	0.210 x 0.180 x 0.140 mm^3
Theta range for data collection	2.032 to 27.152°.	1.942 to 28.331°.
Index ranges	-16<=h<=16, -21<=k<=22, -23<=l<=23	-17<=h<=17, -25<=k<=16, -22<=l<=22
Reflections collected	17142	16559
Independent reflections	4373 [R(int) = 0.0278]	5183 [R(int) = 0.0340]
Completeness to theta = 25.242°	99.9 %	99.9 %
Absorption correction	Semi-empirical from equivalents	Semi-empirical from equivalents
Max. and min. transmission	0.879 and 0.741	0.820 and 0.721
Refinement method	Full-matrix least-squares on F^2	Full-matrix least-squares on F^2
Data / restraints / parameters	4373 / 0 / 249	5183 / 1 / 267
Goodness-of-fit on F^2	1.041	1.050
Final R indices [I>2sigma(I)]	R1 = 0.0291, wR2 = 0.0690	R1 = 0.0387, wR2 = 0.0934
R indices (all data)	R1 = 0.0354, wR2 = 0.0718	R1 = 0.0570, wR2 = 0.1017
Largest diff. peak and hole	0.707 and -0.319 $e.Å^{-3}$	0.841 and -0.659 $e.Å^{-3}$

Table 5.8: Selected bond distances (Å) and angles (˚) for compounds **25** and **27**.

Compound **25**

P(1)-O(1)	1.5014(16)	Zn(1)-O(1)	2.0227(15)
P(1)-S(2)	1.9477(9)	Zn(1)-O(1)#1	2.0227(15)
P(1)-S(1)	2.1270(8)	Zn(1)-N(1)#1	2.1489(19)
S(1)-S(1)#1	2.0668(13)	Zn(1)-N(2)#1	2.1961(18)
O(1)-Zn(1)-O(1)#1	94.39(9)	O(1)#1-Zn(1)-N(1)	95.41(7)
O(1)-Zn(1)-N(1)#1	95.41(7)	N(1)#1-Zn(1)-N(1)	163.28(10)
O(1)#1-Zn(1)-N(1)#1	95.93(7)	O(1)-Zn(1)-N(2)	171.63(7)
O(1)-Zn(1)-N(1)	95.93(7)	O(1)#1-Zn(1)-N(2)	86.15(6)

Compound **27**

N(1)-Zn(1)	2.196(2)	P(1)-S(2)	1.9577(12)
N(2)-Zn(1)	2.161(2)	P(1)-S(1)	2.1204(10)
O(1)-P(1)	1.504(2)	S(1)-S(1)#1	2.0741(15)
O(1)-Zn(1)	2.0256(19)	O(1)#1-Zn(1)-N(1)	169.23(8)
O(1)#1-Zn(1)-O(1)	100.91(11)	O(1)-Zn(1)-N(2)	92.07(8)
O(1)#1-Zn(1)-N(2)#1	92.07(8)	N(2)#1-Zn(1)-N(2)	169.24(12)
O(1)-Zn(1)-N(2)#1	94.78(8)	O(1)#1-Zn(1)-N(1)#1	86.18(8)
O(1)#1-Zn(1)-N(2)	94.78(8)	O(1)-Zn(1)-N(1)#1	169.24(8)

Compound **27** crystallizes in the monoclinic space group C2/c with 4 molecules in the asymmetric unit cell (Table 5.7). Important X-ray crystallographic data and selected bond lengths and angles of compound **27** are shown in Tables **5.7** and **5.8** respectively.

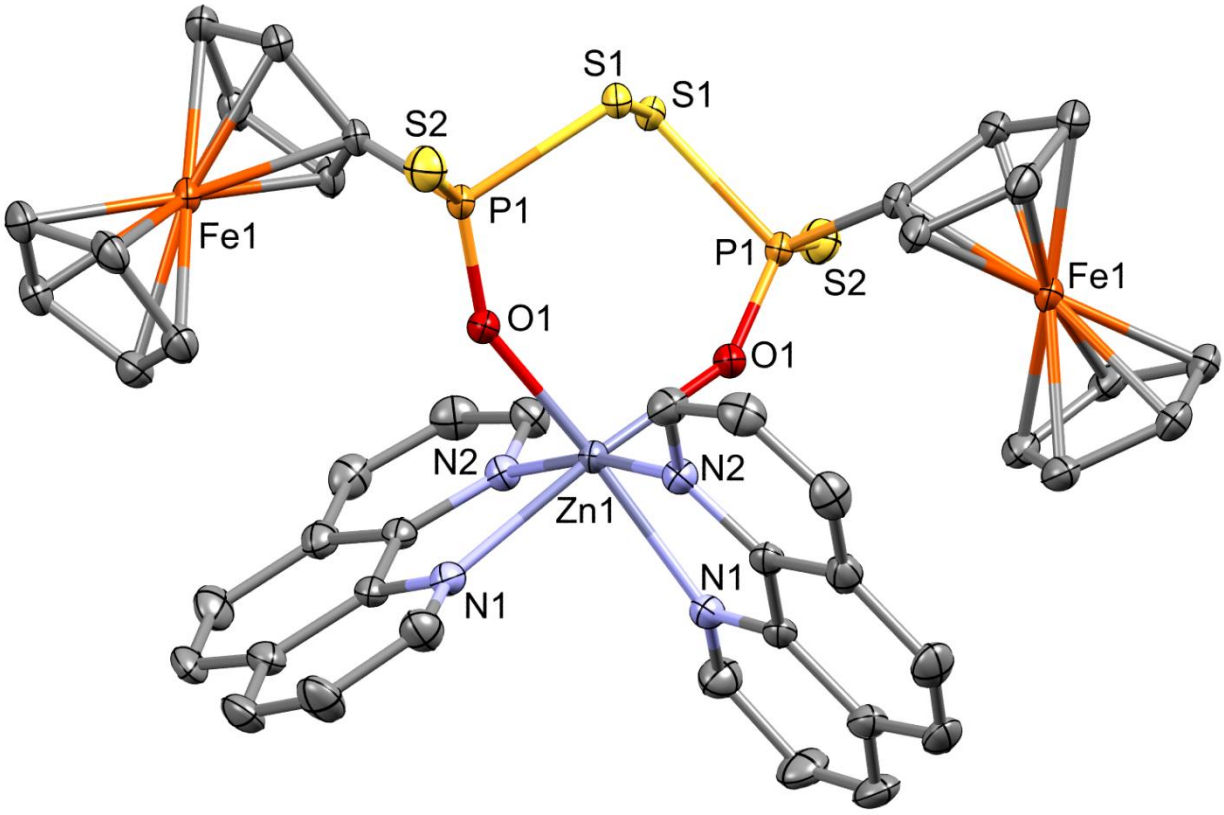

Figure 5.11: Perspective view of the molecular structure of compound **27**. Hydrogen atoms are omitted for clarity.

The P=S bond length of 1.96 Å is shorter than the P-S bond length of 2.12 Å (Table 5.8) as expected. The molecular structure of compound **27** also produces a 7-membered heterocycle (Figure 5.11) similar to compound **25**. The geometry around the coordinated Zn(II) in the molecular structure of compound **27** is distorted octahedral. The S-S bond lengths of the molecular structures of compounds **25** and **27** which are 2.067 and 2.074 Å (Table 5.3), respectively, are in good agreement with each other and literature.[17] The molecular structure of compound **27** also displays the *anti-anti* geometry as shown in Figure 5.11.

5.4 CONCLUSION

This chapter reports four different polymorphs of pentaerythritol derivitised intramolecular S-S coupled dithiophosphonate. The molecular structures of these polymorphs were obtained and compared by molecular overlays to the one already reported in literature. The chapter also reports four new bimetallic

intramolecular S-S coupled dithiophosphonates with the first examples of their respective molecular structures. These compounds were applied as co-sensitizers in DSSC and reported in chapter 6.

5.5 EXPERIMENTAL

5.5.1 Method

Unless otherwise noted, all reactions and manipulations were carried out under an inert atmosphere with a positive nitrogen gas flow using standard Schlenk lines and tubes. Standard Schlenk techniques are critical for these reactions and manipulations to minimize contact with atmospheric oxygen that can oxidize and/or reduce desired compounds.

5.5.2 Materials

Ferrocenyl Lawesson's reagent was prepared according to established literature.[30] Zn/Cd bipyridine and phenanthroline metal precursors $[Zn(bipyOH_2)_2]Cl_2$, $[Cd(bipyOH_2)_2]Cl_2$, $[Zn(phenanOH_2)_2]Cl_2$, $[Cd(phenanOH_2)_2]Cl_2$were also prepared according to established literature.[31] Phosphorus-pentasulfide, ferrocene, bipyridine, phenanthroline and pentaerythritol were purchased from Sigma Aldrich and used without further purification. Ammonia gas was obtained from Afrox (South Africa). Diethyl ether, Toluene and hexane were distilled under dinitrogen over a Na wire with the formation of a benzophenone ketyl indicator. Dichloromethane was distilled over P_4O_{10}. Methanol was distilled from I_2/Mg turnings.

5.5.3 Characterization methods

^1H and ^{31}P NMR spectra were recorded on a Bruker Avance 400 MHz spectrometer. NMR data are expressed in parts per million (ppm) and referenced internally to the residual proton impurity in the deuterated solvent whilst ^{31}P spectra chemical shifts are reported relative to an 85% H_3PO_4 in D_2O external standard solution, all at 298 K. Data are reported as chemical shift position (δ_H), multiplicity, relative integral intensity and assignment. Melting points were determined using a Stuart SMP3 melting point apparatus. Infrared spectra were recorded on a Perkin-Elmer Spectrum 100 FT-IR spectrometer. Mass spectral analyses were performed on a Waters API Quattro Micro spectrometer.

5.5.4 X-ray structure determination

Crystals were mounted on glass fibers with epoxy resin, and all geometric and intensity data were collected on a Bruker APEXII CCD diffractometer equipped with graphite monochromated Mo-Ka radiation ($\lambda = 0.71073$ Å). The data reduction was carried out with SAINT-Plus software.[32] The SADABS program was used to apply empirical absorption corrections.[33] All structures were solved by direct methods and refined by full-matrix least-squares on F2 with SHELXTL software package[34] found in SHELXTL/PC version 5.10.[35] Thermal ellipsoid plots are generated with OLEX2.[36]

5.6 EXPERIMENTAL

Synthesis of $[Zn(OS_2P\text{-}Fc)_2(bipy)_2]$ (25)

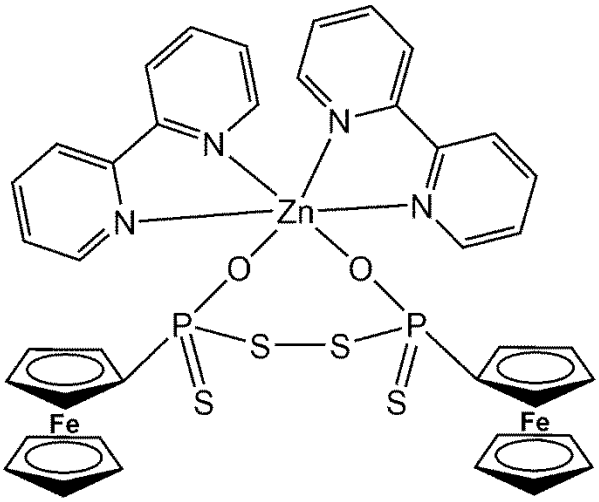

To a stirred solution of **2** (0.30 g, 0.23 mmol) in 20 mL of methanol was added $[Zn(bipyOH_2)_2]Cl_2$ (0.22 g, 0.45 mmol) in 20 mL of ethanol yielding an immediate precipitate. The yellow precipitate was stirred at room temperature for 20 mins, vacuum filtered, extracted into 20 mL DCM and concentrated into a free flowing powder. Yield: 1.15 g, 46%. M.p.: 232 °C (dec). ^{1}H-NMR (400 MHz, DMSO-d_6, ppm): δ 4.05 (2H, d, J=9.85 Hz, Fc), 4.16 (10H, s, Fc), 4.37 (4H, d, J=17.17 Hz, Fc), 4.48 (1H, s, V), 4.58 (1H, s), 7.49 (4H, s, ArH), 7.98 (4H, s, ArH), 8.40 (4H, s, ArH), 8.69 (4H, s, ArH). ^{31}P NMR (400 MHz, DMSO-d_6, ppm): δ 97.29 (s, 2P). ^{13}C NMR (400 MHz, DMSO-d_6): δ 1493.0, 138.2, 124.83, 120.89, 79.23, 78.90, 78.57. Selected FTIR (ν cm^{-1}): 3281 (m), 2952 (m), 1598 (m), 1573 (m), 1005. (s). ESI-MS: $(M\text{-}2Fc)^+$ 595.

Synthesis of $[Cd(OS_2P\text{-}Fc)_2(bipy)_2]$ (26)

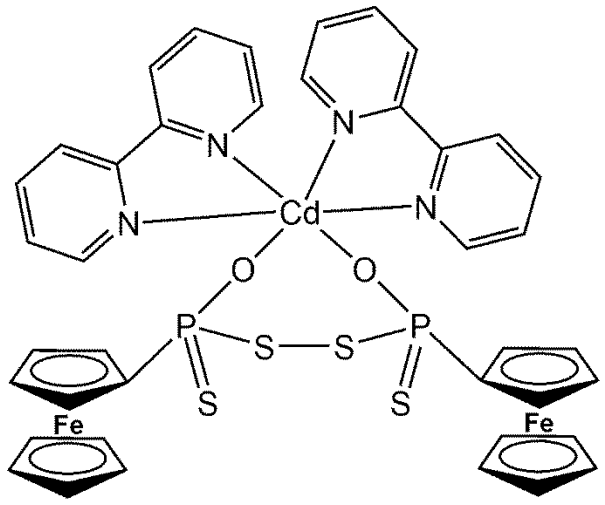

To a stirred solution of **2** (0.30 g, 0.23 mmol) in 20 mL of methanol was added $[Cd(bipyOH_2)_2]Cl_2$ (0.24 g, 0.45 mmol) in 20 mL of ethanol yielding an immediate precipitate. The yellow precipitate was stirred at room temperature for 20 mins, vacuum filtered, extracted into 20 mL DCM and concentrated into a free flowing powder. Yield: 1.3 g, 43 M.p.: 310 °C (dec). ^{1}H-NMR (400 MHz, DMSO-d_6, ppm): δ 4.09 (2H, d, J=9.89 Hz, Fc), 4.20 (10H, s, Fc), 4.41 (4H, d, J=17.21 Hz, Fc), 4.52

(1H, s, Fc), 4.62 (1H, s, Fc). 7.59 (4H, s, ArH), 8.08 (4H, s, ArH), 8.50 (4H, s, ArH), 8.79 (4H, s, ArH). ^{31} P NMR (400 MHz, DMSO-d_6, ppm): δ 103.29 (s, 2P). ^{13}C NMR (400 MHz, DMSO-d_6): δ 148.02, 137.25, 123.83, 119.89, 78.23, 77.90, 77.57. Selected FTIR (ν cm^{-1}): 2939 (m), 1593 (m), 1427 (w), 1001 (m). ESI-MS: $(M\text{-}2FcSP)^+$ 461.

Synthesis of $[Zn(OS_2P\text{-}Fc)_2(phenan)_2]$ (27)

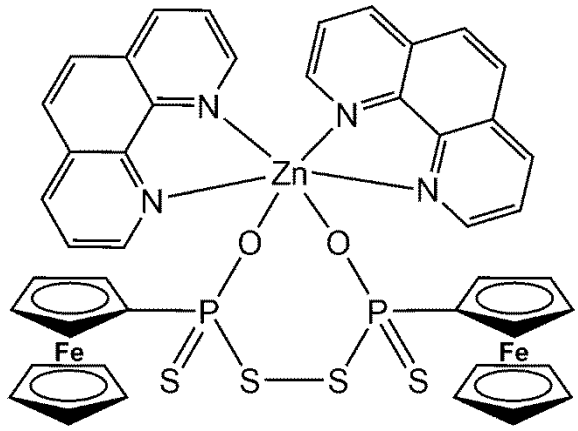

To a stirred solution of **2** (0.30 g, 0.23 mmol) in 20 mL of methanol was added $[Zn(phenanOH_2)_2]Cl_2$ (0.21 g, 0.45 mmol) in 20 mL of ethanol yielding an immediate precipitate. The yellow precipitate was stirred at room temperature for 20 mins, vacuum filtered, extracted into 20 mL DCM and concentrated into a free flowing powder. Yield: 1.3 g, 57%. M.p.: 240 °C (dec). ^{1}H-NMR (400 MHz, DMSO-d_6, ppm): δ 4.19 (2H, d, J=9.89 Hz, Fc), 4.30 (10H, s, Fc), 4.51 (3H, d, J=17.24 Hz, Fc), 4.62 (2H, s, Fc), 4.72 (1H, s, Fc). 7.80 (4H, t, J=5.66 Hz, ArH), 8.05 (4H, s, ArH), 8.60 (4H, s, ArH), 8.83 (4H, s, ArH). ^{31} P NMR (400 MHz, DMSO-d_6, ppm): δ 108.89 (s, 2P). ^{13}C NMR (400 MHz, $CDCl_3$): δ 129.03, 128.22, 125.30, 72.47, 72.05, 70.64. Selected FTIR (ν cm^{-1}): 3277 (m), 2940 (m), 1573 (m), 1455 (m), 1004 (m). ESI-MS: $(1/2M\text{-}FcS)^+$ 401.

Synthesis of $[Cd(OS_2P\text{-}Fc)_2(phenan)_2]$ (28)

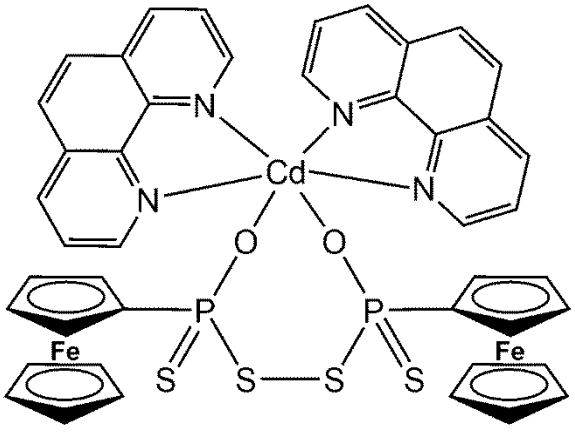

To a stirred solution of **2** (0.30 g, 0.23 mmol) in 20 mL of methanol was added $[Cd(phenanOH_2)_2]Cl_2$ (0.23 g, 0.45 mmol) in 20 mL of ethanol yielding an immediate precipitate. The yellow precipitate was stirred at room temperature for 20 mins, vacuum filtered, extracted into 20 mL DCM and concentrated into a free flowing powder. Yield: 0.9 g, 39 M.p.: 222

°C (dec). ^{1}H-NMR (400 MHz, DMSO-d_6, ppm): δ 4.09 (2H, d, J=9.85 Hz, Fc), 4.20 (10H, s, Fc), 4.41 (2H, d, J=17.21 Hz, Fc), 4.52 (2H, s, Fc), 4.62 (2H, s, Fc). 7.90 (4H, t, J=5.62 Hz, ArH), 8.15 (4H, s, ArH), 8.70 (4H, s, ArH), 8.93 (4, s, ArH). ^{31} P NMR (400 MHz, DMSO-d_6, ppm): δ 98.21 (s, 2P). ^{13}C NMR (400 MHz, $CDCl_3$): δ 131.04, 130.23, 127.30, 74.47, 74.05, 72.64. Selected FTIR (ν cm^{-1}): 2938 (m), 1593 (m), 1427 (m), 1023 (m). ESI-MS: $(M-2Fc)^{+}$ 698.

5.7 REFERENCES

1. D. Klaman, *Verlag-Chemie, Weinheim*, **1984**.
2. I. P. Alimarin and V. M. Ivanov, *Russ. Chem. Rev*, **1989**, 58, 863.
3. M. Fuller, M. Kasraia, J. S. Sheasby, G. M. Bancroft, K. Fyfe and K. H. Tan, *Tribology Lett*, **1995**, 1, 367-378.
4. A. M. Barnes, K. D. Bartle and V. R. Thibon, *Tribology International*, **2001**, 34, 389-395.
5. M. A. Nicholls, T. Do, P. R. Norton, M. Kasrai and G. M. Bancroft, *Tribology International*, **2005**, 38, 15-39.
6. H. Spikes, *Lubricat Sci*, **2008**, 20, 103-136.
7. L. Bromberg, I. Lewin and A. Warshawsky, *Hydrometallurgy*, **1993**, 33, 59-71.
8. P. Patnaik, *A comprehensive guide to the hazardous properties of chemical substances*, John Wiley & Sons, **2007**.
9. T. B. Gaines, *Toxic and Applied Pharm*, **1969**, 14, 515-534.
10. S. E. Livingstone and A. E. Mihkelson, *Inorg. Chem*, **1970**, 9, 2545-2551.
11. W. E. van Zyl, J. M. López-de-Luzuriaga, A. A. Mohamed, R. J. Staples and J. P. Fackler, *Inorg. Chem*, **2002**, 41, 4579-4589.
12. W. E. van Zyl, R. J. Staples and J. P. Fackler Jr, *Inorg. Chem. Comm*, **1998**, 1, 51-54.
13. M. Karakus, *Phosphorus Sulfur Silicon Relat. Elem*, **2011**, 186, 1523-1530.
14. M. Karakus, P. Lönnecke, D. Yakhvarov and E. Hey-Hawkins, *Zeitschrift für anorganische und allgemeine Chemie*, **2004**, 630, 1444-1450.
15. M. Karakus and H. Yilmaz, *Russ. J. Coord. Chem*, **2006**, 32, 437-443.
16. I. P. Gray, A. M. Slawin and J. D. Woollins, *New J. Chem*, **2004**, 28, 1383-1389.
17. M. N. Pillay, H. van der Walt, R. J. Staples and W. E. van Zyl, *J .Organomet. Chem*, **2015**, 794, 33-39.
18. N. Baumann, H.-J. Fachmann, R. Jotter and A. Kubny, in *S Sulfur-Nitrogen Compounds*, Springer, **1994**, pp. 292-321.

19. W. J. Stec, B. Uznanski, A. Wilk, B. L. Hirschbein, K. L. Fearon and B. J. Bergot, *Tetrahedron lett*, **1993**, 34, 5317-5320.

20. B. Miller, *Tetrahedron*, **1964**, 20, 2069-2078.

21. G. P. Stahly, *Cryst. Growth & Des*, **2007**, 7, 1007-1026.

22. C. H. Gu, V. Young and D. J. Grant, *J. Pharm Sci*, **2001**, 90, 1878-1890.

23. S. Khoshkhoo and J. Anwar, *J. Physics D: Applied Physics*, **1993**, 26, B90.

24. N. Fridman, M. Kapon, Y. Sheynin and M. Kaftory, *Acta Crystall. Section B: Stru Sci*, **2004**, **60**, 97-102.

25. W. E. van Zyl and J. D. Woollins, *Coord. Chem. Rev*, **2013**, 257, 718-731.

26. G. A. Zank and T. B. Rauchfuss, *Inorg. Chem*, **1986**, 25, 1431-1435.

27. M. Karakus, J. D. Woollins, P. Lönnecke and E. Hey-Hawkins, *Acta Crystall. Section E: Structure Reports Online*, **2012**, 68, m428-m428.

28. A. Spek, *Inc., Madison, WI*, **2003**.

29. P. Knopik, L. Łuczak, M. J. Potrzebowski, J. Michalski, J. Błaszczyk and M. W. Wieczorek, *J of the Chem Soc, Dalton Trans*, **1993**, 2749-2757.

30. W. E. Van Zyl and J. P. Fackler, *Phosphorus Sulfur Silicon Relat. Elem*, **2000**, 167, 117-132.

31. G. H. Eom, H. M. Park, M. Y. Hyun, S. P. Jang, C. Kim, J. H. Lee, S. J. Lee, S.-J. Kim and Y. Kim, *Polyhedron*, **2011**, 30, 1555-1564.

32. V. SAINT, *Siemens Analytical Instruments Division, Madison, WI*, **1995**.

33. G. Sheldrick, *University of Göttingen, Germany*, **2010**.

34. G. Sheldrick, *University of Göttingen, Germany*, **1997**.

35. V. SHELXTL, *Inc., Madison, WI*, **2001**.

36. C. Júnior and P. de Sousa, Universidade de São Paulo, **2017**.

CHAPTER 6

LIGHT HARVESTING PROPERTIES OF SOME OF THE SYNTHESIZED DITHIOPHOSPHONATE COMPLEXES

6.1 INTRODUCTION

Efficiencies of 7 %[1, 2], 9 %[3], 11 %[4] and 14.7 %[5] have been achieved in dye-sensitized solar cells (DSSCs) using different types of co-sensitizers. Researchers have focused their attention in this field on the selection of the right co-sensitizer. It is clear that access to economically viable renewable energy sources is essential for the development of a globally sustainable society.[6] Among the several approaches for harnessing solar energy and converting it into electricity, dye-sensitized solar cells (DSSCs) represent one of the most promising methods for future large-scale power production from renewable energy sources.[7] Introduced over 20 years ago by Grätzel and O'Reagan,[8] DSSC technology has elicited tremendous interest both in the academic and industrial sector.[1, 7, 9-14] This interest stems from the ability of these systems to convert available sunlight into electricity with simple and low fabrication cost in contrast with conventional silicon-based solar cells. Though these silicon-based cells are still the dominant material for photovoltaic systems, the potential shortage of solar grade silicon, the complicated and energy intensive fabrication process and use of toxic chemicals needed for Si solar cells, along with the cells' heavy weight and high price, have created a strong drive to develop more cost-efficient, versatile and easily producible alternatives to solar energy utilization.[15]. The dominance of Si solar cells in terms of commercial availability compared to DSSCs stems from better cell efficiencies. To overcome this problem, researchers have employed different ways to improve photovoltaic performance of DSSCs. Some of these ways include replacement of the liquid electrolyte with a solid or quasi solid electrolyte,[16-19] use of different organic dyes,[20-26] employing a luminescent polymeric coating material[27] and co-sensitization[9, 23, 28]. Co-sensitization which involves the use of a combination of two or more dyes on the same semiconducting film, which can extend the light-harvesting spectrum of the cells and can in turn increase

the photocurrent of the device maybe an effective approach to improve device performance[9]. Selection of suitable co-sensitizer and sensitizer combinations that can maximize the light-harvesting spectrum to improve photovoltaic performance is therefore important.[9] Metal-organic frameworks have been investigated as co-sensitizers to improve the performance of DSSCs.[29-32]

Our group has studied metal complexes of dithiophosphonates for many years now.[33-37] A survey of literature indicates that these compounds have scarcely been explored as sensitizers or co-sensitizers in DSSCs. On the other hand, sulfur rich compounds and their derivatives have recently been investigated as light-harvesting materials in DSSCs.[9, 38-40] Dithiophosphonates can also be furnished with the ferrocenyl moiety to form the ferrocenyl derivatives. This can become useful since ferrocenyl derivatives' typical electronic absorption band of 450 nm[41] can be capable of compensating the weak (lower-wavelength) absorption region of the N719 dye. Complexes of zinc and cadmium have given good cell efficiencies when employed in DSSCs. For example, Peng and co-workers reported efficiencies of 6.61 %,[42] Gosavi and co-workers reported 6.62 %[43] and Wang and co-workers obtained 7.1 %.[9]

Considering this background, this chapter reports the light harvesting properties of complexes **25-28** reported in chapter 5. Complexes **25-28** were selected for testing as DSSC cells unlike other complexes herein reported because of their optical properties which gave an indication of their potential good performance in these cells.

6.2 RESULT AND DISCUSSION

6.2.1 Optical Properties of Co-Sensitizers 25-28

Optical properties are important deciding factors for the utility of a compound to act as a sensitizer or co-sensitizer as light harvesters in DSSCs. The electronic absorption spectra of co-sensitizers **25-28** with the N719 dye were recorded in DMF solution and are presented in Figure 6.1. The UV-vis spectra show absorptions between 350-450 nm and 460-600 nm. These electronic absorption spectra of the co-sensitized systems indicate enhancement of the absorption spectra of the N719 dye in the wavelength region where the dye has weak absorptions. This observation is consistent with the proposal that the absorptions of the Zn and Cd complexes are capable of compensating the absorption of the N719 dye in the lower-wavelength region and also improving the low-energy absorption of the M/N719 (M = Zn and Cd) systems.[9]

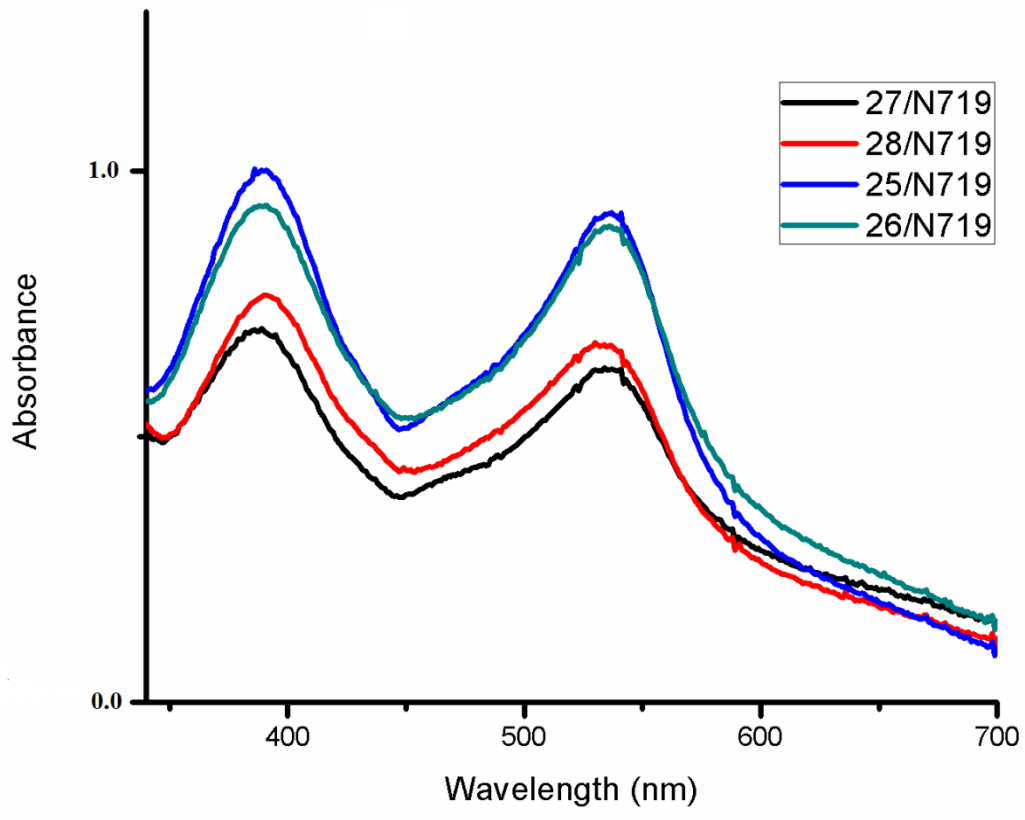

Figure 6.1: Electronic absorption spectral of co-sensitizers/N719 recorded in 10^{-4} M DMF solution.

The solid state emission spectra of the co-sensitizers **25-28** were obtained and are illustrated in Figure 6.2.

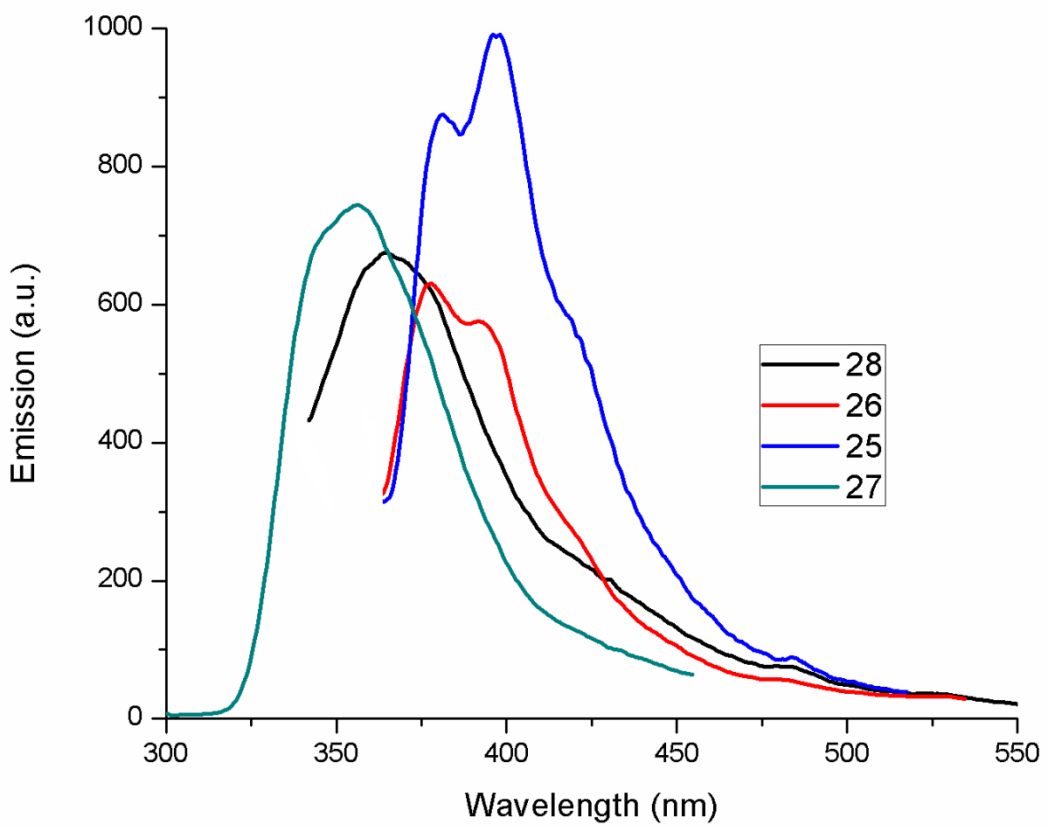

Figure 6.2: Solid state photoluminescent spectra of co-sensitizers.

Following excitation at around 300 and 350 nm, co-sensitizers **27**, **28** and **25**, **26** exhibit strong luminescence in the region 310-400 and 360-470 nm, respectively (Figure 6.2). These emissions overlap with the excitation spectrum of the N719 dye and indicate that the dye may be capable of accepting energy from the incident light as well as from the excited co-sensitizers **25-28**.

6.2.2 Photovoltaic Properties of DSSCs

The sandwich type cells (TiO_2/N719-M/electrolyte containing I^-/I_3^-/Pt counter electrode; M = **25-28**) were fabricated using different co-sensitized dyes (N719/**25**, N719/**26**, N719/**27** and N719/**28**) and their photocurrent-potential (*J*-*V*) curves were determined under stimulated light irradiation with 100 mW cm^{-2} light intensity (Figure 6.3).

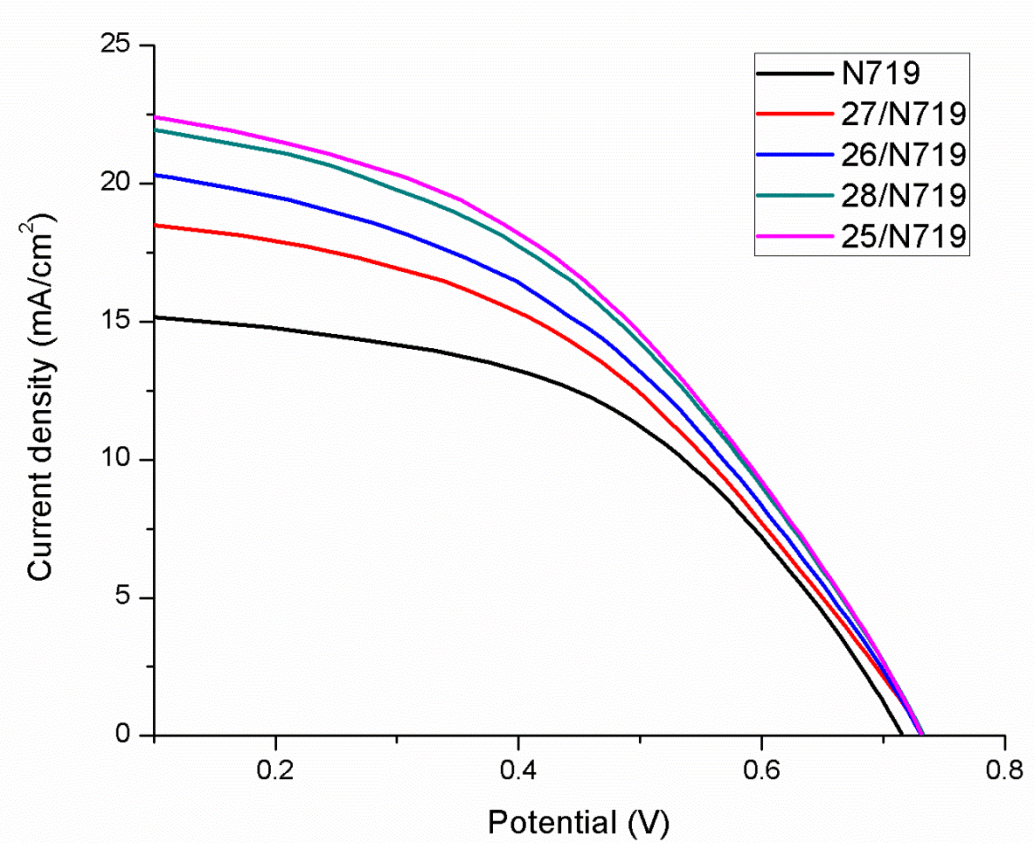

Figure 6.3: Photocurrent-potential curves for DSSCs based on N719-sensitized and co-sensitized photoelectrodes under illumination with 100 mW cm^{-2} light intensity.

The current-voltage characteristics of the DSSC device based on the state of the art N719 dye photoanode was also obtained (Figure 6.3) under identical conditions for comparison basis. The detailed photovoltaic parameters, such as short circuit photocurrent (J_{SC}), open circuit voltage (V_{OC}), fill factor (FF), and power conversion efficiency (η) derived from the J-V curves are summarized in table 6.1.

Table 6.1: Photovoltaic parameters output of DSSCs based on different co-sensitizers and the N719 dye.

Dye	J_{SC} (mA cm^{-2})	V_{OC} (V)	FF	η (%)
N719	15.62	0.709	0.51	5.65
25/N719	22.75	0.726	0.45	7.49
26/N719	20.65	0.725	0.45	6.74
27/N719	18.97	0.726	0.46	6.34
28/N719	22.33	0.727	0.45	7.30

The performances of the co-sensitized cells (**25**/N719, **26**/N719, **27**/N719 and **28**/N719) compared to that of the state of the art dye N719 showed an improved performance. The values for J_{SC}, V_{OC}, and η decrease in the order **25**/N719 > **28**/N719 > **26**/N719 > **27**/N719. All the parameters are significantly better than those of the device sensitized only by the N719. The **25**/N719 device yields a J_{SC} of 22.75 mA cm^{-2}, a V_{OC} of 0.726 V, a fill factor (FF) of 0.45 and a η of 7.49 % whereas the N719 sensitized device shows J_{SC} and η values of 15.62 mA cm^{-2} and 5.65 %, respectively (Table 6.1). The **27**/N719 co-sensitized device with the least power conversion efficiency of 6.34 % improves the performance of the N719 dye by about 11 % while the **25**/N719 cell with the highest conversion efficiency improves the N719 dye by about 33 %.

It can be deduced from the photovoltaic parameters that the complexes **25-28** are not only effectively adsorbed onto the TiO_2 surface but can also compensate the photovoltaic parameters in terms of enhancement of electron collection in TiO_2 and reduced recombination of electrons by providing efficient electron injection in the conduction band of the TiO_2 film.

6.3 CONCLUSION

In summary it can be concluded that the synthesized dithiophosphonate complexes **25-28** used as co-sensitizers and co-adsorbents have a significant effect on the performance of the DSSCs. They are capable of improving the J_{SC}, V_{OC} and η. The device performance decreases in the order **25**/N719 > **28**/N719 > **26**/N719 > **27**/N719, and each of these fabricated cells shows better performance than the DSSC fabricated by using only the N719 dye. The performance of the **25**/N719 was the best with an overall conversion efficiency of 7.49 %. It can therefore be concluded that compounds **25-28** are attractive candidates for improving the performances of DSSCs.

6.4 EXPERIMENTAL

6.4.1 Material

Titanium coated electrodes, platinum counter electrodes, hot melt gaskets, iodolyte PN-50, glass caps, N719 dye, seal film and Vac'n'Fill syringe were purchased purchased from Solaronix and the DSSC fabrication was carried out in a standard solar cell laboratory at the Council for Scientific and Industrial Research, CSIR, South Africa. DSSC fabrication was carried out on dried electrodes which were stored away from air and light prior to use. DCM, methanol, ethanol and DMSO were purchased from Sigma Aldrich and used without further purification.

6.4.2 Method

Ferrocenyl Lawesson's reagent and complexes **25-28** were prepared as outlined in Chapter 5. Titanium coated electrodes, platinum counter electrodes, hot melt gaskets, iodolyte PN-50, glass caps, N719 dye, seal film and Vac'n'Fill syringe purchased from Solaronix were used as received. Dichloromethane was distilled over P_4O_{10}. Methanol and ethanol were distilled from I_2/Mg turnings.

6.4.3 DSSC Fabrication

The co-sensitized photoelectrodes were prepared by immersion of the thin nanoporous TiO_2 layers into a DMSO solution of the compounds **25-28** (10^{-4} M) for 6 hours, washing with ethanol and then blow drying. The electrodes were then dipped into a 10^{-4} M ethanol solution of the N719 dye for 12 hours. Unadsorbed dye was washed off with anhydrous ethanol. The dye adsorbed TiO_2 electrodes and Pt counter-electrodes were assembled in a sealed sandwich-type cell by heating at 120 °C using a hot melt sealant film (Solaronix) as spacer between the electrodes. Iodolyte PN-50 (Solaronix) was used as the electrolyte. A drop of this electrolyte solution was placed in a hole drilled in the counter electrode and driven into the cell by vacuum backfilling. Finally, the hole was sealed by using a sealant and a 0.1 mm thick glass cover.

6.4.4 Characterization

6.4.4.1 Solar Cell Efficiency

The photoelectrochemical performance characteristics (short circuit current, *J*sc, open-circuit voltage, *V*oc, fill factor (FF), and overall conversion efficiency, η) were measured under illumination with a 1000 W xenon lamp (Model 201-100) using a Sciencetech SF-150 solar simulator (Ontario, Canada) at CSIR, South Africa. The light intensity was confirmed to be homogeneous over an 8×8 in^2 area by calibration with a Si solar cell for 1 sun light intensity (AM 1.5G, 100 mW cm^{-2}).

6.5 REFERENCES

1. M. E. Ragoussi, J. J. Cid, J. H. Yum, G. de la Torre, D. Di Censo, M. Grätzel, M. K. Nazeeruddin and T. Torres, *Angew. Chem. Int. Ed*, 2012, **51**, 4375-4378.
2. L. Wei, Y. Yang, R. Fan, P. Wang, L. Li, J. Yu, B. Yang and W. Cao, *RSC Advances*, 2013, **3**, 25908-25916.
3. C.-M. Lan, H.-P. Wu, T.-Y. Pan, C.-W. Chang, W.-S. Chao, C.-T. Chen, C.-L. Wang, C.-Y. Lin and E. W.-G. Diau, *Energy Environ. Sci*, 2012, **5**, 6460-6464.
4. T. Bessho, S. M. Zakeeruddin, C. Y. Yeh, E. W. G. Diau and M. Grätzel, *Angew. Chem*, 2010, **122**, 6796-6799.
5. K. Kakiage, Y. Aoyama, T. Yano, K. Oya, J.-i. Fujisawa and M. Hanaya, *Chem. Comm*, **2015**, 51, 15894-15897.
6. A. Hagfeldt, G. Boschloo, L. Sun, L. Kloo and H. Pettersson, *Chem. Rev*, **2010**, 110, 6595-6663.
7. M. Urbani, M. Grätzel, M. K. Nazeeruddin and T. Torres, *Chem. Rev*, **2014**, 114, 12330-12396.
8. B. O'Regan and M. Gratzel, *Nature*, **1991**, 353, 737-740.
9. R. Yadav, M. Trivedi, G. Kociok-Köhn, R. Chauhan, A. Kumar and S. W. Gosavi, *Euro. J. Inorg. Chem*, **2016**.
10. Z. Zhang, S. M. Zakeeruddin, B. C. O'Regan, R. Humphry-Baker and M. Grätzel, *The J. Phys. Chem. B*, **2005**, 109, 21818-21824.
11. N. A. Lee, B. A. Frenzel, J. Rochford and S. E. Hightower, *Euro. J. Inorg. Chem*, **2015**, 2015, 3843-3849.
12. T. Funaki, H. Kusama, N. Onozawa-Komatsuzaki, K. Kasuga, K. Sayama and H. Sugihara, *Euro. J. Inorg. Chem*, **2014**, 2014, 1303-1311.
13. B. Bozic-Weber, E. C. Constable and C. E. Housecroft, *Coord. Chem. Rev*, **2013**, 257, 3089-3106.
14. M. Grätzel, *Nature*, **2001**, 414, 338-344.

15. M. Toivola, J. Halme, K. Miettunen, K. Aitola and P. D. Lund, *Inter. J. Energy Res*, **2009**, 33, 1145-1160.

16. R. Shanti, F. Bella, Y. Salim, S. Chee, S. Ramesh and K. Ramesh, *Mat. Des*, **2016**, 108, 560-569.

17. J. Y. Lim, J. K. Kim, J. M. Lee, D. Y. Ryu and J. H. Kim, *J. Mat. Chem. A*, **2016**, 4, 7848-7858.

18. S. Yusuf, A. Azzahari, R. Yahya, S. Majid, M. Careem and A. Arof, *RSC Advances*, **2016**, 6, 27714-27724.

19. F. Bella, S. Galliano, M. Falco, G. Viscardi, C. Barolo, M. Grätzel and C. Gerbaldi, *Green Chem*, **2017**.

20. Z.-S. Wang, Y. Cui, Y. Dan-oh, C. Kasada, A. Shinpo and K. Hara, *The J. Phys. Chem. C*, **2007**, 111, 7224-7230.

21. K. Hara, K. Sayama, Y. Ohga, A. Shinpo, S. Suga and H. Arakawa, *Chem. Comm*, **2001**, 569-570.

22. K. Hara, M. Kurashige, Y. Dan-oh, C. Kasada, A. Shinpo, S. Suga, K. Sayama and H. Arakawa, *New J. Chem*, **2003**, 27, 783-785.

23. T. Kitamura, M. Ikeda, K. Shigaki, T. Inoue, N. A. Anderson, X. Ai, T. Lian and S. Yanagida, *Chem. Mats*, **2004**, 16, 1806-1812.

24. S. Kim, H. Choi, D. Kim, K. Song, S. O. Kang and J. Ko, *Tetrahedron*, **2007**, 63, 9206-9212.

25. I. Jung, J. K. Lee, K. H. Song, K. Song, S. O. Kang and J. Ko, *The J. Organic Chem*, **2007**, 72, 3652-3658.

26. S. Ferrere, A. Zaban and B. A. Gregg, *The J. Phys. Chem. B*, **1997**, 101, 4490-4493.

27. G. Griffini, F. Bella, F. Nisic, C. Dragonetti, D. Roberto, M. Levi, R. Bongiovanni and S. Turri, *Advan. Energy Mat*, **2015**, 5.

28. J. N. Clifford, E. Palomares, M. K. Nazeeruddin, R. Thampi, M. Grätzel and J. R. Durrant, *J. American Chem. Soc*, **2004**, 126, 5670-5671.

29. X. Wang, Y. Yang, R. Fan and Z. Jiang, *New J. Chem*, **2010**, 34, 2599-2604.

30. L. Zhang, Y. Yang, R. Fan, P. Wang and L. Li, *Dyes and Pigments*, **2012**, 92, 1314-1319.

31. X. Wang, Y.-L. Yang, P. Wang, L. Li, R.-Q. Fan, W.-W. Cao, B. Yang, H. Wang and J.-Y. Liu, *Dalton Trans*, **2012**, 41, 10619-10625.

32. S. Gao, R. Q. Fan, X. M. Wang, L. S. Qiang, L. G. Wei, P. Wang, H. J. Zhang, Y. L. Yang and Y. L. Wang, *J. Mat. Chem. A*, **2015**, 3, 6053-6063.

33. W. E. van Zyl, R. J. Staples and J. P. Fackler Jr, *Inorg. Chem. Comm*, **1998**, 1, 51-54.

34. W. E. van Zyl, J. M. López-de-Luzuriaga, A. A. Mohamed, R. J. Staples and J. P. Fackler, *Inorg. Chem*, **2002**, 41, 4579-4589.

35. F. K. Keter, I. A. Guzei, M. Nell, W. E. v. Zyl and J. Darkwa, *Inorg. Chem*, **2014**, 53, 2058-2067.

36. W. E. Van Zyl and J. P. Fackler, *Phosphorus Sulfur Silicon Relat. Elem*, **2000**, 167, 117-132.

37. M. N. Pillay, H. van der Walt, R. J. Staples and W. E. van Zyl, *J. Organomet. Chem*, **2015**, 794, 33-39.

38. A. Kumar, R. Chauhan, K. C. Molloy, G. Kociok-Köhn, L. Bahadur and N. Singh, *Chem–A Euro. J*, **2010**, 16, 4307-4314.

39. V. Singh, R. Chauhan, A. N. Gupta, V. Kumar, M. G. Drew, L. Bahadur and N. Singh, *Dalton Trans*, **2014**, 43, 4752-4761.

40. S. K. Singh, R. Chauhan, B. Singh, K. Diwan, G. Kociok-Köhn, L. Bahadur and N. Singh, *Dalton Trans*, **2012**, 41, 1373-1380.

41. H. B. Gray, Y. Sohn and N. Hendrickson, *J. American Chem. Soc*, **1971**, 93, 3603-3612.

42. L. Yu, K. Fan, T. Duan, X. Chen, R. Li and T. Peng, *ACS Sust. Chem. Eng*, **2014**, 2, 718-725.

43. Y.-W. Dong, R.-Q. Fan, P. Wang, L.-G. Wei, X.-M. Wang, S. Gao, H.-J. Zhang, Y.-L. Yang and Y.-L. Wang, *Inorg. Chem*, **2015**, 54, 7742-7752.

CHAPTER 7

ANTIBACTERIAL SUSCEPTIBILITY TESTS OF SYNTHESIZED DITHIOPHOSPHONATE COMPOUNDS

7.1 INTRODUCTION

Microorganisms have existed on the earth for many years and exhibit the greatest genetic and metabolic diversity.[1] Presently, resistance to antimicrobial agents among bacteria, parasites, viruses and other disease-causing organisms has become a public health challenge worldwide.[2]

A major setback in the development of antibiotics and their application to clinical medicine has resulted in the increment in resistance of bacteria towards antibacterial drugs. This may be largely due to constant use of antibiotics which in turn increases selective pressure in the bacteria population, thereby permitting the survival of the resistant bacteria and eradication of the susceptible ones.[3] Since antimicrobial resistance is fast becoming a global concern and with rapid increase in multidrug-resistant bacteria,[4] there is need for continued search for new compounds including coordination complexes with antimicrobial activity.[5] Antimicrobial activity of dithiophosphonate complexes become attractive candidates in this regard.[6] Though dithiophosphonate ligands and complexes of different types have been reported in literature, only a few have been screened for their antibacterial activity.[7-9] It is important to note too that ethambutol has been employed as a TB drug and it will be useful to assess the antibacterial activity of its derivatives.

Considering this background, this chapter reports the antibacterial activity of some of the new dithiophosphonate compounds synthesized. In this study, three Gram-positive bacteria including sensitive *S. aureus* ATCC 29213, Methicillin-resistant *S. aureus* ATCC 43300 and Vancomycin-resistant *E. faecalis* ATCC 51299 were used. The anti-bacteria susceptibility tests also included three Gram-negative bacteria including Sensitive *E. coli* and QC organism ATCC 25922, β-lactam resistant *E. coli* ATCC 35218 and Multidrug resistant *P. aeruginosa* ATCC 27853.

7.2 RESULTS AND DISCUSSION

7.2.1 Antibacterial activity of synthesized compounds with Gram positive bacteria

Compounds **1-29** were tested for antibacterial activity by screening them against 3 Gram positive bacteria including sensitive *S. aureus* ATCC 29213, methicillin-resistant *S. aureus* ATCC 43300 and vancomycin-resistant *E. faecalis* ATCC 51299 using the agar-well diffusion method. The potency of compounds **1-29** screened against the 3 Gram positive bacteria evaluated quantitatively is given in Table 7.1. The following zone diameter (for 20 mm discs) criteria were used to assign susceptibility or resistance to tested compounds: Susceptible (S) ≥ 15 mm, Intermediate (I) = 11-14 mm, and Resistant (R) ≤ 10 mm[10]. The criteria for assigning susceptibility or resistance to the standard antimicrobial agents were as follows: AMP10; (S) ≥ 17 mm, (I) = 14–16 mm, (R) ≤ 13 mm, CIP5; (S) (I) (R) and TET30; (S) ≥ 19 mm, (I) = 15–18 mm, (R) ≤ 14 mm[11].

The antibacterial susceptibility screenings for compounds **1-23** against the tested Gram positive bacteria exhibit broad antibacterial activity for *S. aureus* ATCC 29213 and *S. aureus* ATCC 43300 while no activity was observed for *E. faecalis* ATCC 51299 (Table 7.1). *S. aureus* ATCC 29213 was intermediately susceptible to compounds **3**, **4**, **8**, **10**, and **17** at 1000 µg/L. It was susceptible at 1000 µg/L for compounds **1** and **2**. *S. aureus* ATCC 29213 was also intermediately susceptible at 500 and 1000 µg/L to compounds **5** and **19** and susceptible at 500 – 1000 µg/L for compounds **9**, **13**, **14**, **16**, and **18** respectively.

Table 7.1: Diameter of zones of inhibition (mm) of compounds **1-28** against Gram positive isolates at 500 & 1000 μg/L.

Compound	***S. aureus* ATCC 29213**		***S. aureus* ATCC 43300**		***E. faecalis* ATCC 51299**	
	500	1000	500	1000	500	1000
1	- (R)	18 (S)	- (R)	- (R)	- (R)	- (R)
2	- (R)	16 (S)	11 (I)	15 (S)	- (R)	- (R)
3	- (R)	14 (I)	- (R)	14 (I)	- (R)	- (R)
4	- (R)	14 (I)	- (R)	- (R)	- (R)	- (R)
5	14 (I)	20 (S)	15 (S)	18 (S)	- (R)	- (R)
6	- (R)	- (R)	- (R)	11 (I)	- (R)	- (R)
7	- (R)	- (R)	- (R)	13 (I)	- (R)	- (R)
8	- (R)	11 (I)	- (R)	- (R)	- (R)	- (R)
9	15 (S)	18 (S)	11 (I)	14 (I)	- (R)	- (R)
10	- (R)	12 (I)	11 (I)	15 (S)	- (R)	- (R)
12	- (R)	- (R)	- (R)	- (R)	- (R)	- (R)
13	19 (S)	23 (S)	21 (S)	25 (S)	- (R)	- (R)
14	20 (S)	25 (S)	15 (S)	17 (S)	- (R)	- (R)
15	- (R)	- (R)	11 (I)	11 (I)	- (R)	- (R)
16	19 (S)	24 (S)	12 (I)	15 (S)	- (R)	- (R)
17	- (R)	12 (I)	- (R)	12 (I)	- (R)	- (R)
18	16 (S)	20 (S)	- (R)	12 (I)	- (R)	- (R)
19	12 (I)	17 (S)	12 (I)	15 (S)	- (R)	- (R)
20	- (R)	- (R)	- (R)	- (R)	- (R)	- (R)
21	- (R)	- (R)	- (R)	- (R)	- (R)	- (R)
22	- (R)	16 (S)	- (R)	12 (I)	- (R)	- (R)
23	- (R)	12 (I)	14 (I)	20 (S)	- (R)	- (R)

Compound	*S. aureus* ATCC 29213	*S. aureus* ATCC 43300	*E. faecalis* ATCC 51299
AMP10	25 (S)	20 (S)	25 (S)
CIP5	27 (S)	28 (S)	Nt
TET30	28 (S)	36 (S)	0 (R)

Standard antimicrobial agents: AMP10 (Ampicillin), CIP5 (Ciprofloxacin), TET30 (Tetracycline). Negative control: DMSO. Solvent used: DMSO. Susceptibility parameters: R (Resistant), I (Intermediate), S (Susceptible). Nt (Not tested).

Compounds **1-23** were also screened against *S. aureus* ATCC 43300. Intermediate susceptibility was observed at 1000 µg/L with compounds **3**, **6**, **7**, **17**, and **18** and for compounds **9** and **15** at 500 – 1000 µg/L (Table 7.2). Intermediate susceptibility at 500 µg and susceptibility at 1000 µg was observed for compounds **2**, **10**, **16**, and **19** with 11/12 and 15 mm inhibition zones. This isolate was susceptible to compounds **5**, **13** and **14** at 500 – 1000 µg/L.

7.2.2 Antibacterial activity of synthesized compounds with Gram negative bacteria

Compounds **1-29** were also tested for antibacterial activity by screening them against 3 Gram negative bacteria. The 3 Gram negative bacteria used were sensitive *E. coli* and QC organism ATCC 25922, β-lactam resistant *E. coli* ATCC 35218 and multidrug resistant *P. aeruginosa* ATCC 27853. There was limited antibacterial activity against Gram-negative *E. coli* and *P. aeruginosa*. Compounds **1-23** were ineffective against *P. aeruginosa*, with only compounds **6** and **19** demonstrating intermediate activity at 1000 µg/L. No activity was observed against the susceptible *E. coli* ATCC 25922 for all compounds. Intermediate activity was observed with compound **19** at 1000 µg/L for *E. coli* ATCC 35218 and susceptible activity for compounds **3**, **5**, **6 and 9** at 500-1000 µg/L. Compound **5** however showed more activity compared to compounds **3**, **6** and **9**.

Table 7.2: Diameter of zones of inhibition (mm) of compounds **1-28** against Gram negative isolates at 500 & 1000 μg/L.

Compounds	***P. aeruginosa* ATCC 27853**		***E. coli* ATCC 25922**		***E. coli* ATCC 35218**	
	500	1000	500	1000	500	1000
1	- (R)	- (R)	- (R)	- (R)	- (R)	- (R)
2	- (R)	- (R)	- (R)	- (R)	- (R)	- (R)
3	- (R)	- (R)	- (R)	- (R)	- (R)	16 (S)
4	- (R)	- (R)	- (R)	- (R)	- (R)	- (R)
5	- (R)	- (R)	- (R)	- (R)	31 (S)	33 (S)
6	- (R)	12 (I)	- (R)	- (R)	- (R)	15 (S)
7	- (R)	- (R)	- (R)	- (R)	- (R)	- (R)
8	- (R)	- (R)	- (R)	- (R)	- (R)	- (R)
9	- (R)	- (R)	- (R)	- (R)	19 (S)	22 (S)
10	- (R)	- (R)	- (R)	- (R)	- (R)	- (R)
12	- (R)	- (R)	- (R)	- (R)	- (R)	- (R)
13	- (R)	- (R)	- (R)	- (R)	- (R)	- (R)
14	- (R)	- (R)	- (R)	- (R)	- (R)	- (R)
15	- (R)	- (R)	- (R)	- (R)	- (R)	- (R)
16	- (R)	- (R)	- (R)	- (R)	- (R)	- (R)
17	- (R)	- (R)	- (R)	- (R)	- (R)	- (R)
18	- (R)	- (R)	- (R)	- (R)	- (R)	- (R)
19	- (R)	14 (I)	- (R)	- (R)	- (R)	13 (I)
20	- (R)	- (R)	- (R)	- (R)	- (R)	- (R)
21	- (R)	- (R)	- (R)	- (R)	- (R)	- (R)
22	- (R)	- (R)	- (R)	- (R)	- (R)	- (R)

Compounds	*P. aeruginosa* ATCC 27853		*E. coli* ATCC 25922		*E. coli* ATCC 35218	
23	- (R)	- (R)	- (R)	- (R)	- (R)	- (R)
AMP10	20 (S)		- (R)		- (R)	
CIP5	35 (S)		30 (S)		35 (S)	
TET30	27(S)		23 (S)		15 (I)	

Standard antimicrobial agents: AMP10 (Ampicillin), CIP5 (Ciprofloxacin), TET30 (Tetracycline). Negative control: DMSO. Solvent used: DMSO. Susceptibility parameters: R (Resistant), I (Intermediate), S (Susceptible).

7.3 CONCLUSION

This study reported the antibacterial susceptibility tests for Gram negative and positive bacteria including sensitive *E. coli* and QC organism ATCC 25922, β-lactam resistant *E. coli* ATCC 35218, multidrug resistant *P. aeruginosa* ATCC 27853, sensitive *S. aureus* ATCC 29213, methicillin-resistant *S. aureus* ATCC 43300 and vancomycin-resistant *E. faecalis* ATCC 51299 against new dithiophosphonate compounds synthesized using the agar-well diffusion method. The susceptibility tests showed a range of activity ranging from zero (resistant) to intermediate and in some cases susceptible. Compounds **3**, **5** and **9** showed good antibacterial activity compared to the standard antimicrobial agents for Gram negative bacteria while compounds **5**, **9**, **13**, **14**, **16** and **18** also showed similar results for the gram positive bacteria respectively.

7.4 EXPERIMENTAL

7.4.1 Evaluation of antimicrobial activity for dithiophosphonate compounds by agar-well diffusion assay

Compounds **1-29** were subjected to antibacterial screening using the agar-well diffusion method (CLSI, 2012). Stock solutions of compounds **1-29** (10 mg) were prepared in DMSO (1 mL). Three Gram-negative bacteria (*Escherichia coli* ATCC 25922, *E. coli* ATCC 35218, and *Pseudomonas aeruginosa* ATCC 27853) and three Gram-positive (*Staphylococcus aureus* ATCC 29213, *S. aureus* ATCC 43300 and *Enterococcus faecalis* ATCC 51299) were selected for the study. Bacterial isolates, grown overnight on TSA agar plates, were re-suspended in sterile distilled water and the turbidity of cell suspensions adjusted equivalent to that of a 0.5 McFarland standard. Inocula were used to swab Mueller-Hinton (MH) agar plates. Wells (6 mm) punched into the swabbed agar surface were loaded with 50 µL (500 µg) and 100 µL (1000 µg) of all compounds respectively. Three standard antimicrobial agents (Oxoid, UK), i.e., ampicillin (AMP10, 10 µg per disc), ciprofloxacin (CIP, 5 µg per disc), tetracycline (TET30, 30 µg per disc) as well as a negative control (DMSO-impregnated discs) were also assessed. Diameters of zones of inhibition (Figure 7.1) were measured with the aid of transparent calibrated ruler. The following zone diameter criteria were used to assign susceptibility or resistance to tested compounds: Susceptible (S) ≥ 15 mm, Intermediate (I) = 11-14 mm, and Resistant (R) ≤ 10 mm (Chenia, 2013). The criteria for assigning susceptibility or resistance to AMP10 was as follows: (S) ≥ 17 mm, (I) = 14–16 mm, (R) ≤ 13 mm, CIP5 (S) (I) (R), while those for TE30 were: (S) ≥ 19 mm, (I) = 15–18 mm, (R) ≤ 14 mm (CLSI, 2012).

Figure 7.1: Incubated plates showing the diameter of zones of inhibition against test isolates.

7.5 REFERENCES

1. E. Dun, *J. Biol. Med.,* **1999**, 72 281–285.
2. T. Y. Saga, K. *JMAJ,* **2009**, 52**,** 103-108.
3. J. X. Yanling, L. Zhiyuan, L., *InTech.* , **2013**, 289-308.
4. S. Saha, Dhanasekaran, D., Chandraleka, S., Thajuddin, N. and Panneerselvam, A. , *Advances in Bio. Res,* (**2010**) 4, 224-229.
5. N. Farrell, *Comprehensive Coord. Chem*, **2003**, 9, 809-840.
6. H. P. S. Chauhan, U. P. Singh, N. M. Shaik, S. Mathur and V. Huch, *Polyhedron*, **2006**, 25, 2841-2847.
7. R. A. Cherkasov, I. S. Nizamov, G. T. Gabdullina, L. A. Almetkina, R. R. Shamilov and A. V. Sofronov, *Phosphorus, Sulfur, Silicon Relat. Elem*, **2013**, 188, 33-35.
8. C. Aydemir, S. Solak, G. Acar Doganlı, T. Sensoy, D. Arar, N. Bozbeyoglu, N. Mercan Dogan, P. Lönnecke, E. Hey-Hawkins, M. Sekerci and M. Karakus, *Phosphorus, Sulfur, Silicon Relat. Elem*, **2015**, 190, 300-309.
9. M. Karakus, Y. Ikiz, H. I. Kaya and O. Simsek, *Chem. Cent. J*, **2014**, 8, 18.
10. H. Y. Chenia, *Sensors*, **2013**, 13, 2802-2817.
11. P. Wayne, *Performance standards for antimicrobial susceptibility testing*, **2007**, 17.

CHAPTER 8

CONCLUSION AND PROSPECTIVE WORK

8.1 CONCLUSION

This thesis reports on new dithiophosphonate ligands synthesized from the reaction between Phenetole Lawesson's reagent and its ferrocenyl analogue with a tetraol and an aromatic alcohol (pentaerythritol and diphenyl methanol). The dithiophosphonate ligands synthesized were employed to prepare new Zn, Cd and Ni complexes that were characterized spectroscopically and in representative cases by molecular structures. The molecular structures of the Zn complexes obtained were distorted tetrahedral while that of Ni was distorted square planar. Compounds 7-10 were UV-Vis active between 240-320 nm. Compounds **7-10**, **16** and **18** displayed solid state luminescence between 320-450 nm. The reaction between Phenetole Lawesson's reagent and its ferrocenyl analogue with ethambutol yielded new dithiophosphonate zwitterions while coordination compounds of ethambutol were obtained by the reaction of Ni and Cu salts with ethambutol in water. The ability of these compounds to exhibit polymorphism was also reported in chapter 5. The reaction of EMB.2HCl with Cu resulted in a hexanuclear cluster while that of Cu gave trigonal bipyrimidal geometry, all characterised structurally. The solubility of all the complexes was also studied. The light harvesting properties of some of the synthesized compounds were assessed as dye sensitized solar cell application. Compounds **25-28** used as co-sensitizers and co-adsorbents had a significant effect on the performance of the DSSCs. They cells were capable of improving the J_{SC}, V_{OC} and η. The device performance decreased in the order **25**/N719 > **28**/N719 > **26**/N719 > **27**/N719, and each of these fabricated cells showed better performance than the DSSC fabricated by using only the N719 dye. The performance of the **25**/N719 was the best with an overall conversion efficiency of 7.49 %. The thesis concluded that the tested compounds are attractive candidates as co-sensitizers in DSSCs.

The thesis also reported the results of the antibacterial screenings of these compounds.

8.2 PROSPECTIVE WORK

This study can be possibly taken further in a number of ways, some of which are highlighted below.

- Ethambutol could be derivitized to incorporate two functionalities (dithiocarbamate and xanthate) yielding ‘complexes of complexes’ (Scheme 8.1). The geometry of these ‘complexes of complexes’ would be interesting.
- The ‘complex of complex’ can be extended with the dithiophosphonate and amido dithiophosphonate functionality on EMB as shown in Scheme 8.2.
- These compounds can then be applied as DSSCs and/or screened for anti-bacterial activity.

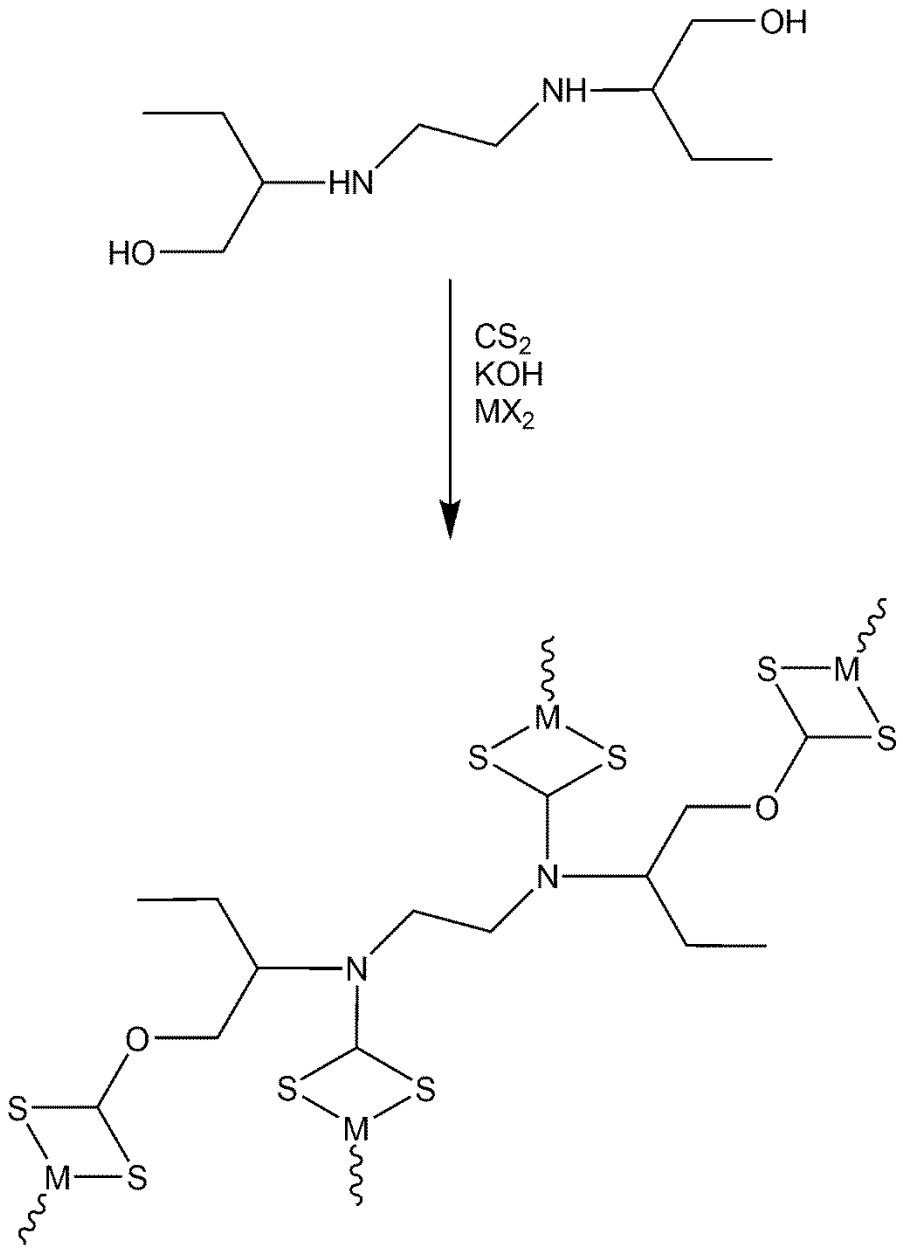

Scheme 8.1: Prospective ‘complex of complex’ incorporating dithiocarbamate and xanthate.

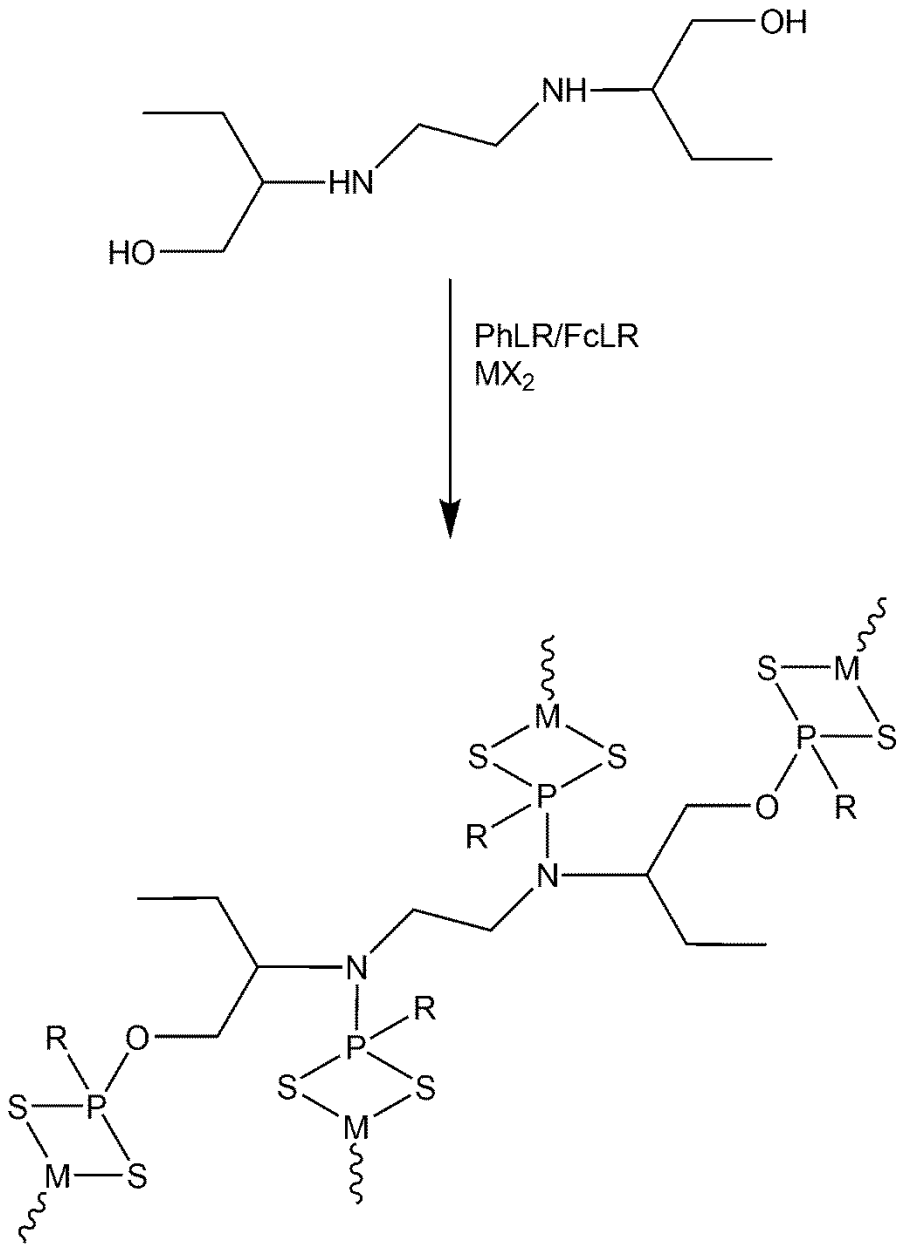

Scheme 8.2: Prospective 'complex of complex' incorporating dithiophosphonate and amido dithiophosphonate.

APPENDIX

The accompanying CD serves as an appendix to this thesis and contains ^{1}H NMR, ^{31} P NMR, ^{13}C NMR, FTIR and Mass spectra. It also contains the cif files of the crystallographic data.